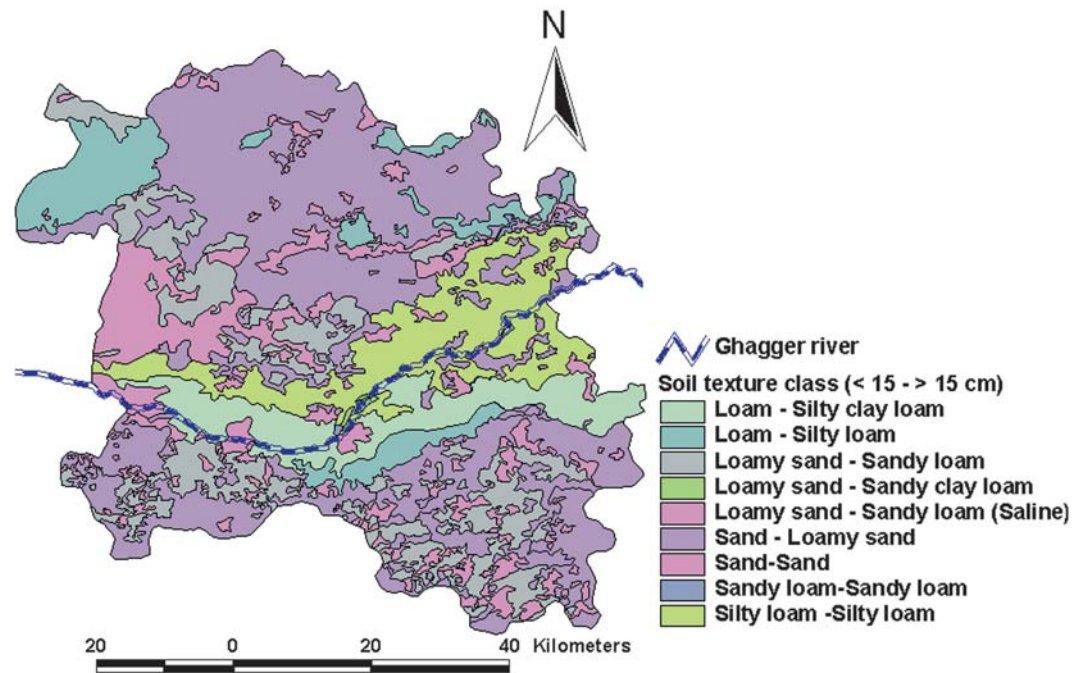
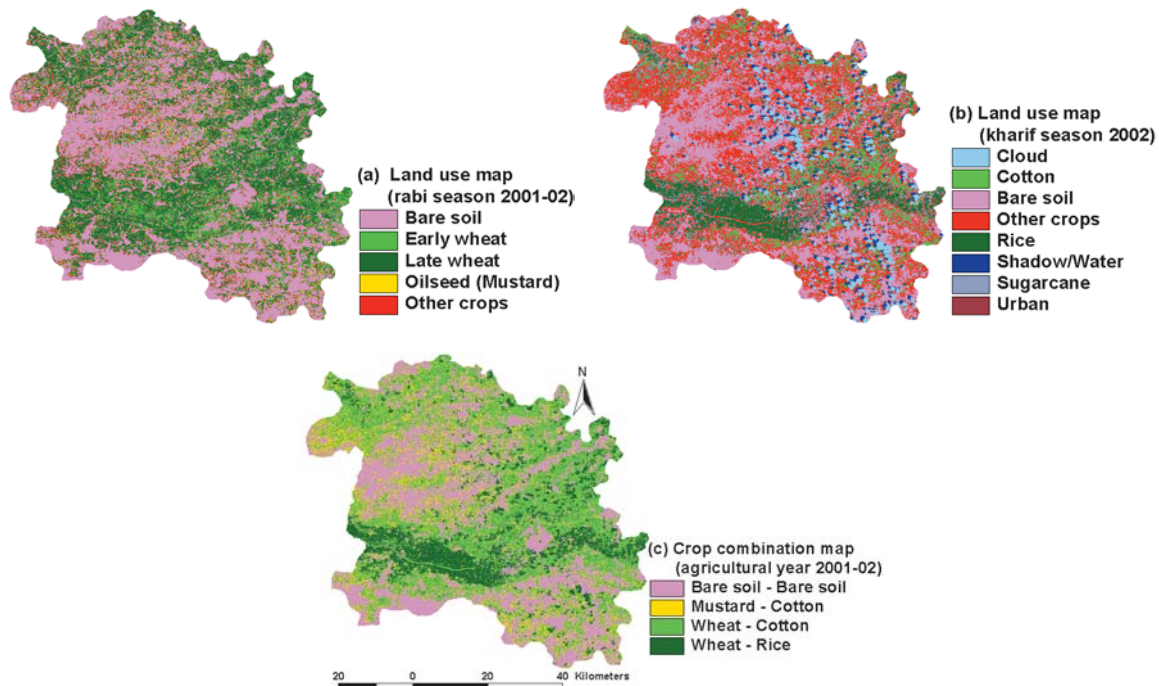


Water productivity analysis from field to regional scale

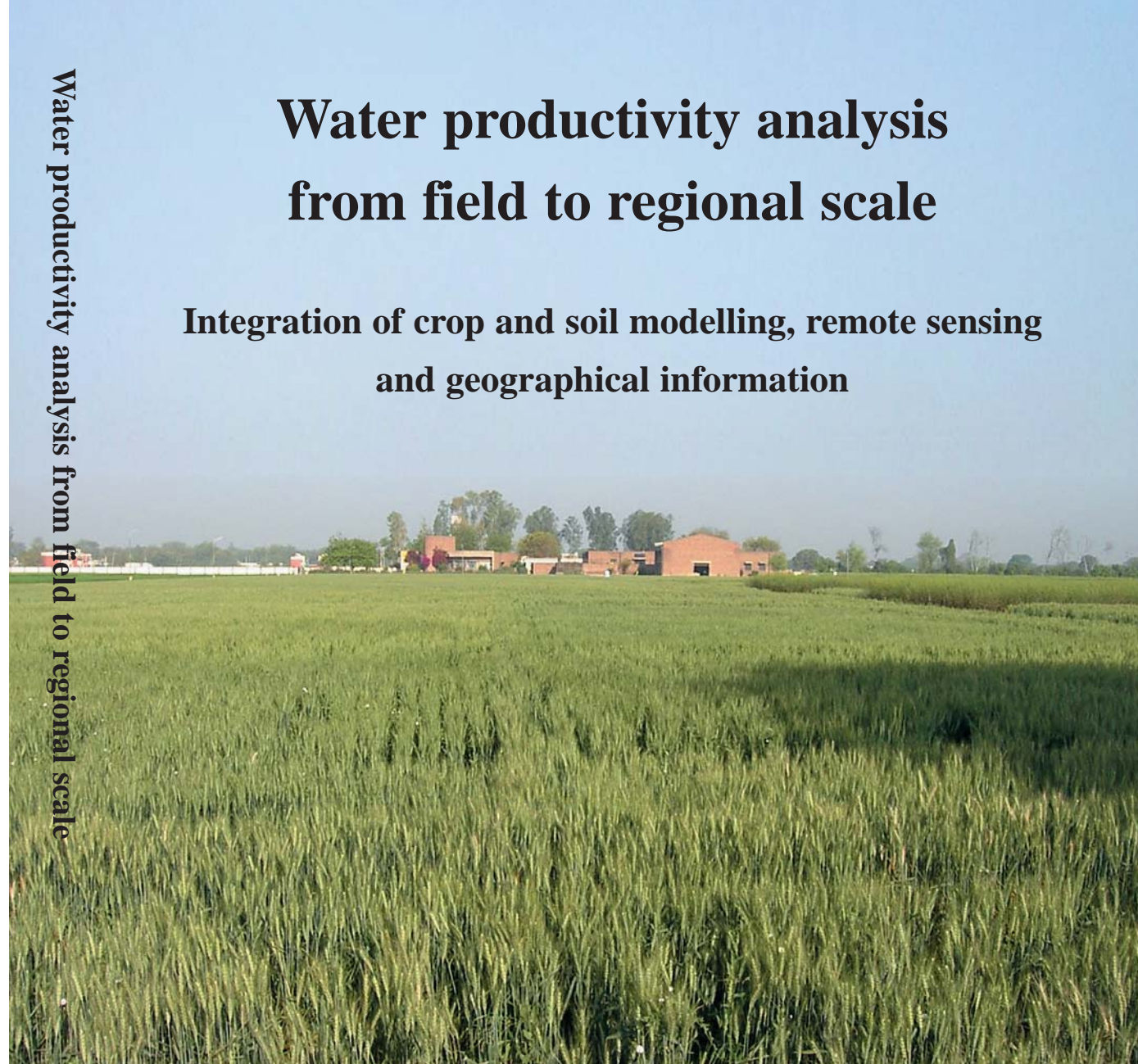
Integration of crop and soil modelling, remote sensing and geographical information



Soil map of Sirsa district (Ahuja et al. 2001)



Land use classification of Sirsa district based on satellite images (Landsat TM7, spatial resolution 30m x 30m) during the agricultural year 2001-02: (a) the *rabi* season (Mar 18, 2002), (b) the *kharif* season (Sept 10, 2002), and (c) resulting crop combination map (based on the reclassification).



Propositions

1. Efforts to increase water productivity in Sirsa district (Haryana), India should focus not only on the water and salt stress, but also on nutritional, pest or disease stresses.
 - This Thesis
2. The concept of water productivity is useful to understand water utilization, but does not describe the sustainability of an irrigation system.
 - This Thesis
3. The present thesis is just a drop in the ocean of gap between the created potential for real world simulation and its utilization.
4. We realize that what we are accomplishing is a drop in the ocean. But if this drop were not in the ocean, it would be missed.
 - Mother Teresa
5. Think of the poorest person you have ever seen and ask if your next act will be of any use to him.
 - Mahatma Gandhi
6. Without water, we will not be focused on impressive progress, but on mere survival.

Singh, R. 2005. *Water productivity analysis from field to regional scale: integration of crop and soil modelling, remote sensing and geographical information*. Doctoral thesis, Wageningen University, Wageningen, The Netherlands.

Water productivity analysis from field to regional scale:

Integration of crop and soil modelling, remote sensing and geographical information

Promotor: Prof. dr. ir. R. A. Feddes
Hoogleraar in de Bodemnatuurkunde, agrohydrologie en
grondwaterbeheer

Co-promotor: Dr. ir. J. C. van Dam
Universitair hoofddocent, sectie Waterhuishouding

Samenstelling promotiecommissie:

Prof. dr. K. E. Giller,
Wageningen Universiteit

Prof. dr. ir. A. Veldkamp,
Wageningen Universiteit

Dr. Peter Droogers,
FutureWater, Arnhem

Ir. G. H. van Vuren,
Wageningen Universiteit

Dit onderzoek is uitgevoerd binnen de onderzoekschool WIMEK-SENSE.

Water productivity analysis from field to regional scale:

Integration of crop and soil modelling, remote sensing and
geographical information

Ranvir Singh

Proefschrift
ter verkrijging van de graad van doctor
op gezag van de Rector Magnificus
van Wageningen Universiteit,
Prof. dr. ir. L. Speelman
in het openbaar te verdedigen op
dinsdag 22 maart 2005
des namiddags te vier uur in de Aula

ISBN: 90-8504-155-4

Ranvir Singh
Email: khatri_ranvir@yahoo.com

Ranvir Singh, 2005

Water productivity analysis from field to regional scale: integration of crop and soil modelling, remote sensing and geographical information / Singh, R. Doctoral thesis, Wageningen University, Wageningen, The Netherlands - with references - with summaries in English and Dutch.

“Water is probably the only natural resource to touch all aspects of human civilization
from
agricultural and industrial development
to
cultural and religious values embedded in society.”

– *Koichiro Matsuura, Director General, UNESCO*

*This work is dedicated to my parents,
Om Parkash and Murti devi*

Abstract

Singh, R. 2005. *Water productivity analysis from field to regional scale: integration of crop and soil modelling, remote sensing and geographical information*. Doctoral thesis, Wageningen University, Wageningen, The Netherlands.

In agricultural production systems, a profound water productivity analysis requires quantification of different hydrological variables such as transpiration, evapotranspiration and percolation, and biophysical variables such as dry matter and grain (or seed) production in relation to different irrigation and agricultural management practices. Sirsa district, located in the Bhakra Irrigation System in Haryana (India), has been selected for a case study. The study area, covering 0.42 million ha, is characterized by typical problems of canal water scarcity, poor groundwater quality, rising and declining groundwater levels, waterlogging and secondary salinization, and less than optimal crop production.

The field scale ecohydrological Soil-Water-Atmosphere-Plant (SWAP) model when coupled with field experiments, remote sensing and GIS as used in this study, increases the capabilities of reliable simulation of water productivity from field to regional scale. SWAP was calibrated and validated using the observations at different farmer fields representing various combinations of soil, crop, and irrigation amount and its quality. Inverse modelling was used to determine indirectly the soil hydraulic parameters at field scale, and the observed soil moisture and salinity profiles were used as system response. The calibrated and validated SWAP including detailed crop growth simulations was extended in a distributed mode to quantify the required hydrological and biophysical variables at regional scale. Field experiments, satellite images and existing geographical data were used to derive and aggregate the input parameters and boundary conditions at the appropriate scales. The accuracy and reliability of spatial aggregation of representative input parameters was determined by comparing the evapotranspiration simulated by distributed SWAP modelling with independent satellite remote sensing based evapotranspiration data at different spatial and temporal scales.

The water productivity WP was computed for different scales and in different forms viz., crop yield per unit amount of water used in transpiration T , evapotranspiration ET , or ET plus percolation from field irrigations and seepage losses from the conveyance system. Considerable spatial variation in WP values was observed not only for different crops but also for the same crop. For instance, the WP_{ET} , expressed in the terms of grain yield per unit amount of ET , for wheat varied from 1.22 to 1.56 kg m⁻³ among different farmer fields monitored in Sirsa district during the agricultural year 2001-02. At field scale, the average WP_{ET} (kg m⁻³) was 1.39 for wheat, 0.94 for rice and 0.23 for cotton, and represents its average values for the climatic and growing conditions in Northwest India. Factors responsible for low values of WP include a high share (20 to 40%) of soil evaporation into ET for rice, percolation from fields and seepage losses (34 to 43% of the total canal inflow) from the conveyance system. The simulated water and salt limited crop yields were higher than the recorded crop yields, and indicate substantial nutritional, pest and disease stresses. Also, the study revealed a considerable fluctuation of the estimated net groundwater recharge and salt build-up over the main canal commands in Sirsa district. Better crop management, reduction in seepage losses and canal water reallocation (15%) from the northern to the central canal commands are recommended to improve the WP , and to halt the rising and declining groundwater levels.

Although ecohydrological models offer predictions for the future, they may become inaccurate due to over- or underparameterisation, especially in case of distributed modelling at regional scale. Therefore, a sequential 'updating' algorithm has been developed to improve the simulated total dry matter production in SWAP, whenever an observation of total dry matter production is available.

Key words: distributed modelling, inverse modelling, data assimilation, irrigation water management, salinization, Bhakra Irrigation System, India.

Acknowledgements

Successful completion of a doctoral thesis requires research interest, hard work, dedication and teamwork. Following my studies in Agricultural Engineering with specialised in Soil and Water Engineering, my research interests are in productive and sustainable water management in agriculture. The idea to start a doctoral thesis was realized when I met with Dr. Jos C van Dam during his visit to CCS Haryana Agricultural University (CCS HAU), Hisar (Haryana), India in the year 2001. Following the discussion, this doctoral thesis was designed in the framework of the WATPRO project in Sirsa district (Haryana), India from 2001 to 2003. With great pleasure, I enjoyed working with the various individuals involved in this project, and later during the tenure of this thesis. I feel indebted and wish to express my gratitude to all of them for their support and contribution in one or another way.

First, I would like to express my sincere gratitude to Dr. Jos C van Dam, for his faith shown in me. Not only he facilitated all my work, but also supervised it throughout the development of this thesis. This thesis would not have been possible without his continued support, guidance and consistent encouragement to finish it in time. I gratefully acknowledge his intellectual guidance, explaining SWAP model, discussing problems, valuable insights and especially correcting my English in the many versions of thesis drafts. Discussions with him have been of great benefit not only to this thesis but also to my inexperienced research and scientific writing career. What I have learned while working with him is far beyond the contents of this thesis. Besides his scientific advice and support, what I really enjoyed with him was occasionally biking and especially walking through 'Rhenen and Veluwe zoom' forests during the summer time in Wageningen. Jos: Thanks a lot for your scientific advice and friendly behaviour!

I am very grateful to, and would like to pay my kind regards to my promotor, Prof. Dr. Reinder Feddes. Without his critical reading and comments on the drafts of the different chapters, there could have been no guarantee of the academic qualification of this thesis. His suggestions and remarks have helped significantly to shape this work.

The generous efforts of Dr. Raj Kumar for his constructive comments and invaluable suggestions to improve the contents of this thesis are highly acknowledged. He has been a source of inspiration to me, and undoubtedly also to many other students at CCS HAU, Hisar. Raj: it has been an honour for me to be your student!

A major part of this thesis includes the fieldwork and data collection in Sirsa district in the framework of the WATPRO project. Special appreciation goes to Ir. Arne Roelevink, who did his master thesis within this project. We spent a couple of months at CCS HAU, Hisar, and later at Altera Research Centre, Wageningen while working on a digital database for regional analysis. My special thanks go to the Research Associates Mr. Sher Singh, Udaivur, Jhaber Mal and Devender, as without them collection of the necessary field data was impossible. I am highly grateful to Dr. R.S. Malik, Prof. Ranvir Kumar, Dr. A.S. Dhindwal, Dr. B. S. Jhorar and Dr. M. S. Bhattoo who guided and helped me during the fieldwork. I respectfully acknowledge the scientific knowledge and help received from Mr. Joop Kroes, Dr. Peter Droogers, Dr. Wim Bastiaanssen, Dr. Janette Bessmbinder and Dr. Peter Leffelaar.

My memories go back to when I came the first time in Wageningen to work on this thesis. I missed my friends a lot, especially Sanjeev Balyan, Pankaj Rana, Pardeep Bhai Sahab, Mahesh Khatri, Satish Ahlawat, Kulbir, Piyush Sund, Vikas, Naveen Kohar, Kuldeep Dahiya,

Ashish Mudgal, Vivek, Anil Saroha, Sonu and Arti, with whom I was living happily at CCS HAU, Hisar. As life started in Wageningen, I met new friends Kirtiman, Shibu Ebrahim, Ajay Awati, Arun Mishra, Anjal Parkash, Anand, Sharad, Bobby, Palvinder and Karin Viergever, and enjoyed their company. I enjoyed playing squash with Esther Bloem, Tineke van der Ploeg, Jeannette Kluess, Geraldine Klarenberg and Berry van Wases. My whole heartily thanks go to Gina Homs Aubia, she always encouraged me whenever I felt down towards my work while writing this thesis. Thanks to all my friends, you made my life easy and happy in Wageningen!

I enjoyed the friendly working atmosphere at the Sub-department of Water Resources at WUR (Wageningen). I sincerely appreciate the secretarial staff, Mrs. Henny van Werven and Mrs. Annemarie Hofs, for their prompt help on different administrative matters. Thanks are also due to Mr. Piet Warmerdam for his support in coordinating the financial matters. I also thankfully acknowledge the staff Department for Education and Student Affairs at WUR, particularly Maria Wijkniet for the help she provided to get my residence and working permit during my stay in Wageningen. To deal with Dutch bureaucratic matters, of course in Dutch language, would not have been possible without her help.

I would like to express my deepest appreciation to my parents and other family members. Their continuous moral support and encouraging words always helped me to finish my duties. I am extremely grateful to my father for his encouragement and kind help. Though my late mother could not see this occasion, she always encouraged me for higher studies.

Ranvir Singh
March 2005,
Wageningen, The Netherlands

Contents

1	Introduction	1
1.1	Water for food	1
1.2	Water management and related issues in Haryana state (India)	3
1.3	Problem statement	4
1.4	Research objectives and outline of thesis	7
2	Description of Sirsa study area	9
2.1	Introduction	9
2.2	Physical environment	10
2.2.1	Climate	10
2.2.2	Soil	11
2.2.3	Groundwater level and its quality	11
2.3	Irrigation water management	13
2.3.1	Canal water	13
2.3.2	Groundwater use	15
2.4	Cropping pattern and yields	16
3	Framework for regional water productivity analysis	19
3.1	Introduction	19
3.2	Schematisation of framework for regional water productivity analysis	20
3.3	Soil-Water-Atmosphere-Plant (SWAP) model	21
3.4	Calculation and aggregation of water productivity	28
3.5	Overview of data requirement and collection	30
3.5.1	Field scale	30
3.5.2	Regional scale	34
4	Water productivity analysis of irrigated crops at field scale	37
4.1	Introduction	37
4.2	Input parameters of SWAP model	37
4.2.1	Upper boundary	38
4.2.2	Crop parameters	39
4.2.3	Soil hydraulic parameters: Inverse modelling	39
4.2.4	Lower boundary and initial conditions	42
4.3	Results and discussion	42
4.3.1	Parameter estimation	42
4.3.2	Water and salt balances	45
4.3.3	Water productivity	48
4.4	Conclusions	51

5	Water productivity analysis of irrigated crops at regional scale	53
5.1	Introduction	53
5.2	Schematisation and aggregation of spatial information	53
5.3	Parameterisation of distributed SWAP model	62
5.4	Results and discussion	65
5.4.1	Cropping pattern and irrigation water distribution	65
5.4.2	Comparison of distributed modelling and satellite remote sensing	68
5.4.3	Regional water and salt balances	72
5.4.4	Regional water productivity	74
5.5	Conclusions	77
6	Impact of alternative water management scenarios on regional water productivity and groundwater behaviour in Sirsa district	79
6.1	Introduction	79
6.2	Current and alternative water management	79
6.3	Distributed modelling	81
6.4	Results and discussion	84
6.4.1	<i>'Business as usual'</i>	84
6.4.2	Regional water productivity	85
6.4.3	Net groundwater recharge	88
6.4.4	Salt build-up	90
6.5	Conclusions	91
7	Sequential assimilation of the observed total dry matter production in SWAP model	93
7.1	Introduction	93
7.2	Data assimilation methods	94
7.3	Application to study sites in Sirsa district	97
7.4	Results and discussion	98
7.4.1	The <i>'forcing'</i> vs. <i>'updating'</i> method	98
7.4.2	The <i>'calibration'</i> vs. <i>'updating'</i> method	100
7.5	Conclusions	102
	Summary and conclusions	105
	Samenvatting en conclusies	115
	References	125
	Appendices	135
	A Determination of solar net radiation	135
	B Soil profiles in Sirsa district (Haryana), India	137
	List of frequently used symbols	139
	List of abbreviations	143
	Curriculum vitae	145

Chapter 1

Introduction

1.1 Water for food

Water, a scarce natural resource and vital for life, plays a key role in the growth and development of human society. It is an essential input in agricultural production systems for food and fibre. The growing human population keeps this demand high, and forces to produce more food with the limited natural resources of land and water. Most of the human population growth occurs in third world countries, especially in Asia and Africa. For instance, the population in India has increased with a factor of three during the last 50 years, from 0.36 billion in 1951 to 1.02 billion in 2001. Concurrent growth in the total food grain production, from 51 million ton in 1951 to 212 million ton in 2002 (Fig. 1.1), has provided India with food security. The average food grain yield, defined as total food grain produced per unit area, has also increased substantially from 0.5 ton ha⁻¹ in 1951 to 1.7 ton ha⁻¹ in 2002.

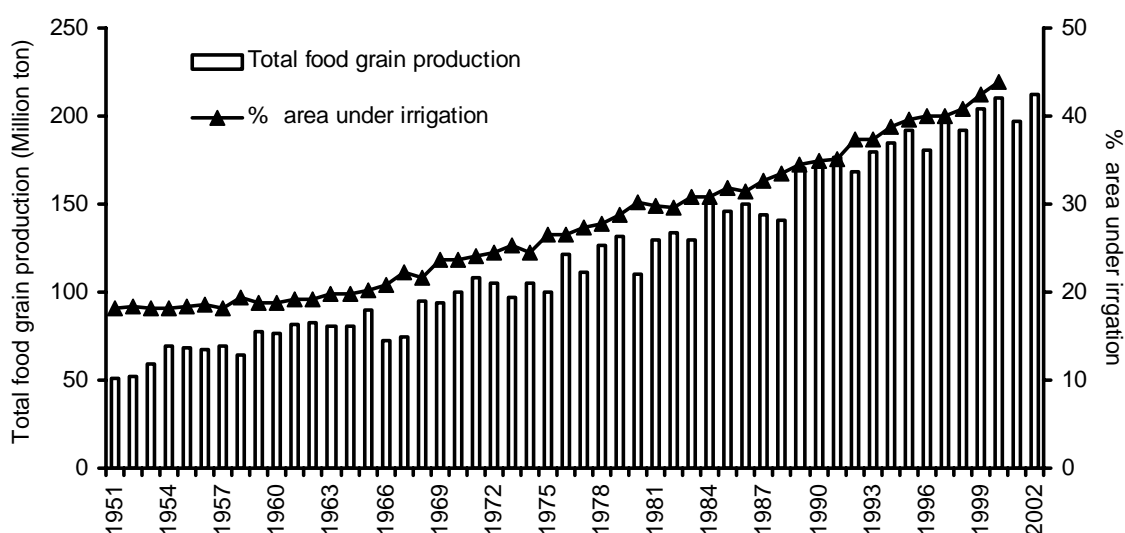


Figure 1.1 Trend of the total food grain production and % area under irrigation in India from 1951 to 2002. (Source: <http://www.agricoop.nic.in/statistics2003/>)

This huge leap in food grain production in India started in 1960's, and is described as the '*Green Revolution*'. Current higher production levels are mainly attributed to improved crop varieties, increased fertilization and especially more extensive irrigation (Fig. 1.1).

With the current population growth rate, India's population will amount 1.40 billion by the year 2025, which may outweigh the growth of food grain production. The domestic food grain demands for the year 2020 are estimated from 241 to 245 million ton (Kumar, 2001). According to estimates by Brown and Kane (1994), India will face again food shortage by the year 2030, and at that time will have to import 45 million ton of food grain. Also, the annual per capita fresh water availability in India has decreased from 5177 m³ in 1951 to 1820 m³ in 2001. Countries with annual per capita water availability of less than 1700 m³ are denoted as water stressed, and less than 1000 m³ as water scarce (IWRS, 1999).

Taking into account the increase in population up to 1.40 billion by the year 2025, India will need 2380 billion m³ of water per year to be above the water stress zone and 1400 billion m³ of water per year to avoid being a water scarce country. However, the total annual renewable water resources in India are assessed at 1869 billion m³, of which 690 billion m³ of surface water and 432 billion m³ of groundwater is utilizable (Ministry of Water Resources, 2003). Irrespective of certain assumptions and uncertainties involved in these future water and food demand projections, it is obvious that the agricultural sector has to produce more food with the same or less amount of land and water resources.

The average food grain yield in India is lower than what has been achieved in other countries like Egypt, USA and China. Further, there exists large variation in the average food grain yields among different states of India. For instance, average food grain yield during the agricultural year 2001-02 varied from 0.9 ton ha⁻¹ in Maharashtra to 4.04 ton ha⁻¹ in Punjab (Fig. 1.2). These low food grain yields and its large variation among different states offer a great potential to increase the food grain production, and to maintain Indian food security.

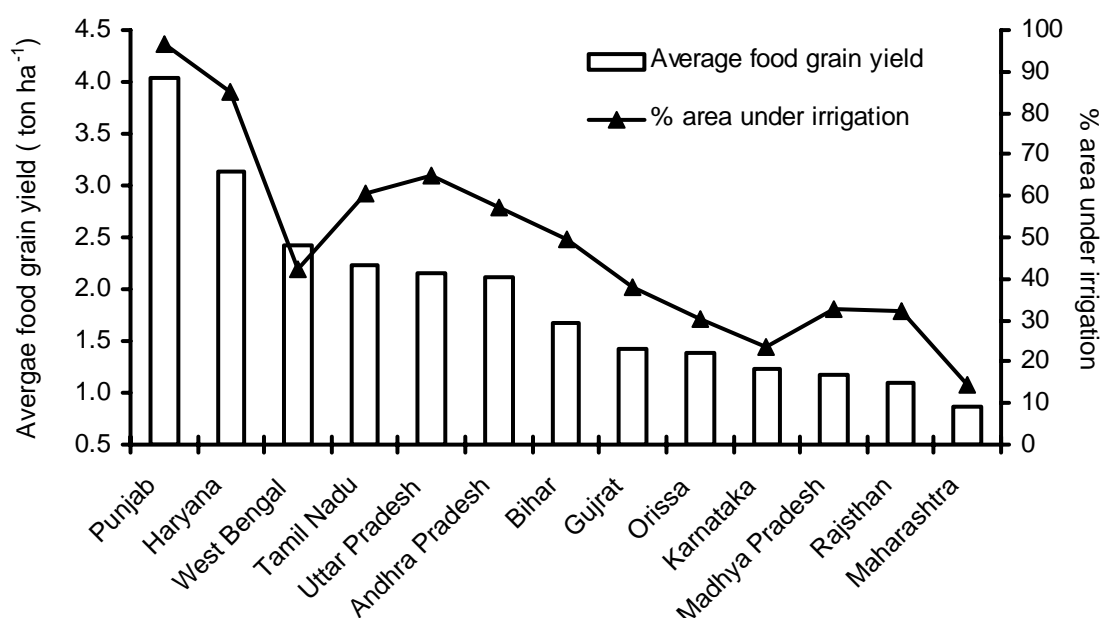


Figure 1.2 Average food grain yields and % area under irrigation in different states of India during the agricultural year 2001-02. (Source: <http://www.agricoop.nic.in/statistics2003/>)

In low rainfall regions like India, irrigated agriculture is significantly more productive than rainfed agriculture. Fig. 1.1 and 1.2 clearly present that the total food grain production and average food grain yields are related to the irrigation developments in India. Nearly 60% of the total agricultural output comes from irrigated agriculture, which covers only 40% of the total agricultural area. This significant contribution of irrigated agriculture, however, requires more than 70% of the Indian fresh water withdrawals.

The scope of meeting the growing demand of water for food through more intensive use of water resources is limited, as its exploitation in most of the river basins is already on its maximum. The urban, industrial and environmental users are also calling for their legitimate share of water, which will certainly cut down the water availability for irrigated agriculture.

Since it is hardly possible to withdraw more water from natural resources, future food production must focus on the improvement of water productivity i.e. 'more crop per drop' (IWMI, 2000).

1.2 Water management and related issues in Haryana state (India)

Haryana state, located in Northwest of India, has 82% of its total geographical area (44200 km²) under cultivation. The cropping intensity is about 177% with cultivation of two crops per year: *rabi* (winter) crop and *kharif* (summer) crop. The climate in the region is arid to semi-arid with an average annual rainfall of 545 mm y⁻¹. Successful crop production is not possible without supplemental irrigation. Current wheat yields in Haryana are around 4.2 ton ha⁻¹ under irrigated conditions. Major constraint to further increase the food grain production is limited surface water availability (Aggarwal et al., 2001). At present, only 40% of the total cultivated area is under surface (canal) water irrigation. The limited surface water for crop production is supplemented by the groundwater pumping, and hence the net irrigated area increased to 80% of the total cultivated area. This over-exploitation of good quality groundwater, especially in the eastern parts of Haryana, resulted in the decline of groundwater levels with a rate of 9 to 10 cm y⁻¹ during the last 25 years. Further, the inefficient utilization of water has caused unfavourable ecohydrological conditions as waterlogging and salinization in the central and northwest parts. The long-term (1974-2000) trend of the measured groundwater levels in Sirsa district, located in the western part of Haryana, shows an average annual rise of 0.31 m y⁻¹ (Groundwater Atlas of Sirsa district, 2002). In June 2000, Sirsa district already had a critical groundwater level (< 3 m) in nearly 5% of its total geographical area of 4270 km². These water management issues are very complex, and must be addressed by better planning and management.

Concept of water productivity

In traditional approaches, improvement of 'irrigation efficiency', defined as the ratio of soil water storage in the root zone to the total water diverted from the source, was promoted as a solution to improve water management, especially in water scarce environments. Recent approaches show that improving irrigation efficiency is not the proper solution. For instance, the on-farm irrigation efficiency of most canal irrigation systems in India ranges from 30 to 40% (Navalawala, 1999a; Singh, 2000) whereas, the irrigation efficiency at basin level is as high as 70 to 80% (Chaudhary, 1997). Improving on-farm irrigation efficiency presents a 'dry' saving of water, which is due to the reuse of groundwater at basin level. Therefore, instead of 'irrigation efficiency', 'water use efficiency' was promoted to describe the performance of irrigation systems.

In agronomic terms, 'water use efficiency' is defined as the amount of organic matter produced by a plant divided by the amount of water used by the plant in producing it (De Wit, 1958). This definition relates both production and utilization of water resources in agricultural production systems. However, the used terminology 'water use efficiency' does not follow the classical concept of 'efficiency', which uses the same units for input and output. The classical concept of efficiency as used by engineers omits production values. International Water Management Institute (IWMI), therefore, has proposed a change of the nomenclature from 'water use efficiency' to 'water productivity'.

In a broader sense, ‘*water productivity*’ is related to the value or benefit derived from the use of water. Therefore, the concept of water productivity in agricultural production systems is focused on ‘*producing more food with the same water resources*’ or ‘*producing the same amount of food with less water resources*’. In a simple way, water productivity is defined as ‘*crop production*’ per unit ‘*amount of water used*’ (Molden, 1997). It can be further defined in several ways according to the purpose, scale and domain of analysis (Molden et al., 2001; Bastiaanssen et al., 2003a). This flexibility in defining the water productivity provides a conceptual framework and common language between different stakeholders, researchers and water managers (Table 1.1).

Table 1.1 Some examples of stakeholders and definitions in the concept of water productivity (Adapted from Bastiaanssen et al., 2003a).

Stakeholder	Definition	Scale	Target
Plant physiologist	Dry matter / transpiration	Plant	Utilize light and water resources
Agronomist	Yield / evapotranspiration	Field	Sufficient food
Farmer	Yield / irrigation	Field	Maximize income
Irrigation engineer	Yield / canal water supply	Irrigation scheme	Proper water allocation
Policy maker	\$ / available water	River basin	Maximize profits

For example, obtaining more kg of dry matter or grain per unit amount of transpiration or evapotranspiration is the key issue for plant breeders and agronomic scientists. The definition of water productivity, therefore, brings both the plant breeders and the agronomists to a common communication platform, and can be used as a standard unit of evaluation. Low values of water productivity in terms of kg of grain per unit amount of evapotranspiration suggest an agronomist to reduce soil evaporation by improving agronomic practices such as mulching. Similarly low crop yields under high irrigations at field scale indicate poor field irrigation management or the status of other management factors such as nutrient, pest and disease control. For irrigation engineers, canal water supply is a key factor. They will evaluate their own water productivity based on the crop yields in relation to the canal water supplies.

Water productivity can also be defined in economic terms: \$ / amount of water used. These economic values are useful to compare different crops and to evaluate the net benefits derived from a particular crop. The economic definition of water productivity also provides a better basis for policy makers to decide on agricultural and non-agricultural utilization of water such as for industries, bird habitats and tourism. In summary, *the concept of water productivity describes various aspects of water management such as production, utilization and economy* (Molden and Sakthivadivel, 1999; Molden et al., 2001; Droogers and Bastiaanssen, 2002; Kijne et al., 2003), *and therefore deserves to get more attention.*

1.3 Problem statement

In order to improve the water productivity, a comprehensive water use analysis is required to understand and quantify different water balance components, and their short as well as long-term impact on ecohydrological conditions and agricultural production of the system. The bottleneck is that tools are absent to make such detailed analysis of irrigation systems,

especially at regional scale. Various approaches such as field measurements (Hussain et al., 2003), satellite remote sensing (Bastiaanssen et al., 2003b) and simulation modelling (Droogers and Kite, 2001) are investigated to quantify the water productivity values of irrigation systems.

Traditionally field experiments are conducted to quantify and evaluate alternative water management practices to improve the water productivity. To conduct field experiments for all ecohydrologic conditions is expensive, laborious and time consuming, especially if they should be representative for a sequence of years. The measurement of water balance components such as transpiration, soil evaporation and percolation under field conditions is also difficult, and need sophisticated instrumentation and / or installation of lysimeters. *However, field experiments are essential for the detailed knowledge of crop growth, water flow and salt transport processes at field scale.* These location specific findings at field scale need to be generalized to all ecohydrological conditions in the considered region. Using measured data at 216 farmer fields in Kaithal district (Haryana), Hussain et al. (2003) developed statistical yield functions to estimate the combined effect of various production factors on wheat yields in Haryana. The measured wheat yields were related to location specific factors such as soil salinity and rainfall, and management factors such as seed variety, cropping calendar, source and amount of irrigation, dosage of fertilizers, pesticides and weedicides. There was significant variation in wheat grain yields across farmer fields ranging from 3.0 to 5.7 ton ha⁻¹. The amount of irrigation applied at these fields varied from 746 to 4332 m³ ha⁻¹. They found an average wheat production of 1.47 kg grain per m³ of irrigation water applied. Hussain et al. (2003) concluded that promoting on-farm agronomic practices such as improved seed varieties, and dissemination of the knowledge on sowing dates and timings and application rates of inputs, especially of water, fertilizer and weedicide are important factors for the yield increase in Haryana. *Such developed statistical yield functions, however, do not give any information on the actual water and salt balances, and their long-term impact on ecohydrological conditions and agricultural production of the irrigation system.*

In satellite remote sensing, the accumulated scientific knowledge between agricultural researchers and radiation physicists has evolved in the development of quantitative algorithms to convert remotely sensed spectral radiances into useful information such as land use, evapotranspiration fluxes and crop yields. These algorithms e.g. Surface Energy Balance Algorithm for Land (SEBAL) (Bastiaanssen et al., 1998) can analyze the water productivity at irrigation system and basin level. Bastiaanssen et al. (2003b) applied SEBAL to process the high resolution (Landsat TM7, spatial resolution 30 m × 30 m) and low resolution (NOAA-AVHRR, spatial resolution 1.1 km × 1.1 km) satellite images, and obtained spatially distributed evapotranspiration fluxes and crop yields in Sirsa district during the agricultural year 2001-02. Estimation of water balance components such as percolation, and distinction between soil evaporation vs. crop transpiration is not possible with the current remote sensing algorithms such as SEBAL. As a result, *satellite remote sensing gives limited information on the water productivity: kg crop yield per unit amount of evapotranspiration.* Further, the evaluation of alternative water management options is not possible with the satellite remote sensing techniques. *However, satellite remote sensing provides spatial variables such as land use, which can be of great help in water productivity analysis at regional scale.*

In recent decades, researchers have devoted much effort to develop physical based simulation models to analyze the environmental and water use problems. With the gained theoretical and practical experience on crop growth, water flow and salt transport processes under different ecohydrological conditions in Haryana, Bastiaanssen et al. (1996) developed a distributed On-Farm Irrigation and drainage Management Decision Support System (FIRM). This system linked the field scale Soil-Water-Atmosphere-Plant (SWAP) model with a geographical information system (GIS) and a multi-objective optimisation procedure (ELECTRE). The developed FIRM system contains a procedure to infer geographically different units with respect to soil, rainfall, and groundwater level and its quality. Combinations of six major crop rotations and four water management strategies were explored and analyzed in terms of different water management response indicators. Results indicate that the total fresh surface water and fresh or brackish groundwater resources available in Haryana are sufficient to establish a productive and sustainable agricultural system. In a more recent study, Jhorar (2002) used a distributed irrigation water management model, called FRAME (Boels et al., 1996), to analyze the performance of Sirsa Irrigation Circle (Haryana), India. The FRAME is composed of two model packages, SIMulation of Water management in Arid REgions (SIWARE) for canal and on-farm water management (Boels et al., 1989; Sijtsma et al., 1995) and Standard Groundwater Model Package (SGMP) for regional groundwater flow (Boonstra and De Ridder, 1990). He calibrated the regional soil hydraulic parameters through inverse modelling using the evapotranspiration fluxes estimated by the remote sensing algorithm SEBAL and the measured groundwater levels. The calibrated and validated FRAME model was used to predict the impact of water management strategies on evapotranspiration, soil salinity and groundwater levels. Results revealed that the groundwater of relatively poor quality (4 to 6 dS m⁻¹) can be used, and the sustainability of Sirsa Irrigation Circle depends on the rainfall received and its distribution.

The main limitation of the simulation models used in both above presented studies was pre-defined crop growth during the evaluation of water management strategies at regional scale. However, the physiological growth of crops is affected by the spatial variability in terms of weather, soil, irrigation and groundwater level and its quality in a region. The used pre-defined or simple crop growth model did not simulate any interaction between the crop growth and different water and salt stress conditions, and therefore had disadvantage for the simulations at regional scale. Neither of these studies tried to address the concept of water productivity at field or regional scale.

In this study, we focus on water productivity analysis from field to regional scale through a physical based simulation modelling approach. The field scale ecohydrological SWAP model when coupled with field experiments, remote sensing and GIS as used in this study, increases the capabilities of reliable simulation of water productivity at regional scale. For evaluation of water management strategies, a feedback mechanism between the physiological crop growth and different water and salt stress conditions is essential, which is achieved through the detailed crop growth modelling. Recently, a detailed generic crop growth model WORld FOod STudies (WOFOST) (Supit et al., 1994) has been implemented in SWAP for the simulation of crop growth in close interaction with dynamics of water flow and salt transport in soils (Van Dam et al., 1997; Kroes and Van Dam, 2003). This detailed crop model describes the

photosynthesis process accurately, and has the advantage of accounting the effects of different water and salt stress conditions on the physiological growth of crops.

Sirsa district (Haryana), India has been selected for this study. Water management problems in Sirsa district represent the typical problems in Haryana of canal water scarcity, poor groundwater quality, rising or declining groundwater levels, waterlogging and secondary salinization, and less than optimal crop production.

1.4 Research objectives and outline of thesis

The main research objective of this study is to integrate the operational knowledge of crop growth, soil water flow and salt transport modelling with field experiments, remote sensing and GIS for water productivity analysis from field to regional scale. For understanding and improving regional irrigation water management and its productivity, this approach uses simulation modelling in order to be flexible in revisiting the past, analyzing the present and predicting the future.

The specific research objectives of this study are:

- 1. Calibration and validation of an advanced field scale ecohydrological model using data from farmer fields with current practices.*
- 2. Application of a field scale ecohydrological model for water productivity analysis of irrigated crops at regional scale.*
- 3. Analysis of the impact of water management strategies on regional water productivity and groundwater levels in the study area.*
- 4. Analysis of the methodology combining crop growth, soil water flow and salt transport modelling with remote sensing and GIS to improve regional irrigation water management and its productivity.*

Chapter 2 gives a brief introduction of the study area, Sirsa district. An overview is given of its physical environment, irrigation and cropping system. This chapter also highlights the important issues related to water management in Sirsa district.

Chapter 3 presents the framework for regional water productivity analysis, which integrates crop growth, soil water flow and salt transport modelling with field experiments, remote sensing and GIS. Simulation approaches such as simple and detailed crop growth, soil water flow and salt transport included in the Soil-Water-Atmosphere-Plant (SWAP) model are briefly introduced. This chapter also presents the calculation and aggregation of different water productivity definitions and their significance at different scales. An overview is given of the data requirement and its collection at field as well as regional scale.

In Chapter 4, the SWAP model is calibrated and validated using the observations at farmer fields in Sirsa district during the agricultural year 2001-02. Inverse modelling is briefly discussed for the estimation of soil hydraulic parameters. The detailed crop growth module of

SWAP is compared with the simple crop module, the latter is based on the measured crop growth. Finally, the water productivity and its variation for wheat, cotton and rice in Sirsa district is simulated and analyzed at field scale.

Chapter 5 deals with the implementation of the proposed framework for regional water productivity analysis in Sirsa district during the agricultural year 2001-02. Effects of spatial heterogeneity on the regional water and salt balances, and on the water productivity are analyzed through a distributed modelling: running field scale SWAP model for all combinations of *weather-crop-soil-water* in Sirsa district. The aggregation of these combinations and their attached spatial input parameters through field experiments, satellite images and existing geographical data are discussed in detail. Further, the accuracy and reliability of the spatial aggregation of input parameters is evaluated by comparing the evapotranspiration simulated by distributed SWAP modelling with independent satellite remote sensing based evapotranspiration data at different spatial and temporal scales. The simulated water and salt balances, crop yields, and subsequently water productivity values of irrigated crops in Sirsa district are analyzed at regional scale.

In Chapter 6, various feasible water management options are discussed to improve regional irrigation water management and its productivity in Sirsa district. Further, the current and proposed water management scenarios are evaluated through a physical based distributed modelling coupled with field experiments, remote sensing and GIS. The simulation results are analysed to select appropriate recommendations for a productive and sustainable water management in the district.

In recent years, a strong research interest has been developed in integrating the physical based models with satellite remote sensing data to improve their prediction capabilities, especially at regional scale. In Chapter 7, different data assimilation methods such as '*forcing*', '*calibration*' and '*updating*' are discussed to assimilate the observed (remotely) state variables into the physical based models. A relatively simple sequential '*updating*' algorithm is investigated to assimilate the observed total dry matter production in SWAP model. The results with synthetic and observed total dry matter data are discussed to explore the relative merits and demerits of different assimilation methods.

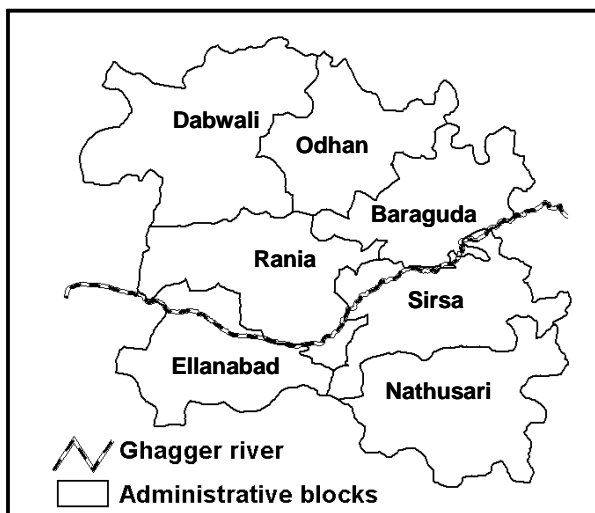
Finally, the results of this study are summarized with key conclusions and recommendations to improve regional irrigation water management and its productivity in Sirsa district. A future research outlook is given with respect to distributed modelling at regional scale.

Chapter 2

Description of Sirsa study area

2.1 Introduction

The study area, Sirsa district, is located in the extreme western corner of Haryana State, India. It covers around 4270 km², stretching between latitude 29.1⁰ to 30.0⁰ North and longitude 74 2⁰ to 75 2⁰ East, and is politically bounded by the state of Punjab in the north and northeast, and by the state of Rajasthan in the west and south. Sirsa district is further divided into seven administrative blocks: Dabwali, Odhan, Baragudha, Rania, Sirsa, Ellanabad and Nathusari (Fig. 2.1).



The current population of Sirsa district is about 1.1 million, and their main occupation is agriculture. About 90% of the total geographical area of the district is under cultivation with a mean cropping intensity of 157%.

Figure 2.1 Geographical location of Sirsa district (Haryana), India.

During the year 2000, Sirsa district occupied about 10% of the total geographical, 12% of the net irrigated, 18% of the canal irrigated and 5% of the groundwater irrigated area of Haryana (Fig. 2.2a). The average crop yields in Sirsa district are at the same level as the average crop yields in Haryana State (Fig. 2.2b).

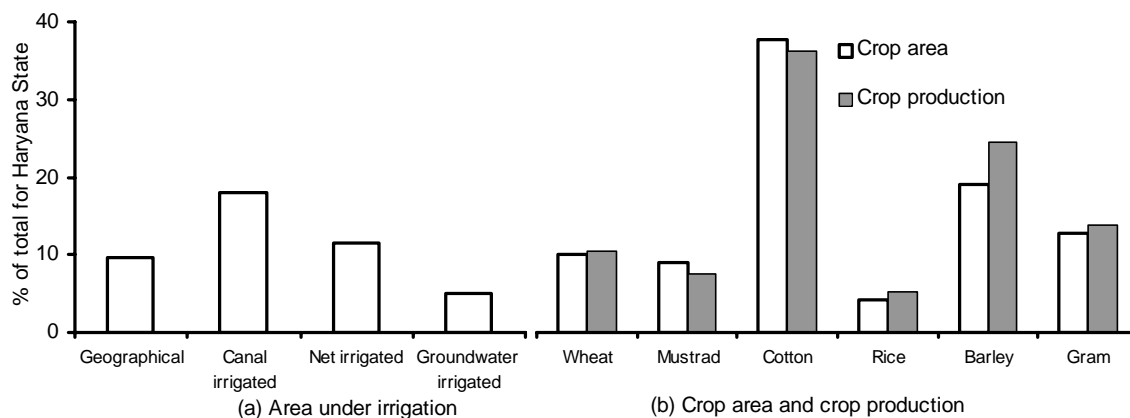


Figure 2.2 The percentage share of Sirsa district as part of Haryana agriculture sector in the year 2000. (Source: Statistical Abstract of Haryana, 2001)

The ephemeral river Ghagger flows from East to West, and drains through the central part of Sirsa district (Fig. 2.1). The absence of any perennial river in and around the district illustrates the dryness of the study area. The water management in Sirsa district, like in other arid and semi-arid regions, is of very complex nature. *The key problematic factors related to its water management are low and erratic rainfall, canal water scarcity, high evaporative demands, marginal to poor groundwater quality, rising and declining groundwater levels and sandy soils with low water holding capacity.* Beside these factors, other factors such as delay and failure of monsoon, fluctuations in canal water supply and seepage losses from the conveyance system are also limiting the crop production and water productivity in the district.

2.2 Physical environment

2.2.1 Climate

The climate of Sirsa district can be defined as sub-tropical, semi-arid and continental with monsoon. Four distinct seasons can be distinguished: cold, dry hot, monsoon (rainy) and post-monsoon season. In the cold season from December to February, the daily mean temperature varies from 5 to 21°C. The cold season is followed by a dry hot season, which lasts till the end of June. During the hottest period from May to June, mean daily maximum temperature rises up to 41-46°C. On individual days during the hottest period, it may rise up to 49°C. Hot winds with low relative humidity often cause dust storms during this season. The period from July to September constitutes the southwest monsoon (rainy) season. About 80% of the annual rainfall occurs during this season. The average annual rainfall varies from 100 to 400 mm, which is only 10 to 25% of the reference evapotranspiration (Fig. 2.3).

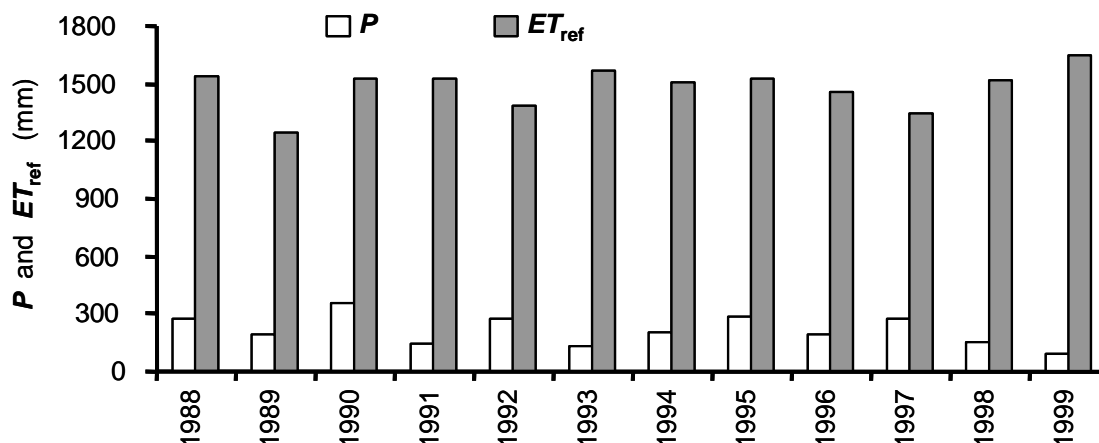


Figure 2.3 Inter-annual variation of rainfall P and reference evapotranspiration ET_{ref} in Sirsa district.

The rainfall in Sirsa district can be characterised as low and highly erratic in its occurrence and spatial distribution. It increases generally from West to East. Occasionally, heavy storms containing a large portion of the total rainfall cause temporary ponding of field crops, particularly in low-lying areas. After the withdrawal of monsoon in the end of September, temperature begins to decrease and leads to the cold season. This period from September till November is distinguished as the post-monsoon season. In summary, the climate of Sirsa district is characterized by its dryness, extremes of temperature and scanty rainfall. Crop production is very limited without irrigation, even in the monsoon (rainy) season.

2.2.2 Soil

Sirsa district is a part of Indo-Gangetic alluvial plain, which has been formed by the alluvial deposition of the Himalayan rivers into the trough between the Himalayas in the North and the Deccan plateau in the South of India. The quaternary formations comprising alluvial and aeolian plains occupy the entire district. These quaternary formations can be roughly divided into three different geomorphical units: aeolian plains, old alluvial plains and recent alluvial plains. The aeolian plains are characterised by sand dunes, and confined to the southern and the western parts of Sirsa district. The vast surface of flat and rolling old alluvial plains extends from north to south, while recent alluvial plains exist in the central parts, along the belt of Ghagger river. The plain elevations vary from 192 to 207 m above Mean Sea Level, and exhibit a small slope in the direction of northeast to southwest. The soil deposits in these plains consist of fine to medium sand, silt and clay, and are heterogeneous in character. The soil texture in the most parts of Sirsa district varies from sand to sandy loam, except a belt of silty loam to silty clay loam along Ghagger river (Fig. 2.4).

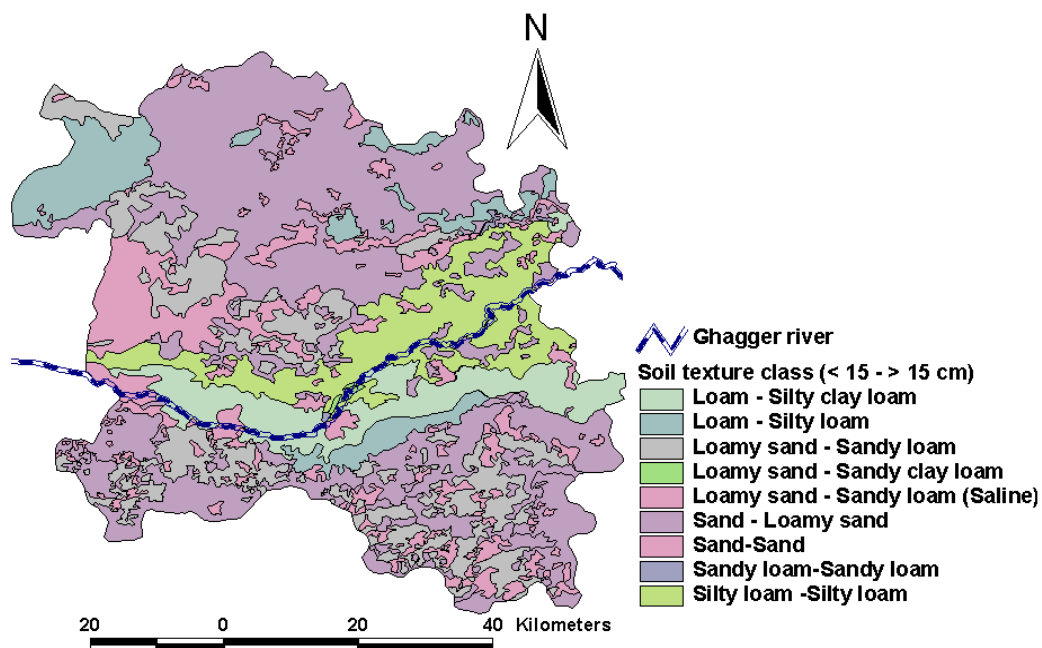


Figure 2.4 Soil map of Sirsa district (Ahuja et al., 2001) (For colour figure see cover page).

Most of the soils in the district can be characterised as deep and well drained, yellowish brown to dark yellowish brown in colour, single grained structure and loamy sand to sandy loam in texture. The low water holding capacity, high infiltration rate, low organic matter, poor fertility status, waterlogging and salinity are main issues related to the soils in Sirsa district.

2.2.3 Groundwater level and its quality

The groundwater in Sirsa district occurs under unconfined and semi-confined aquifer conditions. The major sources of its recharge are rainfall, percolation from field irrigations and seepage losses from the canal network and the Ghagger river. The groundwater level and its quality vary both in space and time. The groundwater elevation above Mean Sea Level

varies from 204 m in the eastern to 178 m in the western parts. It follows the topography of Sirsa district with a very gentle groundwater movement in the southwest direction. In June 2000, the groundwater depth varied from less than 3 m to more than 25 m below surface. The northern (Dabwali, Odhan, Baragudha) and the southern (Nathusari) blocks have experienced a rise in groundwater levels (Fig. 2.5), while groundwater levels are declining in the central (Sirsa and Rania) and the southwest (Ellanabad) blocks. The average groundwater depth below surface in Sirsa district has decreased from 18 m in 1974 to 10 m in 2000, and presents an annual groundwater rise of 0.31 m y^{-1} .

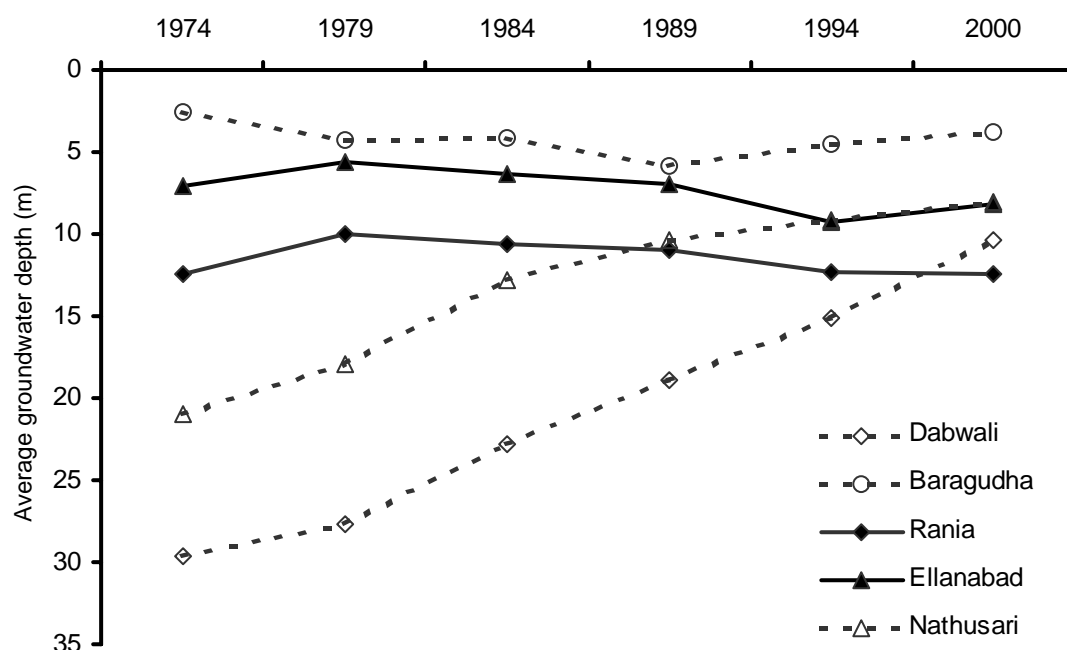


Figure 2.5 Inter-annual behaviour of groundwater depth (m, below surface) in different blocks of Sirsa district. The location of blocks is shown in Fig. 2.1. (Source: Groundwater Atlas of Sirsa district, 2002)

The groundwater quality in Haryana is classified in three categories: good ($EC_{gw} < 2 \text{ dS m}^{-1}$), marginal ($2 \text{ dS m}^{-1} < EC_{gw} < 6 \text{ dS m}^{-1}$) and poor ($EC_{gw} > 6 \text{ dS m}^{-1}$), where EC_{gw} is the electrical conductivity of groundwater. In June 2000, the groundwater quality was good in 16%, marginal in 69% and poor in 15% area of Sirsa district (Groundwater Atlas of Sirsa district, 2002).

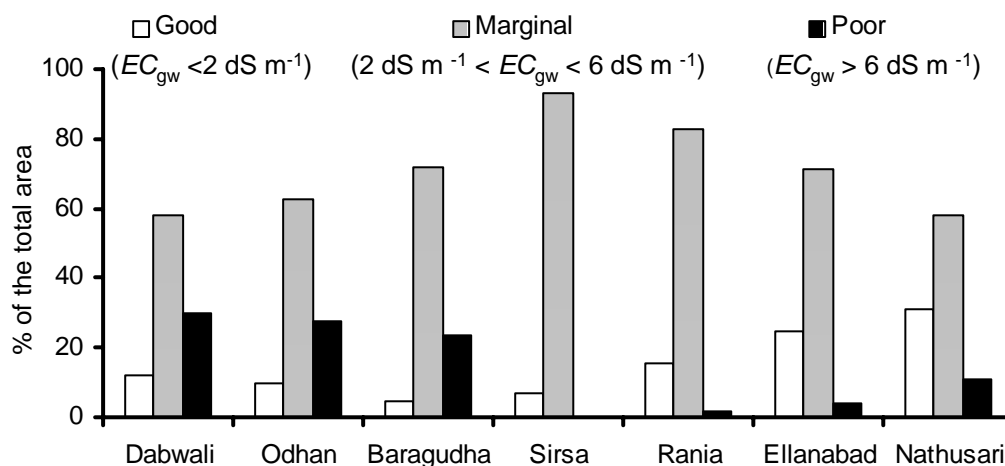


Figure 2.6 Blockwise % area under different groundwater quality zones in Sirsa district in June 2000. The location of blocks is shown in Fig. 2.1. (Source: Groundwater Atlas of Sirsa district, 2002)

The groundwater quality in the northern (Dabwali, Odhan and Baraguda) and the southern (Nathusari) blocks is poor as compared to the central (Rania and Sirsa) and the southwest (Ellanabad) blocks (Fig. 2.6). In some areas, a high amount of residual sodium carbonate ($>2.5 \text{ meq l}^{-1}$) is observed in the groundwater. Use of this groundwater requires the application of gypsum to prevent the sodification of fine-textured soils.

2.3 Irrigation water management

2.3.1 Canal water

Sirsa Irrigation Circle (SIC), located at the tail end of Bhakra Irrigation System, is an irrigation administrative unit covering the entire Sirsa district and a part of adjacent Fatehabad district. Since mid 1950's, Bhakra Irrigation System is serving the semi-arid tracts of Punjab, Haryana and a part of Rajasthan State in the northwest of India. The water supply in this system originates from Gobind Storage Reservoir located at about 400 km distance in the state of Himachal Pradesh.

Because of limited water supply, Bhakra Irrigation System was designed for an average irrigation intensity of 62% of the cultivable command area of 11700 km² (Reidinegr, 1971). To prevent crop failure, irrigation systems in Haryana were designed to serve the biggest number of farmers possible, and deliver the limited water supply over the largest area possible. The canal water distribution among farmers follows the '*principle of equity*', which means water amounts in proportion to their land holding size. To achieve this equal canal water distribution, irrigation systems are operated under the '*rostering*' and '*warabandi*' procedure. Following the '*rostering*', the limited water supply is rotated among groups of canals during a period of 24 days. Typically all canals in an irrigation system are divided into three rotational groups: A, B and C. During the first 8 days of a rotation, group A has the first priority and receives full water supply, group B has the second priority and receives reduced water supply in case of water shortage, and group C has the last priority and does not receive water unless supply to the irrigation system is sufficient. After each period of 8 days, the priority order changes, and the last priority group moves to the first priority. The distribution of water among farmers at watercourse level is based on a weekly fixed rotational system called '*warabandi*'. To ensure a uniform volumetric water distribution, water is allocated to the individual farmer for a specified period per week in proportion to his landholding in that particular watercourse. During his turn, the farmer decides the amount of water to be applied at each field. Surface flooding is the most common method of irrigation application in Sirsa district. Ease in operation and minor management problems are the main advantages of this '*rostering*' and '*warabandi*' system. The main disadvantage is its rigid water distribution in proportion to landholding size, without considering the soil type, crop water requirement and local ecohydrological conditions.

SIC has an extensive canal network resulting into about 84 canal commands varying in size from 1.98 to 41 km². It is served by three main canals: Bhakra Main Branch (BMB) in the northern, Sukchain distributary (SUK) in the central and Fatehabad Branch (FB) in the southern parts (Fig. 2.7). Tails of these canals supply water to the adjoining state of Rajasthan. During the monsoon period, water from the ephemeral river Ghagger is partly diverted to canals for irrigation in the central and the southwest parts of Sirsa district.

In case of low discharges in the river (non-monsoon period), this area is fed by the Otu feeder canal, which receives supply from Bhakra Main Branch. A recently constructed dam, 'Otu weir' on Ghagger river near Sirsa town, is expected to increase the amount and reliability of irrigation water from the river.

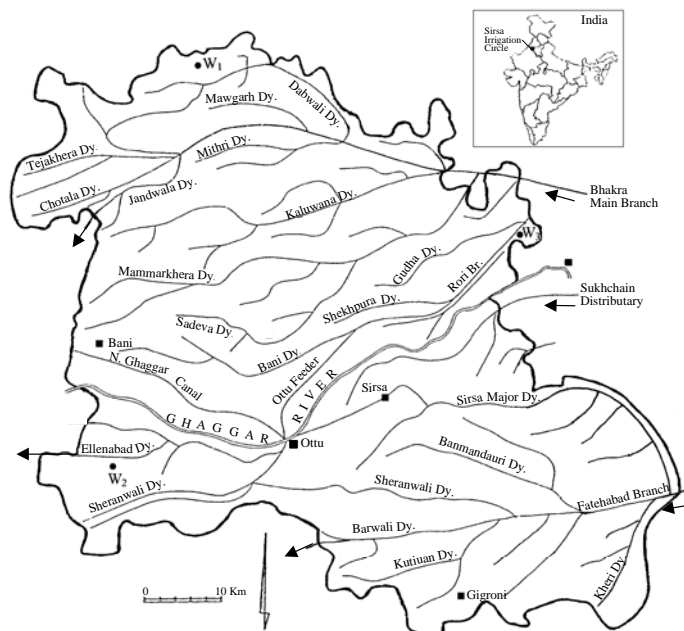


Figure 2.7 Location of Sirsa Irrigation Circle showing the canal network in the study area.

The total annual volumetric intake of SIC including deliveries to the state of Rajasthan generally exceeds 2000 million m³. About 2850 km² in Sirsa district corresponding to 80% of its net irrigated area receives the canal water supply. The average canal water delivery of 1.5 mm d⁻¹ is only 1/3 of the average reference evapotranspiration of 4.7 mm d⁻¹ (Bastiaanssen et al., 1999).

The limited canal water supply is further reduced by the seepage losses in main canals, distributaries and watercourses. The measured discharge values revealed a significant seepage loss of about 33% for lined and 48% for unlined watercourses (Table 2.1). Most of the canals and watercourses in Sirsa district are lined, while the field channels that distribute canal water among fields are still unlined.

Table 2.1 Measured discharges in head, middle and tail reaches of watercourses in Sirsa district (Tyagi, 1996).

Distributaries	Watercourse name	Lined/unlined	Location	Discharge (l s ⁻¹)
Kutiana	780L	Lined	Head	39.5
			Middle	32.7
			Tail	26.4
Sheronwali	2000R	Unlined	Head	30.5
			Middle	20.7
			Tail	15.8

2.3.2 Groundwater use

The limited canal water supply in Sirsa district is supplemented by the groundwater use. The groundwater pumping is implemented in two ways: by deep direct augmentation tubewells and by shallow tubewells. The Haryana State Government operates the deep direct augmentation tubewells, which supply water to the canals. The major portion of the groundwater use takes place through the shallow tubewells operated by individual farmers at their own fields. The appropriate depth of shallow and deep tubewells varies from 20 to 80 m, and discharge ranges from 6 to 18 l s⁻¹ (Groundwater Atlas of Sirsa district, 2002).

The groundwater quality is a major factor for the extent of groundwater use in a region. The Haryana State Government agency, Haryana State Minor Irrigation and Tubewells Corporation (*HSMITC*), prepared a groundwater quality map of Haryana in the year 2001. According to this map, the deep groundwater quality in Sirsa district was poor in 64% of the total area, while the shallow groundwater quality was poor in 8% of the total area only. These figures indicate that a relatively better quality shallow groundwater layer has developed over the deep poor quality groundwater layer. Over the years, percolation and seepage losses of good quality canal water might be contributing to this build-up of a good quality shallow groundwater layer in Sirsa district. For instance, the good quality groundwater in the central parts is mainly due to the seepage from Ghagger river, especially during the monsoon season. This development has stimulated the farmers in this region to install shallow tubewells for irrigation. The total number of tubewells in Sirsa district, therefore, has increased from 8217 in the year 1976 to 32000 in the year 2000. This increase in number of tubewells is concentrated in good quality groundwater areas: Rania, Ellanabad and Sirsa blocks (Fig. 2.8a). The high tubewell density, defined as number of tubewells / km², and the decline in groundwater levels in these blocks (Fig 2.5) indicate the high exploitation of groundwater in the central and southwestern parts of Sirsa district. On the other side, poor quality groundwater in the northern and southeastern parts restricts the groundwater use. This is reflected by the rising groundwater levels (Fig. 2.5) and low tubewell density (Fig. 2.8a) in the northern and southeastern blocks: Dabwali, Odhan, Baragudha and Nathusari.

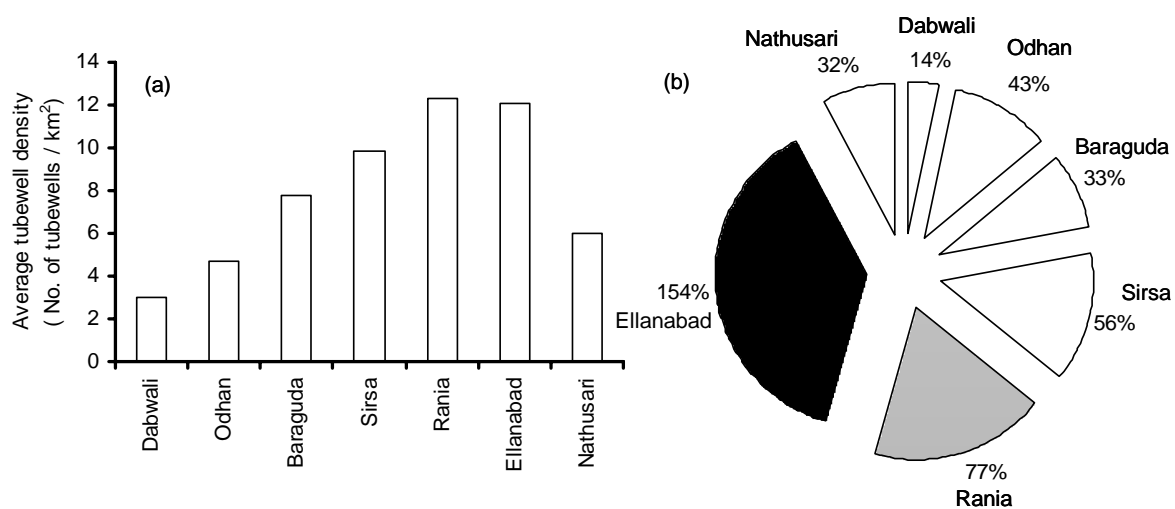


Figure 2.8 Groundwater use in different blocks of Sirsa district in the year 2000: (a) average tubewell density, defined as number of tubewells/km² (Source: District Statistical Abstract, 2001), and (b) groundwater development, defined by the groundwater extraction as % of the total annual groundwater recharge. (Source: Groundwater Atlas of Sirsa district, 2002). The location of blocks is shown in Fig. 2.1.

The extent of groundwater use also can be expressed in so-called groundwater development categories. Each category is defined by the groundwater extraction as % of the total annual groundwater recharge. In India, three major categories are distinguished: White (< 65%), Grey (65 to 85%) and Dark (>85%). The level of groundwater development in Sirsa district varies from 14% in Dabwali block to more than 154% in Ellanabad block (Fig. 2.8b). The high groundwater development in Ellanabad (dark) followed by Rania (grey) block suggests either to decrease the groundwater pumping or increase the groundwater recharge in the central and southwestern parts of Sirsa district. On the other side, the northern (Dabwali, Odhan and Baragudha) and southeastern (Nathusari) parts need more attention to halt a rise in groundwater levels, which presents a threat of waterlogging and salinization. Already about 5% of the district, mainly in the northeast (Baragudha) parts, had a critical groundwater level (< 3 m) in June 2000.

2.4 Cropping pattern and yields

The climatic conditions in Sirsa district allow two crops per year: *rabi* (winter) crop and *kharif* (summer) crop. The cropping system can be classified into the rain-based and the irrigation-based cropping system. The rain-based cropping system consists of the low yielding but less water demanding crops such as *gram* (chickpea) and *bajra* (pearl millet). These crops can be grown with the low rainfall amounts received in the study area. The irrigation-based cropping system consists of the high yielding but more water demanding crops such as wheat, rice and cotton. Successful production of these crops without supplemental irrigation is hardly possible even in the monsoon season. The total irrigation requirements vary from 35 to 40 cm for wheat, from 40 to 50 cm for cotton and from 120 to 150 cm for rice (Singh and Sharma, 1993; Sharma, 1995).

In response to the ‘Green Revolution’ strategies for increasing food grain production in Northern India, the irrigation development in Sirsa district during the last 25 years has resulted in the cultivation of wheat, rice and cotton as major crops replacing *gram* and *bajra* (Fig 2.9). From the year 1975 to 2001, the area under rice has increased with more than 200%, wheat with 190% and cotton with 170%. On the other side, the area under *gram* and *bajra* has decreased with 95%. In the year 2000-01, the area under the rain-based cropping system was only 80 km² for *gram* and 30 km² for *bajra*.

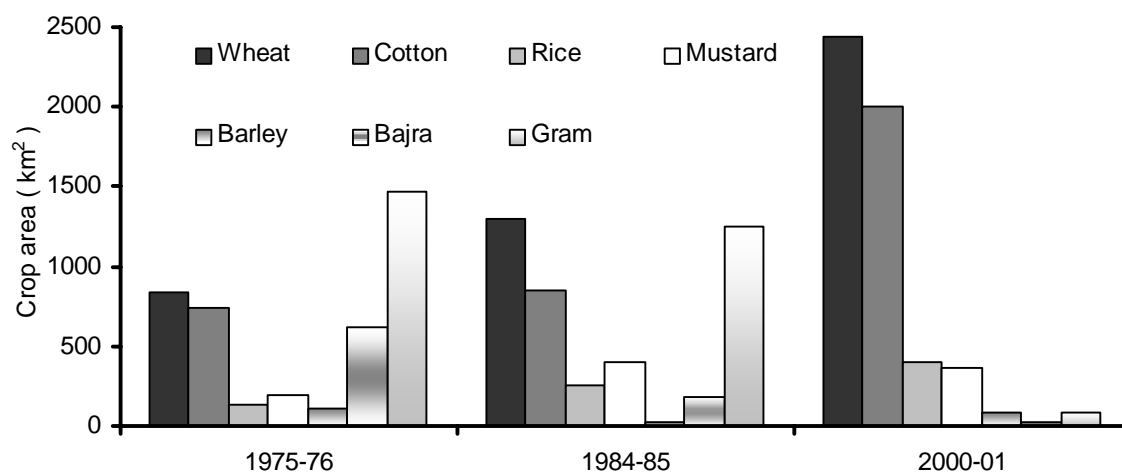


Figure 2.9 Change in cropping pattern in Sirsa district over the period from 1975 to 2001. (Source: <http://sirsa.nic.in/htfiles/25agriculture.html>)

Wheat and mustard (oilseed) are the main crops during the *rabi* (winter) season, which are followed by cotton and rice during the *kharif* (summer) season. Wheat-cotton is the dominant crop combination. Intensive irrigation coupled with high yielding varieties, increased use of fertilizer and weedicides over the years has increased the crop yields, especially for wheat and rice (Fig. 2.10). For instance, the average wheat grain yield of 4.3 ton ha⁻¹ in the year 2000 has been doubled since 1975. The average crop yields (ton ha⁻¹) during the year 2000 were recorded at 4.3 for wheat, 1.1 for mustard (oilseed), 0.4 for cotton (lint) and 3.0 for rice (Source: Department of Agriculture, Sirsa). However, current increase in crop yields is either marginal or reversed, especially in case of rice.

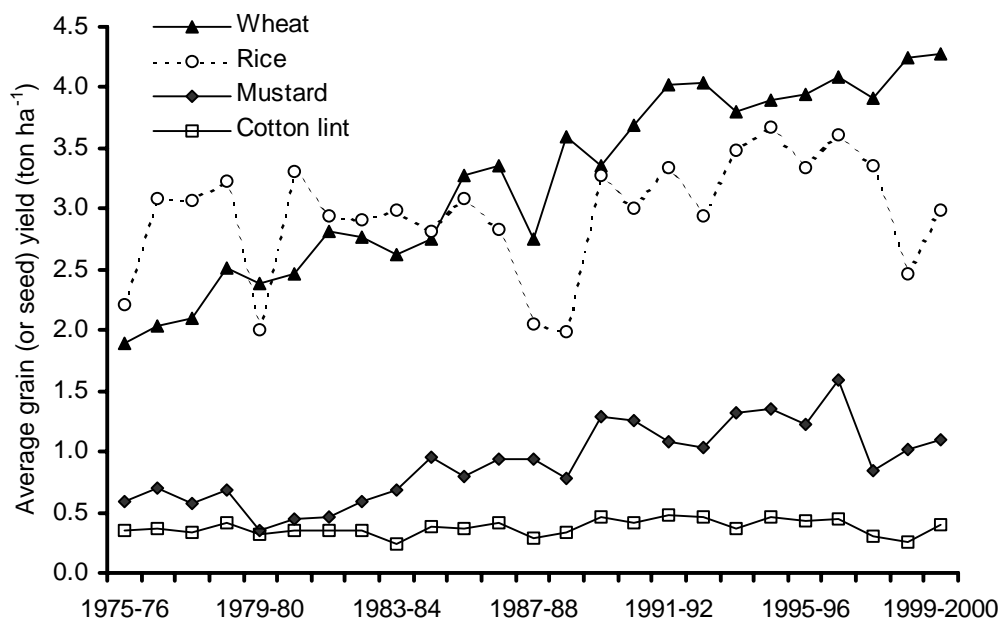


Figure 2.10 Average grain (or seed) yield of the main crops in Sirsa district over the period from 1975 to 2000. (Source: Department of Agriculture, Sirsa)

Chapter 3

Framework for regional water productivity analysis

3.1 Introduction

In order to improve water management and its productivity, we need to reveal the cause-effect relationships between hydrological variables such as soil evaporation, transpiration, percolation or capillary rise, and biophysical variables such as dry matter and grain yields under different ecohydrological conditions. Spatial-temporal quantification of these required variables is a challenge, especially at regional scale. The problems, often encountered are:

- i) limited availability of ecohydrological information,
- ii) field experiments are expensive, laborious and time consuming,
- iii) measurements of evapotranspiration and its partitioning into soil evaporation and crop transpiration under partial soil cover, and of percolation are rather difficult,
- iv) tools are absent to make a detailed hydrological analysis, especially at regional scale.

In this context, scientists and researchers have devoted much effort to develop system simulation models to quantify the required hydrological and biophysical variables at the appropriate scale. Fundamental in the modelling approach is an appropriate physical description of various hydrological, chemical and biological processes occurring in the natural system. In this system simulation approach related to water management, a system can be defined as a plant, as the local soil-water-atmosphere-plant continuum and more complex as regional domains e.g. an irrigation system. The dominant processes in the defined system are extracted and put into an interactive framework to simulate the water and salt balances. Assuming homogeneous system characteristics, the physical description of hydrological, chemical and biological processes is attractive at field scale, and results into one-dimensional field scale models like ecohydrological SWAP model.

Complexity increases when moving to the regional scale, where heterogeneity must be considered. *The one-dimensional structure and inherent spatial limitation of field scale models are major constraints to describe directly the spatial heterogeneity encountered at regional scale.* The limited ecohydrological information available at non-measured fields further hampers the application of field scale models at regional scale.

Increasing use of remote sensing and development of sophisticated computational tools such as GIS are providing new opportunities to increase the capabilities of field scale models to describe the hydrological and biophysical processes at regional scale (Droogers et al, 2000; Droogers and Kite, 2002). In this chapter, a distributed modelling approach integrating the operational knowledge of crop growth, soil water flow and salt transport modelling with field experiments, remote sensing and GIS is proposed to describe the hydrological and biophysical processes, and subsequently to analyze water productivity from field to regional scale.

3.2 Schematisation of framework for regional water productivity analysis

The main hypothesis postulated in this framework is that an ensemble of individually homogeneous regions can equivalently represent a spatially heterogeneous region. It is further postulated that the effects of spatial heterogeneity on the regional water and salt balances, and on the water productivity can be analyzed by running a field scale model for all combinations of *weather-crop-soil-water* in the study area. This hypothesis can be made only in areas without significant runoff and with deep groundwater levels.

The application of field scale model in such a distributed mode, therefore, requires the derivation of all combinations of *weather-crop-soil-water* at regional scale. These combinations are hereafter referred to as ‘simulation units’ (SU). The aggregation of simulation units, termed as ‘stratification’, is performed in a GIS environment by overlaying the thematic maps of different spatial variables such as weather, land use, soil, irrigation, groundwater level and its quality in the study area. Spatial variables such as land use can be derived by remote sensing techniques with a high accuracy of 80 to 90% (Bastiaanssen and Bos, 1999).

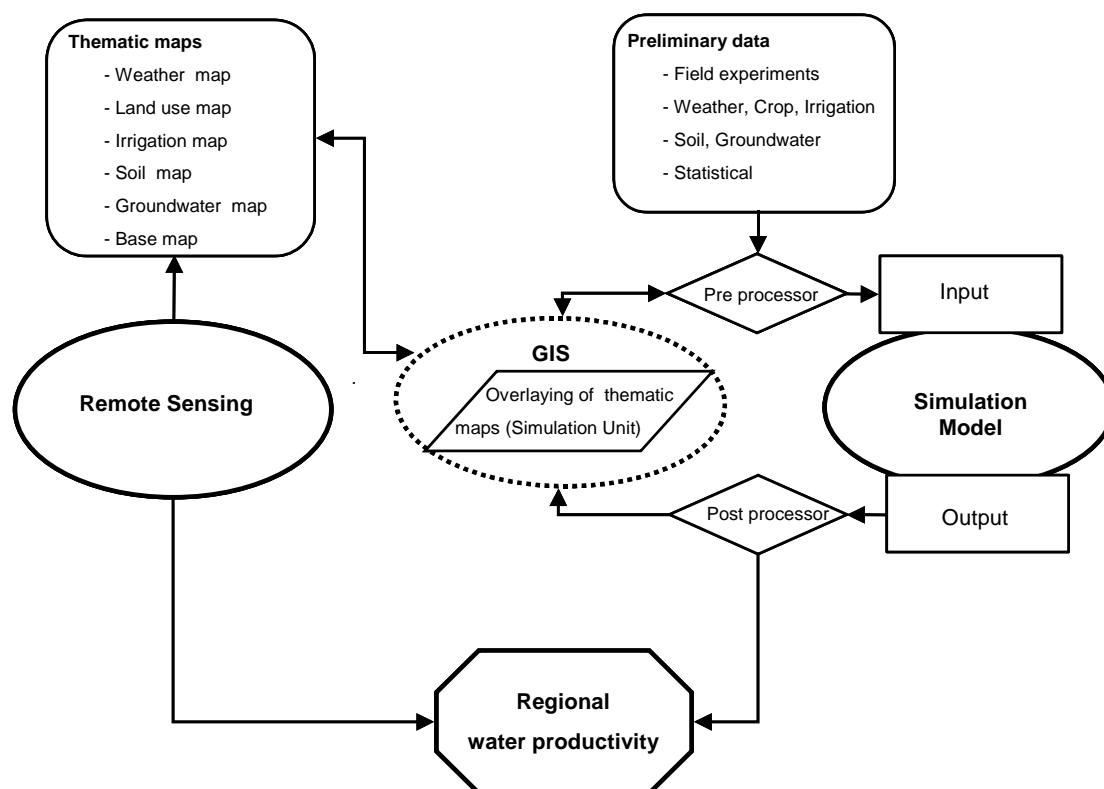


Figure 3.1 Schematisation of framework for regional water productivity analysis.

The model input parameters attached to the simulation units are preprocessed using the information derived from experimental stations, farmer fields, satellite images and existing geographical data. Subsequently, independent runs of a field scale model simulate the water and salt balances and crop yields for each simulation unit. The outputs of independent model runs are finally synthesized with the help of post-processors and GIS to analyze water productivity at regional scale.

In this study, a field scale ecohydrological SWAP model is used in a distributed mode to simulate the spatial water and salt balances and crop yields, and subsequently to analyze water productivity from field to regional scale. For linking of SWAP, remote sensing and GIS, we adopted a loose coupling approach, which involves transfer of data from one system to another. The term ‘loose coupling’ allows the use of different existing models and tools using appropriate pre- and post-processors.

3.3 Soil-Water-Atmosphere-Plant (SWAP) Model

The Soil-Water-Atmosphere-Plant (SWAP) is an ecohydrological model based on the deterministic and physical laws for essential hydrological, chemical and biological processes occurring in the soil-water-plant-atmosphere continuum. Assuming the main flow process in vertical direction, SWAP simulates the vertical soil water flow and salt transport in close interaction with the crop growth (Fig. 3.2).

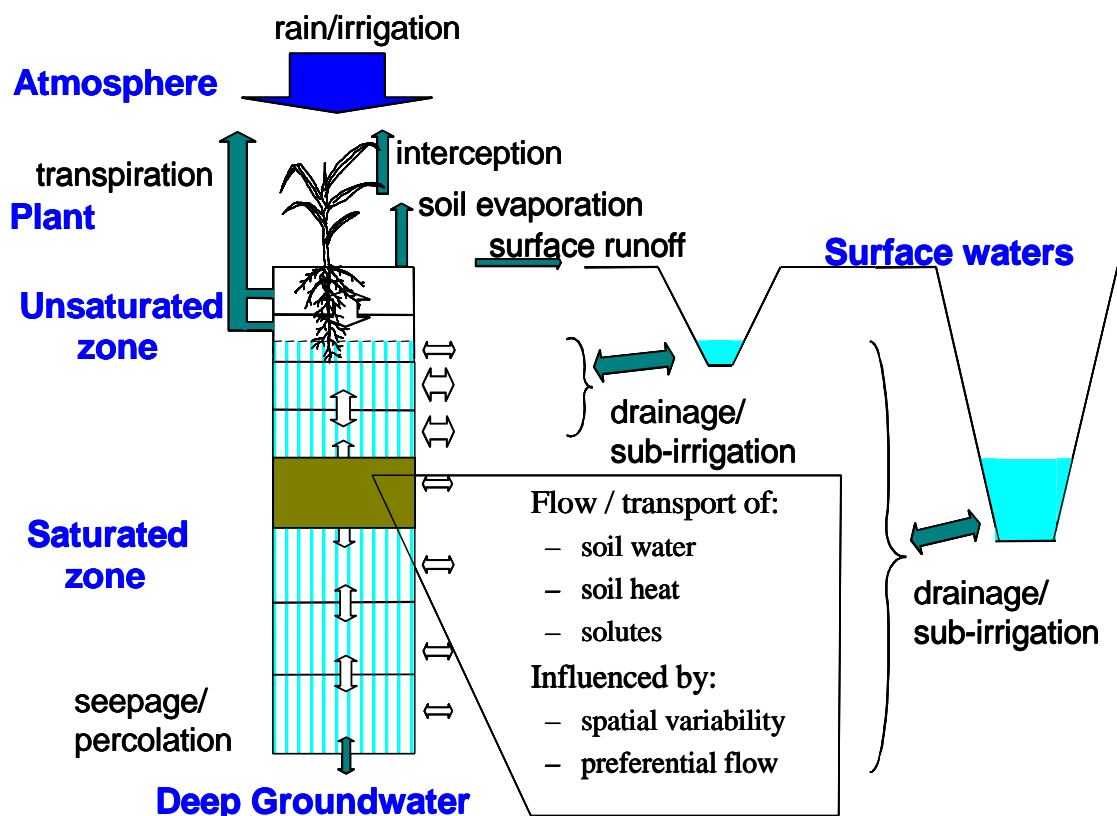


Figure 3.2 Schematisation of hydrological process involved in SWAP (Van Dam, 1997).

Crop growth

SWAP includes both a simple and detailed crop growth module. *The simple crop module prescribes the crop growth according to the measured crop growth during field experiments.* In this module, the measured leaf area index, crop height and rooting depth are prescribed as a function of crop development stage, which is either controlled by the temperature sum or linear in time. These measured data are sufficient to determine the rainfall interception, potential soil evaporation and crop transpiration at upper boundary for a specific situation. When the simple crop module is used, the effect of water and salt stress on crop production in

semi-arid and arid regions might be quantified using a simplified linear relationship between relative yield Y/Y_p and relative transpiration T/T_p (De Wit, 1958; Hanks, 1974, 1983; Stewart et al., 1977; Feddes, 1985):

$$\frac{Y}{Y_p} = \frac{T}{T_p} \quad (3.1)$$

where Y and Y_p are the actual and potential crop yields [$M L^{-2}$], and T and T_p are the actual and potential transpiration [L].

The simple crop module does not simulate any interaction between the crop growth and the water and salt stress conditions. Therefore, it has disadvantage for situations that have a different water and salt stress than in the situation for which crop growth was measured. In actual field conditions, the spatial variability in terms of soil, salinity and irrigation affects the physiological growth of crops.

The detailed generic crop growth model *World Food Studies (WOFOST)* has the advantage of a feedback between the crop growth and the water and salt stress conditions. Recently, WOFOST has been implemented in SWAP for simulation of crop growth in close interaction with the dynamics of soil water movement. Fig. 3.3 shows the main processes incorporated in WOFOST.

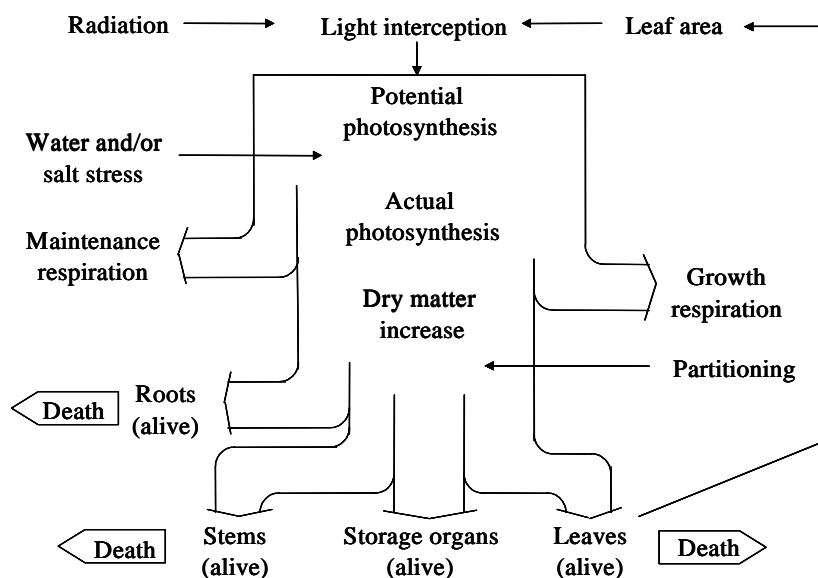


Figure 3.3 Schematisation of crop growth process involved in WOFOST (Spitters et al., 1989; Supit et al., 1994).

The potential production of a crop depends on the solar radiation, air temperature and plant characteristics (Fig. 3.4). About 50% of the incoming total solar radiation (wavelength 300-3000 nm) is photo-synthetically active radiation (*PAR*) (wavelength 400-700 nm), which is used by plants for photosynthesis. The potential production is the maximum level of crop production, which can be achieved only under optimal conditions i.e. ample supply of water and nutrients, and absence of any pest, weed and disease. WOFOST simulates the potential

gross CO₂ assimilation rate of a crop based on the incoming *PAR* absorbed by the crop canopy, and on the photosynthetic leaf characteristics. This potential gross CO₂ assimilation rate is reduced to the water and salt limited gross CO₂ assimilation rate due to the water and salt stress in field conditions (Fig. 3.4). The ratio of actual and potential transpiration T/T_p is used to quantify the effect of water and salt stress on crop production.

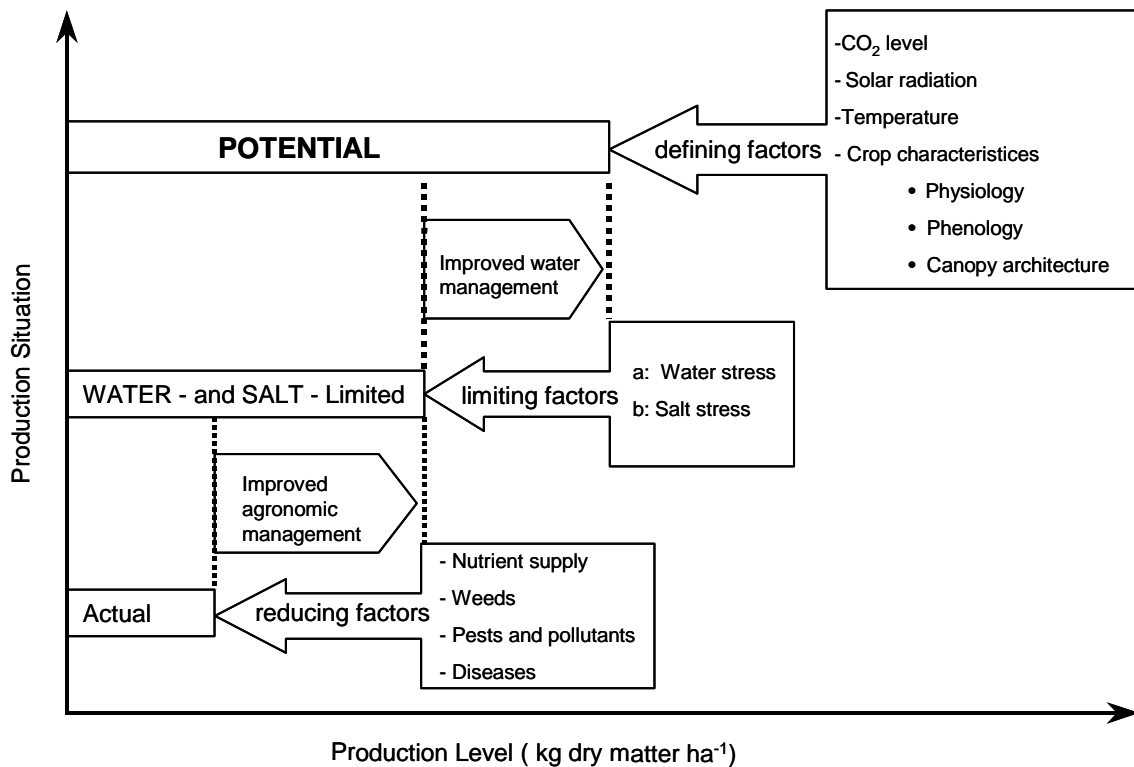


Figure 3.4 Production hierarchy in the crop production system (Adapted after Lövenstein et al., 1995).

The produced water and salt limited assimilates provide energy for the maintenance and growth respiration for plant organs, and increase the dry matter of crop. The amount of dry matter produced is partitioned among roots, leaves, stems and storage organs. This partitioning is a function of crop development stage. The increased leaf dry matter determines the leaf area development, and hence the amount of light interception for photosynthesis, except for the initial stage. During the initial stage, the rate of leaf appearance and final leaf size are constrained by temperature, rather than by the supply of assimilates. The dry weights of plant organs are obtained by integrating their growth and death rates over time. Leaf senescence occurs due to water stress, shading (high leaf area index), and also due to life span exceedance. The death rates of plant organs are crop specific, and are defined as a daily fraction of living biomass. It is defined zero for the storage organs. The death rates are also considered as a function of crop development stage.

The crop development rate before anthesis is controlled by the day length and / or temperature, while temperature is considered to affect the development rate after anthesis. The ratio of accumulated daily effective temperature after emergence divided by temperature sum from emergence to anthesis, determines the crop development stage. The details of the light

interception and CO₂ assimilation as growth driving processes and the crop phenological development as growth controlling process included in WOFOST are described in Spitters et al. (1989) and Supit et al. (1994).

In addition to the water and salt stress, nutrient supply, weeds, pest and disease may affect the crop production in actual field conditions. This reduces the water and salt limited production further to the actual production (Fig. 3.4). *The effects of nutrient supply, weeds, pest and disease on crop growth and its production are not implemented in the present version of WOFOST.*

The above described both simple and detailed crop growth simulation approaches are included in the present version SWAP 3.03 model (Kroes and Van Dam, 2003). To distinguish the simulations in this study, SWAP 3.03 when used with the simple crop growth module is called *SWAP* hereafter, and when used with the detailed crop growth module is called *SWAP-WOFOST*.

Soil water flow

The Richards' equation (Richards, 1931) is applied to compute transient soil water flow:

$$C(h) \frac{\partial h}{\partial t} = \frac{\partial}{\partial z} \left[K(h) \left(\frac{\partial h}{\partial z} + 1 \right) \right] - S_a(z) \quad (3.2)$$

where C is the differential soil water capacity [L⁻¹], h is the soil water pressure head [L], K is the hydraulic conductivity [L T⁻¹], S_a is the root water extraction rate [T⁻¹], and z is the vertical coordinate [L] (positive upward).

SWAP solves the Richards' equation numerically using an implicit finite difference scheme as described by Van Dam and Feddes (2000). The numerical solution of Eq. 3.2 is subjected to specified initial and boundary conditions, and requires known relationships between soil hydraulic variables: moisture θ , pressure head h and hydraulic conductivity K . The following relations between these variables has been used (Van Genuchten, 1980; Mualem, 1976):

$$\theta(h) = \theta_{\text{res}} + \frac{\theta_{\text{sat}} - \theta_{\text{res}}}{\left[1 + |\alpha h|^n \right]^{\frac{n-1}{n}}} \quad (3.3)$$

$$K(\theta) = K_{\text{sat}} S_e^\lambda \left[1 - \left(1 - S_e^{n/n-1} \right)^{\frac{n-1}{n}} \right]^2 \quad (3.4)$$

where θ_{res} is the residual water content [L³ L⁻³], θ_{sat} is the saturated water content [L³ L⁻³], $S_e = (\theta - \theta_{\text{res}}) / (\theta_{\text{sat}} - \theta_{\text{res}})$ is the relative saturation [-], α is the empirical shape factor [L⁻¹], n is the empirical shape factor [-], K_{sat} is the saturated hydraulic conductivity [L T⁻¹], and λ is an empirical coefficient [-].

The upper boundary condition is determined by the potential evapotranspiration rate ET_p , and irrigation I and rainfall P fluxes. The ET_p [$L T^{-1}$] is estimated by the Penman-Monteith equation (Monteith, 1965, 1981; Smith, 1992; Allen et al., 1998):

$$ET_p = \frac{\frac{\Delta_v}{\lambda_w}(R_n - G) + \frac{p_1 \rho_{air} C_{air}}{\lambda_w} \frac{e_{sat} - e_a}{r_{air}}}{\Delta_v + \gamma_{air} \left(1 + \frac{r_{crop}}{r_{air}}\right)} \quad (3.5)$$

where Δ_v is the slope of the vapour pressure curve [-], λ_w is the latent heat of vaporization [$L^2 T^{-2}$], R_n is the net radiation flux density [$M T^{-3}$] above the canopy, G is the soil heat flux density [$M T^{-3}$], p_1 accounts for unit conversion ($= 86400 \text{ s d}^{-1}$), ρ_{air} is the air density [$M T^{-3}$], C_{air} is the heat capacity of moist air [$L T^{-1} \Theta^{-1}$], e_{sat} is the saturation vapour pressure [$M L^{-1} T^{-2}$], e_a is the actual vapour pressure [$M L^{-1} T^{-2}$], r_{air} is the aerodynamic resistance [$L^{-1} T$], γ_{air} is the psychrometric constant [$M L^{-1} T^{-2} \Theta^{-1}$], and r_{crop} is the crop resistance [$L^{-1} T$]. In order to solve Eq 3.5, daily weather data of solar radiation, air humidity, wind speed and air temperature are required. In addition, crop characteristics such as minimum resistance, reflectance (albedo) and crop height are needed (Allen et al., 1998).

Under field conditions where crops partly cover the soil, ET_p is partitioned into potential soil evaporation rate E_p [$L T^{-1}$] and potential transpiration rate T_p [$L T^{-1}$]. This partitioning is achieved through the leaf area index LAI [-] as a function of crop development stage (Goudriaan, 1977; Belmans, 1983):

$$E_p = ET_p e^{-K_{gr} LAI} \quad (3.6)$$

where K_{gr} is the extinction coefficient for global solar radiation [-].

Under wet soil conditions, actual soil evaporation rate E [$L T^{-1}$] is governed by the atmospheric demand, and equals E_p . Under dry soils conditions, E is governed by the maximum soil water flux E_{max} [$L T^{-1}$] in top soils, which can be quantified by Darcy's law as:

$$E_{max} = K_{1/2} \left(\frac{h_{atm} - h_1 - z_1}{z_1} \right) \quad (3.7)$$

where $K_{1/2}$ is the mean hydraulic conductivity [$L T^{-1}$] between the soil surface and first node, h_{atm} is the soil water pressure head [L] in equilibrium with the air humidity, h_1 is the soil water pressure head [L] of first node, and z_1 is the soil depth [L] of first node.

Due to splashing rain, dry crust formation, root extension, wind erosion and various cultivation practices, the validity of soil hydraulic parameters of top few soil centimetres by parameters of ordinary soil columns is still not clear. Consequently, the Darcy's law may overestimate the actual soil evaporation flux (Van Dam, 2000). In addition to Eq. 3.7, SWAP computes the soil evaporation rate using empirical functions E_{emp} , and determines the actual evaporation rate E by taking the minimum value of E_p , E_{max} and E_{emp} . For this study, we used the empirical function of Black et al. (1969) to limit the soil evaporation rate.

The potential transpiration rate T_p [$L T^{-1}$] follows from the balance:

$$T_p = \left(1 - \frac{P_i}{ET_{p0}}\right) ET_p - E_p \quad \text{with} \quad T_p \geq 0 \quad (3.8)$$

where P_i is the rainfall intercepted [$L T^{-1}$] by vegetation, and ET_{p0} is the potential evapotranspiration [$L T^{-1}$] of a wet crop, which can be estimated by the Penman-Monteith equation (Eq. 3.5) assuming zero crop resistance. The ratio P_i/ET_{p0} denotes the day fraction during which interception water evaporates and transpiration is negligible.

The actual transpiration rate is governed by the root water extraction rate of a crop, which depends upon the rooting depth and its distribution, and actual soil water pressure heads in the root zone. For practical reasons, we adopted a homogeneous root distribution over the rooting depth. The maximum root water extraction rate $S_{\max}(z)$ [T^{-1}] is then calculated by distributing the T_p over the rooting depth:

$$S_{\max}(z) = \frac{T_p}{z_{\text{root}}} \quad (3.9)$$

where z_{root} is the rooting depth [L].

Under non-optimal conditions either too dry, too wet or too saline, $S_{\max}(z)$ will be reduced to the actual root water extraction rate. To account for water stress, Feddes et al. (1978) proposed a water stress reduction function as depicted in Fig. 3.5a. The critical pressure head h_3 for too dry conditions depends on the T_p . The values of input variables h_1 , h_2 , h_{3h} , h_{3l} and h_4 [L] are assumed crop specific, and can be found in literature (Taylor and Ashcroft, 1972; Doorenbos and Kassam, 1979; Wesseling et al., 1991; Smith, 1992).

In case of salt stress, the reduction in crop yields may be linearly related to the soil water electrical conductivity EC (Maas and Hoffman, 1977). Assuming a one to one relationship between the relative yield Y/Y_p and relative transpiration T/T_p , they proposed a salt stress reduction function as depicted in Fig. 3.5b.

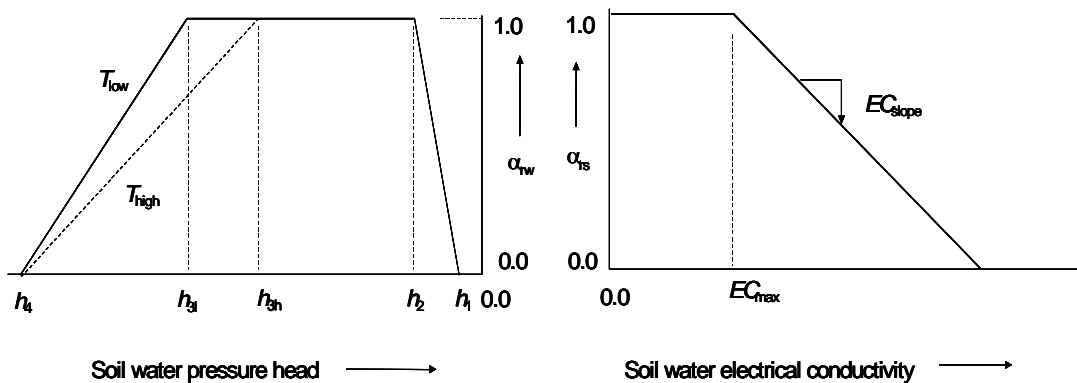


Figure 3.5a Reduction coefficient α_w as function of soil water pressure head h and potential transpiration rate T_p (Feddes et al., 1978).

Figure 3.5b Reduction coefficient α_{ts} as function of soil water electrical conductivity EC (Mass and Hoffman, 1977).

In line with recommendations of Cardon and Letey (1992), SWAP calculates the actual root water extraction rate $S_a(z)$ [T^{-1}] as the product of both the water and salt stress:

$$S_a(z) = \alpha_{rw} \alpha_{rs} S_{max}(z) \quad (3.10)$$

where α_{rw} is the reduction coefficient for water stress [-], and α_{rs} for salt stress [-]. Finally, the actual transpiration rate T [$L T^{-1}$] follows from the integration of $S_a(z)$ over the rooting depth.

The lower boundary condition is defined by the fluxes at the bottom of soil profile. In case of groundwater levels more than 3 m below surface (deep groundwater conditions), we applied the free drainage condition to calculate the bottom flux q_{bot} [$L T^{-1}$]:

$$q_{bot} = -K(h) \left(\frac{\partial h}{\partial z} + 1 \right) = -K(h)(0+1) = -K(h) \quad (3.11)$$

In case of groundwater levels less than 3 m below surface (shallow groundwater conditions), we may assume the presence of a semi-confined layer in the soil profile, and subsequently apply the Cauchy condition to calculate the bottom flux q_{bot} from a given hydraulic head of a deep aquifer.

$$q_{bot} = \frac{\phi_{aquif} - \phi_{gwl}}{c_{conf}} \quad (3.12)$$

where ϕ_{aquif} is the hydraulic head [L] in the semi-confined layer, ϕ_{gwl} is the groundwater level [L], and c_{conf} is the vertical resistance [T] of the semi-confined layer.

Salt transport

The movement of salts in a soil profile is mainly governed by convection, diffusion and dispersion. The diffusion process under irrigated field conditions is much slower than the dispersion process, and is neglected in this study. Under laminar flux conditions, the dispersion flux density is proportional to the salt concentration gradient and water flux density (Bear, 1972). The total salt flux J [$M L^{-2} T^{-1}$], therefore, is described as:

$$J = qC + qL_{dis} \frac{\partial C}{\partial z} \quad (3.13)$$

where q is the water flux density [$L T^{-1}$], C is the salt concentration [$M L^{-3}$], and L_{dis} is the dispersion length [L].

The principle of salt mass conservation gives for an elementary soil volume:

$$\frac{\partial \theta C}{\partial t} = - \frac{\partial J}{\partial z} \quad (3.14)$$

In Eq. 3.14, the decomposition and root uptake of salts are also neglected. Combination of Eq. 3.13 and 3.14 results in the much applied convection-dispersion equation:

$$\frac{\partial \theta C}{\partial t} = \frac{\partial}{\partial z} \left[q L_{\text{dis}} \frac{\partial C}{\partial z} \right] - \frac{\partial q C}{\partial z} \quad (3.15)$$

Eq. 3.15 is valid for dynamic, one-dimensional, convective-dispersive salt transport, and permits the simulation of root water uptake reduction due to salt stress in unsaturated / saturated soils (Van Genuchten and Cleary, 1979; Boesten and Van der Linden, 1991). SWAP solves this equation numerically using specified initial salt concentrations and concentrations in the irrigation and groundwater.

Water and salt balance

The water balance of a vertical soil column with vegetation *integrated over a certain period* can be written as:

$$\Delta W = P + I - SR - P_i - T - E - E_w + Q_{\text{bot}} \quad (3.16)$$

where ΔW is the change in soil water storage [L], P is the rainfall [L], I is the irrigation [L], SR is the surface runoff [L], P_i is the rainfall interception [L] by vegetation, T is the actual transpiration [L], E is the actual soil evaporation [L], E_w is the evaporation of ponding water [L], and Q_{bot} is the water percolation [L] at the soil column bottom (positive upward).

The salt balance of the soil column over that time interval also can be written as:

$$\Delta C = P C_p + I C_i + Q_{\text{bot}} C_{\text{bot}} \quad (3.17)$$

where ΔC is the change in salt storage [$M L^{-2}$], C is the solute concentration [$M L^{-3}$], and subscript 'p' refers to rainfall, 'i' to irrigation, and 'bot' to bottom flux.

3.4 Calculation and aggregation of water productivity

In agricultural production systems, the definition of water productivity accounts for 'crop production' per unit 'amount of water used' (Molden, 1997; Molden et al., 2001). The actual transpiration represents the lower limit of water used by the crop. Therefore, water productivity is expressed in terms of crop grain (or seed) yield Y_g per unit amount of transpiration T :

$$WP_T = \frac{Y_g \text{ (kg m}^{-2}\text{)}}{T \text{ (m}^3 \text{ m}^{-2}\text{)}} = \frac{Y_g}{T} \text{ (kg m}^{-3}\text{)} \quad (3.18)$$

WP_T depends on the crop type e.g. C3 or C4 and its variety, and indicates the physiological performance of a certain crop. The dry matter production and transpiration rate of a crop are related to the diffusion rates of CO_2 and H_2O molecules at stomatal aperture of leaves. Since under a fixed set of environmental conditions, the diffusion rates of CO_2 and H_2O molecules vary proportionally to the size of stomatal aperture of a certain crop, the ratio of these rates remains constant. For such conditions, WP_T for a certain crop is expected to remain constant (Leffelaar et al., 2003). However, continuously changing environmental conditions in terms of the CO_2 concentration in air, radiation, temperature and vapour pressure result in varying evaporative demands, and subsequently the transpiration rate vary at a given stomatal aperture.

As a result, WP_T for a certain crop shows a considerable variation depending on the ecohydrological conditions of a region. For instance under extreme conditions such as high radiation levels in arid and semi-arid regions, the CO_2 assimilation by crops may become light saturated while the transpiration rate may still increase, and result in relatively low WP_T values. Similarly, the dry matter production rate of a crop under extreme moisture deficit conditions may not change proportionally to the transpiration rate, mainly due to the biochemical adaptations in CO_2 assimilation and respiration (Lövenstein et al., 1992). Therefore, *improved crop varieties, well chosen sowing dates and sufficient water supply can increase the low WP_T values for a crop.*

The inevitable loss of water due to soil evaporation E decreases the water productivity from WP_T to WP_{ET} , which is expressed in terms of Y_g per unit amount of evapotranspiration ET :

$$WP_{ET} = \frac{Y_g}{E+T} = \frac{Y_g}{ET} \text{ (kg m}^{-3}\text{)} \quad (3.19)$$

The ET represents the actual amount of water used in crop production, and must be used as productive as possible. *Relative low values of WP_{ET} as compared to WP_T indicate the need to reduce soil evaporation by agronomic measures such as soil mulching and conservation tillage.*

Similarly, including percolation Q_{bot} from field irrigations enlarges the denominator in expression of water productivity, and hence decreases it from WP_{ET} to WP_{ETQ} . The seepage losses Q_{SL} from the conveyance system further decrease WP_{ETQ} at regional scale.

$$WP_{ETQ} = \frac{Y_g}{ET + Q_{bot} + Q_{SL}} = \frac{Y_g}{ETQ} \text{ (kg m}^{-3}\text{)} \quad \text{with } Q_{SL} = 0 \text{ at field scale} \quad (3.20)$$

Apparently it seems that both percolation and seepage losses reduce the WP_{ETQ} at field and regional scale, but it depends on the groundwater quality of the region. For instance percolation from field irrigations and seepage from the conveyance system recharge to groundwater, which is recycled through groundwater pumping in good quality groundwater regions. If groundwater quality is poor, recycling of this water may not be possible, and any percolation and seepage should be considered as lost water. Therefore, *in poor quality groundwater regions as the northern parts of Sirsa district, WP_{ETQ} must be evaluated to quantify percolation and seepage losses, which might be contributing to the rising groundwater levels or waterlogging risk.*

Water productivity also depends on the spatial scale considered. It is aggregated by taking the ratio of independent summations of Y_g and amount of water used W_{su} per simulation unit area. For instance, the $(WP)_{reg}$ at regional scale is calculated as:

$$(WP)_{reg} = \frac{\sum_{i=1}^{N_{su}} Y_{g,i} \times A_{su,i}}{\sum_{i=1}^{N_{su}} W_{su,i} \times A_{su,i}} \quad (3.21)$$

where Y_g is the amount of crop grain (or seed) yield for a crop (kg m^{-2}), W_{su} is the amount of water used (T , ET , Q_{bot} and Q_{SL}) ($\text{m}^3 \text{m}^{-2}$), A_{su} is the simulation unit area (m^2), i denotes simulation unit, and N_{su} is the total number of simulation units in the study area.

The regional water and salt balances, e.g. $(ET)_{\text{reg}}$, also can be aggregated as:

$$(ET)_{\text{reg}} = \frac{\sum_{i=1}^{N_{\text{su}}} ET_i \times A_{\text{su},i}}{\sum_{i=1}^{N_{\text{su}}} A_{\text{su},i}} \quad (3.22)$$

Using Eqs. 3.21 and 3.22, the simulated water and salt balances, crop yields, and water productivity values can be aggregated at different spatial scales.

The used definitions of water productivity in this study are summarized in Table 3.1. This flexibility in defining water productivity provides useful indicators to evaluate the water utilization, and to identify where and when water can be saved.

Table 3.1 Definitions of water productivity WP (kg m^{-3}) expressed as crop production (kg m^{-2}) per unit amount of water used ($\text{m}^3 \text{m}^{-2}$). Y_g is the crop grain (or seed) yield, T is the actual transpiration, E is the actual soil evaporation, Q_{bot} is the percolation from field irrigations, and Q_{SL} is the seepage losses from the conveyance system.

WP	Definition	Unit	Field scale	Regional scale
WP_T	Y_g / T	kg m^{-3}	T	T
WP_{ET}	Y_g / ET	kg m^{-3}	$E + T$	$E + T$
WP_{ETQ}	Y_g / ETQ	kg m^{-3}	$ET + Q_{\text{bot}}$	$ET + Q_{\text{bot}} + Q_{\text{SL}}$

3.5 Overview of data requirement and collection

The proposed framework for regional water productivity analysis has been implemented and evaluated in Sirsa district (Chapter 2). The information used in this study was collected in the frame of the WATER PROductivity (WATPRO) project in Sirsa district from 2000 to 2003 (Van Dam and Malik, 2003). This information was derived from two different sources: specific field experiments and existing secondary information. Further, the required and collected information can be categorized into two main categories: at field and regional scale.

3.5.1 Field scale

Most of the input parameters of SWAP are site specific, and can be obtained by field measurements. Some of the input parameters such as soil hydraulic parameters are difficult to measure directly under field conditions, and might be determined through the calibration and validation of the model. The calibration and validation of *SWAP-WOFOST* also requires detailed crop measurements under controlled field conditions. Field experiments for two main crops, i.e. wheat during the *rabi* (winter) season and cotton during the *kharif* (summer) season, during the agricultural year 2001-02 were conducted at the Cotton Research Station (CRS), Sirsa. Several cultivars and different levels of soil moisture availability were included in these experiments (Table 3.2).

Table 3.2 Overview of crop experiments conducted at the Cotton Research Station, Sirsa (Haryana) during the agricultural year 2001-02 (Malik et al., 2003). *I* is the irrigation, *CPE* is the cumulative pan evaporation, and *CRI* is the crown root initiation.

Crop	Experiment	Cultivars	Treatments	Emergence
Wheat	Moisture	PBW343	1. <i>I / CPE</i> = 0.9 after <i>CRI</i> 2. <i>I / CPE</i> = 0.7 after <i>CRI</i> 3. <i>I / CPE</i> = 0.5 after <i>CRI</i>	Dec. 13, 2001
Wheat	Cultivar	PBW343, PBW373, HD2329, HD2687, WH711, WH147, Raj3765	Optimum moisture (5 post-sown irrigation)	Dec. 13-15, 2001
Cotton	Moisture + Cultivar	H1098 LHH144	1. Optimum moisture (4 post-sown irrigation) 2. Medium moisture (3 post-sown irrigation) 3. Low moisture (2 post-sown irrigation)	May 21, 2002

Table 3.3 gives an overview of the data collected for calibration and validation of SWAP in Sirsa district. The required input parameters can be categorized into meteorological, soil, water and crop parameters. SWAP uses the daily meteorological data to calculate the potential evapotranspiration rate (Eq. 3.5). These meteorological data, including minimum and maximum temperature, relative humidity, vapour pressure, sunshine hours, wind speed and rainfall, were collected from the meteorological station installed at the Indian Council of Agricultural Research-Cotton Research Institute (ICAR-CRS) (lat. 29° 35'; long. 75° 08') in Sirsa district. The obtained meteorological data contained some missing data and errors. Therefore, a comparison with data from the meteorological station (lat. 29° 10'; long. 75° 46') of CCS Haryana Agricultural University (CCS HAU), Hisar (about 90 km from Sirsa) was made. If needed, corrections were made using multiple regression relations between the data of Sirsa and Hisar (Roelevink, 2003). In the case of wind speed, data from Hisar were used. The solar radiation values were calculated from measured sunshine hours using the Angstrom formula (Appendix A) with coefficients $a_s = 0.29$ and $b_s = 0.41$, which are specific for Sirsa region.

To obtain the soil parameters at the monitored fields, samples were taken from five different soil depths: 0-15, 15-30, 30-60, 60-90 and 90-120 cm. These samples were analysed for basic physio-chemical properties such as soil texture, bulk density, saturated hydraulic conductivity, saturation percentage, pH, electrical conductivity (*EC*) and organic carbon.

The source (canal or tubewell), amount and quality of each irrigation gift were recorded. The detailed crop growth in terms of density (number of tillers per unit area), height, leaf area index, dry matter and its partitioning, and rooting depth at different crop development stages were measured. The Sunscan canopy analysis system was used for the measurement of light interception i.e. photosynthetically active radiation (*PAR*) absorbed by the canopy. Total dry matter, grain (or seed) and straw yields were measured at the harvest time of the crop.

These measurements (Table 3.3) at the experimental stations (Table 3.2) were used to calibrate and validate SWAP-WOFOST for wheat and cotton in Sirsa district (Bessembinder et al., 2003). They also did this for rice using similar measurements (Table 3.3) at two farmer fields, denoted as S1F2 and S2F6, in Sirsa district.

Table 3.3 Overview of the data collected for calibration and validation of SWAP model at experimental stations and farmer fields in Sirsa district (Malik et al., 2003).

Data	Method / source	Frequency	Purpose
Meteorological data			
	Meteorological station	Daily	Input derivation
Soil physio-chemical properties			
Texture	International Pipette Method (Piper, 1996), USDA classification	Once	Input derivation
Bulk density	Core Method	Once	Input derivation
Saturated hydraulic conductivity	Constant Water Head Method (Klute and Dirksen, 1986)	Once	Input derivation
Saturation percentage / moisture	Saturation Paste Method	Once	Input derivation
Soil moisture	Gravimetric Method	Before and after irrigation	Calibration and validation
pH	In soil-water suspension of 1:2 by pH meter	Before and after irrigation	General
Electrical Conductivity	In soil-water suspension of 1:2 by Conductivity meter	Before and after irrigation	Calibration and validation
Organic Carbon	Wet digestion method (Walkley and Black, 1934 and Jackson, 1973)	Before sowing	Input derivation
Irrigation regime			
Discharge of Irrigation source i.e. canal water or tubewell water	Current meter /Co-ordinate method/ Volumetric method	3 - 4 times	Input derivation
Duration of irrigation	Field observation	Each irrigation	Input derivation
Irrigation depth	Irrigation depth were calculated by multiplying the discharge and duration of irrigation and then divided by field area.	Each irrigation	Input derivation
Irrigation quality	Conductivity meter	Each irrigation	Input derivation
Crop growth parameters			
Crop development stage (in days after sowing) i.e. emergence, panicle initiation, anthesis, maturity and harvest	Field observation	4-5 times	Input derivation
Plant density and tillers	Field observation	4 -5 times	Input derivation
Plant height	Field observation	4 -5 times	Input derivation
Dry matter partitioning	Field observation	4 -5 times	Calibration and validation
Leaf area	Leaf area meter	4 -5 times	Calibration and validation
Photosynthetically active radiation (PAR)	Sunscan canopy analysis system	4 -5 times	Input derivation
Rooting depth	Field observation, Auger method	2-3 times	Input derivation
Crop yields	Field observation	at Harvest	Calibration and validation

To obtain the ecohydrological information and its existing variation under actual field conditions, a total of 24 farmer fields at 6 different sites (4 fields at each site), denoted as S1 to S6 (Fig. 3.7), were monitored in Sirsa district during the agricultural year 2001-2002. Wheat-rice combination is mainly grown in the central parts of Sirsa district. The sites S1 and S2 were located in the main wheat-rice belt along the Northern Ghagger canal downstream of the Ottu weir. The heavy soil texture (i.e. clay loam to silt clay loam) and good quality

groundwater are providing suitable growing conditions for wheat-rice in this area. The predominant wheat-cotton (site S3 to S6) combination is cultivated on the light soils i.e. sandy loam to loamy sand. Site S6 was selected in a waterlogged and saline area near Fatehabad Branch canal flowing in the southern part of Sirsa district.

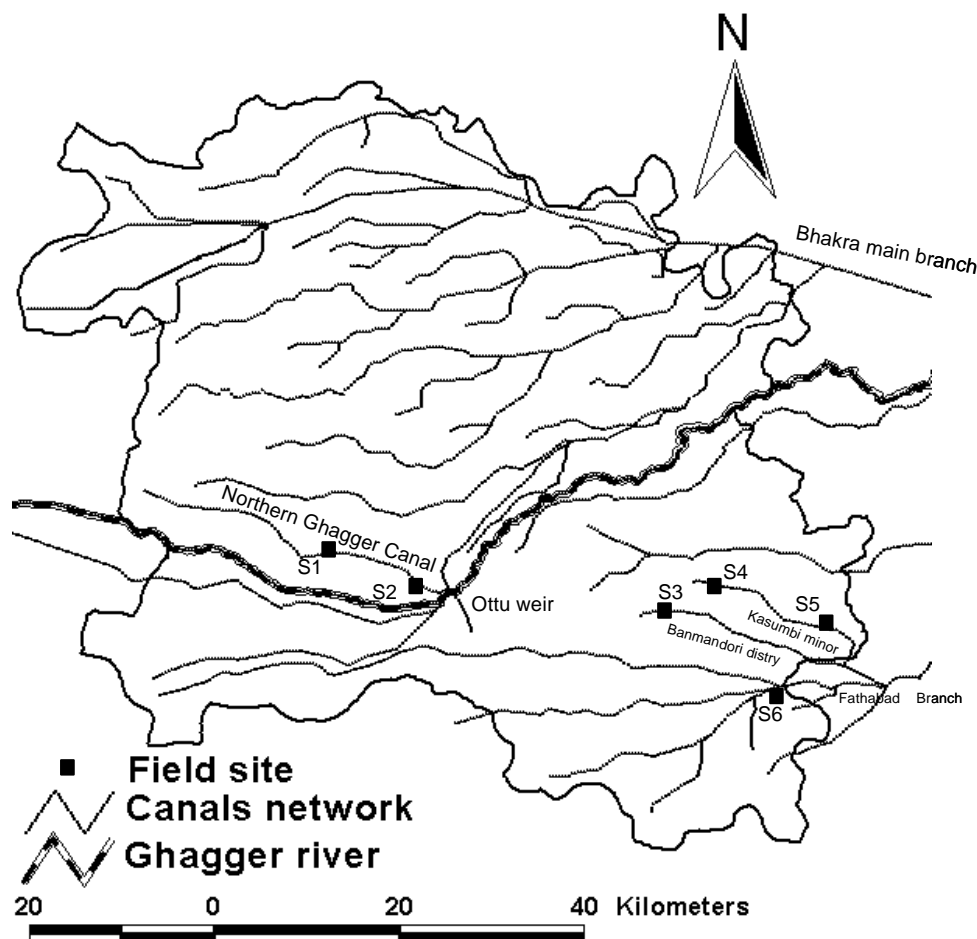


Figure 3.7 Location of farmer fields at 6 sites (denoted as S), which were monitored in Sirsa district during the agricultural year 2001-02.

The collected information (Table 3.3) at the monitored farmer fields in Sirsa district (Fig. 3.7) was used for the calibration and validation of SWAP, and for the water productivity analysis at field scale. The saturation percentage ranges from 46 to 60% for heavy soils in wheat-rice fields, and from 31 to 40% for light soils in wheat-cotton fields. The bulk density ranges from 1.29 to 1.46 g cm⁻³ in wheat-rice fields, and from 1.48 to 1.70 g cm⁻³ in wheat-cotton fields. Most of the soils are low in organic carbon, and sodic with a pH ranging from 8.0 to 9.0. Some of the soils in wheat-cotton fields with shallow groundwater (< 3m) level are saline sodic. Irrigation water comes mainly from tubewells (groundwater) in the wheat-rice area, while canal water is the main source of irrigation in the wheat-cotton area. Canal water at the monitored wheat-rice fields (8) was hardly used: less than 1% of the total irrigation water (canal + groundwater) applied. While at the other monitored wheat-cotton fields (16), the share of canal water in the total irrigation water ranged from 30% (site S3) to 60% (S5), with a maximum of 90% at site S6. The groundwater quality of wheat-rice area is very good: < 2 dS m⁻¹. The groundwater quality of the wheat-cotton area varies from good (< 2 dS m⁻¹, at site S4 and S5) to poor (> 6 dS m⁻¹ at site S6). Site S6 with wheat-cotton combination also

has shallow groundwater depth (< 1.5 m). At each site, one field was observed intensively in terms of soil moisture and salinity profiles before and after each irrigation event, mainly during the *rabi* (winter) season. *The observed soil moisture and salinity profiles were used for the calibration and validation of soil hydraulic parameters at farmer fields.*

3.5.2 Regional scale

The proposed framework for regional water productivity analysis requires a substantial amount of spatial information on weather, land use, soil type, irrigation and groundwater (Table 3.4). Satellite remote sensing techniques generate some of the required spatial information e.g. land use and soil map. The other required information on weather, irrigation, groundwater and statistics of agriculture are obtained from the State Government agencies in Sirsa district.

Bastiaanssen et al. (2003b) performed a satellite image analysis dealing with land use classification, actual evapotranspiration *ET* and dry matter *DM* production in Sirsa district during the agricultural year 2001-02. Two land use maps were produced using the Landsat TM7 image of 18th Mar., 2002 during the *rabi* (winter) season, and of 10th Sept., 2002 during the *kharif* (summer) season. In addition, a record of 249 ground truth points was used. This land use classification was achieved by performing a series of consecutive unsupervised classification steps based on the ISODATA clustering algorithm. They also applied SEBAL algorithm to analyze 12 NOVA-AVHRR and 2 Landsat TM7 images. The estimated total *DM* production was converted to the spatial grain (or seed) yields Y_g , and subsequently the estimated Y_g and *ET* were used to analyze the WP_{ET} for main crops (wheat, rice and cotton) in Sirsa district. Further details of procedures and results of this satellite remote sensing analysis are reported in Bastiaanssen et al. (2003b).

The ICAR-CRS, Sirsa provided an extensive meteorological data set with daily values of minimum and maximum temperature, relative humidity, vapour pressure, sunshine hours, wind speed and rainfall measured over the period from 1990 to 2002. The rainfall is highly erratic in its occurrence and spatial distribution. The rainfall records of seven rain gauges spread over Sirsa district (Abubsher, Kalanwali, K. Malkan, Panjuwana, Sirsa, Ottu and M. Khera) were collected, and used in this study.

The spatial information of soils in Sirsa district was derived from a comprehensive soil report based on a reconnaissance survey (scale 1:50,000) (Ahuja et al. 2001). This survey was carried out using the satellite images (Landsat TM) in conjunction with the ground truth. The soil map was prepared by digitizing 10 distinguished soil series covering the entire district. Soil properties such as texture, organic carbon, $EC_{1.2}$ and pH of different soil horizons of each identified soil series are given (Appendix B). Soil salinity was measured as electrical conductivity $EC_{1.2}$ of the soil-water suspension (one part soil mixed with two parts distilled water), and expressed in $dS\ m^{-1}$.

The unit of salinity account in SWAP is expressed in $mg\ cm^{-3}$. Therefore, the $EC_{1.2}$ was transformed into the salinity concentration in liquid phase ($mg\ cm^{-3}$) using the relations derived for Hisar conditions by Aggarwal and Roest (1996) and Kumar et al. (1996):

$$EC_e = 5.2EC_{1:2} \quad (3.23)$$

$$EC_{FC} = 1.75 EC_e \quad (3.24)$$

$$C_{FC} = 0.707 EC_{FC} \quad (3.25)$$

where EC_e is the electrical conductivity of saturated soil paste ($dS m^{-1}$), EC_{FC} is the electrical conductivity at field capacity ($dS m^{-1}$), and C_{FC} is the soil salinity concentration ($mg cm^{-3}$) at field capacity.

The Department of Agriculture at Sirsa provided agriculture statistics such as total area, cultivable area, net sown area, irrigated area, and average discharge, type and number of tubewells at village level. This information especially average discharge and number of tubewells were used to quantify the groundwater pumping in Sirsa district.

Table 3.4 Overview of the collected regional information and its source in Sirsa district.

Data	Source	Period	Purpose
<i>Land use</i>	Satellite image, ground truth points (Bastiaanssen et. al., 2003b)	2001-2002	Land use map
<i>Meteorological data</i>	Meteorological station, rain gauges	1990-2002	Input derivation
<i>Soil</i>	Soil survey for Sirsa district using satellite image, ground truth points (Ahuja et. al., 2001)	2001	Soil map
<i>Village boundaries</i>	Department of Agriculture, Sirsa	-	Village map
<i>Agriculture statistics at village level: total area, cultivable area, net sown area, irrigated area, and average discharge, type and number of tubewells</i>	Department of Agriculture, Sirsa	1996 -99	Input derivation
<i>Canal inflow: daily discharge of main inflow and outflow canals, discharge inflow from the Ghagger river</i>	Irrigation department, Sirsa	1990-2002	Input derivation
<i>Canal network characteristics: canal design dimensions, area served (CCA) and regulations for water distribution</i>	Irrigation department, Sirsa	2001	Input derivation
<i>Groundwater condition: depth and quality.</i>	Groundwater Cell, Sirsa	1990-2000	Groundwater map

The Irrigation department of Sirsa provided detailed information on the design characteristics and layout of the canal network in Sirsa Irrigation Circle (SIC). To regulate the principle of equal water distribution, this department maintains the records of canal water inflow and area served by each canal. The records of agricultural area attached with canal water rights, called Culturable Command Area (CCA), are available at watercourse level. The canal water flows into SIC through three main canals: Bhakra Main Branch (BMB) serving around 2270 km² in the northern, Sukchain distributary (SUK) serving around 220 km² in the central, and

Fatehabad Branch (FB) serving around 840 km² in the southern parts of the district. At the tails of Jandwala distributary (JDW), Southern Ghagger Canal (SGC) and Baruwali distributary (BRU), canal water is supplied to the adjoining areas of Rajasthan state (Fig 2.7). The daily discharge records of all these main inflow and outflow canals were collected over the period from 1990 to 2002. Irrigation water from the ephemeral river Ghagger is also fed to the area downstream the Ottu weir, mainly during the monsoon season. The discharges of the river and the canals off taking from Ottu weir during the monsoon period were also obtained from Irrigation department, Sirsa.

The Groundwater Cell, Sirsa is responsible for the groundwater measurements in the district. They measure groundwater levels and its quality at 164 observation wells spread over the district, and twice a year: in June (before monsoon) and in October (after monsoon). These measurements were obtained for the period from 1990 to 2000. The groundwater quality measurements for most of the observations points were not available after the year 1995. The Inverse Distance Weighted (IDW) technique in ArcView was used to interpolate between the observation points, and to generate contour maps of groundwater level and its quality in Sirsa district.

Most of the regional information in Sirsa district is available at village level. The village boundaries map of Sirsa district, therefore, was obtained and digitized in ArcView. The collected information was aggregated and processed at this village map, which was subsequently used in the aggregation of simulation units. All the above presented data for Sirsa district over a period of more than 10 years are available on a CD-ROM accompanying the final report of WATPRO project (Van Dam and Malik, 2003).

Chapter 4

Water productivity analysis of irrigated crops at field scale

4.1 Introduction

Water productivity analysis requires the quantification of the hydrological variables transpiration, evapotranspiration and percolation, and the biophysical variables dry matter or grain yield in the agricultural production system. Measurements of these hydrological variables under field conditions are difficult, and need sophisticated instruments or installation of lysimeters. The ecohydrological models like SWAP in combination with field experiments quantify these difficult to measure hydrological and biophysical variables in space and time (Chapter 3).

The accuracy of these predictive models depends upon the proper identification of input parameters. In this chapter, a profound analysis of input parameters and predicted results of SWAP, therefore, is conducted at farmer fields in Sirsa district. Most of the input parameters were measured directly in field experiments with high accuracy, some remained uncertain. Inverse modelling is used to determine indirectly the remaining uncertain soil hydraulic parameters (Jhorar, 2002; Ritter et al., 2003), where the observed soil moisture and salinity profiles are used as system response. Firstly, SWAP with simple crop module, denoted as *SWAP*, is calibrated and validated using measurements at different farmer fields representing various combinations of soil, crop, and irrigation amount and quality. Secondly, *the applicability of SWAP-WOFOST for regional simulations is tested by a comparison with the calibrated and validated SWAP at different farmer fields*. Finally, the water productivity and its variation for wheat, rice and cotton in Sirsa district is simulated and analysed through both *SWAP* and *SWAP-WOFOST* at field scale.

4.2 Input parameters of SWAP model

Most of the input parameters of SWAP could be measured directly in the field or laboratory. Measurements at two wheat-rice fields (denoted as S1F1 and S2F5), and at three wheat-cotton fields (denoted as S3F11, S4F16 and S5F20) are used in this analysis. These farmer fields were monitored in Sirsa district during the agricultural year 2001-02 (Chapter 3).

Early sowing (in October) of wheat is practised at wheat-rice fields, while late sowing (in November) at wheat-cotton fields. In year 2002, the sowing of *kharif* crops (cotton / rice) was delayed by 15 to 20 days due to a late start of monsoon (rain). The late sowing resulted in the late harvesting. Based on the recorded sowing and harvesting dates, experimental period for wheat-rice fields is defined from Oct 1, 2001 to Oct 15, 2002, which is further divided into two crop seasons: *rabi* (wheat) from Oct 1, 2001 to Apr 30, 2002, and *kharif* (rice) from May 1, 2002 to Oct 15, 2002. Similarly, for wheat-cotton fields, it is defined from Nov 1, 2001 to Nov 15, 2002 comprising the *rabi* (wheat) season from Nov 1, 2001 to Apr 30, 2002, and the *kharif* (cotton) season from May 1, 2002 to Nov 15, 2002.

The input parameters of SWAP could be categorized into parameters required to define the upper boundary, crop, soil, lower boundary and initial conditions.

4.2.1 Upper boundary

The potential evapotranspiration ET_p and rainfall P and irrigation I fluxes define the upper boundary of the soil profile. The ET_p is estimated by the Penman-Monteith equation (Eq. 3.5) using the daily meteorological data. The required meteorological data were obtained from the ICAR-CRS, Sirsa. Fig. 4.1 shows the temperature, radiation, rainfall and vapour pressure in Sirsa district during the agricultural year 2001-02. The daily vapour pressure ranged from 0.4 to 3.4 kPa with an average value of 1.8 kPa. The daily maximum temperature reached to 46°C on the individual day during the *kharif* (summer) season. The daily solar radiation varied from 6552 to 26463 kJ m⁻² with an average value of 17680 kJ m⁻². The total rainfall was 188 mm only, out of which 177 mm was received during the *kharif* (monsoon) season.

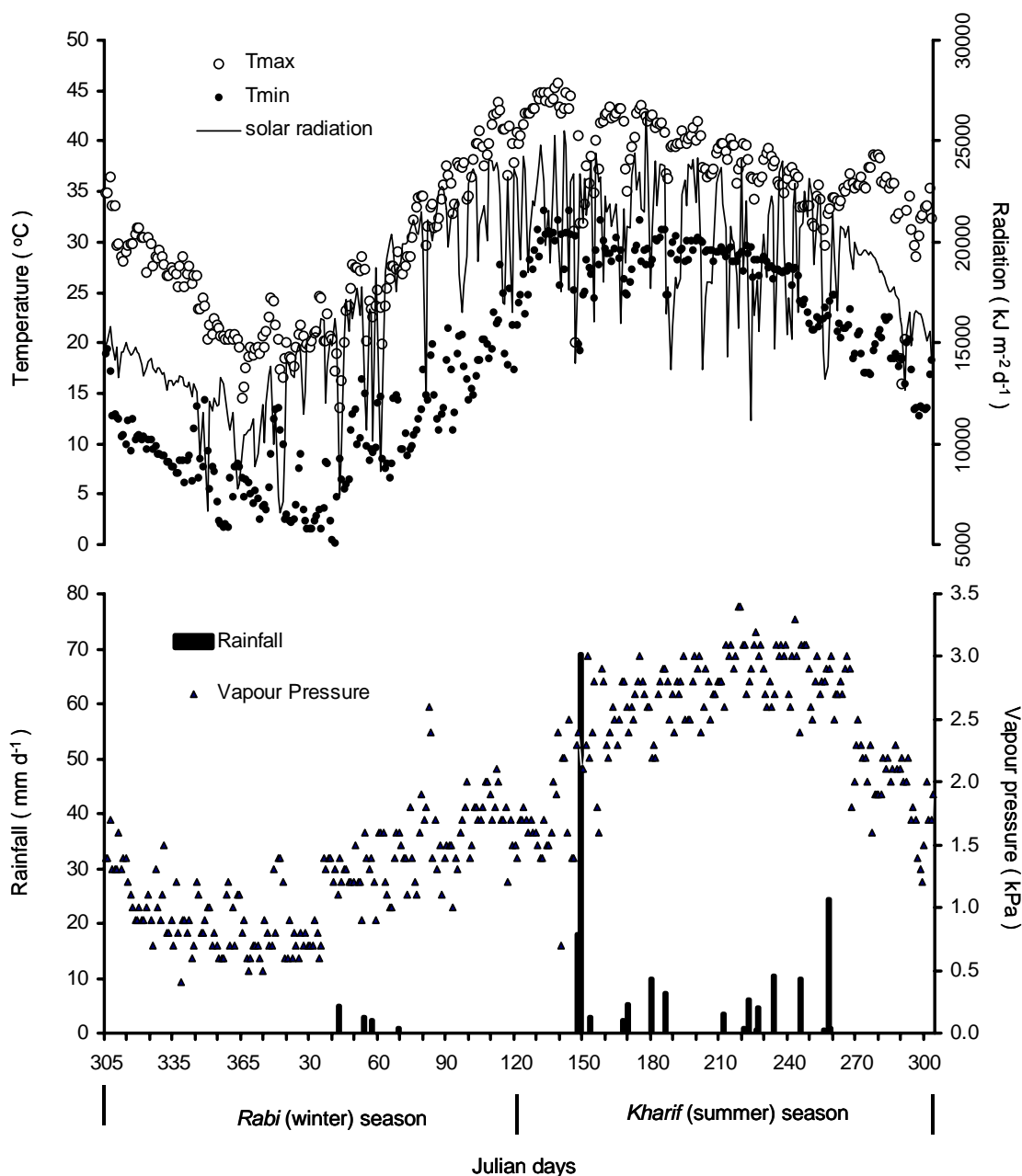


Figure 4.1 Variation of climatic conditions in Sirsa district during the agricultural year 2001-02.

4.2.2 Crop parameters

Most of the crop parameters of *SWAP-WOFOST* are the same summarized by Bessembinder et al. (2003). To calibrate and validate *SWAP-WOFOST*, they used the crop measurements (Table 3.3) for wheat and cotton at the experimental fields (Table 3.2), and for rice at two farmer fields (S1F2 and S2F6) in Sirsa district during the agricultural year 2001-02. The crop growth and its yield at the experimental fields (wheat and cotton) were higher as compared to the farmer fields. This was due to optimal crop management in terms of improved crop varieties, and better nutritional, pest and disease control at the experimental fields. To account for less optimal management at farmer fields, crop parameters such as light use efficiency ε ($\text{kg ha}^{-1} \text{hr}^{-1} / \text{J m}^2 \text{s}^{-1}$) and maximum CO_2 -assimilation rate A ($\text{kg ha}^{-1} \text{hr}^{-1}$) for wheat and cotton were somewhat decreased, using the crop measurements at farmer fields. The various input parameters used for wheat, rice and cotton are summarized in Table 4.1.

Table 4.1 Main crop parameters specified for *SWAP-WOFOST* model in Sirsa district.

Parameter	Wheat*	Rice	Cotton
Temperature sum from emergence to anthesis, TSUMEA (°C)	1480	2060	2390
Temperature sum from anthesis to maturity, TSUMAM (°C)	890	620	760
Minimum canopy resistance, r_{crop} (s m^{-1})	70	70	70
Critical pressure heads, h (cm)			
h_1	-1	100	-1
h_2	-22	55	-22
h_{31}	-1000	-160	-1200
h_{3h}	-2200	-250	-7500
h_4	-16000	-16000	-16000
Light extinction co-efficient, K_{gr}	0.375	0.338	0.450
Light use efficiency, ε ($\text{kg ha}^{-1} \text{hr}^{-1} / \text{J m}^2 \text{s}^{-1}$)	0.45	0.45	0.40
Maximum CO_2 assimilation rate, A ($\text{kg ha}^{-1} \text{hr}^{-1}$)	40	47	50
Salinity			
Critical level, EC_{max} (dS m^{-1})	6.0	5.0	7.7
Decline per unit EC , EC_{slope} ($\% \text{ dS m}^{-1}$)	7.1	9.0	5.4

* For wheat crop at wheat-rice fields, TSUMEA = 1680 °C and TSUMAM = 1015 °C.

In case of *SWAP*, crop parameters were derived from the crop measurements at the corresponding field. The measured leaf area index, crop height and rooting depth were prescribed as a function of crop development stage, which was assumed to be linear in time from emergence to harvest.

4.2.3 Soil hydraulic parameters: Inverse modelling

As important hydrological processes occur in the upper soil layers, a soil profile of 300 cm depth was specified during simulations. The soil profile was divided into one to three layers according to the profile description upto 120 cm soil depth (Fig. 4.2). The soil domain was further discretized into a total of 44 compartments with a nodal distance of 1 cm for the top 10 compartments, followed by 5 cm for the next 10 compartments and 10 cm for the remaining soil profile. This soil domain specification is acceptable as the actual soil

evaporation under field conditions is controlled by only the top few centimeters of a soil (Van Dam, 2000).

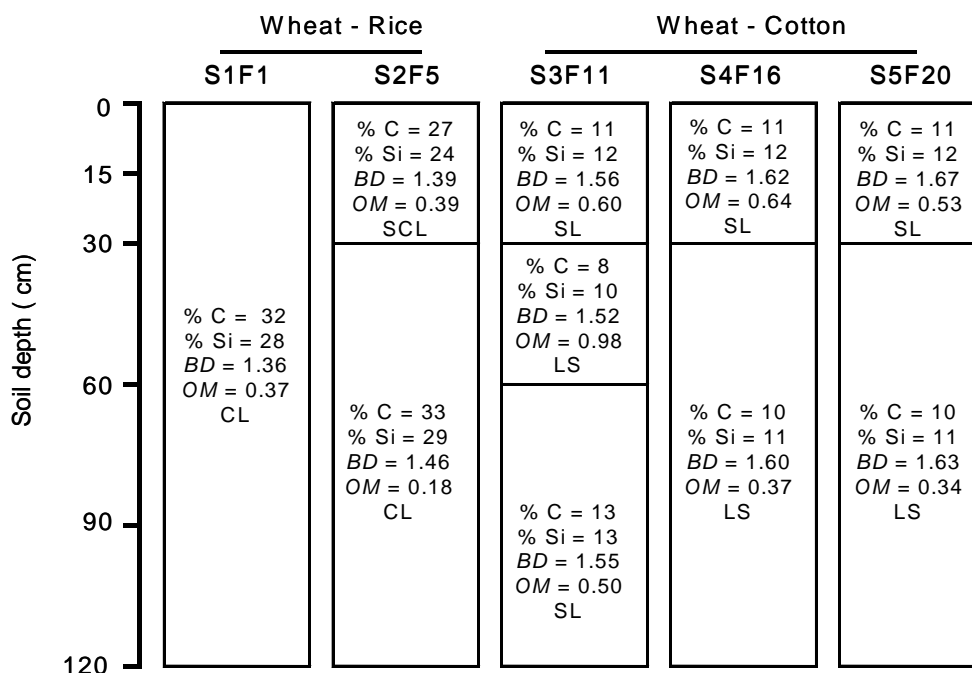


Figure 4.2 Soil information of the selected farmer fields in Sirsa district. The symbol C stands for clay, Si for silt, S for sand, and L for loam. Accordingly soil texture CL means clay loam, and SL sandy loam. *BD* is the bulk density (g cm^{-3}) and *OM* is the percentage organic matter.

For salt transport in irrigated field soils, the dispersion length L_{dis} (Eq. 3.15) was set to 5 cm (Nielsen et al., 1986). In addition to Eq. 3.7, a coefficient of 0.35 cm d^{-1} according to Black et al. (1969) was used to limit the soil evaporation rate.

Inverse modelling: a technique for parameter estimation

Water flow and salt transport is very sensitive to the soil hydraulic functions $\theta(h)$ and $K(\theta)$. The parameters describing these functions (Eq. 3.3 and 3.4) were based on the measured texture (Fig. 4.2) and so-called pedotransfer functions (Wösten et al., 1998), which relate soil texture to $\theta(h)$ and $K(\theta)$. The accuracy of pedotransfer functions is limited for site-specific water flow and salt transport. Therefore, we might calibrate the soil hydraulic parameters either manually or automatically.

We performed automatic calibration, which is also known as inverse modelling. A non-linear parameter estimation program PEST (Doherty et al., 1995) was linked with SWAP model (Fig. 4.3).

Reliable estimation of soil hydraulic parameters by inverse modelling requires other measured inputs with high accuracy, and field observations, which characterize the system behaviour. In addition, the parameters, which are optimized, should be sufficiently sensitive to these field observations. The soil moisture and salinity profiles observed at different fields were used for the calibration of soil hydraulic parameters. *SWAP* using the measured crop growth was used in the calibration process.

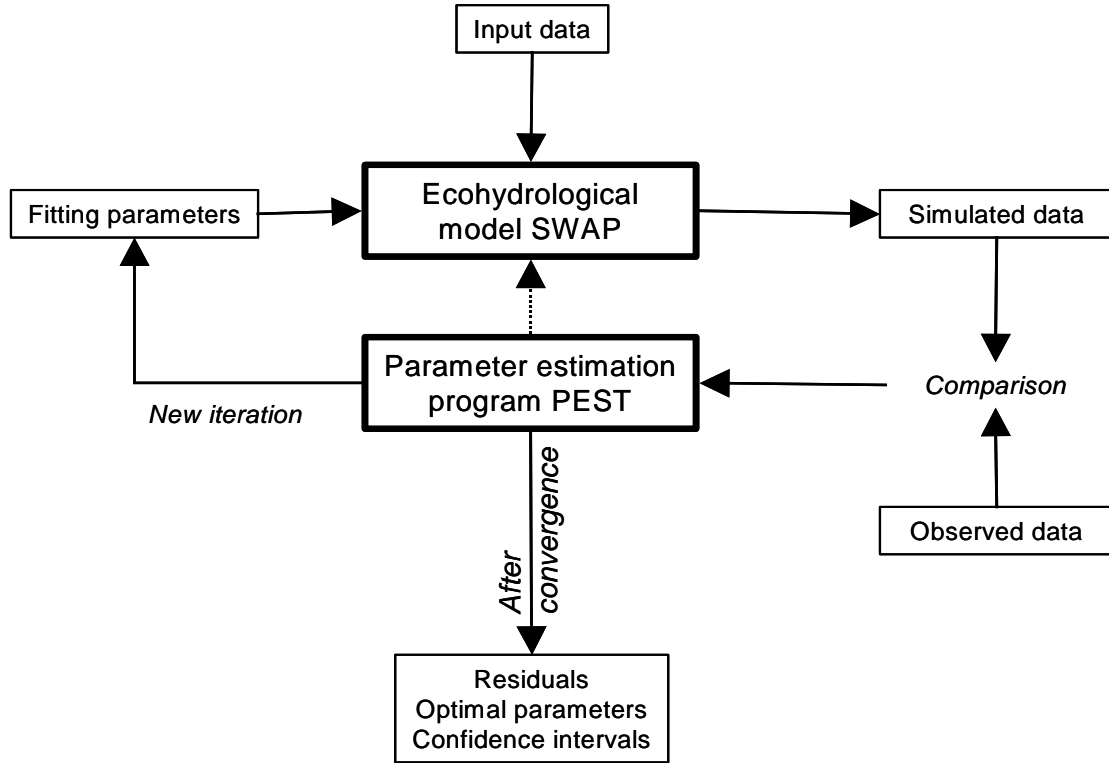


Figure 4.3 Communication between the ecohydrological model SWAP and the parameter estimation program, PEST.

The objective function quantifies the differences between model results and observations. If the observation errors follow a multivariate normal distribution with zero mean, no correlation, and constant variance for each observation type, maximization of the probability of reproducing the observed data leads to the weighted least squares objective function $\Phi(\mathbf{b})$:

$$\Phi(\mathbf{b}) = \sum_{i=1}^N \left[\left\{ W_{\theta} (\theta_{\text{obs}}(t_i) - \theta_{\text{sim}}(\mathbf{b}, t_i)) \right\}^2 + \left\{ W_{\text{EC}} (EC_{\text{obs}}(t_i) - EC_{\text{sim}}(\mathbf{b}, t_i)) \right\}^2 \right] \quad (4.1)$$

where $\theta_{\text{obs}}(t_i)$ and $EC_{\text{obs}}(t_i)$ are the observed soil moisture and salinity at time t_i , N is the number of observations, $\theta_{\text{sim}}(\mathbf{b}, t_i)$ and $EC_{\text{sim}}(\mathbf{b}, t_i)$ are the simulated values of θ and EC using an array with parameter values \mathbf{b} . W_{θ} and W_{EC} are the weight associated with θ_{obs} and EC_{obs} , respectively.

In case of random observation errors only, according to Maximum Likelihood the weighting factor for a particular observation should be equal to the inverse of the standard deviation of the observation error of that particular observation type. Gribb (1996) weighted each different data type by the inverse of the mean values. We used $W_{\theta}=1$ and $W_{\text{EC}}=10\%$ of average $\theta_{\text{obs}}/EC_{\text{obs}}$. In this way, we accounted for observation unit differences of θ and EC , and at the same time gave relatively more weight to the soil moisture content observations.

The inverse problem should be well posed in order to achieve unique and stable parameter values. In general, a well posed inverse problem can be realized by a small number of fitting parameters (Kool and Parker, 1988). Of the parameters describing the soil hydraulic functions

(Eq. 3.3 and 3.4), θ_{sat} ($\text{cm}^3 \text{cm}^{-3}$) and K_{sat} (cm d^{-1}) have a clear physical meaning, and can be measured directly. So the values of these parameters were taken from the measurements at the corresponding field. The θ_{res} ($\text{cm}^3 \text{cm}^{-3}$), which might be assigned a value near to zero (Russo, 1988), and empirical shape parameter λ [-] were derived from the pedotransfer functions. Both parameters show less sensitivity to soil water flow and salt transport. Two parameters remain uncertain: α (cm^{-1}) and n [-]. As the fields considered in this analysis have one to three soil layers (Fig. 4.2), the total number of parameters to be optimised is 2 to 6. In case of regular measurements at ordinary field conditions, 4 to 8 hydrological parameters could be estimated uniquely with a low coefficient of correlation and variation (Van Dam, 2000). Pedotransfer functions (Wösten et al., 1998) were used to derive reasonable initial estimates of the soil hydraulic parameters for the optimisation process.

In actual field conditions, the farmers puddle the soil before rice transplantation in the field. The purpose of soil puddling is to reduce the percolation below rootzone, and thereby to maintain water ponding on the soil surface for optimal rice growing conditions. Because of this management practice, the hydraulic conductivity of the puddled layer is decreased. In order to capture the reduced percolation in the simulation of water flow during the rice growing period, the K_{sat} of the upper 30 cm soil layer of wheat-rice fields was reduced to 20% (Singh et al., 2001). The reduction in the soil evaporation rate according to the empirical function of Black et al. (1969) was also set off during the rice growing period.

4.2.4 Lower boundary and initial conditions

The groundwater level at the selected farmer fields was deeper than 3 m below soil surface. Therefore, the free drainage condition (Eq. 3.11) was applied as lower boundary.

Initial salinity profiles were derived from the measurements at the corresponding field. Unfortunately, the initial soil moisture contents were not measured. The initial soil moisture profile at each field, therefore, were generated by running SWAP for one year in advance with the same inputs, and using the final soil moisture as initial condition.

4.3 Results and discussion

4.3.1 Parameter estimation

The soil moisture and salinity profiles observed during the *rabi* (wheat) season were used for the calibration and validation of soil hydraulic parameters. The calibration process was performed with the first part of observations (Jan-Feb), and the second part of observations (Mar-Apr) was used for the validation. Soil hydraulic parameters α and n of the different soil layers of stratified soil profile (Fig. 4.2) were optimized simultaneously. The optimized values of α and n together with the other soil hydraulic parameters (θ_{res} , θ_{sat} , K_{sat} and λ), which were input to the model, are given in Table 4.2.

Repetition of the optimization process with different initial values of α and n resulted in the same values, which showed the uniqueness of the solution. The coefficient of variation and correlation coefficients of the optimized parameters also should be small during proper calibration.

Table 4.3 lists the coefficient of variation (i.e. ratio of standard deviation and mean) and the correlation between the optimised parameters α and n . The coefficient of variation was relatively low for parameter n as compared to parameter α . This is attributed to the higher sensitivity of parameter n to the soil water flow. Table 4.3 also shows that the correlation coefficients were acceptably small.

Table 4.2 Derived soil hydraulic parameters at different farmer fields. Parameters α and n were optimized.

Field No.	Soil Layer (cm)	Texture	Soil hydraulic parameters					
			θ_{res} (cm ³ cm ⁻³)	θ_{sat} (cm ³ cm ⁻³)	K_{sat} (cm d ⁻¹)	α (cm ⁻¹)	λ [-]	n [-]
Wheat - Rice fields								
S1F1	0 - 300	CL	0.01	0.57	1.57	0.005	-2.57	1.93
S2F5	0 - 30	SCL	0.01	0.50	2.63	0.010	-2.53	1.40
	30 - 300	CL	0.01	0.58	1.87	0.005	-2.37	1.77
Wheat - Cotton fields								
S3F11	0 - 30	SL	0.01	0.34	61.82	0.011	-1.55	1.42
	30 - 60	LS	0.01	0.33	73.81	0.052	-1.35	1.19
	60 - 300	SL	0.01	0.38	60.58	0.005	-1.58	1.58
S4F16	0 - 30	SL	0.01	0.31	101.71	0.014	-1.67	1.29
	30 - 300	LS	0.01	0.32	120.87	0.036	-0.87	1.19
S5F20	0 - 30	SL	0.01	0.34	138.69	0.041	-1.56	1.20
	30 - 300	LS	0.01	0.31	141.62	0.024	-0.80	1.16

Table 4.3 Coefficients of variation and correlation matrix of optimized parameters α and n . Two typical examples: fields S2F5 (Wheat-Rice) and S5F20 (Wheat-Cotton).

Field No.	Soil layer (cm)	Parameter	Optimized value	Coefficient of variation	Correlation coefficient			
					α_1	n_1	α_2	n_2
S2F5	0 - 30	α_1	0.010	0.271	1.00			
		n_1	1.40	0.06	0.15	1.00		
	30 - 300	α_2	0.005	0.504	0.59	0.86	1.0	
		n_2	1.77	0.02	0.26	0.38	0.4	1.0
S5F20	0 - 30	α_1	0.041	1.474	1.00			
		n_1	1.20	0.10	-0.77	1.00		
	30 - 300	α_2	0.024	1.182	0.53	0.12	1.0	
		n_2	1.16	0.01	0.23	-0.09	0.2	1.0

The Root Mean Square Error (*RMSE*) is useful to quantify the difference between the observed and simulated data with the optimised parameters:

$$RMSE = \sqrt{\frac{1}{N} \sum_{i=1}^N [Obs(t_i) - Sim(t_i, \mathbf{b})]^2} \quad (4.2)$$

where $Obs(t_i)$ and $Sim(t_i, \mathbf{b})$ are the observed and simulated values for a output variable at time t_i , and N is the total number of observations.

As a typical example, Fig. 4.4 shows the observed and simulated soil moisture θ and salinity $EC_{1:2}$ profiles of the field S5F20 during the *rabi* (wheat) season. During the calibration period, the average *RMSE* at this field was $0.022 \text{ cm}^3 \text{ cm}^{-3}$ for θ and 0.09 dS m^{-1} for $EC_{1:2}$. The average *RMSE* was also small during the validation period: $0.022 \text{ cm}^3 \text{ cm}^{-3}$ for θ and 0.07 dS m^{-1} for $EC_{1:2}$.

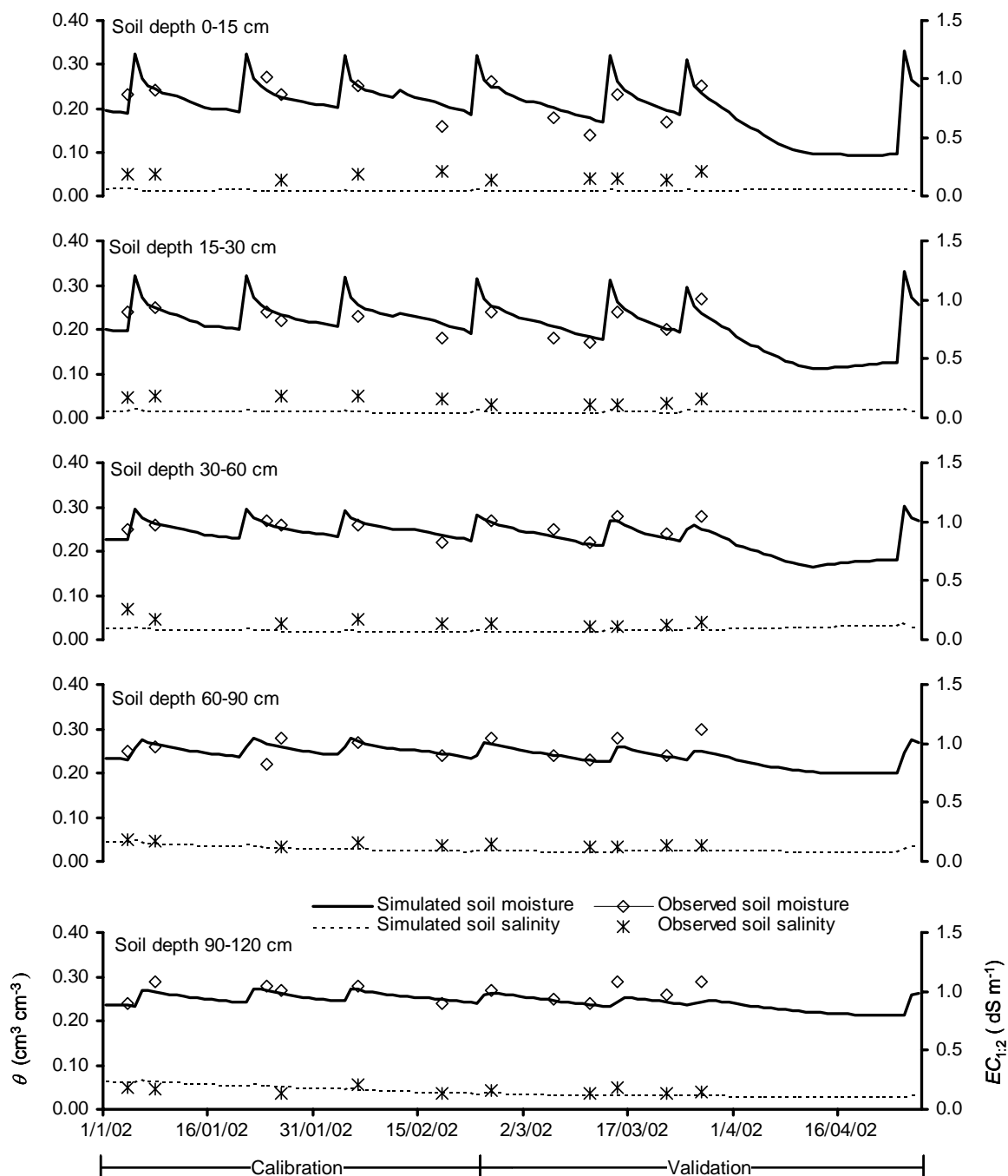


Figure 4.4 The observed and simulated soil moisture θ and salinity $EC_{1:2}$ profiles at the field S5F20 during the *rabi* (wheat) season of the agricultural year 2001-02. The calibration was performed with the first part of observations (Jan-Feb), and the second part of observations (Mar-Apr) was used for the validation.

Table 4.4 lists the *RMSE* values for both the calibration and the validation period at different fields. The *RMSE* of θ ranged from 0.016 to 0.033 $\text{cm}^3 \text{cm}^{-3}$, and of $EC_{1:2}$ from 0.09 to 0.31 dS m^{-1} . These small values reveal that soil water flow and salt transport were well simulated by *SWAP* at different fields.

Table 4.4 Number of observations N and root mean square error *RMSE* of soil moisture contents θ and salinity concentrations $EC_{1:2}$ for both the calibration (Jan-Feb) and validation period (Mar-Apr) during the *rabi* (wheat) season of the agricultural year 2001-02.

Field No.	Calibration				Validation			
	θ ($\text{cm}^3 \text{cm}^{-3}$)		$EC_{1:2}$ (dS m^{-1})		θ ($\text{cm}^3 \text{cm}^{-3}$)		$EC_{1:2}$ (dS m^{-1})	
	N	<i>RMSE</i>	N	<i>RMSE</i>	N	<i>RMSE</i>	N	<i>RMSE</i>
S1F1	15	0.032	10	0.18	13	0.023	15	0.20
S2F5	15	0.016	15	0.20	15	0.027	15	0.25
S3F11	20	0.025	20	0.25	20	0.033	20	0.31
S4F16	25	0.022	25	0.15	20	0.026	20	0.10
S5F20	30	0.022	25	0.09	30	0.022	25	0.07

As no systematic under- or overestimation of θ and $EC_{1:2}$ was observed, the differences between the observed and simulated θ and $EC_{1:2}$ are contributed to the spatial heterogeneity and observation errors, which are inevitable under field conditions.

4.3.2 Water and salt balances

The calibrated soil hydraulic parameters (Table 4.2) were used in both *SWAP* and *SWAP-WOFOST* to simulate the water and salt balances at different fields. To avoid confusion in this section only, the water and salt balance components simulated by *SWAP* are distinguished with the superscript ‘s’, and by *SWAP-WOFOST* with the superscript ‘sw’. For example, the potential evapotranspiration ET_p is denoted as ET_p^s when simulated by *SWAP*, and as ET_p^{sw} when simulated by *SWAP-WOFOST*. First, the water and salt balances simulated by *SWAP* are analysed, and second they are compared with those simulated by *SWAP-WOFOST*.

The average annual Class A pan-evaporation E_{pan} for Hisar-Sirsa regions is established at 2124 mm through the measurements over the period from 1984 to 1994 (Bastiaanssen et al., 1996). Multiplication with the reasonable pan-coefficient of 0.80 and crop-coefficient of 1.20 (Perreira et al., 1995; Allen et al., 1998) indicates an annual ET_p of 2039 mm in Sirsa district. The simulated annual ET_p^s varied from 1963 to 2021 mm at wheat-rice fields, and from 1897 to 2204 mm at wheat-cotton fields. These simulated values of ET_p^s are in agreement with the above estimated indicative value of 2039 mm. The variation in annual ET_p^s at different fields with same crop combination was mainly due to the differences in measured crop height, which determines the aero-dynamic term in the Penman-Monteith equation (Eq. 3.5).

Under field conditions, water and salt stress reduce the ET_p to the actual evapotranspiration ET . Measurements of the ET , being rather difficult under field conditions, are not common in Sirsa district. Doorenbos and Kassam (1979) mentioned a range of ET from 450 to 650 mm for wheat. Based on an analysis of satellite images with SEBAL, Bastiaanssen et al. (2003b)

estimated mean *ET* of 360 mm with a standard deviation of 15 mm over the wheat areas in Sirsa district during the period from Nov 1, 2001 to Apr 30, 2002. During the same period, *SWAP* simulated *ET*^s varied from 338 to 355 mm at wheat-cotton fields, and shows an agreement with the above mentioned values. During the *rabi* (wheat) season, the *ET*^s at wheat-rice fields was higher than the *ET*^s at wheat-cotton fields (Table 4.5). This was mainly due to the one month longer growing season at wheat-rice fields, i.e. from Oct 1, 2001 to Apr 30, 2002, as compared to wheat-cotton fields, i.e. from Nov 1, 2001 to Apr 30, 2002.

Table 4.5 Simulated water and salt balances⁽¹⁾ at farmer fields in Sirsa district during the *rabi* (wheat) season of the agricultural year 2001-02. *SWAP* refers to the simple crop module, and *SWAP-WOFOST* refers to the detailed crop growth module.

Component	<i>SWAP</i> model					<i>SWAP-WOFOST</i> model				
	S1F1*	S2F5*	S3F11	S4F16	S5F20	S1F1*	S2F5*	S3F11	S4F16	S5F20
Water balance (mm)										
<i>P</i>	13	13	11	11	11	13	13	11	11	11
<i>I</i>	343	424	430	391	568	343	424	430	391	568
<i>I_{cw}</i>	0	0	50	0	0	0	0	50	0	0
<i>I_{gw}</i>	343	424	380	391	568	343	424	380	391	568
<i>T</i>	363	326	244	253	245	312	291	215	223	245
<i>ET</i>	452	425	338	351	355	405	397	313	329	353
<i>Q_{bot}</i>	-329	-195	-77	-6	-171	-334	-200	-86	-7	-160
ΔW	-426	-185	23	42	52	-387	-162	40	64	63
Salt balance (mg cm⁻²)										
<i>I C_i</i>	20	24	102	25	20	20	24	102	25	20
<i>Q_{bot} C_{bot}</i>	-30	-75	-19	-3	-49	-31	-77	-21	-3	-46
ΔC	-11	-51	83	22	-30	-11	-53	81	22	-27

* Wheat-rice fields. ⁽¹⁾ Height soil column considered is 300 cm.

Table 4.6 Simulated water and salt balances⁽¹⁾ at farmer fields in Sirsa district during the *kharij* (cotton/rice) season of the agricultural year 2001-02. *SWAP* refers to the simple crop module, and *SWAP-WOFOST* refers to the detailed crop growth module.

Component	<i>SWAP</i> model					<i>SWAP-WOFOST</i> model				
	S1F1*	S2F5*	S3F11	S4F16	S5F20	S1F1*	S2F5*	S3F11	S4F16	S5F20
Water balance (mm)										
<i>P</i>	177	177	177	177	177	177	177	177	177	177
<i>I</i>	1250	1062	301	554	737	1250	1062	301	554	737
<i>I_{cw}</i>	0	0	162	0	0	0	0	162	0	0
<i>I_{gw}</i>	1250	1062	139	554	737	1250	1062	139	554	737
<i>T</i>	457	536	277	582	685	472	546	317	586	632
<i>ET</i>	862	960	427	745	827	858	949	456	740	758
<i>Q_{bot}</i>	-121	-98	-86	-25	-132	-133	-100	-96	-41	-159
ΔW	440	175	-37	-44	-51	430	184	-78	-58	-11
Salt balance (mg cm⁻²)										
<i>I C_i</i>	74	61	33	36	26	74	61	33	36	26
<i>Q_{bot} C_{bot}</i>	-11	-41	-22	-11	-38	-13	-38	-25	-19	-46
ΔC	63	19	11	24	-12	61	21	7	17	-20

* Wheat-rice fields. ⁽¹⁾ Height soil column considered is 300 cm.

Doorenbos and Kassam (1979) also mentioned a range of ET from 450 to 700 mm for rice, and from 700 to 1300 mm for cotton. Bastiaanssen et al. (2003b) estimated mean ET of 769 ± 50 mm over the rice areas, and of 690 ± 39 mm over the cotton areas in Sirsa district during the period from May 1, 2002 to Oct 31, 2002. During this *kharif* (cotton/rice) season, SWAP simulated ET^s varied from 862 to 960 mm at rice fields, and from 422 to 799 mm at cotton fields (Table 4.6). The simulated ET^s at rice fields was slightly higher than above mentioned values. This is attributed to heavy irrigation applied at these fields: 1062 mm at S2F5 and 1250 mm at S1F1. Further, the simulated ET^s at cotton field S3F11 was significantly low, i.e. 427 mm only, as compared to other fields and above mentioned values. This was a result of less irrigation applied at this field during the *kharif* (cotton) season (Table 4.6).

The percolation Q_{bot}^s at wheat-rice fields is higher than those at wheat-cotton fields. At wheat-rice fields, the irrigation I during the *rabi* (wheat) season was about 1/3 of the I during the *kharif* (rice) season (Table 4.5 and 4.6). Despite this, the Q_{bot}^s was relatively higher during the *rabi* (wheat) season. This was due to the saturated soil profile left after rice and application of two heavy irrigations about 100 mm each in the early stage (Oct-Nov) of the *rabi* (wheat) season at these fields. The heavy irrigations also resulted into high Q_{bot}^s at the wheat-cotton field S4F20. This indicates the practice of over irrigation in Sirsa district.

The use of poor quality groundwater results into a salt build-up in the soil profile. Note that the change in salt storage ΔC at field S3F11 during the *rabi* (wheat) season was high, i.e. 83 mg cm⁻², despite a significant Q_{bot}^s of -77 mm (Table 4.5). This was due to the use of poor quality groundwater (3.73 dS m⁻¹), which supplied a large amount of salts (102 mg cm⁻²). In case of poor quality groundwater, conjunctive use of canal water and groundwater is beneficial in terms of salt build-up. For instance, the conjunctive use of canal water I_{cw} (162 mm) and groundwater I_{gw} (139 mm) at same field S3F11 during the *kharif* (cotton) season resulted into a relatively low ΔC of 11 mg cm⁻² (Table 4.6).

Comparison of water and salt balances simulated by SWAP and SWAP-WOFOST

In this section, the water and salt balances simulated by SWAP-WOFOST are compared with those simulated by the calibrated and validated SWAP at different fields. In both SWAP and SWAP-WOFOST, the simulated potential evapotranspiration rate ET_p is partitioned into the potential soil evaporation rate E_p and the potential crop transpiration rate T_p using the leaf area index LAI (Eq. 3.6). The share of the total potential crop transpiration T_p into the potential evapotranspiration ET_p also depends on the crop duration i.e. from emergence till harvest during the respective crop season. For instance, the T_p^s for cotton at field S3F11 was about 1/2 of the T_p^s at other cotton fields S4F16 and S5F20 (Fig. 4.5). This was a result of relatively poor cotton growth at field S3F11. The measured maximum LAI of cotton was 1.32 only at S3F11, while 3.92 at S4F16 and 4.23 at S5F20. Further, the measured cotton crop duration was 159 days at S3F11, while 189 days at S4F16 and 196 days at S5F20.

In case of SWAP-WOFOST, the ET_p^{sw} is partitioned into the E_p^{sw} and the T_p^{sw} using the simulated LAI and crop duration. SWAP-WOFOST simulates the LAI based the incoming solar radiation, air temperature, plant characteristics, and the water and salt stress on a crop. The

accumulated daily effective temperature and prescribed temperature sum (TSUMs) for a crop determine the crop duration (Chapter 3). Therefore, the comparison of T_p^{sw} and T_p^s could indicate the simulation of crop growth in terms of LAI and crop duration at different fields (Fig. 4.5).

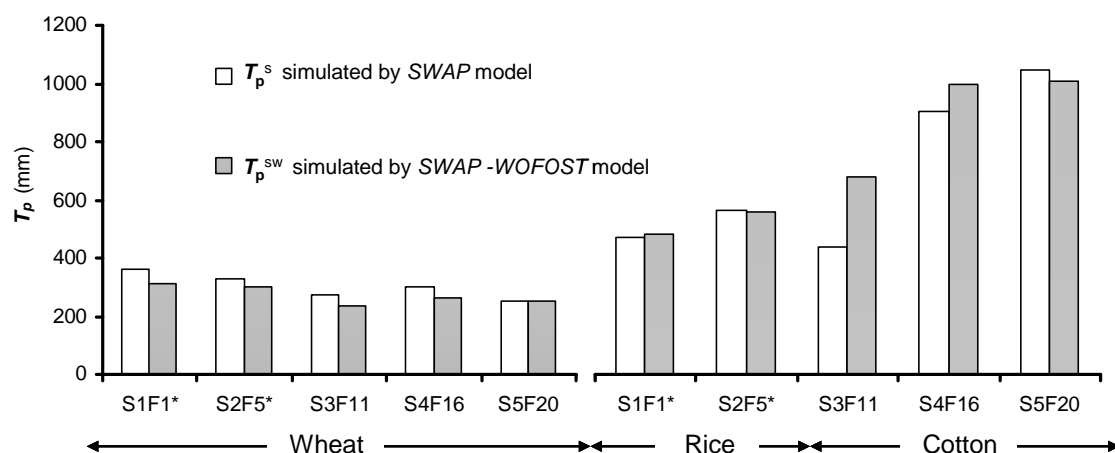


Figure 4.5 Simulated potential transpiration T_p at farmer fields in Sirsa district during the *rabi* (wheat) and *kharif* (cotton / rice) season of the agricultural year 2001-02. SWAP model refers to the simple crop module, and SWAP-WOFOST refers to the detailed crop growth module. * Wheat-rice fields.

The deviation between T_p^{sw} and T_p^s varied from 1 to 14% of the T_p^s at the corresponding field, except at cotton field S3F11. In case of most fields, the T_p^s was slightly higher than the T_p^{sw} . It was expected due to the linear interpolation between two LAI measurements by SWAP. This linear interpolation results into slightly overestimation of LAI, especially in the beginning of crop season, and hence slightly overestimation of T_p^s . In contrast to this, about 56% higher T_p^{sw} than T_p^s for cotton at field S3F11 was clearly a result of higher simulation of LAI and crop duration. However, the T_p^{sw} for cotton at field S3F11 was about 2/3 of the T_p^{sw} at other cotton fields S4F16 and S4F20 (Fig. 4.5). This indicates the response of SWAP-WOFOST towards the water and salt stress at field S3F11.

Similar to the T_p^{sw} and T_p^s (Fig. 4.5), the deviation between ET^{sw} and ET^s varied from 1 to 10% of the ET^s during their respective crop seasons at the corresponding field. The ET^{sw} at field S3F11 during the *kharif* (cotton) season was only 7% higher than the ET^s . Other water and salt balance components such as Q_{bot} , ΔW and ΔC simulated by SWAP-WOFOST were also well comparable with those obtained from the calibrated and validated SWAP (Table 4.5 and 4.6).

4.3.3 Water productivity

The water productivity for wheat, rice and cotton was analysed through both SWAP and SWAP-WOFOST models. First, we calculated the water productivity values (Table 3.1) using the water balance components T , ET and Q_{bot} simulated by SWAP, and the actual grain (or seed) yields Y_g measured at the selected farmer fields (Table 4.7). The average WP_T , expressed as Y_g/T ($kg\ m^{-3}$), was 1.88 for wheat, 1.73 for rice and 0.29 for cotton. *This presents wheat as a highest efficient crop in terms of physical crop production in Sirsa district.* The differences in WP_T for different crops are due to the differences in the chemical composition, harvest index and evaporative demands during the respective seasons. In Sirsa district, temperatures and vapour

pressure deficit are high during the *kharif* (summer) season, which results into high evaporative demands. Consequently, the WP_T , WP_{ET} and WP_{ETQ} of summer crops (cotton and rice) are lower than those for winter crop (wheat).

Based on a review of 82 literature sources with results of experiments in the last 25 years, Zwart and Bastiaanssen (2003) established global benchmark values of WP_{ET} , expressed as Y_g/ET (kg m^{-3}), at 1.08 for wheat, 1.09 for rice and 0.63 for cotton. Droogers and Kite (2001) mentioned a value of WP_{ET} from 0.16 to 0.39 for cotton at basin to field level in Turkey. Similarly, a value of WP_{ET} about 0.27 for cotton is mentioned in a study towards on crop water productivity in Pakistan during 1970s (PARC, 1982). Tuong and Bouman (2003) summarized a range of WP_{ET} from 0.4 to 1.1 for rice in farmer fields and irrigation systems of Northwest India. Hussain et al. (2003) gave a WP_{ET} value of 1.36 for wheat in Haryana region. In our analysis, the average WP_{ET} at the selected farmer fields in Sirsa district was 1.39 for wheat, 0.94 for rice and 0.23 for cotton (Table 4.7), and *presents kind of average values for the climatic and growing conditions in Northwest India.*

To improve the WP_{ET} for a crop, the fraction of soil evaporation E in evapotranspiration ET is important (Eq. 3.19). The high evaporative demands and continuously surface water ponding result in high soil evaporation during the rice growing season. The fraction of E in ET at rice fields, therefore, was as high as 0.44 at field S2F5 and 0.47 at field S1F1 (Table 4.6). Consequently, the average WP_{ET} for rice was 45% lower than the average WP_T . Also, the WP_{ET} for wheat and cotton was 17 to 35% lower than the WP_T at different fields (Table 4.7). *Improving agronomic practices such as soil mulching and especially dry rice cultivation is expected to reduce this non-beneficial loss of water through soil evaporation E , and to improve the WP_{ET} at field scale.*

The percolation Q_{bot} further reduces the WP_{ET} to WP_{ETQ} at field scale (Eq. 3.20). The average WP_{ETQ} , Y_g/ETQ (kg m^{-3}), at the selected farmer fields was 1.04 for wheat, 0.84 for rice and 0.21 for cotton. Note the high reduction from WP_{ET} to WP_{ETQ} for wheat at wheat-rice fields (S1F1 and S2F5) and the wheat-cotton field S5F20 (Table 4.7). This presents the over-irrigation especially at wheat-rice fields during the *rabi* (wheat) season (Table 4.5). Usually in irrigated areas, Q_{bot} contributes to the groundwater recharge, which is recycled through groundwater pumping in good quality groundwater areas. The groundwater pumping is not possible in the poor quality groundwater areas. Therefore, the reduction in Q_{bot} will be beneficial for improving the low WP_{ETQ} values in the poor quality groundwater areas as in the northern parts of Sirsa district. *Optimal irrigation scheduling and precise land levelling can be promoted to reduce the Q_{bot} and hence to improve the WP_{ETQ} at field scale.*

Additionally, the WP_T , WP_{ET} and WP_{ETQ} values were calculated using the water balance components T , ET and Q_{bot} , and the actual grain (or seed) yields Y_g simulated by SWAP-WOFOST (Table 4.7). Accurate simulation of crop yields is necessary for the calculation of reliable water productivity values. In this analysis, the simulated potential Y_g for wheat varied from 7.1 (S4F16) to 9.1 ton ha^{-1} (S1F1) with an average value of 7.7 ton ha^{-1} . These potential productions of wheat in Sirsa district are in agreement with the reported potential Y_g of 7.3 ton ha^{-1} by Aggarwal et al., 2000. They also reported the potential Y_g of 10.8 ton ha^{-1} for rice in Sirsa district. In another study, Aggarwal et al. (2001) mentioned the potential Y_g for cotton

from 4.2 to 5.7 ton ha⁻¹ in Haryana conditions. The simulated potential Y_g for rice and cotton were slightly lower than above mentioned values (Table 4.7). This might be due to high temperatures during the *kharif* (cotton/rice) season of the agricultural year 2001-02 (Fig 4.1). Higher temperatures accelerate the crop development rate, which results into a shorter growing period and a lower crop production.

Taking into account the water and salt stress, *SWAP-WOFOST* reduces the potential Y_g to water and salt limited Y_g . In addition to the water and salt stress, the actual Y_g under field conditions depends on other factors such as nutritional, pest and disease control (Chapter 3). The lowest actual (measured) Y_g of 4.3 ton ha⁻¹ at wheat field S5F20 (Table 4.7) with the high irrigation of 568 mm (Table 4.5) indicates the presence of nutritional, pest and disease stress at farmer fields in Sirsa district. Also, note the high actual Y_g of wheat at field S1F1 as compared to other wheat fields. This is attributed to improved crop management and early sowing (i.e. Oct 25, 2001) of wheat at field S1F1.

Table 4.7 Water productivity for wheat, rice and cotton at farmer fields in Sirsa district during the agricultural year 2001-02. Water productivity WP (kg m⁻³) (Table 3.1) is calculated in different forms viz., Y_g/T (transpiration) or ET (evapotranspiration) or ETQ (evapotranspiration + percolation). Y_g denotes the grain (or seed) yield, and Y_{FM} denotes the total fresh matter yield. In case of *SWAP*, the Y_g and Y_{FM} are the actual (measured) yields, while in case of *SWAP-WOFOST*, the Y_g and Y_{FM} are the simulated water and salt limited yields at the corresponding field.

Water productivity (kg m ⁻³) / Crop yields (ton ha ⁻¹)	SWAP model						SWAP-WOFOST model					
	S1F1	S2F5	S3F11	S4F16	S5F20	Average	S1F1	S2F5	S3F11	S4F16	S5F20	Average
Wheat												
$WP_T (Y_g/T)$	1.94	1.80	1.82	2.05	1.77	1.88	2.90	2.47	3.13	2.81	2.83	2.83
$WP_{ET} (Y_g/ET)$	1.56	1.38	1.31	1.48	1.22	1.39	2.23	1.81	2.15	1.90	1.97	2.01
$WP_{ETQ} (Y_g/ETQ)$	0.90	0.94	1.07	1.45	0.83	1.04	1.22	1.21	1.69	1.86	1.35	1.47
Y_g^*	7.0	5.9	4.4	5.2	4.3	5.4	9.0	7.2	6.7	6.3	6.9	7.2
Y_{FM}^{**}	16.1	15.4	11.3	11.4	9.2	12.7	19.7	18.0	14.1	14.2	14.6	16.1
Potential Y_g^*							9.1	7.6	7.7	7.1	7.2	7.7
Potential Y_{FM}^{**}							19.8	19.2	15.4	15.3	15.3	17.0
Rice												
$WP_T (Y_g/T)$	1.78	1.67				1.73	1.54	1.53				1.54
$WP_{ET} (Y_g/ET)$	0.94	0.93				0.94	0.84	0.88				0.86
$WP_{ETQ} (Y_g/ETQ)$	0.83	0.85				0.84	0.73	0.80				0.77
Y_g^*	8.1	9.0				8.5	7.3	8.4				7.8
Y_{FM}^{**}	18.0	19.0				18.5	17.7	17.5				17.6
Potential Y_g^*							7.5	9.1				8.3
Potential Y_{FM}^{**}							19.1	18.9				19.0
Cotton												
$WP_T (Y_g/T)$			0.14	0.40	0.35	0.29			0.32	0.45	0.42	0.40
$WP_{ET} (Y_g/ET)$			0.09	0.31	0.29	0.23			0.22	0.36	0.35	0.31
$WP_{ETQ} (Y_g/ETQ)$			0.07	0.30	0.25	0.21			0.18	0.34	0.29	0.27
Y_g^*			0.4	2.3	2.3	1.6			1.0	2.6	2.7	2.1
Y_{FM}^{**}			1.3	12.9	14.1	9.4			5.8	13.9	12.8	10.8
Potential Y_g^*									3.3	3.6	4.0	3.6
Potential Y_{FM}^{**}									20.2	22.7	23.5	22.1

* Water and salt limited Y_g considering 80% grain (or seed) in simulated storage organs for wheat, 81% for rice and 44% for cotton. The Y_g includes 14, 16 and 15% moisture in grain (or seed) for wheat, rice and cotton, respectively; and
 ** moisture in air-dry fresh matter: 12% for wheat and rice, and 18% for cotton .

As expected, *SWAP-WOFOST* simulated water and salt limited Y_g for wheat were 20 to 60% higher than actual Y_g at the corresponding field (Table 4.7). Further, the simulated water and salt limited Y_g for wheat were almost equal to the simulated potential Y_g . The relative transpiration (T/T_p) at the selected wheat fields ranged from 0.85 to 1.00. This presents almost negligible water and salt stress on wheat in Sirsa district, while substantial nutritional, pest or disease stress. The differences in WP_T , WP_{ET} and WP_{ETQ} values for wheat obtained from *SWAP* and *SWAP-WOFOST* are mainly due to the differences in actual (measured) and simulated Y_g at the corresponding field. The average WP_{ET} for wheat obtained from *SWAP-WOFOST* was 45% higher than that obtained from *SWAP* (Table 4.7). *Improved crop management in terms of timely sowing and optimal fertilizer, and better pest and disease control is expected to achieve this significant increase in the WP_{ET} for wheat in Sirsa district.*

For rice, the average water and salt limited Y_g was 7.8 ton ha^{-1} , which was slightly lower than the average actual Y_g of 8.5 ton ha^{-1} . Apparently it seems that rice growth at the selected rice fields was hardly limited by the water and salt stress, or reduced by the nutrient deficiency, pest and diseases: the actual Y_g were almost equal to the potential Y_g (Table 4.7). The relative transpiration (T/T_p) at the selected rice fields was about 0.95. The T/T_p at the selected cotton fields ranged from 0.50 to 0.65, and shows water and salt stress on cotton crop. Further, the low actual Y_g of 0.4 ton ha^{-1} at the cotton field S3F11 indicates the crop failure, mainly due to water stress: 301 mm irrigation only. The low rainfall of 177 mm only will have contributed to the water stress on *kharif* (summer) crops, especially cotton (Table 4.6). *The corresponding lower simulation of water and salt limited Y_g of 1.0 ton ha^{-1} confirms that *SWAP-WOFOST* responds well towards the water stress at field S3F11.* The water and salt limited Y_g for cotton were 1.5 to 3.5 times lower than the potential Y_g at the corresponding field (Table 4.7). Also, the WP_T , WP_{ET} and WP_{ETQ} values for cotton obtained from *SWAP-WOFOST* were slightly higher than those obtained from *SWAP*. *This suggests that ensuring the irrigation supplies, especially during the dry years, and improved crop management at cotton fields will increase cotton yields, and subsequently its water productivity in Sirsa district.*

4.4 Conclusions

The main conclusions, which could be drawn from this field scale analysis, are as follows.

- Inverse modelling is efficient in the calibration of model input parameters at field scale. The use of observed soil moisture θ and salinity $EC_{1:2}$ profiles as system response in inverse modelling is successful for the estimation of soil hydraulic parameters. The good agreement between the observed and simulated θ and $EC_{1:2}$ values (Table 4.4) provided confidence to use the calibrated and validated *SWAP* to quantify the water and salt balances at farmer fields.
- Water and salt balances simulated by *SWAP-WOFOST* were well comparable with the results of the calibrated and validated *SWAP*, the latter used the measured crop parameters at the corresponding field. Further, the simulation of crop yields by *SWAP-WOFOST* was found to be well corresponding to the water and salt stress at different fields. For instance, the low simulated water and salt limited yield of 1.0 ton ha^{-1} for cotton at field S3F11 was a result of the low irrigation of 301 mm and

use of poor quality groundwater (3.73 dS m^{-1}). These results show the possibilities for the application of *SWAP-WOFOST* to simulate the crop growth for variable ecohydrological conditions at regional scale.

- Water productivity for wheat, rice and cotton in Sirsa district is a kind of average value for the climatic and growing conditions in Northwest India (Table 4.7). The 20 to 47% share of soil evaporation into evapotranspiration, especially for rice could be identified as a major non-beneficial loss of water. Based on the actual grain (or seed) yields and simulated water balance components (*SWAP*), the calculated average WP_{ET} was significantly lower than the average WP_T : 46% for rice, 26% for wheat and 22% for cotton (Table 4.7). Improving agronomic practices, especially dry rice cultivation, could reduce this non-beneficial loss of water through soil evaporation, and subsequently will improve the WP_{ET} at field scale.
- The simulated water and salt limited yields for wheat were 20 to 60% higher than the actual (measured) yields at the selected wheat fields (Table 4.7). This is attributed to almost negligible water and salt stress at these fields: the relative transpiration (T/T_p) ranged from 0.85 to 1.00. There exist substantial nutrition, pest and disease stress. The presented water productivity analysis indicates that improved crop management in terms of timely sowing, and optimal nutrition, pest and disease control for wheat will multiply its WP_{ET} by a factor of 1.5 in Sirsa district. Moreover, severe water stress was observed on cotton (relative $T/T_p < 0.65$) during the *kharif* (summer) season. As a result, the simulated water and salt limited yields for cotton were 1.5 to 3.5 times lower than the simulated potential yields at the selected cotton fields (Table 4.7). This suggests that benefits in terms of increased cotton yields and its water productivity will be gained by ensuring irrigation supply at cotton fields, especially during the dry years.
- The physical based field scale ecohydrological *SWAP* model in combination with field experiments can be used to quantify hydrological variables such as transpiration, evapotranspiration and percolation, and biophysical variables such as dry matter or crop yields, which are required for water productivity analysis at field scale.

Chapter 5

Water productivity analysis of irrigated crops at regional scale

5.1 Introduction

Water productivity analysis helps to understand and identify where and when water can be saved in an irrigation system. Such detailed water use studies are often not possible with limited available information on different hydrological variables and their short- as well as long- term impact on ecohydrological conditions and crop production. Even tools are absent to quantify the required hydrological and biophysical variables, especially at regional scale. In recent years, attempts have been made with field scale models to accommodate spatial heterogeneity at regional scale (D'Urso et al., 1999; Droogers et al., 2000; Droogers and Kite, 2002; Ines et al., 2002).

In this Chapter, *we investigate the aggregation of all combinations of weather-crop-soil-water with representative model input parameters at regional scale.* (see Chapter 3 for details of the proposed methodology). In this context, a case study is conducted for Sirsa district (Chapter 2). The aggregation of so-called *homogeneous* combinations, denoted as '*simulation*' units, is performed in a GIS environment by overlaying the thematic map of weather, land use, soil, water supply, groundwater level and its quality in Sirsa district. Spatial-temporal representative input parameters and boundary conditions attached to the simulations units are either generated through site-specific experiments and satellite images or existing geographical data. The canal and groundwater irrigations, which are important hydrological variables in Sirsa district, are aggregated for different crop combinations at village level. The field scale ecohydrological SWAP model using detailed crop growth, denoted as *SWAP-WOFOST*, is applied in a distributed mode to quantify the hydrological and biophysical variables for all ecohydrological conditions at regional scale.

Apart from the simplifications in the physical characterization of various processes in the natural system, other major sources of error in this distributed modelling could be uncertainties in composing the representative model input parameters at regional scale. Therefore, *a comparison in terms of evapotranspiration between distributed modelling and satellite remote sensing is carried out at different spatial and temporal scales.* Further, the simulated water balances and crop yields are aggregated and analysed in terms of water productivity at the desired scale.

5.2 Schematization and aggregation of spatial information

Spatial information of the variables listed below was collected and aggregated in Sirsa district during the agricultural year 2001-02. For details of methods and source of data used in this study see Chapter 3.

Weather

Daily weather data including radiation, temperature, relative humidity, vapour pressure, wind speed and rainfall are required to define the upper boundary in *SWAP-WOFOST*. The rainfall in Sirsa district is highly erratic in its distribution, and occurs mainly during the monsoon

season from July to September. Fig. 5.1a confirms its variability and Fig. 5.1b its uneven distribution.

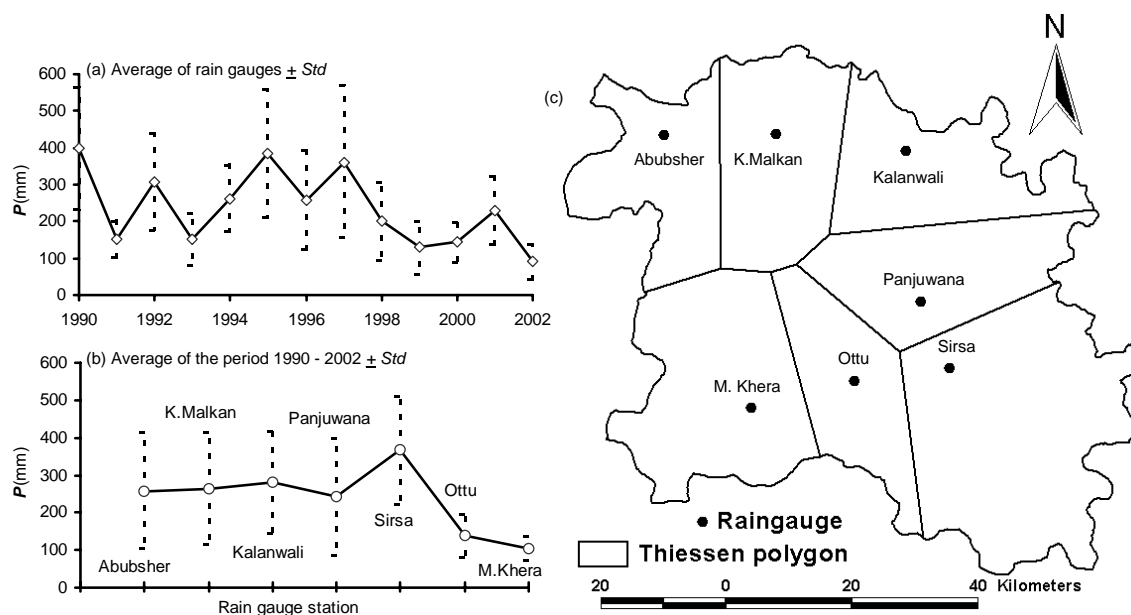


Figure 5.1 The rainfall P (mm) distribution in Sirsa district: (a) temporal variation, (b) spatial variation, and (c) meteorological regions using Thiessen polygons.

The rainfall amount declines from east to west direction. The recorded rainfall during the year 2002 at seven rain gauges spread over the district varied from 60 to 198 mm. It was low as compared to the period from 1990 to 2002, where average annual rainfall amounted from 104 to 367 mm. This spatial and temporal variation in rainfall was taken into account by dividing Sirsa district into seven meteorological regions using the Thiessen polygons (Fig. 5.1c). As there exists no meteorological station in other parts of Sirsa district, the evaporation data from the meteorological station at the ICAR-CRS, Sirsa were assigned to each meteorological region.

Cropping pattern

The satellite remote sensing provides the land use or cropping pattern at regional scale. Bastiaanssen et al. (2003b) performed a land use classification of Sirsa district during the agricultural year 2001-02. A series of consecutive unsupervised classification steps based on the ISODATA clustering algorithm was performed to derive this land use classification. Using two Landsat TM7 images and a record of 249 ground truth points, two land use maps were derived: one for the *rabi* season (Mar 18, 2002) and another for the *kharif* season (Sept 10, 2002). This land use classification resulted into five classes during the *rabi* (winter) with wheat as the main crop, and eight classes during the *kharif* (summer) season (Fig. 5.2a and b).

The local crop data were available only for wheat, cotton and rice (Chapter 3). This limited availability of local crop data and identification of land use classes like shadow/water and other crops (Fig 5.2a and b) affected the reclassification procedure to derive the crop combination map (Fig. 5.2c). In the reclassification, the early and late wheat classes were merged to represent wheat during the *rabi* season. Similarly, the cloud and water/shadow classes identified during the *kharif* season were dissolved to the nearby land use classes. The

reclassified maps of both seasons were combined to derive the crop combination map. Unrealistic combinations, for instance bare soil-rice and wheat-urban, which represented only 2% of the total area, were dissolved to the nearby areas. Considering that wheat was identified with high accuracy, the area under other crops during the *rabi* season was assigned to the second major crop 'oil seed' i.e. mustard. Similarly, assuming that rice was identified with high accuracy due to rice field inundation, the area under other crops during the *kharif* season was assigned to cotton. Finally, four main crop combinations were identified i.e. bare soil-bare soil, wheat-cotton, wheat-rice and mustard-cotton (Fig. 5.2c).

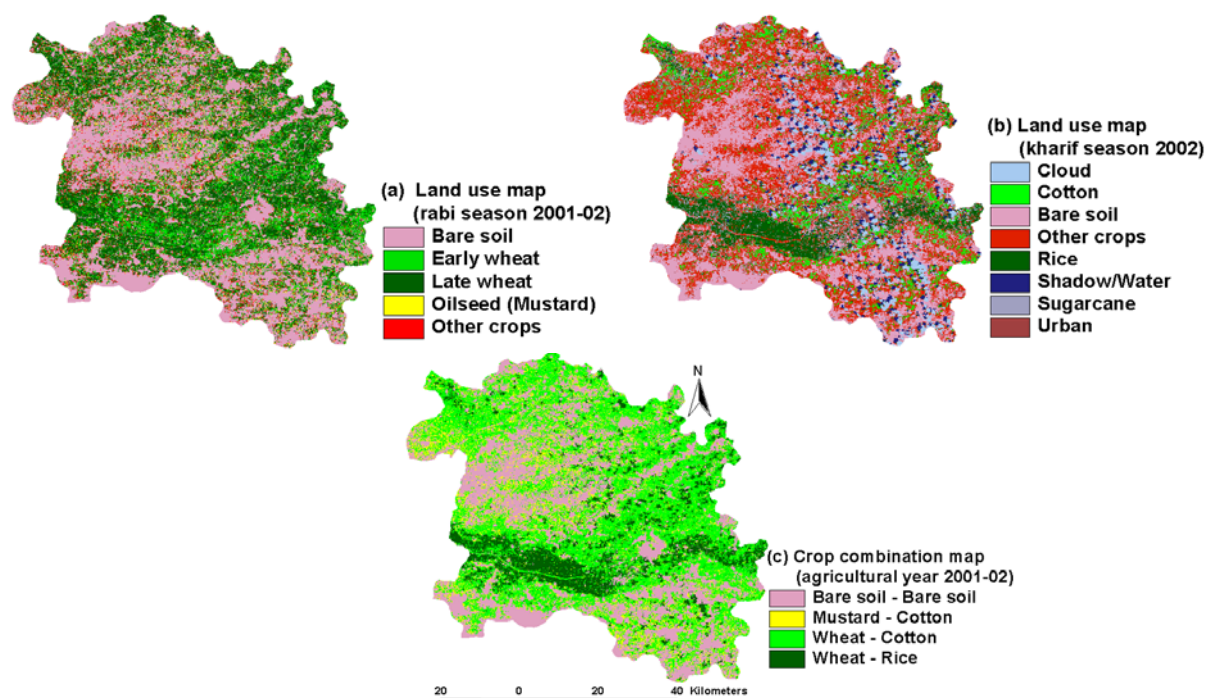


Figure 5.2 Land use classification of Sirsa district based on satellite images (Landsat TM7, spatial resolution 30m × 30m) during the agricultural year 2001-02: (a) the *rabi* season (Mar 18, 2002), (b) the *kharif* season (Sept 10, 2002), and (c) resulting crop combination map (based on the reclassification). (For colour figure see cover page).

Irrigation

Sirsa Irrigation Circle, located at the tail end of Bhakra Irrigation System, distributes the surface irrigation water among the farmers in Sirsa district. To ensure the equal distribution of limited available water, canal supply is rotated over a group of canals according to 'rostering', and then allocated to the individual farmer for a specified period per week in proportion to his land holding at the watercourse level according to 'warabandhi' (Chapter 2). The records of the agricultural area attached with canal water rights, called Culturable Command Area (CCA), are available at watercourse level in each village of Sirsa district. Also, the spatial information on groundwater pumping such as number and average discharge of tubewells is available at village level (Chapter 3). This availability of irrigation information at village level provides opportunities to aggregate irrigation amounts for different crop combinations in each village of Sirsa district.

Canal water supply

To facilitate the canal water distribution, Sirsa district was divided into four main commands (*mc*): Bhakra Main Branch (BMB), Sukchain (SUK), Ghagger (GHG) and Fatehabad Branch (FB) (Fig 5.3). These main commands were further divided into 15 canal commands (*cc*) based on the canals into same priority group i.e. A, B or C. The *CCA* served by the watercourses at village level was accumulated for each canal command, and subsequently for each main command. The agricultural area of a village might be served by more than one canal, and might have *CCA* in several canal commands. In that case, the smallest part of *CCA* was assigned to the largest part, such that a village has only *CCA* in one particular canal command. In this way, each canal command was fitted to the village boundaries (Fig. 5.3).

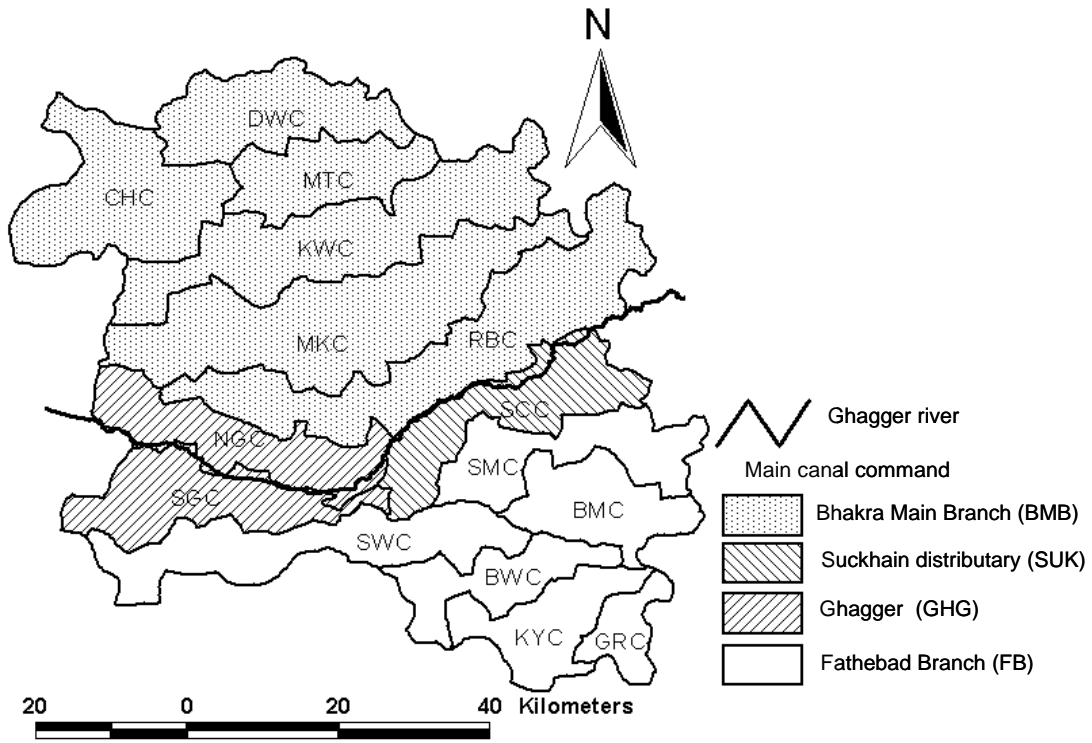


Figure 5.3 Different canal commands in Sirsa district.

The daily water supplies of main commands Q_{mc} [$L^3 T^{-1}$] were calculated from the measured discharge records of inflow and outflow canals, and from Ghagger river (Chapter 3). The calculated Q_{mc} of each main command was rotated every 8 days over canals under different rotational groups i.e. A, B and C giving full water supply to the first priority group, subsequently followed by the second and third priority group:

$$Q_{mc, RG}(t) = \min \left[\sum_{i=1}^{RG} (CCA_i \times CWA), \{Q_{mc} - Q_{SL, mc} - \sum_{i=1}^{RG-1} (CCA_i \times CWA)\} \right] (t) \quad (5.1)$$

where $Q_{mc, RG}$ is the available water supply [$L^3 T^{-1}$] for each rotational group in a main command, $Q_{SL, mc}$ is the seepage loss [$L^3 T^{-1}$] in main canal, CCA is the culturable command area [L^2], CWA is the maximum canal water allowance (1.40 mm d^{-1} for Sirsa Irrigation Circle), i denotes the priority order of the rotational group RG , and t denotes the daily time step.

The calculated $Q_{mc, RG}$ for each rotational group in a main command was allocated to the different canal commands of that particular rotational group. This water allocation is proportional to the CCA served by the canal command:

$$Q_{cc, RG}(t) = \frac{CCA_{cc, RG}}{\sum_{cc, RG=1}^{N_{cc, RG}} CCA_{cc, RG}} Q_{mc, RG}(t) \quad (5.2)$$

where Q_{cc} is the allocated water supply [$L^3 T^{-1}$] to a canal command, and $N_{cc, RG}$ is the total number of canal commands under a particular rotational group in a main command.

In each canal command, the allocated Q_{cc} was converted to the canal water depth $I_{cw, cc}$ [$L T^{-1}$] over the CCA of that canal command:

$$I_{cw, cc}(t) = \frac{(Q_{cc} - Q_{SL, cc} - Q_{SL, wc})}{CCA_{cc}}(t) \quad (5.3)$$

where $Q_{SL, cc}$ and $Q_{SL, wc}$ are the seepage losses [$L^3 T^{-1}$] in distributaries and watercourses in a canal command, respectively.

The calculated $I_{cw, cc}$ of a canal command was assigned uniform to each village served by that particular canal command. Under actual field conditions, the water is allocated to the individual farmers in proportion to their land holding (CCA), while it is distributed over the actual cropped area. Therefore, the assigned $I_{cw, cc}$ was converted to the canal irrigation depth over the crop area of each village:

$$I_{cw}(t) = \frac{I_{cw, cc} \times CCA_{vill}}{CA_{vill}}(t) \quad (5.4)$$

where I_{cw} is the canal irrigation depth [$L T^{-1}$] over the crop area CA_{vill} [L^2] of a village, which was obtained from the reclassified crop combination map (Fig. 5.2c). CCA_{vill} is the culturable command area [L^2] of a village, which was obtained from the records of Irrigation Department, Sirsa.

Estimation of seepage losses requires that dimensions of the conveyance system are known. The conveyance system inside a command has been represented by a hypothetical canal with a discharge capacity equal to the allocated water supply Q_{cc} to this command. The length of the hypothetical canal represents the total length of canals inside the command. The allocated Q_{cc} was distributed linearly over the length of the hypothetical canal.

The dimensions of the assumed hypothetical canal per unit length were computed using empirical relations (Fig. 5.4), which relate the discharge capacity Q to the water flow depth

H_{\max} and bed width W_b . These empirical relations were developed using the design characteristics of the canal network in Sirsa Irrigation Circle.

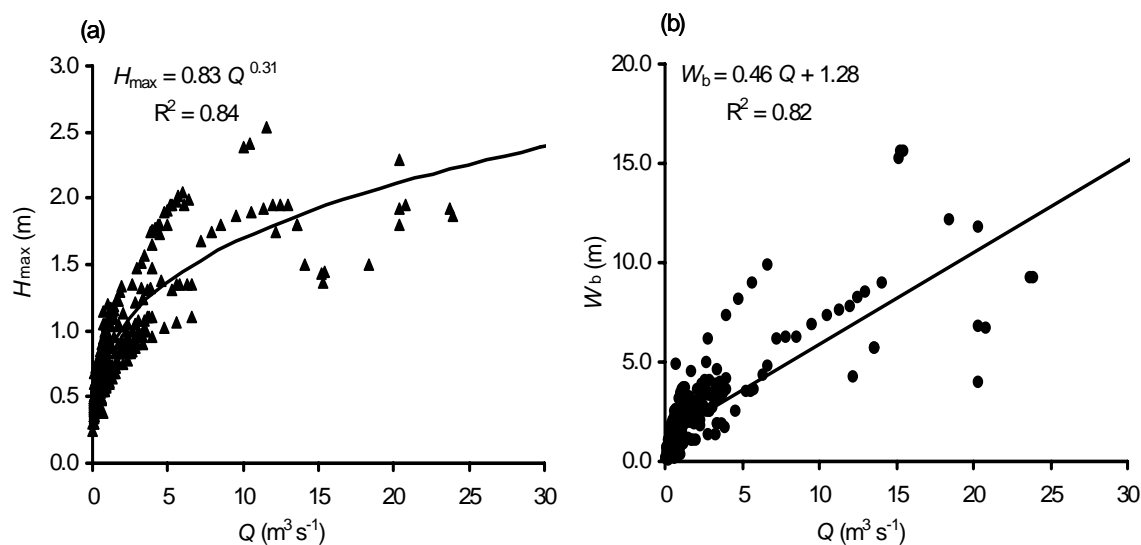


Figure 5.4 Empirical relations for the canal characteristics in Sirsa Irrigation Circle: (a) discharge capacity Q vs. maximum flow depth H_{\max} , and (b) discharge capacity Q vs. bed width W_b .

The seepage loss from the hypothetical canal $Q_{SL,cc}$ [$L^3 T^{-1}$] was estimated:

$$Q_{SL,cc}(t) = SF \times C_{wa}(t) \quad (5.5)$$

where C_{wa} is the wetted area [L^2] of the hypothetical canal, and SF is the seepage factor.

The seepage losses from the main canals $Q_{SL,mc}$ [$L^3 T^{-1}$] and distributaries $Q_{SL,cc}$ [$L^3 T^{-1}$] were estimated using a seepage factor SF equal to $0.065 \text{ m}^3 \text{ d}^{-1} \text{ m}^{-2}$ of the wetted area (*HSMITC* Working Document 1.6).

The seepage loss from the watercourses $Q_{SL,wc}$ [$L^3 T^{-1}$] were estimated by specifying average discharge capacity Q_{wc} [$L^3 T^{-1}$] and seepage rate q_{wc} [$L^3 T^{-1}$] of the watercourses in a canal command:

$$Q_{SL,wc}(t) = q_{wc} \times \frac{(Q_{cc} - Q_{SL,cc})}{Q_{wc}}(t) \quad (5.6)$$

The average discharge capacity Q_{wc} of $3390 \text{ m}^3 \text{ d}^{-1}$ was calculated from the design discharges of the watercourses in Sirsa Irrigation Circle. The specified average seepage rate q_{wc} ranged from 1000 to $1200 \text{ m}^3 \text{ d}^{-1}$ with the higher seepage rate specified for canal commands having lighter textured soils (Table 2.1).

Finally, the seepage losses from the conveyance system Q_{SL} [$L^3 T^{-1}$] were calculated:

$$Q_{SL}(t) = Q_{SL,mc}(t) + Q_{SL,cc}(t) + Q_{SL,wc}(t) \quad (5.7)$$

Groundwater pumping

The crop water requirements represented by the potential evapotranspiration ET_p were estimated by the Penman-Monteith equation (Eq. 3.5) using daily weather data. Simultaneously, the required irrigation depths I_{req} [L] of a crop during the specified irrigation interval I_{int} were calculated by subtracting the rainfall P [L] from the ET_p [L]. The high ET_p rates, particularly during the *khariif* (summer) season, could result in the unrealistic high I_{req} . Therefore, the I_{req} was restricted by a maximum irrigation depth I_{max} [L].

$$I_{req} = \min \left[\sum_{t=1}^{I_{int}} (ET_p - P)(t), I_{max} \right] \quad (5.8)$$

where I_{int} is the irrigation interval (days) of a crop.

The I_{req} are partly supplied through the limited and unreliable canal water irrigation I_{cw} (Eq. 5.4), which is augmented by groundwater pumping in Sirsa district. The irrigation deficit I_{def} [L] during an irrigation interval I_{int} , therefore, was calculated by subtracting the I_{cw} [L] from the I_{req} [L]. Further, the supply of I_{def} through groundwater pumping depends on the maximum groundwater pumping capacity, which is a function of installed pumping capacity and groundwater quality in a region. Hence, the maximum groundwater pumping capacity GW_{max} [$L^3 T^{-1}$] of each village was calculated:

$$GW_{max}(t) = CF_{gw} \times N_{tw} \times D_{tw} \times H_{tw}(t) \quad (5.9)$$

where N_{tw} is the total number of tubewells in a village [-], D_{tw} is the average discharge of the tubewells [$L^3 T^{-1}$], H_{tw} is the average working hours of the tubewells per day [T]. In this study, H_{tw} was specified at 8 hours per day. The groundwater pumping hardly occurs in poor quality ($EC_{gw} > 6 \text{ dS m}^{-1}$) groundwater areas in Sirsa district (Bastiaanssen et al. 1999). In Eq. 5.9, a restriction on groundwater pumping was put through a reduction factor CF_{gw} [-] accounting for groundwater quality EC_{gw} . The value of CF_{gw} was specified at 1.0 for $EC_{gw} < 4 \text{ dS m}^{-1}$, 0.75 for $4 \text{ dS m}^{-1} < EC_{gw} < 6 \text{ dS m}^{-1}$, and 0.5 for $EC_{gw} > 6 \text{ dS m}^{-1}$.

The calculated GW_{max} [$L^3 T^{-1}$] of each village could provide the maximum groundwater irrigation depth $I_{gw, max}$ [$L T^{-1}$] over the crop area CA_{vill} [L^2] of the village:

$$I_{gw, max}(t) = \frac{GW_{max}(t)}{CA_{vill}} \quad (5.10)$$

The actual groundwater irrigation depth I_{gw} [L] during each irrigation interval I_{int} was set equal to the minimum of I_{def} [L] and $I_{gw, max}$ [L]:

$$I_{gw} = \min [I_{def}, (I_{gw, max} \times I_{int})] \quad (5.11)$$

Finally, the actual irrigation depths I [L] for different crops for each irrigation interval were computed by adding I_{cw} [L] and I_{gw} [L] in each village.

The quality of irrigation water C_i [$M L^{-3}$] was calculated as the weighted average based on the depth and quality of both canal and groundwater used:

$$C_i = \frac{C_{cw} I_{cw} + C_{gw} I_{gw}}{I_{cw} + I_{gw}} \quad (5.12)$$

where C_{cw} and C_{gw} are the salt concentration [$M L^{-3}$] of canal I_{cw} and groundwater I_{gw} , respectively. Generally, the irrigation water quality is measured in $dS m^{-1}$, while SWAP simulates the quality as a concentration of solutes. Conversion between the units was carried out using the relation $1 dS m^{-1} = 0.653 mg cm^{-3}$ (Kumar et al., 1996).

Soil

The soil map was prepared by digitizing 10 soil series identified during a reconnaissance survey in Sirsa district (scale 1:50,000) (Ahuja et al., 2001). With the help of soil information on sand, silt, clay and salt concentration of the different soil horizons (Appendix B), the soil profile of each soil series was reduced to two soil layers: topsoil (0-30 cm) and subsoil (30-300 cm) (Table 5.1). The soil map was reduced from 10 to 7 soil types by dissolving the soil series representing about 0.1% of the total area: Khaireka and Jhunpra, and merging the soil series with the same soil texture: Nimla with Ganga (Table 5.1). As an exception, Phaggu and Lambi soil series having similar soil texture were not merged, as Phaggu delineates the saline soils in Sirsa district.

Table 5.1 Information on different soil type in Sirsa district (Ahuja et al., 2001; Malik et al., 2003).

Series No.	Series Name	% area	Soil_ID	% area	Soil depth (cm)	Silt (0.05-0.002)	Clay (<0.002)	OM (%)	C (mg cm ⁻³)	BD (g cm ⁻³)	Soil Texture
1	Nimla	8.6									
2	Saimpal	13.2	1	13.2	0-30 30-300	4.0 5.9	4.0 5.5	0.58 0.38	0.54 0.68	1.65 1.65	Sand Sand
3	Ganga	34.7	2	43.4	0-30 30-300	5.6 9.0	5.6 6.7	0.58 0.38	0.94 0.68	1.65 1.61	Sand Loamy sand
4	Lambi	14.4	3	14.4	0-30 30-300	11.6 9.6	10.3 9.1	0.58 0.49	2.57 11.29	1.65 1.61	Loamy sand Sandy loam
5	Darbi	8.1	4	8.1	0-30 30-300	48.9 66.7	16.7 22.0	0.53 0.25	1.16 2.48	1.37 1.45	Loam Silt loam
6	F. Baidwala	11.0	5	11.2	0-30 30-300	66.7 61.4	20.0 21.3	0.60 0.25	2.44 1.82	1.39 1.45	Silt loam Silt loam
7	H. Khurd	8.4	6	8.4	0-30 30-300	54.0 63.9	23.0 27.7	0.53 0.41	2.57 1.73	1.37 1.47	Loam Silty clay loam
8	Phaggu	1.3	7	1.3	0-30 30-300	20.3 28.0	9.7 12.0	0.46 0.49	27.21 12.70	1.65 1.61	Loamy sand Sandy loam
9	Khaireka	0.1									
10	Jhunpra	0.1									

In most of the district, soil texture varies from sand to sandy loam, except in a belt along Ghagger river where it varies from silt loam to silt clay loam. The organic matter OM and bulk density BD of different soil types were based on the soil analysis of samples from the farmer fields (Malik et al., 2003).

Groundwater level and its quality

The spatial information on groundwater levels and its quality was generated using measurements at 164 observation wells spread over Sirsa district. The Inverse Distance Weighted (IDW) method in ArcView Spatial Analyst was used to interpolate between the observation points, and subsequently to summarize the mean concentrations at village level.

In June 2000, the groundwater level in Sirsa district varied from less than 3 m to 25 m below surface (Fig. 5.5a). A small area of about 5%, mainly in the northeast part of the district, was under shallow groundwater level (i.e. < 3 m).

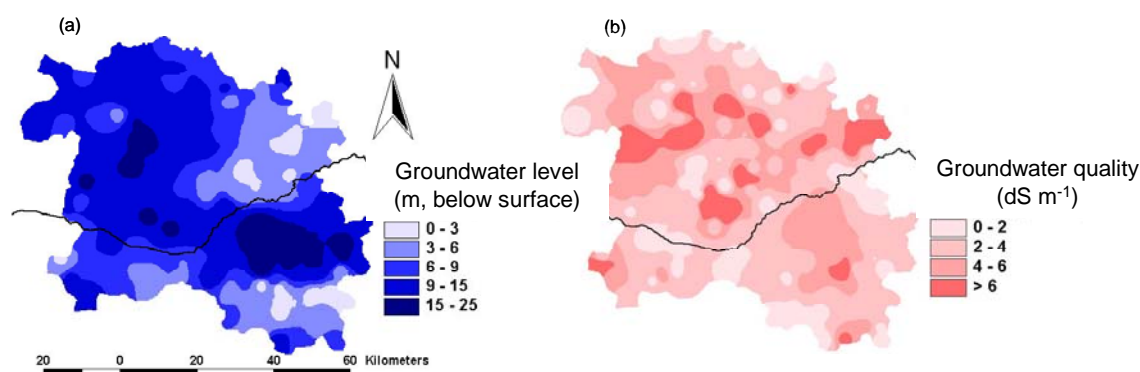


Figure 5.5 Groundwater conditions in Sirsa district: (a) groundwater level (m, below surface) in June 2000, and (b) groundwater quality (dS m^{-1}) in June 1995.

The groundwater quality measurements after the year 1995 were not available at most of the observation wells. The groundwater quality map (Fig. 5.5b) was based on the latest available measurements of the year 1995. In June 1995, the groundwater quality varied from 0.5 to 15.5 dS m^{-1} . It is relatively poor in the northern parts. In the corridor of Ghagger river, the groundwater quality is generally good, which is mainly due to the river seepage during the monsoon (rainy) period.

Stratification

The term ‘*stratification*’ refers to the *process of aggregation* of ‘*simulation*’ units (SU). Most of the spatial information on irrigation, groundwater level and its quality was aggregated at village level in Sirsa district. The weather map was also combined with the village map (323 village boundaries), assigning each village to an individual weather region (Fig. 5.1 c).

The stratification of Sirsa district was finally performed by overlaying 3 thematic maps: crop combination, soil and village boundary (Fig. 5.6). First, the soil map was combined with the crop combination map at grid size of $30\text{m} \times 30\text{m}$ (pixel size of Landsat TM7 image). Second, the derived crop-soil combination was overlaid on the village boundary map, which resulted into a total number of 3168 simulation units. A large number of relatively small simulations units were generated: 50% of the total number of units represented only 7% of the total study area. These small units could be merged to adjoining areas, and almost 50% calculation time could be saved. This merging would further simplify the spatial heterogeneity. We did not merge these small units in order to have an accurate comparison between distributed modeling and satellite remote sensing at regional scale.

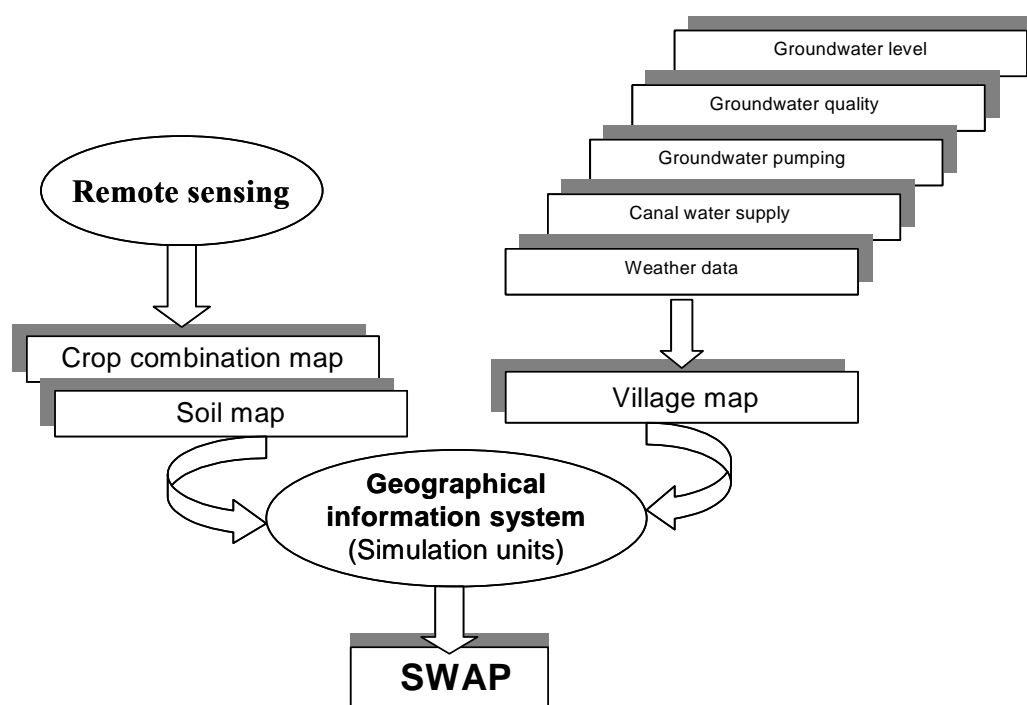


Figure 5.6 Schematic representation of the stratification procedure to aggregate simulation units (SU) for SWAP simulations at regional scale.

5.3 Parameterization of distributed SWAP model

Upper boundary

The upper boundary was specified by the computed potential evapotranspiration ET_p and spatially distributed irrigation I and rainfall P fluxes. The ET_p was computed by the Penman-Monteith equation (Eq. 3.5) using the daily meteorological data including variables such as radiation, temperature, humidity and vapour pressure. As there exists no meteorological station in other parts of Sirsa district, the evaporation data from the meteorological station at the ICAR-CRS, Sirsa were assigned to each meteorological region (Fig. 5.1c), while the rainfall was specific.

The crop and irrigation calendar of a crop varies from field to field, generally within a range of 10 to 15 days. Following Eqs. 5.1 to 5.12, the irrigations of different crop combinations were calculated at village level using the specified average crop and irrigation calendar. *In this way, the sowing and irrigations of a particular crop were specified on the same day over the whole study area, which is a simplification of actual conditions.*

Table 5.2 Average crop and irrigation calendar for irrigated crops in Sirsa district.

Crop	Crop Calendar			Irrigation Calendar		
	Sowing	Emergence	Harvest	Irrigation	Pre-sowing	Irrigation interval (days)
Wheat	16-Nov	23-Nov	30-Apr	6	4-Nov	37, 32, 35, 24, 22
Mustard	6-Nov	12-Nov	30-Apr	4	1-Nov	52, 45, 40
Cotton	5-May	9-May	31-Oct	6	2-May	45, 25, 30,30, 35
Rice		21-Jun*	31-Oct	29	19-Jun	7, 4, 4, 5, 5, 5, 4, 3, 3, 3, 5, 3, 3, 3, 3, 3, 3, 3, 3, 4, 4, 3, 3, 4, 4, 4, 4, 4

* Transplanting

The average crop and irrigation calendar (Table 5.2) for wheat, cotton and rice were derived from the observations at farmer fields in Sirsa district (Malik et al., 2003), and for mustard from the existing literature (Singh and Sharma, 1993; Bastiaansen et al., 1996). The pre-sowing irrigation at farmer fields is generally heavier than the following irrigations. Therefore, the maximum pre-sowing irrigation depth (Eq. 5.8) was set equal to 10 cm for wheat and cotton, and 15 cm for mustard and rice. The following irrigations during the growing season were restricted to a maximum depth of 8 cm for wheat, cotton and mustard, and of 5 cm for rice.

Crop data

The detailed crop growth *SWAP-WOFOST* model was applied for simulation of crop growth at regional scale. The applicability of *SWAP-WOFOST* for regional crop simulations has been verified by comparing with the calibrated and validated *SWAP*, the latter used the measured crop growth at farmer fields in Sirsa district (Chapter 4).

In addition to Table 4.1, crop parameters for mustard were derived from the existing literature for the study region and similar climatic conditions (Aggarwal et al., 2001; Aulakh and Pasricha, 1999; Singh et al., 1996; Singh, 1996; Bastiaansen et al., 1996; Arora et al., 1993; Boons-Prins et al., 1993; Tanji, 1990; Penning et al., 1989; van Heemst, 1988). The specified main crop parameters for mustard were as follows:

- Temperature sum from emergence to anthesis, TSUMEA = 750 °C
- Temperature sum from anthesis to maturity, TSUMAM = 1300 °C
- Light extinction co-efficient, K_{gr} = 0.375
- Light use efficiency, ε = 0.40 kg ha⁻¹ hr⁻¹ / J m² s⁻¹
- Maximum CO₂-assimilation rate, A = 40 kg ha⁻¹ hr⁻¹
- Critical salinity level, EC_{max} = 7.4 dS m⁻¹
- Decline per unit EC , EC_{slope} = 6.6 % dS m⁻¹.

The specified critical pressure head, h_1 , h_2 , h_{3h} , h_{3l} and h_4 (cm) values for mustard were the same as for cotton (Table 4.1). In case of bare soils, only soil evaporation was simulated.

Soil data

The specified soil profile was divided into a topsoil (0-30 cm) and subsoil (30-300 cm). The flow domain was further discretized into a total of 49 compartments with a nodal distance of 1 cm for the top 10 compartments, followed by 5 cm for the next 20 compartments and 10 cm for the remaining soil profile. To solve Richards' equation (Eq. 3.2), *SWAP* also requires the soil hydraulic functions $\theta(h)$ and $K(\theta)$ (Eq 3.3 and 3.4).

The direct measurement of these soil hydraulic parameters is difficult, especially at regional scale. As an alternative, *pedotransfer functions* (PTFs) (Wösten et al., 1998) were applied, which relate $\theta(h)$ and $K(\theta)$ to easily measured soil information: soil texture, organic matter and bulk density. This soil information (Table 5.1) in Sirsa district was used to derive the soil hydraulic parameters of different soil types (Fig 5.7).

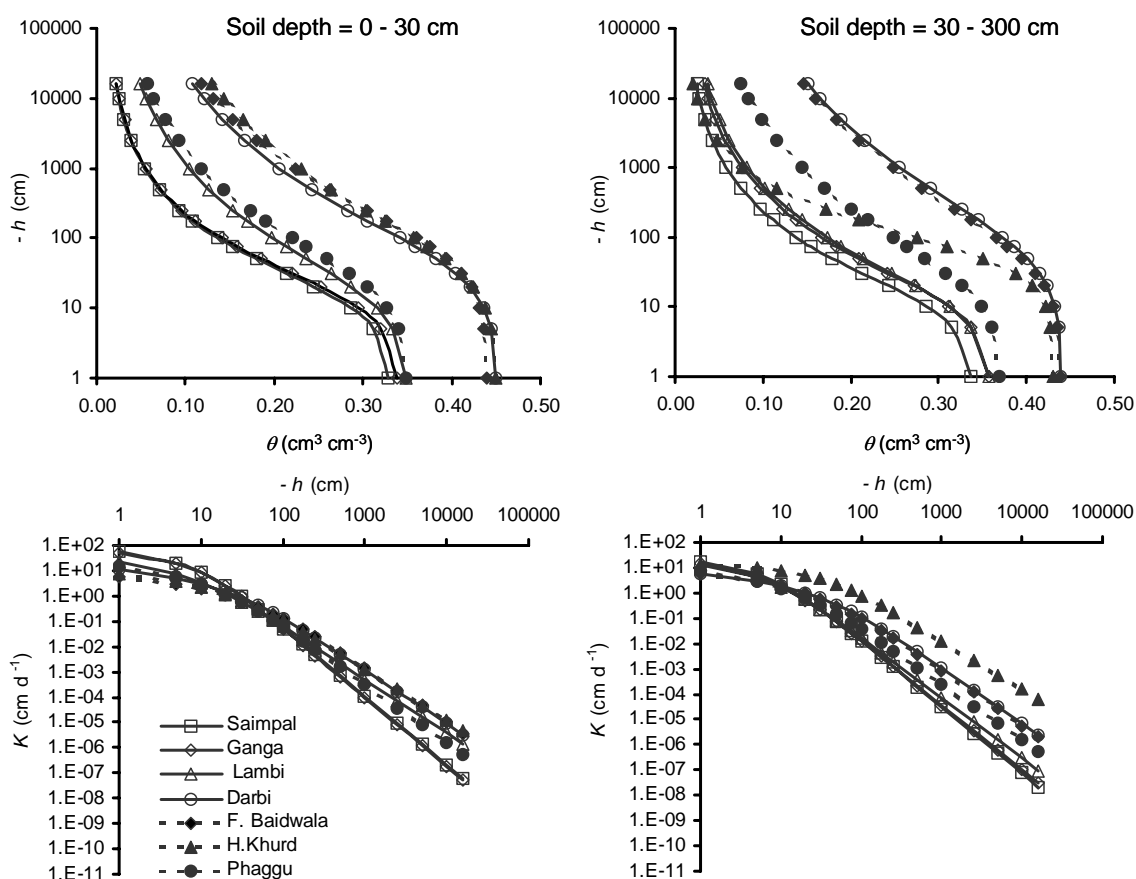


Figure 5.7 The soil retention (pressure head h vs. moisture content θ) and hydraulic conductivity (hydraulic conductivity K vs. pressure head h) curves for different soil types in Sirsa district [derived by the pedotransfer functions (Wösten et al., 1998) using the soil textural information (Table 5.1; Ahuja et al., 2001; Malik et al., 2003)].

For salt transport, the dispersion length L_{dis} (Eq. 3.15) was set to 5 cm (Nielsen et al., 1986). In addition to Darcy's law (Eq. 3.7), the empirical function of Black et al. (1969) was used to limit the soil evaporation rate, and a value of 0.35 cm d^{-1} was specified for the evaporation coefficient. To maintain surface water ponding for optimal rice growing conditions, the soil is puddled to reduce the percolation from field irrigations. In order to capture the reduced percolation in simulation of soil water flow during the rice growing period, the K_{sat} of the upper 30 cm soil layer was reduced to 20% (Singh et al., 2001). The reduction in soil evaporation according to the empirical function of Black et al. (1969) was also set off during the rice growing period.

Lower boundary and initial condition

The bottom fluxes were calculated for two different conditions: shallow ($< 3 \text{ m}$) and deep groundwater level ($> 3 \text{ m}$). We assumed the free drainage (Eq. 3.11) under deep groundwater level conditions. Under shallow groundwater level conditions, the bottom fluxes can be considered as 'flux from deep aquifer' as function of the height of the groundwater level. The presence of a 'deep' aquifer was realized by assuming a semi-confined layer with a vertical resistance c_{conf} of 1000 d. Then, the Cauchy condition (Eq. 3.12) was applied to calculate the

bottom flux q_{bot} from the head difference between the phreatic groundwater level ϕ_{gwl} and the hydraulic head ϕ_{aquif} [L] in the deep aquifer, which was prescribed assuming a sinusoidal wave. No data were available for the year 2001-02, so the groundwater levels were based on the average groundwater levels measured during the years 1999 and 2000. The mean ϕ_{aquif} [L] in the aquifer was set equal to the mean groundwater levels measured during June and October, and the amplitude of the sinus wave was the difference between the mean groundwater level and the groundwater level measured in June. First day number with high ϕ_{aquif} [L] was specified according to the measurements either on July 1 or October 1 in a year.

The initial soil salinity concentrations in the soil profiles were specified according to the collected soil information in Sirsa district (Table 5.1). Running SWAP for one year in advance with the same input generated the spatial variation of soil moisture at the start of study period.

5.4 Results and Discussion

After assigning the spatially varying rainfall, irrigation, crop, soil and lower boundary condition, *SWAP-WOFOST* was run independently for each simulation unit for two years starting from Nov 1, 2000 to Oct 31, 2002. In this analysis, the simulated water and salt balances and crop yields from Nov 1, 2001 to Oct 31, 2002 were aggregated following Eqs. 3.21 and 3.22, and were analyzed at the desired scales in Sirsa district. The experimental year was further divided into two crop seasons: *rabi* (wheat/mustard) from Nov 1, 2001 to Apr 30, 2002, and *kharif* (cotton/rice) from May 1, 2002 to Oct 31, 2002.

5.4.1 Cropping pattern and irrigation water distribution

Table 5.3 presents the results of land use identified by satellite remote sensing and its reclassification for regional analysis. The identification of land use classes like cloud, shadow/water and other crops (Fig 5.2a and b) affected the reclassified crop combination map (Fig. 5.2c). *The extent of the main crops (wheat, mustard, cotton and rice) in Sirsa district was well represented in the reclassified crop combination map.* Note that the latter map, which was involved in this regional analysis, was limited to the main crop combinations i.e. bare soil-bare soil, wheat-rice, wheat-cotton and mustard-cotton (Fig. 5.2c). It implies that some other crops in Sirsa district were represented by one of the main crops. This simplification, however, was considered to be acceptable as, according to the statistical data of the year 2000-01, the area under other crops was very small (Table 5.3).

The large portion of other crops identified by satellite remote sensing was due to the poor land use classification. For instance 34% of other crops identified during the *kharif* season was likely to be cotton, as the cotton area identified by satellite remote sensing was approximately 1/5 of the statistical record. The accuracy of land use classification depends on several factors such as quality of satellite images (cloud freeness), number of images processed and extent of ground truth data. The land use during the *kharif* season identified as shadow/water and cloud show that the quality of the used Landsat TM7 image (Sept. 10, 2002) is poor. The identification of cotton was further poor due to insufficient ground truth data (i.e. only 75 records) and poor crop stand (Bastiaanssen et al., 2003b).

Table 5.3 Land use classification (% of the total area of 4270 km²) in Sirsa district during the *rabi* (winter) and the *kharif* (summer) season of the agricultural year 2001-02.

Land use	Reclassification		Satellite remote sensing		Statistical (2000-01)	
	<i>rabi</i>	<i>kharif</i>	<i>rabi</i>	<i>kharif</i>	<i>rabi</i>	<i>kharif</i>
Wheat	55	-	47	-	57	-
Cotton	-	56	-	9	-	47
Rice	-	13	-	10	-	9
Oil seed (Mustard)	14	-	3	-	9	-
Sugarcane	-	-	-	5	-	-
Other crop	-	-	9	34	1	4
Bare soil / settlements	31	31	41	30	33	40
Water / shadow	-	-	-	4	-	-
Cloud	-	-	-	8	-	-
Total Crop Area	69	69	59	58	67	60

During the agricultural year 2001-02, about 69% of the total area (4270 km²) of Sirsa district was under cultivation (Table 5.3). Fig. 5.8 clearly presents wheat as a dominating crop during the *rabi* (winter), and cotton during the *kharif* (summer) season. The wheat intensity, defined as % of the total crop area, varied from 63 to 93% among different canal commands with an average of 80% for Sirsa district (Fig. 5.8a). Similarly, cotton intensity ranged from 44 to 95% among different canal commands with an average of 82% for the district (Fig. 5.8b).

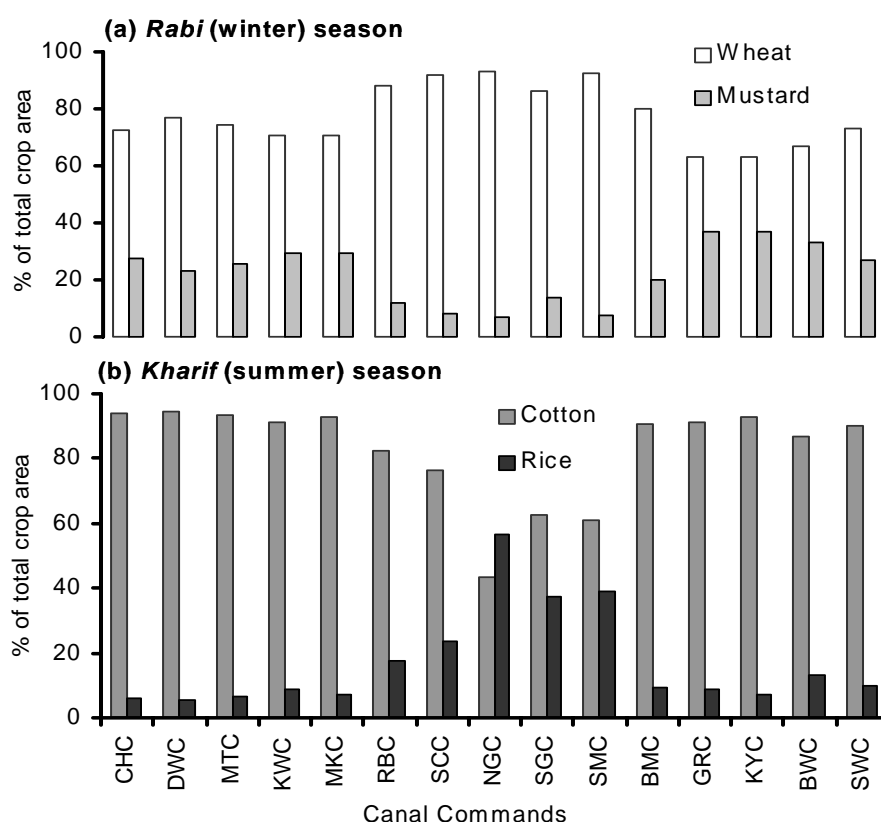


Figure 5.8 Intensity (% of the total crop area) of the main crops in different canal commands of Sirsa district during (a) the *rabi* (winter), and (b) the *kharif* (summer) season of the agricultural year 2001-02. This figure is based on the reclassified crop combination map (Fig 5.2c). The location of different canal commands is shown in Fig. 5.3.

The other major crops in Sirsa district are mustard during the *rabi* (winter), and rice during the *kharif* (summer) season. Rice is mainly cultivated in the central commands: NGC, SGC, SMC and SCC. The highest rice intensity of 56% in NGC is the result of fine textured soils (i.e. silt loam to silt clay loam) and access to good quality ($< 4 \text{ dS m}^{-1}$) groundwater along the belt of Ghagger river.

Successful production of these high water demanding crops in Sirsa district is not possible without supplemental irrigation, even in the monsoon season. During the agricultural year 2001-02, the net measured canal water inflow in Sirsa district was 1920 million m^3 . Following Eqs. 5.1 to 5.7, this measured canal water inflow into the four main commands (BMB, SUK, GHG and FB) was distributed to different canal commands in proportion to their CCA (Table 5.4).

Table 5.4 Estimated canal water inflow in Sirsa district during the agricultural year 2001-02.

Spatial Scale	CCA	Crop area	Canal inflow	Seepage loss	Average canal irrigation *
	(km^2)	(km^2)	Mill. $\text{m}^3 \text{ y}^{-1}$	(%)	(mm y^{-1})
District level					
Sirsa	3332	2959	1920	40.8	384
Main Canal Command level					
Bhakra Main Canal (BMB)	1850	1599	1314	42.1	476
Sukchain (SUK)	222	228	53	39.6	140
Ghagger (GHG)	423	435	137	36.9	199
Fathebad (FB)	837	698	417	38.3	368
Canal Command level					
Chotala distry. (CHC)	321	280	223	40.8	473
Dabwali distry. (DWC)	217	181	151	39.7	502
Mithri distry. (MTC)	172	137	120	39.1	531
Kaluwana distry (KWC)	402	327	280	40.4	510
Mammer Khera distry (MKC)	296	255	206	41.6	472
Rori branch (RBC)	442	418	308	42.5	424
Sukchain canal (SCC)	222	228	53	39.6	140
Northern ghagger canal (NGC)	226	235	73	33.5	207
Southern ghagger canal (SGC)	197	200	64	40.7	189
Sirsa Major distry. (SMC)	192	188	95	38.1	313
Banmandori distry. (BMC)	144	119	71	39.5	364
Gigorani distry. (GRC)	54	43	27	34.4	408
Kutiyana distry. (KYC)	124	97	61	33.6	421
Baruwali distry. (BWC)	122	97	60	35.7	402
Sheranwali distry. (SWC)	201	156	99	41.6	372

* Average canal irrigation is calculated over the crop area based on the reclassified crop combination map (Fig. 5.2c)

The seepage losses (canal + watercourses) from the conveyance system were estimated at 34 to 43% of the net canal inflow in different canal commands. Based on a comprehensive water distribution modelling, Boels et al. (1996) also estimated about 35% of the total annual net inflow as average annual seepage loss from the conveyance system of Sirsa Irrigation Circle during the period from 1977 to 1991. In a recent study, Mandal (2003) observed a reduction

in discharge from upstream end to downstream end of 36 to 54% in two watercourses in Hisar district, which adjoins to Sirsa district.

Fig. 5.9 presents the estimated mean annual canal and groundwater irrigation over the crop area in different canal commands. The canal irrigation varied from 140 mm y⁻¹ (SCC) in the central parts to 531 mm y⁻¹ (MTC) in the northern parts (Fig. 5.9a). The large share of the measured canal inflow as compared to the share of CCA and crop area in BMB (Fig. 5.9b) confirms a relatively high canal water supply in the northern parts of Sirsa district. On the other side, the low share of the measured canal inflow as compared to the share of CCA and crop area in GHG and SUK presents the high groundwater use in the central parts. Following Eqs. 5.8 to 5.11, the estimated mean annual groundwater irrigation were higher in the central commands: NGC, SGC and SCC (Fig. 5.9a). The highest groundwater irrigation was estimated at 1021 mm y⁻¹ in NGC, which was pumped to irrigate the high water consuming wheat-rice cultivation (Fig. 5.8).

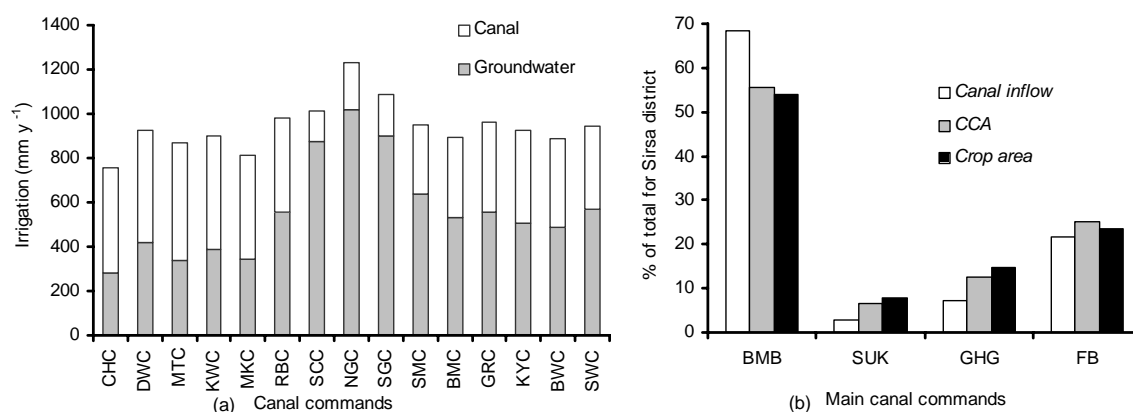


Figure 5.9 (a) Estimated mean annual canal and groundwater irrigation (mm y⁻¹) over the crop area of different canal commands, and (b) % share of the measured canal inflow, CCA and crop area of different main commands in Sirsa district during the agricultural year 2001-02. The crop area was derived from the reclassified crop combination map (Fig 5.2c). The location of different canal and main commands is shown in Fig. 5.3.

The estimated canal irrigation over the entire Sirsa district was about 1.05 mm d⁻¹, which was only 20% of the estimated average ET_p rate of 5.5 mm d⁻¹. In other words, considering an average annual irrigation requirement of 1000 mm for crop production, the canal irrigation of 384 mm y⁻¹ was only sufficient for 1/3 of the crop area. As a result, the groundwater pumping over the entire district was as high as 560 mm y⁻¹.

5.4.2 Comparison of distributed modelling and satellite remote sensing

To evaluate the accuracy and reliability of spatial aggregation of representative input parameters, the evapotranspiration ET simulated by distributed *SWAP-WOFOST* modelling was compared with independent satellite remote sensing based ET data at different spatial and temporal scales. The satellite remote sensing ET data used in this study were estimated by SEBAL during the same period (Bastiaanssen et al., 2003b). For this comparison in this section only, the ET estimated by SEBAL and distributed *SWAP-WOFOST* modelling is referred to as ET_{RS} and ET_{SW} , respectively.

Note that the aggregated simulation units were based on the reclassified crop combination map (Fig. 5.2c). Therefore, a one to one comparison of ET_{RS} and ET_{SW} for all these units makes no sense. For instance the SEBAL algorithm did not estimate ET_{RS} of pixels identified as shadow and cloud. However, these pixels might be assigned to the crop area during the reclassification procedure, and subsequently simulated as a crop by *SWAP-WOFOST*.

For a fair comparison, the simulated ET_{SW} for independent simulation units (3168) was downscaled to the scale of ET_{RS} estimation ($30\text{m} \times 30\text{m}$, pixel size of Landsat TM7 image), and subsequently aggregated over the main land use areas identified by satellite remote sensing. Note that cotton area identified by satellite remote sensing was only 9% of the total area, which was approximately 1/5 of the statistical record of cotton area (Table 5.3). The other crops identified by satellite remote sensing, corresponding to 34% of the total area during the *kharif* season, were likely to be cotton. Therefore, after merging the other crops with the cotton, the ET_{RS} and ET_{SW} were compared over the 43% cotton area. Fig. 5.10 shows a close agreement between ET_{RS} and ET_{SW} over the wheat, mustard and rice areas, with a slightly lower simulation of ET_{SW} over the cotton area. The mean ET_{SW} over the cotton area was 526 mm, which was 15% lower than the mean ET_{RS} .

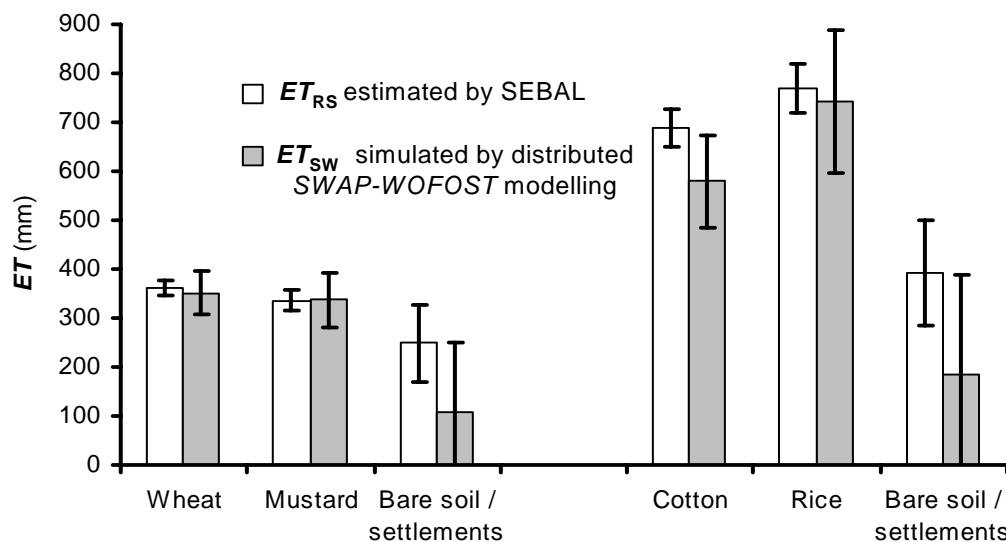


Figure 5.10 Actual evapotranspiration ET (mm) (mean \pm standard deviation) estimated by the remote sensing algorithm SEBAL and the distributed *SWAP-WOFOST* modelling over the main land use in Sirsa district during the agricultural year 2001-02. The main land uses were identified in a land use classification by the ISODATA clustering algorithm using two Landsat TM7 images: one (Mar. 18, 2002, Fig. 5.2a) for the *rabi* (winter) season, and another (Sept. 10, 2002, Fig. 5.2b) for the *kharif* (summer) season.

Fig. 5.10 further shows a high discrepancy between ET_{RS} and ET_{SW} over the bare soil/settlements area, termed as bare soil hereafter. For further insight, the ET_{RS} and ET_{SW} were compared at 314 selected bare soil simulation units of size ranging from 1.21 to 32.80 km², which represented about 88% of the total bare soil area (1281 km²) identified by satellite remote sensing. The simulated ET_{SW} of these bare soil units varied from 11 to 25 mm during the *rabi* season (Fig. 5.11a), and from 45 to 123 mm during the *kharif* season (Fig. 5.11b). This bare soil simulation accounts for soil evaporation only, which corresponds to the rainfall received. The total rainfall recorded at seven meteorological regions of Sirsa district (Fig. 5.1c) varied from 3 to 11 mm during the *rabi* (non-monsoon) season, and from 62 to 177 mm

during the *kharif* (monsoon) season. The aggregated ET_{RS} over the same selected bare soil units varied from 111 to 301 mm during the *rabi* season (Fig. 5.11a), and from 122 to 506 mm during the *kharif* season (Fig. 5.11b). Further, the ET_{RS} of an individual bare soil pixel (30m \times 30m) was as high as 391 mm during the *rabi* season, and 849 mm during the *kharif* season. This indicates that poor or small size crop fields lying in the dominating bare soil areas might be identified as bare soil by satellite remote sensing. Note that the area identified as bare soils by satellite remote sensing was 25% higher than the statistical record of the bare soil during the *rabi* season of the agricultural year 2000-01 (Table 5.3).

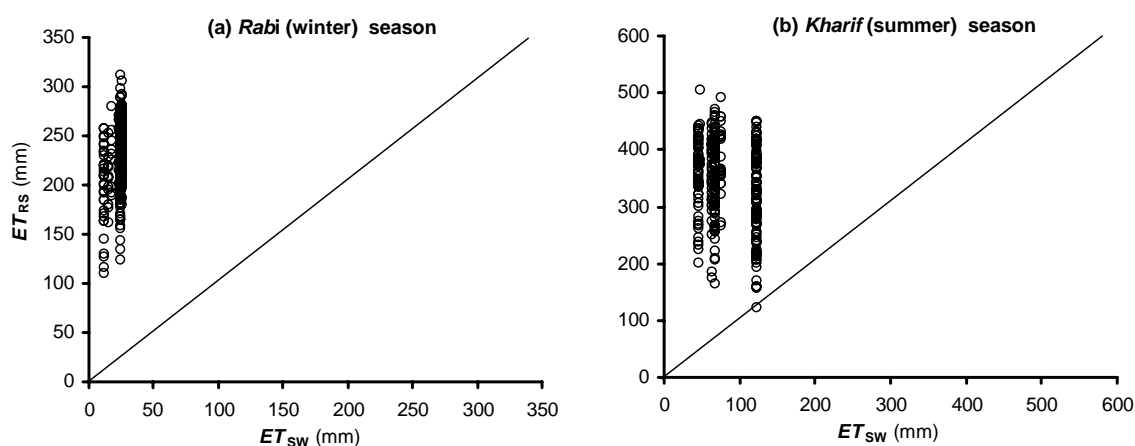


Figure 5.11 ET_{RS} vs. ET_{SW} over the bare soils in Sirsa district during (a) the *rabi* (winter), and (b) the *kharif* (summer) season of the agricultural year 2001-02. The bare soils were identified in a land use classification by the ISODATA clustering algorithm using two Landsat TM7 images: one (Mar. 18, 2002, Fig. 5.2a) for the *rabi* (winter) season, and another (Sept. 10, 2002, Fig. 5.2b) for the *kharif* (summer) season.

The parameterization of distributed *SWAP-WOFOST* modelling depends upon the type of land use or crop identified, which subsequently affects the simulation of water and salt balances and crop yields. Therefore, *the low accuracy in the land use classification might affect the results of distributed modelling at regional scale.*

The simulated ET_{SW} of the selected bare soil units varied from 11 to 25 mm during the *rabi* season (Fig. 5.11a), and from 45 to 123 mm during the *kharif* season (Fig. 5.11b). At the same time, the simulated mean ET_{SW} over the whole bare soil area identified by satellite remote sensing was 107 mm during the *rabi* season, and 183 mm during the *kharif* season (Fig. 5.10). This was due to the assignment of some bare soil area to the crop area during the reclassification procedure (Fig 5.2c). For instance 41% area identified as bare soil/settlements by satellite remote sensing during the *rabi* season was reduced to 31% bare soil in the reclassified crop combination map (Table 5.3). To evaluate the effect of such simplifications, a comparison of the aggregated annual ET_{RS} and ET_{SW} was carried out for different commands in Sirsa district (Fig. 5.12).

The simulated mean annual ET_{SW} over different canal commands was 1 to 29% lower than the mean annual ET_{RS} . Figure 5.12 clearly presents that the differences in ET_{RS} and ET_{SW} were low in the canal commands with high crop area, presented as % of the total area. Note the small differences of 13 and 38 mm in the annual ET_{RS} and ET_{SW} for SCC and NGC with 87 and 94% crop area, respectively. The simulated mean annual ET_{SW} over the entire Sirsa

district was 689 mm, which was 15% lower as compared to the mean annual ET_{RS} of 809 mm. This was caused mainly by the differences in ET_{RS} and ET_{SW} over the bare soils (Fig. 5.10 and 5.11)

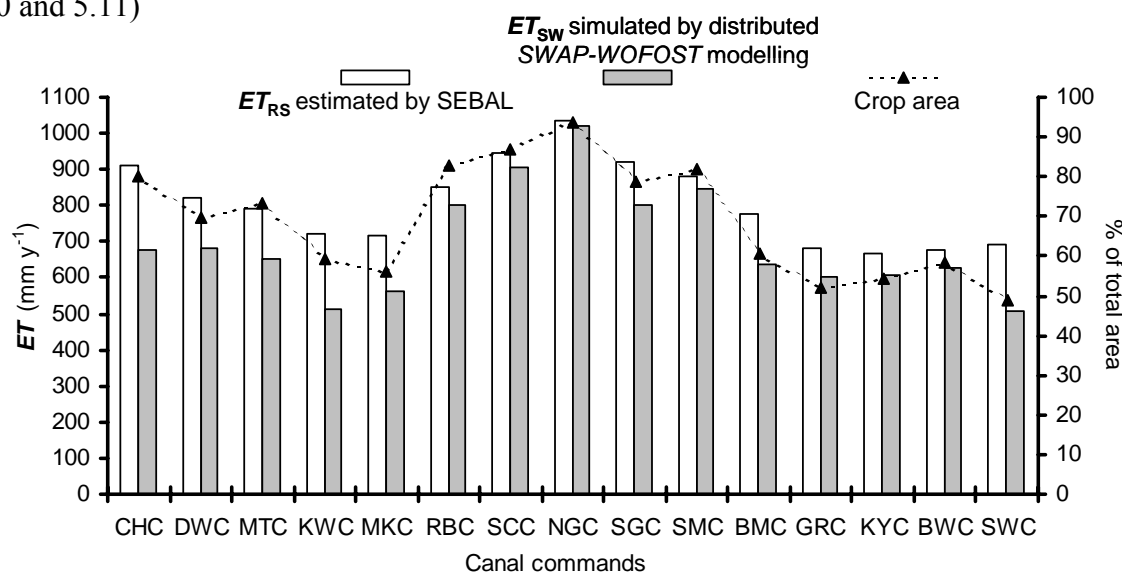


Figure 5.12 Mean annual actual evapotranspiration ET (mm y^{-1}) estimated by the remote sensing algorithm SEBAL and the distributed *SWAP-WOFOST* modelling, and crop area of different canal commands in Sirsa district during the agricultural year 2001-02. The crop area, presented as % of the total area, is based on the reclassified crop combination map (Fig 5.2c). The location of different canal commands is shown in Fig. 5.3.

The accuracy and reliability of spatial aggregation of representative input parameters was further evaluated by comparing the simulated crop yields with independent data obtained through satellite remote sensing, field experiments and statistical records (Table 5.5). Malik et al. (2003) conducted the crop cutting measurements at 17 farmer fields for wheat, 10 for cotton and 5 for rice in Sirsa district during the agricultural year 2001-02. Bastiaanssen et al. (2003b) applied SEBAL to estimate the total dry matter DM production of wheat, cotton and rice over the entire Sirsa district during the same year. They estimated the mean grain (or seed) yields Y_g using an effective harvest index HI , defined as the ratio of Y_g/DM . The simulated mean water and salt limited Y_g for wheat, cotton and mustard are in agreement with SEBAL estimation, field measurements and statistical data (Table 5.5).

Table 5.5 Mean crop grain (or seed) yields Y_g (ton ha^{-1}) of the main crops (wheat, mustard, cotton and rice) obtained through the distributed *SWAP-WOFOST* modelling (this study), the remote sensing algorithm SEBAL (Bastiaanssen et al., 2003b) and the field measurements (Malik et al., 2003) in Sirsa district during the agricultural year 2001-02. *Mean* values apply to the entire area under a particular crop. *Std* denotes the standard deviation, and *HI* denotes the effective harvest index, defined as the ratio of grain (or seed) yield Y_g to the total dry matter DM production.

Source / Crop	Wheat			Mustard			Cotton			Rice		
	Mean	Std	HI	Mean	Std	HI	Mean	Std	HI	Mean	Std	HI
<i>SWAP-WOFOST</i> *	4.8	1.0	0.35	1.6	0.4	0.25	2.0	0.5	0.22	3.5	2.5	0.42
SEBAL	4.4	0.3	0.39				2.2	0.3	0.21	3.7	1.1	0.45
Field measurements	4.5	1.5	0.42				2.1	1.1	0.16	8.1	0.6	0.46
Statistical data**	4.2			1.4						3.2		

* Water and salt limited Y_g considering 80% grain (or seed) in simulated storage organs for wheat, 81% for rice and 44% for cotton and mustard. The Y_g include 14% moisture for wheat, 16% for rice and 15% for cotton and mustard.

** Statistical data recorded by Department of Agriculture, Sirsa for wheat and mustard during the agricultural year 2000 - 01, and for rice during the agricultural year 2001-02 (Source <http://sirsa.nic.in/htfiles/25agriculture.html>).

The measured mean Y_g of 8.1 ton ha⁻¹ at the selected rice fields was almost double the amount simulated by distributed *SWAP-WOFOST* modelling, and estimated by SEBAL over the entire district. The standard deviation of rice Y_g estimated by SEBAL was high, which shows large variations in the rice growing conditions in Sirsa district. The low standard deviation (0.6 ton ha⁻¹) of rice Y_g during the field measurements clearly indicates that the selected rice fields were located in the high productive areas. The simulated water and salt limited Y_g at two of these selected rice fields were about 7.3 and 8.4 ton ha⁻¹ (Chapter 4).

The Department of Agriculture, Sirsa reported average rice Y_g of 3.2 ton ha⁻¹ in Sirsa district during the agricultural year 2001-02. The World Rice Statistics published by IRRI also presents average rice Y_g of 3.8 ton ha⁻¹ for Haryana in the year 2000. The mean water and salt limited rice Y_g simulated by the distributed *SWAP-WOFOST* modelling was 3.5 ton ha⁻¹, and shows an agreement with the SEBAL estimation and statistical data (Table 5.5).

5.4.3 Regional water and salt balances

Table 5.6 presents regional water and salt balances simulated and aggregated over the entire main crop combination in Sirsa district during the agricultural year 2001-02. The simulated mean annual *ET* was 1114 mm over the wheat-rice, 925 mm over the wheat-cotton and 883 mm over the mustard-cotton areas. The annual *ET* over the bare soils accounted for the soil evaporation of 100 mm, which corresponds to the annual rainfall *P* of 103 mm. The low rainfall contributed only 9 to 11% of the annual *ET* over the crop areas. The irrigation water including both canal and groundwater supplies the major part of *ET* in Sirsa district. A significant part about 26 (wheat-rice) to 49% (mustard-cotton) of annual *ET* was supplied by canal irrigation I_{cw} , and the rest came from groundwater irrigation. The share of annual groundwater irrigation I_{gw} into the total irrigation *I* varied from 46% over the mustard-cotton area to 78% over the wheat-rice area.

Table 5.6 Simulated water and salt balances⁽¹⁾ of the main crop combinations in Sirsa district for both the *rabi* (Apr 1, 2001 to Apr 30, 2002) and the *kharif* (May 1, 2002 to Oct 31, 2002) seasons. Mean values are aggregated over the entire area of crop.

Crop season / Component	Wheat - Cotton		Wheat - Rice		Mustard - Cotton		Bare soil - Bare soil	
	<i>rabi</i>	<i>kharif</i>	<i>rabi</i>	<i>kharif</i>	<i>rabi</i>	<i>kharif</i>	<i>rabi</i>	<i>kharif</i>
Water balance (mm)								
<i>P</i>	7	90	6	92	7	91	7	96
<i>I</i>	425	456	432	881	354	450	0	0
I_{cw}	174	219	118	177	192	243	0	0
I_{gw}	251	237	314	704	162	207	0	0
<i>T</i>	254	480	263	342	266	447	0	0
<i>ET</i>	349	576	364	751	341	541	22	78
Q_{bot}	-22	-37	-129	-144	-13	-14	-18	-10
ΔW	60	-67	-55	79	7	-14	-34	8
Salt balance (mg cm⁻²)								
IC_i	58	56	62	142	40	52	0	0
$Q_{bot}C_{bot}$	-6	-10	-45	-61	-5	-4	-6	-3
ΔC	53	50	18	80	31	54	-6	-3

⁽¹⁾ Height soil column considered is 300 cm.

The annual groundwater pumping I_{gw} over the wheat-rice area is 2 to 3 times higher as compared to the wheat-cotton and the mustard-cotton areas. This is mainly to maintain the surface water ponding for optimal rice cultivation conditions. Moreover, maintaining the topsoil saturated during the rice growing period resulted into the high annual percolation Q_{bot} of -273 mm over the wheat-rice area. The high groundwater pumping I_{gw} , especially over the wheat-rice area, is also contributing to a salt build-up ΔC in Sirsa district.

The net groundwater recharge R is an integration of important hydrological processes in the soil-water-atmosphere-plant-continuum. It indicates sustainability in terms of rising or declining groundwater levels in a region. The simulated water balances of the simulation units were aggregated to compute the R over different canal commands in Sirsa district:

$$R = P + Q_{cw} - ET - \Delta W \quad (5.13)$$

where R is the net groundwater recharge [L], ET is the actual evapotranspiration [L], P is rainfall [L], Q_{cw} is the total canal water inflow (i.e. canal irrigation + seepage losses from the conveyance system), and ΔW is the change in the soil water storage [L]. A positive value of R represents a rise and a negative value represents a decline in the groundwater level.

Fig. 5.13 clearly presents that current irrigation practices are contributing to the rising and declining groundwater levels in Sirsa district. The estimated annual R varied from 82 mm y^{-1} in KWC to -679 mm y^{-1} in NGC. The R in most of the northern (BMB) commands is either positive or negligible negative, which indicates a rise of groundwater levels in the northern parts of Sirsa district. On the other side, the estimated annual R in the central commands (SCC, NGC and SGC) varied from -494 to -679 mm y^{-1} . This presents the over-exploitation of groundwater in the central parts along the belt of Ghagger river. Note that the seepage losses from Ghagger river were not accounted in the estimation of annual R for the central commands. Although the seepage losses from river partly compensate the groundwater exploitation, the high negative values of R in the central commands (SCC, NGC and SGC) confirm a decline of groundwater levels in the central parts of Sirsa district.

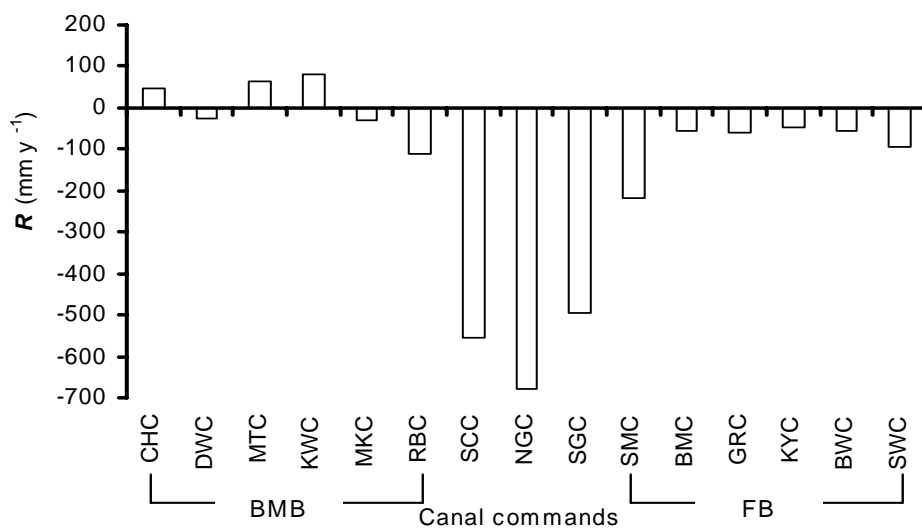


Figure 5.13 Net groundwater recharge R (mm y^{-1}) estimated by the distributed SWAP-WOFOST modelling over different canal commands in Sirsa district during the agricultural year 2001-02. Mean values apply to the entire area: cropped as well as bare soil. The location of different canal commands is shown in Fig. 5.3.

The long-term (1990-2000) trend of the measured groundwater levels in Sirsa district shows a mean annual rise of 90 mm y^{-1} . Multiplying with a specific yield of 12% of the aquifer in Sirsa district (Boonstra et al., 1996), this annual rise corresponds to an annual R of 11 mm y^{-1} . In our analysis, the annual R over the entire Sirsa district during the agricultural year 2001-02 was estimated at -127 mm y^{-1} , which presents a decline of about 1 m of groundwater levels. This is contributed to the low annual rainfall of 99 mm only, and consequently high groundwater pumping, especially during the *kharif* (summer) season of the agricultural year 2001-02.

5.4.4 Regional water productivity

The water productivity was calculated using the simulated water balance and crop yields of individual simulation units, and was aggregated following the Eq. 3.21. Table 5.7 presents the simulated water and salt limited WP_T , WP_{ET} and WP_{ETQ} values and its variation for the main crops (wheat, mustard, cotton and rice) in Sirsa district during the agricultural year 2001-02. Note that these values are based on the simulated numbers, which might deviate to a certain extent from the real values. However, they represent the current utilization of water resources and their effect on existing physical environment.

The WP_T , WP_{ET} and WP_{ETQ} values for winter crops (wheat and mustard) were higher as compared to summer crops (cotton and rice). The high relative transpiration ($T/T_p > 0.80$) for wheat and mustard showed that irrigation supplies were sufficient during the *rabi* (winter) season. The T/T_p during the *kharif* (summer) season was low (0.50 for cotton and 0.70 for rice), and showed the water stress on summer (cotton and rice) crops. This is assigned to the low rainfall received during the *kharif* season of the agricultural year 2001-2002 (Table 5.6). In addition, high temperatures and vapour pressure deficit during this season resulted into high evaporative demands. Also, high temperatures might have accelerated the crop growth rate, and resulted into a shorter growing period and a lower crop production. Consequently, the simulated water and salt limited WP_T , WP_{ET} and WP_{ETQ} values were low for summer crops (cotton and rice), especially for rice.

Table 5.7 Simulated water and salt limited water productivity of the main crops (wheat, mustard, cotton and rice) in Sirsa district during the agricultural year 2001-02. Water productivity WP (Table 3.1) is calculated in different forms viz., $kg Y_g$ (grain or seed yield) / $m^3 T$ (transpiration) or ET (evapotranspiration) or ETQ (evapotranspiration + percolation + seepage loss). *Mean* values apply to the entire area under a particular crop, and *Std* denotes the standard deviation.

Water productivity ($kg m^{-3}$)	Wheat		Mustard		Cotton		Rice	
	Mean	Std	Mean	Std	Mean	Std	Mean	Std
$WP_T (Y_g/T)$	1.89	0.24	0.60	0.11	0.43	0.06	1.04	0.46
$WP_{ET} (Y_g/ET)$	1.37	0.20	0.47	0.09	0.36	0.05	0.47	0.30
$WP_{ETQ} (Y_g/ETQ)$	0.94	0.20	0.33	0.08	0.27	0.05	0.35	0.21

The coefficient of variation CV of WP_{ET} was calculated as 15 to 19% for wheat, cotton and mustard (Table 5.7). The CV of WP_{ET} was 64% for rice, and there exists relatively more scope to improve the water productivity. The WP_T , expressed as Y_g/T ($kg m^{-3}$), represents the highest attainable value in the agricultural production system, and accounts for the minimum

amount of water used: the crop transpiration T only. For wheat, mustard and cotton, the mean WP_{ET} , expressed as Y_g/ET (kg m^{-3}), was 17 to 27% lower than the mean WP_T . Again, in case of rice there is a wide scope for improvement of water productivity: the mean WP_{ET} was 54% lower than the mean WP_T . Percolation Q_{bot} from field irrigations and seepage losses Q_{SL} from the conveyance system further reduce WP_{ET} to WP_{ETQ} (Eq. 3.20). Accounting for Q_{bot} only, the mean WP_{ET} was reduced by 4 to 5% for mustard and cotton, and by 12 to 16% for wheat and rice. We calculated WP_{ETQ} values (Table 5.7) accounting for both Q_{bot} and Q_{SL} in Sirsa district. Including 34 to 43% of the annual canal inflow as seepage losses Q_{SL} , the mean WP_{ET} was reduced by 25% for cotton and rice, and by 30% for wheat and mustard. Usually in irrigated areas, the Q_{bot} and Q_{SL} contribute to the groundwater recharge, which is recycled through groundwater pumping in good quality groundwater areas. The groundwater pumping is not possible in poor quality groundwater areas, where these losses contribute to waterlogging and secondary soil salinization. In some parts, especially in the northern parts of Sirsa district, the groundwater quality is poor i.e. $> 6 \text{ dS m}^{-1}$ (Fig. 5.5). *The low values of WP_{ETQ} in these areas must be improved by reducing the seepage losses through proper maintenance and lining of the conveyance system.*

Water productivity also depends on the spatial scale, mainly due to the differences in environmental and physical conditions such as weather, soil and moisture availability in root zone. The simulations performed by *SWAP-WOFOST* in a distributed mode enabled us to capture this variation in water productivity at regional scale (Fig. 5.14).

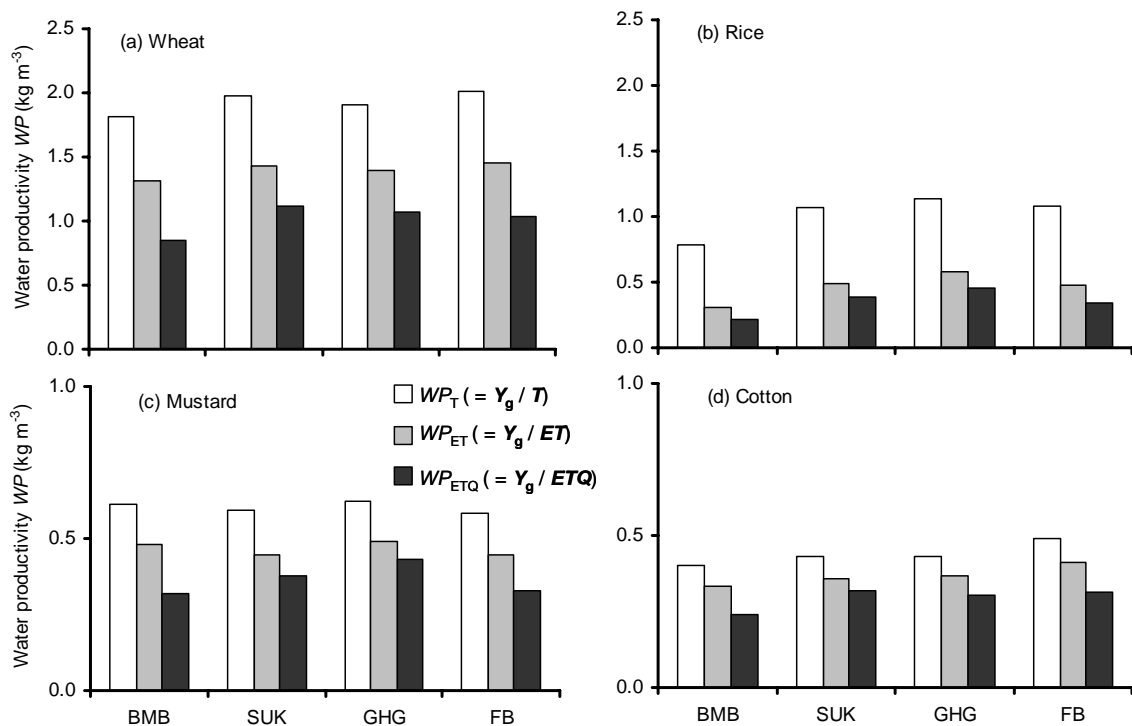


Figure 5.14 Spatial variation of simulated water and salt limited water productivity for the main crops (a) wheat, (b) rice, (c) mustard, and (d) cotton in different main commands of Sirsa district during the agricultural year 2001-02. Water productivity WP (Table 3.1) is calculated in different forms viz., $\text{kg } Y_g$ (grain or seed yield) / $\text{m}^3 T$ (transpiration) or ET (evapotranspiration) or ETQ (evapotranspiration + percolation + seepage loss). Values apply to the entire area under a particular crop in each main command. The location of different main commands is shown in Fig. 5.3.

The simulated water and salt limited WP_T , WP_{ET} and WP_{ETQ} values for wheat, cotton and especially rice were higher in the southern (FB) and the central (GHG and SUK) commands than in the northern (BMB) command. The mean WP_{ET} for wheat was highest (1.46 kg m^{-3}) in FB, while lowest (1.32 kg m^{-3}) in BMB. This is related to the poor quality groundwater in BMB.

The spatial variation in simulated water and salt limited WP_T , WP_{ET} and WP_{ETQ} values was higher for rice (Fig. 5.14b). Other crops performed more or less equal in all main commands. The mean WP_{ET} for rice was highest (0.58 kg m^{-3}) in GHG, which is the main rice belt of Sirsa district. This is a result of fine textured soils (i.e. silt loam to silt clay loam) and access to good quality ($< 4 \text{ dS m}^{-1}$) groundwater along the belt of Ghagger river. In the northern command BMB, the mean WP_{ET} for rice was 47% lower than its mean value of 0.47 kg m^{-3} for the entire district. At the same time, the mean WP_{ET} for cotton in this command was only 8% lower than its mean value of 0.36 kg m^{-3} for the entire district. Also, the high percolation from rice fields is contributing to the rising groundwater levels in this command. Therefore, *efforts to improve the water productivity must focus on the northern parts, and replacing rice cultivation by cotton should be promoted in BMB command.*

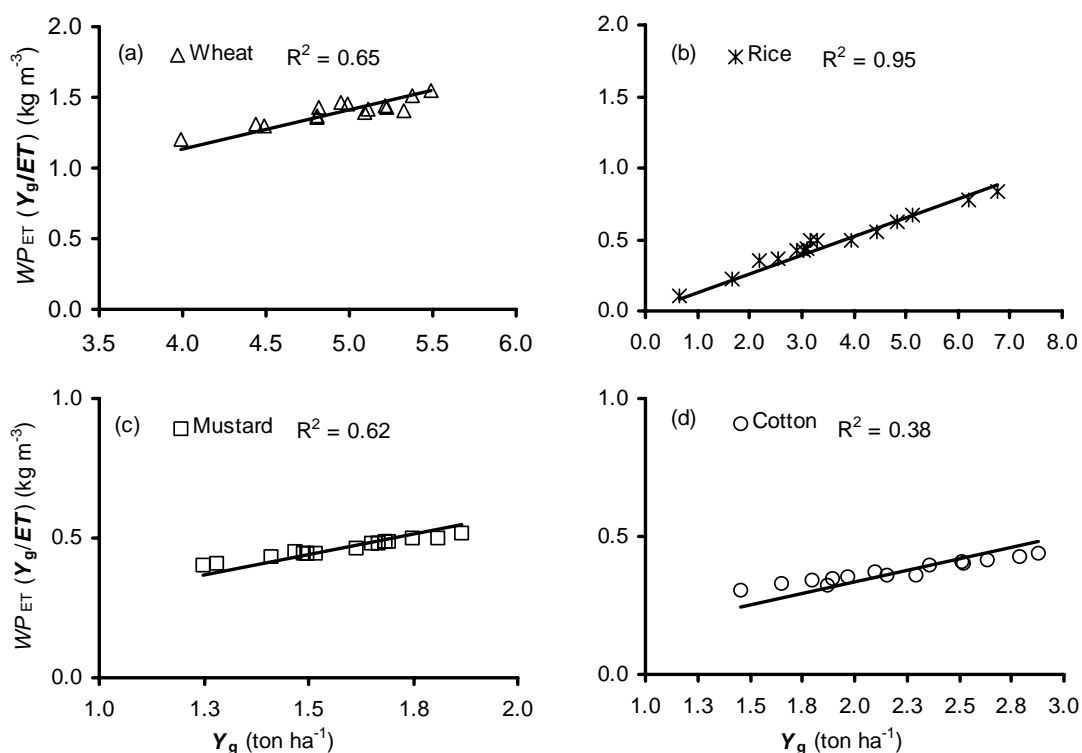


Figure 5.15 Relationship (linear trend line with zero intercept) between simulated water and salt limited water productivity $WP_{ET} (Y_g/ET) (\text{kg m}^{-3})$ and crop grain (or seed) yields $Y_g (\text{ton ha}^{-1})$ of the main crops (a) wheat, (b) rice, (c) mustard, and (d) cotton in Sirsa district during the agricultural year 2001-02. One value represents the mean value for one canal command (Fig. 5.3).

For a certain crop type and its variety, values of WP_T and WP_{ET} are expected to remain more or less constant under a range of water availability, when other factors are optimal. Fig. 5.15 shows that the response of Y_g to ET not remains constant, and WP_{ET} increases with increased Y_g . The positive value of R^2 (0.38 to 0.95) for the fitted linear trend line with zero intercept

(Fig. 5.15) indicates that efforts to increase crop yields, especially for rice, are in line with the improvement of water productivity.

5.5 Conclusions

The main conclusions, which could be drawn from this regional analysis, are as follows.

- The concept of water productivity is a useful indicator of the efficient utilization of water resources in agricultural production systems. The used definitions of water productivity (Table 3.1) explain the variations in water use at different temporal and spatial scales, and successfully identify where and when water can be saved.
- Effects of spatial heterogeneity on the regional water and salt balances, and on the water productivity can be analyzed by a field scale model applied in a distributed mode to all combinations of *weather-crop-soil-water* in the study area. The discrepancy in the actual evapotranspiration estimated by the remote sensing algorithm SEBAL and the distributed *SWAP-WOFOST* modelling over the bare soils (Fig. 5.11) shows the importance of proper land use classification in the proposed distributed modelling approach. A low accuracy in the land use classification can mislead the parameterization of *SWAP-WOFOST*, which subsequently can result in unrealistic water and salt balances. Despite the simplifications involved, the proposed methods of stratification and parameterization such as the use of pedotransfer functions, irrigation water distribution resulted into the simulated water and salt balances and crop yields, which compared well to other independent approaches like satellite remote sensing and field measurements.
- The simulated water and salt limited WP_{ET} , expressed as Y_g/ET (kg m^{-3}), was 1.37 for wheat, 0.36 for cotton and 0.47 for mustard and rice in Sirsa district during the agricultural year 2001-02 (Table 5.7). The coefficient of variation of WP_{ET} was high as 15% for wheat and cotton, 19% for mustard and especially 64% for rice. *Further, 50% of the total evapotranspiration ET for rice is lost through soil evaporation, a non-beneficial use of water.* High seepage losses (40% of the net canal inflow) from the conveyance system along with percolation from field irrigations are responsible for a significant reduction (25 to 30%) from WP_{ET} to WP_{ETQ} . This presents the large potential for the improvement of water productivity in Sirsa district.
- The simulated water and salt limited WP_T , WP_{ET} and WP_{ETQ} values for wheat, cotton and especially rice were higher in the southern (FB) and central (GHG and SUK) commands than in the northern (BMB) command. In BMB, the mean WP_{ET} for rice was 47% lower than its mean value of 0.47 kg m^{-3} for the entire district. Also, the high percolation from rice fields is contributing to the rising groundwater levels in this command. Therefore, *efforts to improve the water productivity must focus on the northern parts, and replacing rice cultivation by cotton should be promoted in BMB command.* The positive relationship between simulated water and salt limited WP_{ET} and crop grain (or seed) yields Y_g emphasizes that increase of crop yields will lead to improved water productivity (Fig. 5.15).

- The current cultivation and irrigation practices are leading to unfavorable ecohydrological conditions in Sirsa district. The high intensity of more water consuming wheat and rice crops and relatively low canal inflow, inducing high groundwater use, are resulting in the declining groundwater levels in the central parts (Fig. 5.13). On the other side, relatively high canal inflow and low groundwater pumping, restricted due to relatively poor groundwater quality, are resulting into positive net groundwater recharge in most of the northern canal commands. This presents a threat of waterlogging and secondary soil salinization in the northern parts of Sirsa district.
- The physical based field scale ecohydrological SWAP model, when coupled with field experiments, remote sensing and GIS demonstrated the potential of producing information required to evaluate the water management and its productivity at different spatial and temporal scales.

Chapter 6

Impact of alternative water management scenarios on regional water productivity and groundwater behaviour in Sirsa district

6.1 Introduction

The current irrigation systems in Haryana State are causing problems of rising or declining groundwater levels, waterlogging and salinization (Aggarwal and Roest, 1996). This is also evident in Sirsa district: the measured groundwater levels show a rise in the northern parts and a decline in the central parts. In June 2000, about 5% area, mainly in the northeast parts, experienced a critical groundwater level (< 3 m, below surface) (Chapter 2). Further, the average water productivity WP_{ET} , expressed in the measured kg grain (or seed) per m^3 of evapotranspiration, at farmer fields in Sirsa district is about 1.39 for wheat, 0.94 for rice and 0.22 for cotton. This corresponds to kind of average values for the climatic and growing conditions in Northwest India (Chapter 4). As water and land for irrigated agriculture are increasingly scarce, ways must be found to develop the productive and sustainable water management of irrigation systems.

The impact of implemented water management on the regional water and salt balances, and on the water productivity largely depends on the ecohydrological conditions of the area considered. In addition, problems and prospects associated with a particular water management option are often not recognised until they are well advanced. In this chapter, we focus on the identification of appropriate water management options to improve water management and its productivity in Sirsa district. First, the feasible water management options are proposed and second, the impact of the proposed scenarios on the regional water productivity and groundwater behaviour are quantified. The field scale ecohydrological SWAP model coupled with field experiments, remote sensing and GIS is extended in a distributed mode to produce the required information to evaluate alternative water management scenarios at regional scale. To identify appropriate recommendations for a productive and sustainable water management in Sirsa district, the simulated results of the current and alternative water management scenarios are analysed at different spatial and temporal scales.

6.2 Current and alternative water management

The canal water distribution in Sirsa district is based on the assumption that ecohydrological conditions in the district are homogeneous, and follows the principle of equal water distribution in proportion to land surface i.e. '*rostering*' and '*warabandhi*' (Chapter 2). This limited canal water distribution is characterized as '*protective irrigation*', which is meant to prevent crop failure due to drought. In the current irrigation system, irrigation charges to the farmers are fixed and based on crop type and actual area irrigated. It implies that farmers will have to pay less if they irrigate less area with the same amount of water. The current system, therefore, could lead to over-irrigation (Aggarwal and Roest, 1996). This over-irrigation might be contributing to the rising groundwater levels, especially in poor quality groundwater areas, where recycling of groundwater is not possible. Based on a regional water management analysis using SIWARE (Boels et al., 1996) for surface water and SGMP (Boonstra, 1996) for groundwater flow, Aggarwal and Roest (1996) recommended '*water pricing*' and a

'demand driven' system instead of 'warabandi', which is a 'supply driven' system. To solve the problems of rising groundwater levels, waterlogging and salinization, both options seem to be an effective, but not a feasible solution. For instance, implementation of the 'demand driven' system would require a complete change of the existing infrastructure, which historically has been designed for the 'warabandi' system. Moreover, the capacity to manage and maintain a 'demand driven' system is not available in Sirsa district.

In contrast to the above presented view, Navalawala (1999b) concluded that the prevailing water availability and its charges are very low, and have hardly any influence on management decisions of farmers for irrigation water use. Hellegers and Perry (2003) also tested 'water pricing' as a feasible management tool to improve water management in Sirsa district. Since the returns on the water are on an average about 100 times the price of water delivery, they concluded that a social-political unacceptable increase in the water price is required to influence the farmer's decisions for irrigation water use. Berkoff (1990) further advocated the rigid 'warabandi' system as a self-enforcing system. He concluded that a relative short supply, proper functioning and reliable water delivery manner i.e. 'farmers know what to expect', are important factors for farmers to plan their selection of crops, and to optimize the returns. Knowing that they cannot fully saturate the root zone with irrigation water, farmers typically plant such a mix of irrigated and non-irrigated crops that overall yield risks are minimal. Moreover, the farmers check for the unauthorized use of water during their turns.

Taking into account above discussed two different views, we propose the following feasible water management options within the existing irrigation infrastructure of Sirsa district. These water management options are focused to improve the water productivity, and to halt the rising and declining groundwater levels in the district.

Improved crop management (improved crop varieties, efficient irrigation, optimal nutrient supply, and better pest and disease control)

Effects of improved crop management are indicated by the ratio Y_g/I , where Y_g is the measured grain (or seed) yield and I is the amount of irrigation applied. In Sirsa district, the ratio Y_g/I was calculated using the measured values of Y_g and I at 24 farmer fields and experimental fields during the agricultural year 2001-02 (Chapter 3). At farmer fields, the average value of Y_g/I , expressed in kg m^{-3} , was calculated at 0.94 for wheat and 0.35 for cotton. At experimental fields, the same ratio for the same crops was calculated relatively high: 1.65 for wheat and 0.68 for cotton. The high ratio Y_g/I at experimental fields is attributed to improved crop varieties, efficient irrigation, optimal nutrient supply, and better pest and disease control. If we assume that this improved crop management at experimental fields is adopted at farmer fields, then in case of wheat $100 (1 - 0.94/1.65) = 43\%$, and in case of cotton $100 (1 - 0.35/0.68) = 48\%$ less water is required to produce the same amount of food. The positive value of R^2 (0.38 to 0.95) for the fitted linear trend line between the simulated water and salt limited Y_g and WP_{ET} (Chapter 5) also indicate that *efforts to increase the crop yields will result in improved water productivity, and therefore must be evaluated.*

Reduction in seepage losses

Jacobs and de Jong (1997) made a detailed study on the 'warabandi' system at two watercourses in Hisar district, which adjoins to Sirsa district. They concluded that seepage

losses coupled with groundwater flow and absence of natural drainage are main factors for waterlogging and salinization in Hisar district. The seepage losses in Sirsa district are also high: 30 to 40% of total canal inflow (Boels et al., 1996; Chapter 5). Accounting for both the percolation Q_{bot} and especially seepage losses Q_{SL} reduced the simulated water and salt limited water productivity from WP_{ET} to WP_{ETQ} by 25 to 30% for the main crops (wheat, cotton, mustard and rice) in Sirsa district during the agricultural year 2001-02 (Table 5.6). These significant seepage losses recharge to the groundwater, and are recycled through groundwater pumping in good quality groundwater areas. However, recycling of this water is not possible in poor quality groundwater areas like in the northern parts of Sirsa district, where they are contributing to the rising groundwater levels. Therefore, *the reduction in seepage losses is expected to improve the water productivity and performance of the irrigation system.*

Canal water reallocation

The long-term (1974-2000) trend of the measured groundwater level in Sirsa district shows a mean annual rise of 0.31 m y^{-1} (Groundwater Atlas of Sirsa district, 2002). Interesting is that the measured groundwater rise over the last 10 years (1990-2000) was 0.09 m y^{-1} only. It clearly shows that over the years the rate of rise in groundwater levels has decreased. This is attributed mainly to the increased groundwater pumping to irrigate more water consuming crops such as wheat, rice and cotton, which has been replacing less water consuming crops such as *gram* (chickpea) and *bajra* (pearl millet) (Chapter 2). The total number of tubewells in Sirsa district since 1976 has been multiplied by a factor of 4. Taking into account this continued increase in groundwater use, the measured annual rise of 0.09 m y^{-1} is expected to decrease further or even to reverse in future. However, the groundwater pumping in the northern parts is low due to the poor quality groundwater, which is compensated through a relatively high canal water supply (Chapter 5). The low groundwater pumping and high seepage losses from the conveyance system are contributing to the rising groundwater levels in the northern parts. On the other side, over-exploitation of good quality groundwater to irrigate high water consuming wheat and rice crops is resulting in the declining groundwater levels in central parts. Therefore, *canal water reallocation from the rising to the declining groundwater level areas can be explored for a sustainable water management in Sirsa district.*

6.3 Distributed modelling

In this study, we followed a distributed modelling approach: running a field scale model for all combinations of *weather-water-crop-soil-groundwater* in the study area. The ecohydrological SWAP model including detailed crop growth processes, denoted as *SWAP-WOFOST*, is extended in a distributed mode for simulations of hydrological and biophysical variables at regional scale. Details of this approach and data used in this study are described in Chapter 3 through Chapter 5. This distributed modelling serves two purposes: first, to understand the current situation and processes, and second, to evaluate alternative water management scenarios.

Implementation of alternative water management scenarios

In this chapter, the 5 scenarios of Table 6.1 were implemented, and their consequences on the regional water and salt balances, and on the water productivity in Sirsa district were

evaluated. The regional water and salt balances and crop yields were simulated over a period of 10 years from Nov 1, 1991 to Oct 31, 2001. The spatial model input information such as weather, canal water supply, and number of tubewells was variable over the simulation period, and derived from the collected information in Sirsa district (Chapter 3). The variation in cropping pattern, cultivation area and groundwater quality over the years could not be considered due to the limited data availability at regional scale. The aggregated ‘simulation’ units during the year 2001-02 (Chapter 5), therefore, were used for the simulation over the entire period from 1991 to 2001.

Scenario 1, ‘Business as usual’ or ‘reference situation’, shows the variability between meteorological years and related canal water supply in Sirsa district. It quantifies the expected rise or decline in groundwater levels and crop production with current water management, and serves as basis for further analysis.

Table 6.1 Alternative water management scenarios in Sirsa district. BMB is Bhakra Main Branch command in the northern parts, SUK and GHG are Sukchain and Ghagger command in the central parts of Sirsa district, respectively (Fig. 5.3).

Scenario	Description
1	'Business as usual' or 'reference situaion'
2	Increased (10 to 20%) crop yields
3	Reduced seepage losses at 25 to 30%
4	Canal water reallocation (15%) from the BMB to the GHG and SUK
5	Combination of Scenarios 2, 3 and 4

Scenario 2, ‘Increased (10 to 20%) crop yields’, was formulated to quantify the impact of increased crop yields on the regional water and salt balances, and on the water productivity. Efforts to increase crop yields such as improved crop varieties are expected to increase the maximum CO₂ assimilation rate and light use efficiency of the crop. Scenario 2, therefore, was implemented by adjusting two crop input parameters: maximum CO₂ assimilation rate A (kg ha⁻¹ hr⁻¹) and light use efficiency ε (kg ha⁻¹ hr⁻¹ / J m² s⁻¹). In order to achieve 10 to 20% increased crop yields with the same water supply, these parameters for simulated crops (Table 4.1 and Section 5.3: Crop data) were increased by 5% for mustard, 10% for wheat and rice, and 15% for cotton (Fig. 6.1).

Scenario 3, ‘Reduced seepage losses at 25 to 30%’, targets the rising groundwater levels, especially in the northern parts of Sirsa district. The seepage losses from the conveyance system were estimated at 34 to 43% of the net canal inflow in different canal commands during the agricultural year 2001-02 (Table 5.4). In scenario 3, the input parameters SF (Eq. 5.5) and q_{wc} (Eq. 5.6) were adjusted to reduce the seepage losses at 25 to 30%, which implies 70 to 75% conveyance efficiency. Proper lining and adequate maintenance of the irrigation system should be able to achieve this conveyance efficiency.

Scenario 4, ‘Canal water reallocation (15%) from the BMB to the GHG and SUK’, was formulated to target both the rising groundwater levels in the northern parts, and the declining

groundwater levels in the central parts. In this scenario, 15% of the measured canal water inflow in the northern Bhakra Main Branch (BMB) command was reallocated to the central Ghagger (GHG) and Sukchain (SUK) commands. This extra canal water inflow received by GHG and SUK was divided in proportion to their CCA, the agricultural area attached with canal water rights (Table 5.4).

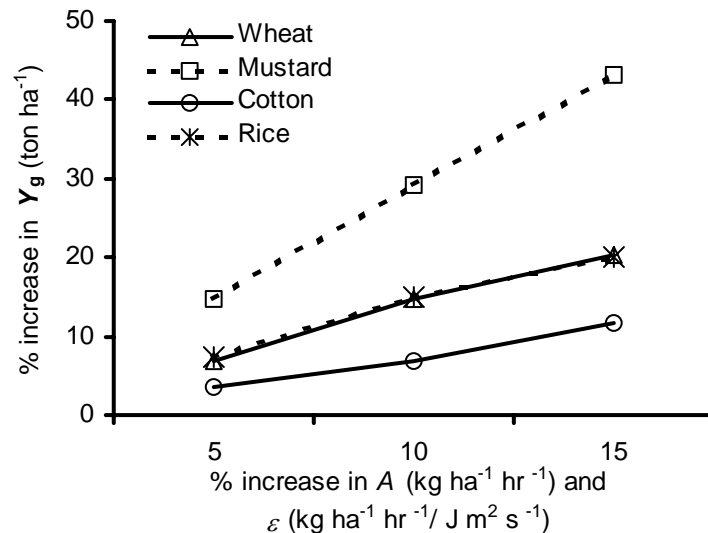


Figure 6.1 Sensitivity of the crop parameters: maximum CO₂ assimilation rate A ($\text{kg ha}^{-1} \text{hr}^{-1}$) and light use efficiency ε ($\text{kg ha}^{-1} \text{hr}^{-1} / \text{J m}^2 \text{s}^{-1}$) to simulated water and salt limited grain (or seed) yields Y_g (ton ha^{-1}) in SWAP-WOFOST. This figure is based on the simulations for 21 simulation units representing the combination of 3 crop rotations (Fig. 5.2c) and 7 soil types (Table 5.1) over the period of 10 years (1991-2001). The model input parameters such as weather, irrigation, and initial and boundary conditions were the same as for the ‘reference situation’. The used crop parameters for wheat, rice and cotton are shown in Table 4.1, and for mustard in Chapter 5 (Section 5.3:crop data).

Scenario 5, ‘Combination of Scenarios 2, 3 and 4’, evaluates the impact of integrated efforts on the regional water productivity, and on the rising and declining groundwater levels in Sirsa district.

Performance indicators

In this study, we focused on the improvement of regional water productivity, and on the rising and declining groundwater levels in Sirsa district, and therefore used the following performance indicators:

- **Water productivity:** Water productivity quantifies the ultimate goal of crop production per unit amount of water used (Table 3.1). The flexibility in defining water productivity provides useful indicators to evaluate water utilization, and to identify where and when water can be saved in the irrigation system.
- **Net groundwater recharge R :** The net groundwater recharge R , an integration of all hydrological processes in the soil-water-atmosphere-plant continuum (Eq. 5.13), quantifies the water exchange between unsaturated and saturated zone. A positive value of R represents a rise, and a negative value represents a decline in the groundwater levels.

- **Salt build-up ΔC** : For long-term sustainability of irrigated agriculture, the salt build-up in the soil profile (root zone) must be kept below the critical level, beyond which crop yields are affected. Therefore, alternative water management scenarios are evaluated on the increase or decrease in the salt build-up ΔC (Eq. 3.17) in the soil profile.

6.4 Results and discussion

After assigning the spatial-temporal input parameters for each considered scenario of Table 6.1, *SWAP-WOFOST* was run in a distributed mode for all simulation units (3168) from Nov 1, 1990 to Oct 31, 2001. Each experimental year was further divided into two crop seasons: *rabi* (wheat/mustard) season from Nov 1 to Apr 30, and *kharif* (cotton/rice) season from May 1 to Oct 31. The simulated water and salt balances and crop yields from Nov 1, 1991 to Oct 31, 2001 were aggregated following Eqs. 3.21 to 3.22, and subsequently were analyzed at different spatial and temporal scales in Sirsa district.

6.4.1 ‘Business as usual’

Table 6.2 presents the mean annual water and salt budgets for the entire Sirsa district and its four main commands (BMB, SUK, GHG and FB) over the period of 10 years (1991-2001). The annual rainfall P varied from 149 to 388 mm y^{-1} with a mean value of 256 mm y^{-1} . The canal water inflow Q_{cw} in Sirsa district was 1889 million $m^3 y^{-1}$ with a standard deviation of 213 million $m^3 y^{-1}$. About 41% of this annual Q_{cw} was estimated as seepage losses Q_{SL} from the conveyance system, which contributes to the groundwater recharge.

Table 6.2 Annual water and salt budget (‘Business as usual’ or Scenario 1) for the entire Sirsa district and its four main commands: BMB, SUK, GHG and FB (Fig. 5.3). Mean values (\pm standard deviation) are based on the distributed *SWAP-WOFOST* simulations for the unsaturated zone (0-300 cm) over the period of 10 years (1991-2001), and apply to the entire area (cropped as well as bare soil). The total area of Sirsa district is about 4270 km^2 , out of which 69% is under cultivation.

Spatial scale / Component	Sirsa district		Sirsa district		BMB		SUK		GHG		FB	
	Mean	Std	Mean	Std	Mean	Std	Mean	Std	Mean	Std	Mean	Std
Water budget ($10^6 m^3 y^{-1}$)												
					Water balance ($mm y^{-1}$)							
P	1083	369	256	87	248	111	292	98	113	33	324	104
Q_{cw}	1889	213	446	50	549	84	190	95	382	111	328	43
I	2471	123	583	29	542	39	744	53	910	24	486	23
I_{cw}	1123	130	265	31	318	51	115	58	244	72	204	51
I_{gw}	1348	117	318	28	224	27	629	50	666	75	283	35
T	2205	162	520	38	505	40	668	54	635	44	468	41
ET	3061	152	722	36	694	40	909	49	879	29	669	46
Q_{bot}	-463	153	-109	36	-89	41	-123	33	-143	20	-132	57
ΔW	27	151	6	36	6	43	4	35	2	19	9	41
Q_{SL} (% of Q_{cw})	41		41		42		39		36		38	
R	-117	292	-27	69	97	82	-432	85	-385	108	-26	82
Salt budget ($10^6 ton y^{-1}$)												
					Salt balance ($mg cm^{-2} y^{-1}$)							
IC_i	3.1	0.2	73	6	64	6	113	8	120	12	59	7
$Q_{bot} C_{bot}$	-2.3	0.9	-53	22	-39	20	-67	30	-104	29	-56	29
ΔC	0.8	1.1	20	25	25	23	46	32	16	29	4	32

The canal water irrigation I_{cw} provided 45% of the annual irrigation I for crop production, and the rest came from groundwater pumping I_{gw} . The total annual water supply of 839 mm y^{-1} , accounting for both the annual P and I , contributes to the annual evapotranspiration ET , which was simulated at 722 mm y^{-1} . About 13% of the total annual water supply percolated to the groundwater: Q_{bot} equal to -109 mm y^{-1} . The total contribution from percolation Q_{bot} and seepage losses Q_{SL} to the groundwater recharge was estimated at 292 mm y^{-1} , which was recycled through the groundwater pumping I_{gw} of 318 mm y^{-1} . *This presents nearly a closed water balance for Sirsa district.*

The measured mean groundwater level below soil surface in Sirsa district has been raised from 10.7 m in 1990 to 9.8 m in 2000. Multiplying with a specific yield of 12% of the aquifer in Sirsa district (Boonstra et al., 1996), this measured groundwater level rise of 90 mm y^{-1} translates to an annual R of 11 mm y^{-1} . This marginal measured annual R of 11 mm y^{-1} confirms a closed water balance for Sirsa district. In our analysis, the net groundwater recharge R was estimated at -27 mm y^{-1} , and presents a decline in the groundwater levels in Sirsa district. The difference of 38 mm y^{-1} between the measured and estimated annual R is only 5% of the annual surface water inflow, which accounts for both the rainfall P and the canal water inflow Q_{cw} . This difference might be due to several reasons such as: regional subsurface groundwater inflow, seepage from the Ghagger river, and change in cropping pattern and cultivation area over the years (1991-2000). These factors were not considered in this study. However, *large fluctuations of the estimated R and the salt build-up ΔC over the main commands suggest that interventions are required for a sustainable water management in Sirsa district* (Table 6.2).

6.4.2 Regional water productivity

Table 6.3 presents the impact of the 5 considered scenarios of Table 6.1 on the simulated water and salt limited grain (or seed) yields Y_g , water balance components T , ET and Q_{bot} , and subsequently on the water productivity WP_T , WP_{ET} and WP_{ETQ} values for the main crops (wheat, mustard, cotton and rice) in Sirsa district.

The average actual Y_g (ton ha^{-1}) in Sirsa district over the period of 10 years (1991-2001) are recorded at 4.1 for wheat, 1.2 for mustard (oilseed) and 3.2 for rice (Fig. 2.10) (Source: Department of Agriculture, Sirsa). The average cotton yield is based on lint, which is usually about 1/3 of the seed amount. The recorded average cotton (lint) yield of 0.4 ton ha^{-1} translates to a cotton Y_g of 1.2 ton ha^{-1} . In this study, *SWAP-WOFOST* simulates the water and salt limited Y_g taking into account the water and salt stress, but not the nutritional, pest and disease stress on the crop (Chapter 3). In case of 'Business as usual' (Scenario 1), the simulated water and salt limited Y_g during the same period from 1991 to 2001 were 1.2 to 2.0 times higher than the above mentioned recorded Y_g , especially for rice and cotton (Table 6.3). *This indicates substantial nutritional, pest or disease stresses on crop production in Sirsa district.*

The simulated average water and salt limited Y_g , and the WP_T , WP_{ET} and WP_{ETQ} values during the period from 1991 to 2001 were further higher than those obtained during the agricultural year 2001-02 (Table 5.7). This is assigned to the low rainfall received during the *kharif* (summer) season of the agricultural year 2001-2002 (Table 5.5). In addition, high

temperatures and evaporative demands during the 'dry year' 2001-02 resulted into low WP_T , WP_{ET} and WP_{ETQ} values, especially for summer crops (rice/cotton).

In Scenario 2, 'Increased (10 to 20%) crop yields', the increased maximum CO_2 assimilation rate A ($kg\ ha^{-1}\ hr^{-1}$) and light use efficiency ε ($kg\ ha^{-1}\ hr^{-1}/J\ m^2\ s^{-1}$) parameters of the simulated crops resulted into the increased Y_g by 12% for cotton, 15% for wheat, 16% for mustard and 17% for rice (Table 6.3). In field conditions, the increased Y_g implies a higher crop growth or leaf area development, which increases the transpiration of the crops. For simulated 12 to 17% increased Y_g , the transpiration T was increased by 2 to 8% for different crops. There was hardly any increase in the evapotranspiration ET , especially for summer (cotton/rice) crops. Even for winter (wheat/mustard) crops, the ET was increased by 2 to 3% only. This is because soil evaporation E relative to ET decreased as T increased under higher crop growth or leaf area development. Further, the percolation Q_{bot} from field irrigations was reduced: about 6% for rice and wheat, and about 15% for cotton and mustard. Therefore, the simulated WP_T , WP_{ET} and WP_{ETQ} values for different crops obtained in Scenario 2 were 8 to 19% higher than those obtained in Scenario 1.

The reduction in seepage losses Q_{SL} (Scenario 3) has a similar impact on the T and ET , while it acts opposite on the Q_{bot} as compared to the increased crop yields Y_g (Scenario 2). Reduction in seepage losses from the conveyance system implies more availability of canal water for irrigations, which may prompt the farmers to apply higher irrigation. In Scenario 3, the reduction in Q_{SL} at 25 to 27% (Table 6.3) provided 23% higher canal irrigation I_{cw} over the entire Sirsa district as compared to Scenario 1 (Table 6.2). Subsequently, the groundwater irrigation I_{gw} was decreased by 8% only, and total irrigation I was increased by 6%. This increased I resulted into 6 to 52% higher Q_{bot} for different crops in Scenario 3 as compared to Scenario 1. This might decrease the WP_{ETQ} at field scale. The WP_{ETQ} accounts for ET and Q_{bot} at field scale, and for ET , Q_{bot} and Q_{SL} at regional scale (Table 3.1). The increased use of good quality canal water in Scenario 3, however, resulted into 4 to 9% higher simulated Y_g for different crops as compared to Scenario 1. This neutralized the adverse impact of increased ET and especially Q_{bot} on the WP_{ETQ} at field scale. Additionally, the reduction of seepage losses at 25 to 27% (Scenario 3) increased the WP_{ETQ} by 6 to 12% for different crops at regional scale (Table 6.3). Also, the WP_T and WP_{ET} values obtained in Scenario 3 were slightly higher than those obtained in Scenario 1.

In Scenario 4, 15% of the measured canal water inflow in the northern BMB command was reallocated to the central GHG and SUK commands. This reallocation resulted into 16% less canal irrigation I_{cw} in BMB in Scenario 4 as compared to Scenario 1 (Table 6.2). The groundwater quality in the northern parts of Sirsa district is relatively poor, which restricts groundwater pumping. In Scenario 4, the groundwater pumping I_{gw} in BMB was increased by 11% only, and hence the total irrigation I was decreased by 5%. This lower amount of irrigation and increased use of poor quality groundwater increased the water and salt stress on crops in BMB, which accounts for 54% of the total crop area in Sirsa district. As a result, Scenario 4 has slightly adverse impact on the simulated Y_g , and subsequently on the WP_T , WP_{ET} and WP_{ETQ} values for all crops. The reduction of 15% canal water inflow from BMB might be made up again by the reduction in seepage losses in Scenario 3.

Table 6.3 Simulated water and salt limited water productivity of the main crops (wheat, mustard, cotton and rice) under the 5 scenarios (Table 6.1) in Sirsa district. Water productivity WP (Table 3.1) is calculated in different forms viz., $\text{kg } Y_g$ (grain or seed yield) / $\text{m}^3 T$ (transpiration) or ET (evapotranspiration) or ETQ ($ET + Q_{\text{bot}} + Q_{\text{SL}}$). Q_{bot} is the percolation from field irrigations, and Q_{SL} represents the estimated seepage loss (% of the total canal inflow) from the conveyance system. Values are based on the distributed *SWAP-WOFOST* simulations for the unsaturated zone (0-300 cm) over the period of 10 years (1991-2001), and apply to the entire area under a particular crop.

Water productivity / Water balance	Scenario 1				Scenario 2				Scenario 3				Scenario 4				Scenario 5			
	Wheat	Mustard	Cotton	Rice	Wheat	Mustard	Cotton	Rice	Wheat	Mustard	Cotton	Rice	Wheat	Mustard	Cotton	Rice	Wheat	Mustard	Cotton	Rice
$WP_T (Y_g/T)$ (kg m^{-3})	2.03	0.66	0.48	1.66	2.20	0.75	0.52	1.79	2.06	0.69	0.48	1.67	2.02	0.65	0.48	1.65	2.22	0.77	0.52	1.79
$WP_{ET} (Y_g/ET)$ (kg m^{-3})	1.43	0.50	0.41	0.94	1.60	0.57	0.46	1.11	1.46	0.52	0.42	0.98	1.42	0.48	0.41	0.95	1.62	0.58	0.46	1.14
$WP_{ETQ} (Y_g/ETQ)$ (kg m^{-3})	0.94	0.34	0.31	0.70	1.07	0.39	0.35	0.83	1.03	0.38	0.33	0.76	0.93	0.33	0.32	0.69	1.16	0.44	0.38	0.88
Y_g^* (ton ha^{-1})	4.90	1.72	2.56	6.45	5.63	1.99	2.87	7.55	5.11	1.87	2.68	6.83	4.81	1.64	2.53	6.50	5.79	2.09	2.95	7.95
T (mm)	243	256	534	392	258	262	550	425	249	269	558	411	240	249	526	396	263	270	565	447
ET (mm)	342	341	622	687	352	346	624	687	349	355	644	700	339	334	614	688	357	354	639	701
Q_{bot} (mm)	-58	-25	-53	-126	-54	-21	-45	-118	-66	-38	-67	-133	-56	-23	-50	-125	-60	-27	-52	-123
Q_{SL} (% of Q_{ew})	41	41	41	39	41	41	41	39	27	27	27	25	41	41	41	38	27	27	27	25

* Water and salt limited Y_g considering 80% grain (or seed) in simulated storage organs for wheat, 81% for rice and 44% for cotton and mustard. The Y_g include 14% moisture for wheat, 16% for rice and 15% for cotton and mustard.

The impact of these integrated actions on the regional water productivity was quantified in Scenario 5, which combined Scenarios 2, 3 and 4. The simulated Y_g , and the WP_T , WP_{ET} and WP_{ETQ} values for all crops in Scenario 5 were the highest among all scenarios (Table 6.3). For instance, WP_{ET} in Scenario 5 was higher about 12% for wheat and cotton, 16% for mustard and 21% for rice as compared to Scenario 1 i.e. ‘business as usual’. This significant gain in the WP_T , WP_{ET} and WP_{ETQ} values was mainly due to the simulated 12 to 17% increased Y_g (Scenario 2). *Improved crop management in terms of timely sowing, optimal nutrient supply and better pest and disease control is expected to achieve these higher simulated water and salt limited Y_g , and WP_T , WP_{ET} and WP_{ETQ} values in Sirsa district.* The reduction in seepage losses Q_{SL} at 25 to 27% (Scenario 3) also contributed to these improved WP_T , WP_{ET} and WP_{ETQ} values.

6.4.3 Net groundwater recharge

The net groundwater recharge in a region varies over time and space, and depends on several variables such as rainfall, canal water inflow, groundwater pumping, crop water use or ET , percolation from the field irrigations, seepage losses from the conveyance system and rivers, and last but not least regional subsurface groundwater inflow. For the 5 considered scenarios of Table 6.1, we estimated the net groundwater recharge R according to Eq. 5.13 using the simulated water balances in Sirsa district and its four main commands over the years from 1991 to 2001 (Fig. 6.2). Note that factors such as regional subsurface groundwater inflow, seepage from Ghagger river and change in cropping pattern and cultivation area over the years were not considered in this study. The estimated R , therefore, might deviate for a certain extent to that of the real situation during the period from 1991 to 2001. However, the relative values of R under different scenarios quantify the impact of alternative water management scenarios on the groundwater behaviour in Sirsa district. A positive value of R represents a rise, and a negative value represents a decline in the groundwater levels.

For ‘Business as usual’ (Scenario 1), the R of 97 mm y^{-1} in BMB confirms a rise in groundwater levels in the northern parts of Sirsa district. This is due to the low pumping of poor quality groundwater I_{gw} in this region, which is compensated through a relatively high canal water inflow Q_{cw} (Table 6.2). On the other hand, there is over-exploitation of good quality groundwater to irrigate the high water consuming wheat and rice grown along the belt of Ghagger, flowing through the central parts of Sirsa district. The estimated mean annual I_{gw} in SUK and GHG, therefore, was almost 2 times of that for the entire Sirsa district (Table 6.2). Hence, the R in SUK and GHG was estimated at -432 and -385 mm y^{-1} , respectively. This presents a decline in groundwater levels in the central parts. The estimated R in FB was low about -26 mm y^{-1} only. Therefore, *the BMB, SUK and GHG commands need more attention to halt the rise and decline in groundwater levels in Sirsa district.*

In Scenario 2, the increased Y_g implies a higher crop growth or leaf area development, which increases the crop transpiration T , and decreases the percolation Q_{bot} at field scale (Table 6.3). As a result, Scenario 2 has a slightly favourable impact in BMB, and decreased the R from 97 to 90 mm y^{-1} . The R in the central commands was also slightly decreased from -432 to -442 mm y^{-1} in SUK, and from -385 to -396 mm y^{-1} in GHG (Fig. 6.2). This implies that increased crop yields will reduce the rise in groundwater levels in the northern parts, while it will accelerate the decline in groundwater levels in the central parts. The reduction in seepage

losses (Scenario 3) also has a similar impact as Scenario 2 on the groundwater behaviour in Sirsa district. In Scenario 3, the reduction in seepage losses at 25 to 27% decreased the R from 97 to 71 mm y^{-1} in BMB, and presents a significant contribution to halt the rise of groundwater levels in the northern parts. The R in SUK and GHG were again decreased by 2 to 4% as compared to Scenario 1.

Scenario 4, ‘Canal water reallocation (15%) from the BMB to the GHG and SUK’, was mainly formulated to target the rise in groundwater levels in BMB, and the decline in groundwater levels in GHG and SUK. In Scenario 4, the reallocation of 15% of the measured canal water inflow Q_{cw} from BMB to GHG and SUK provided about 16% less canal irrigation I_{cw} over the entire BMB as compared to Scenario 1 (Table 6.2). On the other hand, the I_{cw} was increased by 130% over SUK and 57% over GHG. As a result, the high groundwater pumping I_{gw} in SUK and GHG in Scenario 1 (Table 6.2) was decreased by 18% in Scenario 4. Further, the evapotranspiration ET in SUK and GHG was increased by 2 to 3% only. As expected, Scenario 4 resulted into a desirable impact on all three commands: BMB, SUK and GHG. The estimated R in BMB was decreased from 97 to 33 mm y^{-1} . The R in the central commands was also increased from -385 to -182 mm y^{-1} in SUK, and from -432 to -213 mm y^{-1} in GHG (Fig. 6.2).

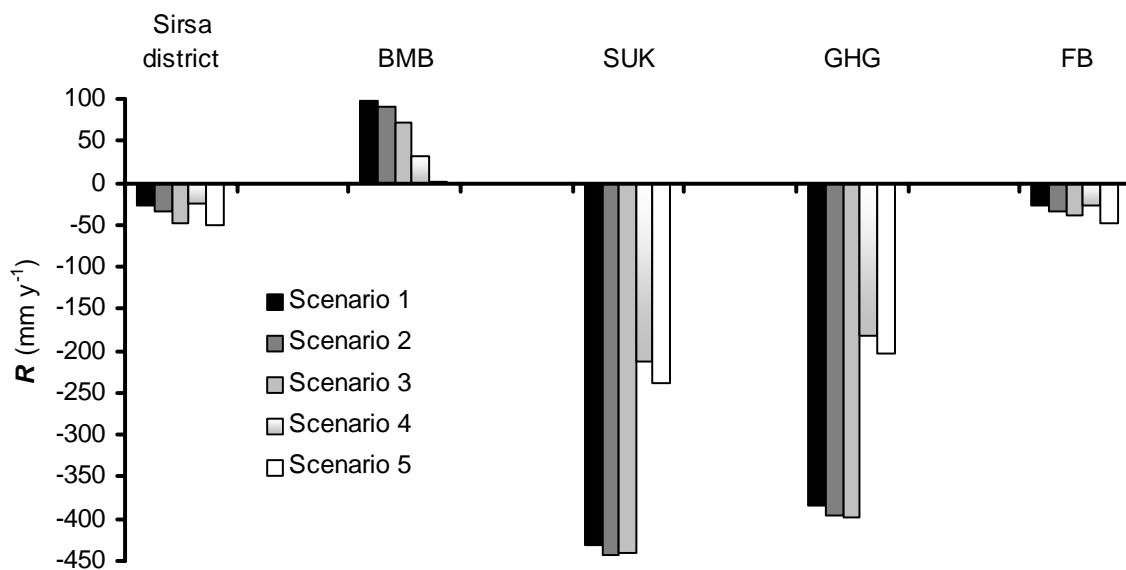


Figure 6.2 Net groundwater recharge R (mm y^{-1}) over the entire Sirsa district and its four main commands (BMB, SUK, GHG and FB; Fig. 5.3) under the 5 scenarios (Table 6.1) in Sirsa district. Mean values are based on the distributed SWAP-WOFOST simulations for the unsaturated zone (0-300 cm) over the period of 10 years (1991-2001), and apply to the entire area (cropped as well as bare soil).

The integrated impact of Scenarios 2, 3 and 4 as implemented through Scenario 5 further decreased the R in BMB from 97 to 1 mm y^{-1} only. Scenario 5 has a slightly unfavourable impact on SUK and GHG as compared to Scenario 4, while a significant favourable impact as compared to Scenario 1. From Fig. 6.2, we conclude that canal water reallocation (15%) from BMB to SUK and GHG (Scenario 4) in combination with reduction in seepage losses (Scenario 3), especially in BMB, is an attractive option to halt the rising groundwater levels in the northern, and the declining groundwater levels in the central parts of Sirsa district.

The recently constructed ‘Ottu weir’ dam on Ghagger river near Sirsa town will further increase the amount and reliability of the canal irrigation in the central commands, especially in GHG.

For the entire Sirsa district, interesting is the decrease of estimated R from -27 mm y^{-1} in Scenario 1 to -50 mm y^{-1} in Scenario 5 (Fig. 6.2). For instance, the measured groundwater level below soil surface in Sirsa district has been raised by 90 mm y^{-1} during the last 10 years (1990-2000). Multiplying with a specific yield of 12% of the aquifer in Sirsa district (Boonstra et al., 1996), this annual rise translates to an annual excess water or recharge R of 11 mm y^{-1} . The decrease of estimated R by -23 mm y^{-1} in Scenario 5 is higher than the measured annual R of 11 mm y^{-1} . This was mainly due to an increase in simulated ET by 20 mm y^{-1} in Scenario 5. This increase in ET is assigned to a simulated reduction in Q_{SL} (Scenario 3) and increased Y_g (Scenario 2) (Table 6.3). *This implies that the increased crop yields and especially reduction in seepage losses will contribute to halt the net rise in groundwater levels in Sirsa district.* Most of the canals and watercourses in Sirsa district are lined, while the field channels that distribute canal water among fields are still unlined.

6.4.4 Salt build-up

In Sirsa district, irrigations with poor quality groundwater are a major source of salt build-up in the soil profile. The capillary rise of poor quality groundwater, and subsequently its evaporation, also contributes to the salt build-up in shallow groundwater level areas. The rainfall and irrigations with canal water of good quality cause leaching of the salts. In this study, the mixed use of canal water and groundwater for irrigation (Eq. 5.13) was simulated over the period of 10 years from 1991-2001. Further, the salt build-up ΔC was estimated according to Eq. 3.17, and aggregated following Eq. 3.22.

Table 6.4 presents the impact of the 5 considered scenarios of Table 6.1 on the ΔC over the entire Sirsa district and its four main commands. For ‘Business as usual’ (Scenario 1), there was a ΔC of $2.0 \text{ ton ha}^{-1} \text{ y}^{-1}$ over the entire Sirsa district (Table 6.4). The highest ΔC of $4.6 \text{ ton ha}^{-1} \text{ y}^{-1}$ in SUK was a result of low canal water inflow Q_{cw} and high groundwater pumping I_{gw} (Table 6.2). Despite the highest Q_{cw} and the lowest I_{gw} , BMB also showed a significant ΔC of $2.5 \text{ ton ha}^{-1} \text{ y}^{-1}$. This is assigned to the relatively poor groundwater quality in the northern parts of Sirsa district (Chapter 2).

In Scenario 2, the simulated increased Y_g decreased the percolation Q_{bot} by 6 to 15% for different crops as compared to Scenario 1 (Table 6.3). The decreased Q_{bot} implies less leaching of salts, and hence Scenario 2 ended up with a slightly increased ΔC in Sirsa district and its four main commands (Table 6.4).

In Scenario 3, the reduction in seepage losses Q_{SL} implies a higher canal irrigation, which will result into low groundwater pumping. As a result, the total salt inflow of $7.3 \text{ ton ha}^{-1} \text{ y}^{-1}$ over the entire Sirsa district in Scenario 1 (Table 6.2) was decreased to $6.8 \text{ ton ha}^{-1} \text{ y}^{-1}$ in Scenario 3. In addition, the Q_{bot} for different crops was increased in Scenario 3 (Table 6.3), which increased the leaching of salts. *As expected, Scenario 3 has a significant favourable impact on the ΔC over the entire Sirsa district and its four main commands* (Table 6.4).

Table 6.4 Salt build-up ΔC (ton ha⁻¹ y⁻¹) over the entire Sirsa district and its four main commands (BMB, SUK, GHG and FB; Fig. 5.3) under the 5 scenarios (Table 6.1) in Sirsa district. Mean values are based on the distributed SWAP-WOFOST simulations for unsaturated zone (0-300 cm) over the period of 10 years (1991-2001), and apply to the entire area (cropped as well as bare soil).

Scenarios / Spatial scale	Scenario 1	Scenario 2	Scenario 3	Scenario 4	Scenario 5
Sirsa district	2.0	2.2	1.3	2.0	1.6
BMB	2.5	2.8	1.7	3.0	2.6
SUK	4.6	5.2	4.4	3.8	3.5
GHG	1.6	2.0	0.6	0.5	-1.0
FB	0.4	0.6	0.1	0.4	0.2

In Scenario 4, canal water reallocation (15%) from BMB to GHG and SUK might increase the use of poor quality groundwater, and decrease the leaching of salts in BMB, and vice-versa in GHG and SUK. Therefore, Scenario 4 resulted into a slightly increased ΔC in BMB, while it was decreased in GHG and SUK. For BMB, the increased ΔC in Scenario 4 might be neutralized by the decreased ΔC in Scenario 3. Therefore, the ΔC in BMB in Scenario 5 was 2.6 ton ha⁻¹ y⁻¹, which was almost equal to that in Scenario 1 (Table 6.4). In addition, *Scenario 5 has a significant favourable impact on the ΔC in GHG, SUK, FB and the entire Sirsa district.*

6.5 Conclusions

The main conclusions, which could be drawn from this scenario analysis, are as follows.

- Sirsa district has a closed water balance as the total annual surface inflow, accounting for both rainfall and canal water inflow, is almost equal to the simulated annual evapotranspiration. This is also confirmed by the measured groundwater levels, which show a marginal annual net groundwater recharge R of 11 mm y⁻¹ only during the period from 1990 to 2000. At the same time, large fluctuations of the estimated net groundwater recharge R and salt build-up ΔC over the main commands (BMB, SUK, GHG and FB) in Scenario 1 ‘*business as usual*’ (Table 6.2) suggest that interventions are required for a sustainable water management in Sirsa district.
- The simulated average water and salt limited grain (or seed) yields Y_g of main crops (wheat, mustard, cotton and rice) are 1.2 to 2.0 times higher, especially for rice and cotton, than the average actual (recorded) Y_g over the period of 10 years (1991-2001). This indicates substantial nutritional, pest or disease stresses on crop production in Sirsa district. Efforts to increase crop yields will certainly improve the WP_{ET} , expressed as Y_g/ET (kg m⁻³), which represents the actual amount of water used in agricultural production systems. In this study, the simulated 12 to 17% increased Y_g in Scenario 2 increased the WP_{ET} by 12% for wheat and cotton, 14% for mustard and 18% for rice as compared to Scenario 1 ‘*business as usual*’ (Table 6.3).

- The simulated reduction in seepage losses Q_{SL} from 39-41% in Scenario 1 to 25-27% in Scenario 3 improved the water and salt limited WP_T , WP_{ET} and especially WP_{ETQ} by 6 to 12% for different crops (Table 6.3). In addition, Scenario 3 contributed significantly to the decrease of net groundwater recharge R in BMB (Fig. 6.2) and salt build-up ΔC over the entire Sirsa district (Table 6.4). The reduction in seepage losses in Sirsa district, therefore, is strongly recommended, especially in the northern BMB command with relatively poor groundwater quality.
- Canal water reallocation (15%) from BMB to GHG and SUK (Scenario 4) will have a slightly adverse impact on the simulated water and salt limited WP_T , WP_{ET} and WP_{ETQ} values, and on the salt build-up ΔC in BMB. This decreased canal water inflow in BMB might be made up again by the reduction in seepage losses (Scenario 3). Further, Scenario 4 has a tremendous favorable impact to decrease the net groundwater recharge R in BMB, and to increase the R in the central commands: GHG and SUK (Fig. 6.2). Therefore, canal water reallocation (15%) from BMB to GHG and SUK (Scenario 4) in combination with the reduction in seepage losses at 25 to 30% (Scenario 3) is suggested to halt the rising groundwater levels in the northern, and the declining groundwater levels in the central parts of Sirsa district.
- In Scenario 5, combining Scenarios 2, 3 and 4, the water and salt limited WP_T , WP_{ET} and WP_{ETQ} values (Table 6.3), the large fluctuations of the estimated net groundwater recharge R (Fig. 6.2) and the high salt build-up ΔC (Table 6.4) have been significantly improved as compared to Scenario 1. The simulated ET of 722 mm y^{-1} over the entire Sirsa district in Scenario 1 (Table 6.2) was increased by 20 mm y^{-1} in Scenario 5, which is higher than the measured annual R of 11 mm y^{-1} . This suggests that the integrated impact of the proposed alternative water management scenarios (Table 6.1) will significantly contribute to a productive and sustainable water management in Sirsa district.
- The physical based field scale ecohydrological SWAP model, when coupled with field experiments, remote sensing and GIS, demonstrates its capabilities to analysis the impact of alternative water management scenarios on the regional water productivity and groundwater behaviour. The developed distributed SWAP modelling can quantify the net groundwater recharge R , which is a necessary component for the groundwater management in a region. Spatially-temporally quantification of net groundwater recharge R from the unsaturated zone can serve as input to regional saturated groundwater flow models. Combination of both distributed SWAP modelling and regional groundwater flow models should be investigated for regional surface and groundwater management.

Chapter 7

Sequential assimilation of the observed total dry matter production in SWAP model

7.1 Introduction

Ecohydrological models like SWAP are suitable to describe the hydrological and biophysical processes at field scale, and can be applied in a distributed mode at regional scale (Chapter 4 and 5). However, SWAP uses a large number of input parameters to accurately reproduce hydrological variables such as transpiration, evapotranspiration, percolation, and biophysical variables such as dry matter and grain (or seed) yield. In case of the use of inaccurate input parameters, the estimation of these variables may be erroneous. Moreover, model input parameters may be measurable in theory, but some of them are difficult to measure under field conditions. This is accommodated by the process of calibration and validation of the model, which requires field observations characterizing the system behaviour such as soil moisture, leaf area index, dry matter production and evapotranspiration fluxes (Chapter 4; Bessembinder et al., 2003; Jhorar, 2002). At regional scale, field measurement of these variables is not possible, and the satellite remote sensing comes in.

In principle, satellite images record spatially distributed spectral radiances in various wavelength bands, but cannot measure a desired hydrological and biophysical variable directly. Cooperation between agricultural researchers and radiation physicists, therefore, has evolved in the development of empirical and more advanced quantitative algorithms to convert remotely sensed spectral radiances into useful information such as leaf area index, dry matter production and evapotranspiration fluxes. For instance, the Surface Energy Balance Algorithm for Land (SEBAL) (Bastiaanssen et al., 1998) computes evapotranspiration fluxes and dry matter production using the energy exchanges between atmosphere and land surface (Bastiaanssen et al., 2003b). Satellite remote sensing offers the possibility of observations at regional scale, and hence one obtains the spatial variability. In addition, one can obtain the temporal variability if observations are made repeatedly. However, SEBAL computations depend upon the revisit frequency of the satellite and the availability of cloud free images. In most climates, images can be analysed for a few days during the entire growing season. The ecohydrological models are expected to fill this temporal gap of the remotely sensed hydrological and biophysical variables at regional scale. The remote sensing techniques further can analyze only the current and past situation. In contrast, physical models may evaluate alternative scenarios, and offer future predictions.

A major problem with models may be inaccurate parameterisation and uncertainty, and hence a low prediction performance. Assimilation of satellite remote sensing data into the physical based ecohydrological models is expected to improve their predictive performance, especially at regional scale (Droogers and Kite 2002; Jhorar, 2002; Schuurmans et al., 2003; Boegh et al., 2004). Various data assimilation methods have been developed to assimilate observations into physical based models (Houser et al., 1998; Moulin et al., 1998; Makowski et al., 2003, Paniconi et al., 2003). These methods involve the correction of the inputs or the state variables of these models, which characterize the system behaviour.

In this chapter, *different data assimilation methods such as forcing, calibration and updating are investigated to assimilate the remotely sensed observations into a relatively complex ecohydrological SWAP model*. Relative merits and demerits of these data assimilation methods are explored through the assimilation of synthetic (numerical) and observed total dry matter production data at field scale.

7.2 Data assimilation methods

As a typical example, the following data assimilation methods apply to the assimilation of total dry matter production in the detailed crop module of SWAP model, denoted as *SWAP-WOFOST*. The subscript ‘obs’ refer to the observed total dry matter *TDM*, and ‘sim’ to the simulated *TDM* at time t . Similar methods, with modifications specific to the state variables, can be investigated to assimilate other variables like leaf area index *LAI* and evapotranspiration *ET* fluxes.

The ‘calibration’ method

In this method, the model input parameters are adjusted to obtain an optimal agreement between TDM_{obs} and TDM_{sim} . The sensitive and uncertain input parameters might be calibrated either manually or automatically by running the model with various combinations of their values with a realistic range. An optimisation algorithm like PEST (Doherty et al., 1995) can easily be linked to the model to perform the automatic calibration process (Fig. 4.3), and a smallest possible deviation between TDM_{obs} and TDM_{sim} can be achieved within a certain pre-set criterion. The objective function quantifies the differences between TDM_{obs} and TDM_{sim} . If the observation errors follow a multivariate normal distribution with zero mean, no correlation, and constant variance for each measurement type, maximization of the probability of reproducing TDM_{obs} leads to the weighted least squares objective function $\Phi(\mathbf{b})$:

$$\Phi(\mathbf{b}) = \sum_{i=1}^N \left[\left\{ W_{\text{obs}} (TDM_{\text{obs}}(t_i) - TDM_{\text{sim}}(t_i, \mathbf{b})) \right\}^2 \right] \quad (7.1)$$

where $TDM_{\text{obs}}(t_i)$ is the observed total dry matter production at time t_i , N is the number of observations, and $TDM_{\text{sim}}(t_i, \mathbf{b})$ is the simulated total dry matter production using an array with parameter values \mathbf{b} . The W_{obs} is the weight associated with a particular TDM_{obs} .

The ‘forcing’ method

The ‘forcing’ method replaces TDM_{sim} with TDM_{obs} as state variable into the model. The direct use of TDM_{obs} to prescribe a driving state variable requires the availability of TDM_{obs} at each model time step, which is daily in case of *SWAP-WOFOST*. In reality, remotely sensed TDM_{obs} are available at time of satellite passage only. To derive TDM_{obs} at daily model time step, some interpolation techniques should be used to fill the gaps between two observations.

In this study, we linearly interpolated between two TDM_{obs} to derive the daily TDM_{obs} values. In order to validate this assumption, *SWAP-WOFOST* simulated *TDM* of wheat at a farmer field in Sirsa district (Chapter 4) is shown in Fig. 7.1. It is clear from the figure that the *TDM* of wheat can be interpolated linearly, provided the observation interval is less than 30 days.

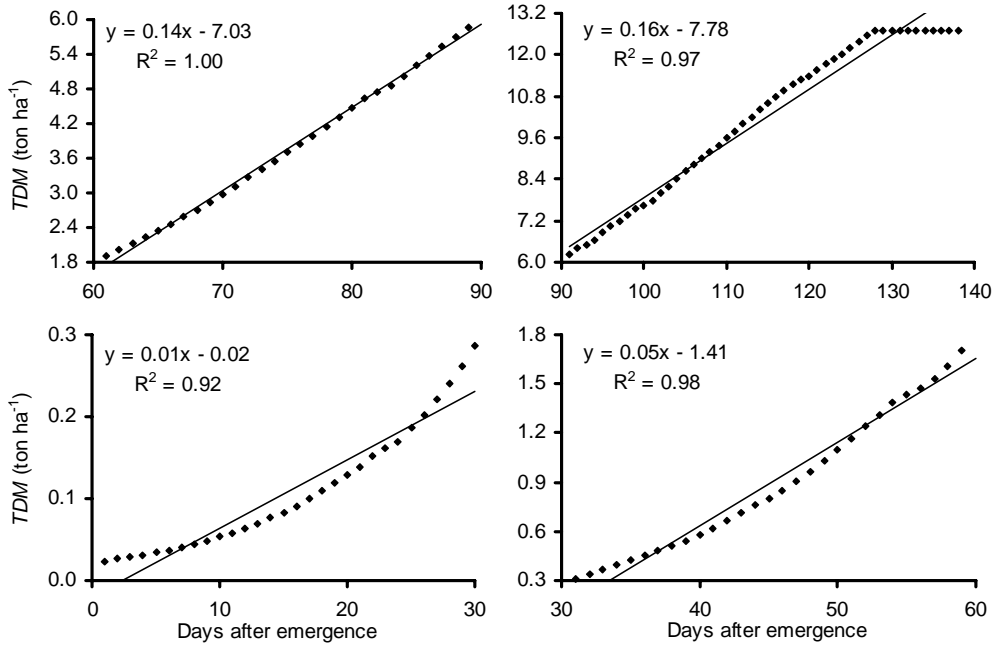


Figure 7.1 Total dry matter (TDM) production (ton ha^{-1}) vs. days after emergence with a fitted linear trend line. This figure is based on the simulation by *SWAP-WOFOST* model for wheat at a farmer field (S4F16) in Sirsa district during the *rabi* (winter) season of the agricultural year 2001-02 (Chapter 4).

The ‘updating’ method

The ‘updating’ method consists of the continuously updating TDM_{sim} , whenever a TDM_{obs} is available. In this study, a simple sequential ‘updating’ algorithm is developed to assimilate the TDM_{obs} into *SWAP-WOFOST*. This algorithm is based on the assumption that a better TDM_{sim} at day t will also improve the accuracy of TDM_{sim} at succeeding days.

$$TDM_{\text{upd}}(t) = TDM_{\text{sim}}(t) + K_g [TDM_{\text{obs}}(t) - TDM_{\text{sim}}(t)] \quad (7.2)$$

where TDM_{upd} is the updated total dry matter production at time t . The factor ‘ K_g ’ represents the optimal gain in the simple sequential ‘updating’ algorithm (Fig. 7.2). In principle, the TDM_{sim} contains certain errors due to the simplified representation of the complex crop growth processes into the model, and due to uncertainty in crop input parameters. On the other hand, the TDM_{obs} also includes observation errors. The optimal gain factor ‘ K_g ’ is associated with the errors into both TDM_{sim} and TDM_{obs} values:

$$K_g = \frac{\sigma_{\text{sim}}^2}{\sigma_{\text{sim}}^2 + \sigma_{\text{obs}}^2} \quad (7.3)$$

where σ_{sim}^2 is the variance of model error in TDM_{sim} , and σ_{obs}^2 is the variance of observation error in TDM_{obs} . In the sequential ‘updating’ process, the errors into both TDM_{sim} and TDM_{obs} values are calculated through a statistical model, and next TDM_{sim} is updated (Fig. 7.2) based on the relative magnitudes of the model and the observation errors (Aubert et al., 2003; Makowski et al., 2003).

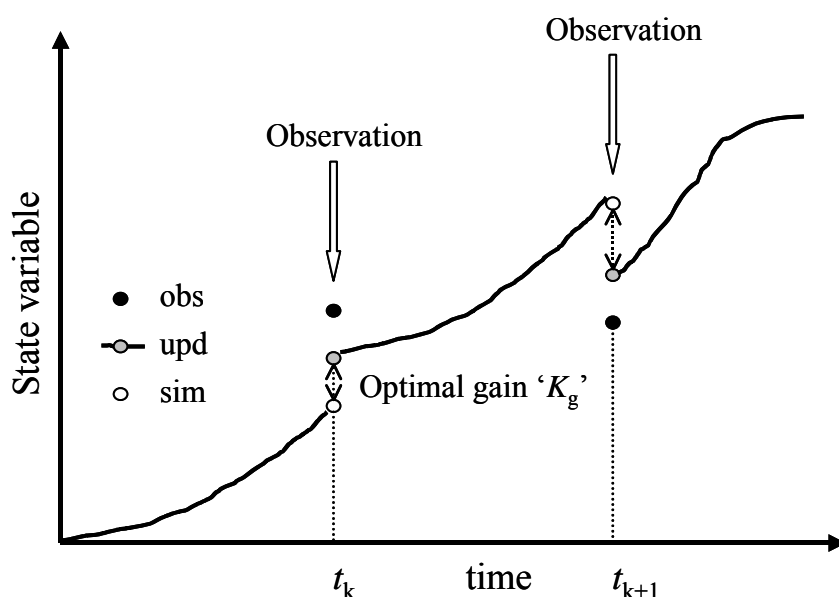


Figure 7.2 Schematic representation of the sequential ‘updating’ algorithm to update the model state variables whenever an observation is available (Adapted from Aubert et al., 2003).

In this algorithm, a correction factor C_F is used to derive TDM_{sim} from TDM_{obs} values:

$$C_F = \frac{TDM_{upd}}{TDM_{sim}} \quad (7.4)$$

To use the C_F for the assimilation of TDM_{obs} into *SWAP-WOFOST*, it must be translated to the model’s calculation procedure. *SWAP-WOFOST* simulates the potential gross CO_2 assimilation rate A^1_{pgross} ($kg\ CO_2\ m^{-2}\ leaf\ d^{-1}$) of a crop based on the absorbed photosynthetically active radiation PAR , and on the photosynthetic leaf characteristics. Under actual field conditions, the crop characteristics, day temperature, and water and salt stress reduce the A^1_{pgross} to daily gross CO_2 assimilation rate A_{pgross} ($kg\ ha^{-1}\ d^{-1}$):

$$A_{pgross} = \frac{30}{40} f_{7min} \frac{T}{T_p} A^1_{pgross} \quad (7.5)$$

where the factor $30/44$ accounts for conversion of each $kg\ CO_2$ to biomass (CH_2O), relative transpiration T/T_p quantifies the effect of water and salt stress, and f_{7min} is a reduction factor for low temperature. In addition to water and salt stress, management factors such as nutrient, pest and disease control affect crop growth, and hence they reduce the A_{pgross} of crop under actual field conditions. The effects of nutrient supply, weeds, pest and disease on crop growth and its production are not implemented in the present version of *SWAP-WOFOST* (Van Dam et al., 1997; Kroes and Van Dam, 2003) (Chapter 3).

In *SWAP-WOFOST*, the simulated A_{pgross} ($kg\ ha^{-1}\ d^{-1}$) is related non-linearly with total dry matter production (Fig. 7.3). Therefore, a direct correction of the simulated A_{pgross} with the correction factor C_F (Eq. 7.4), based on TDM_{upd} and TDM_{sim} , is not possible.

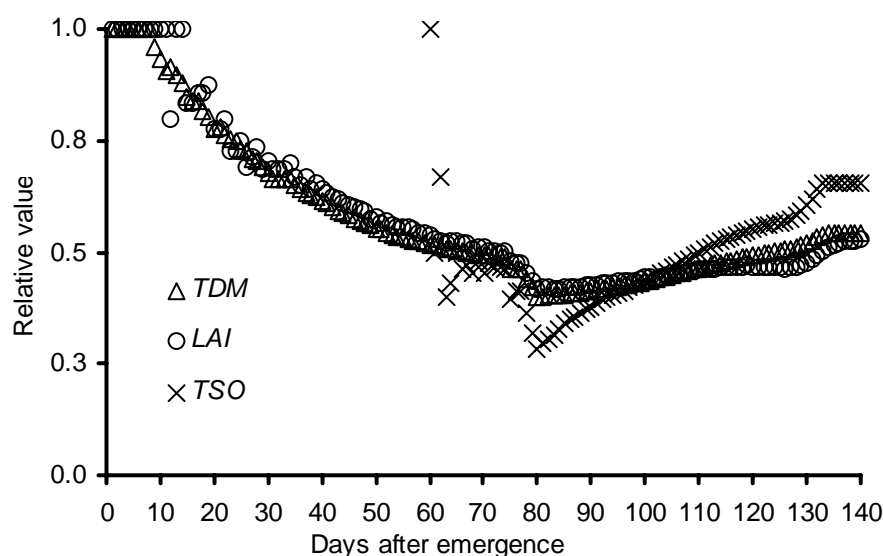


Figure 7.3 Relative values of total dry matter *TDM*, total storage organs *TSO* and leaf area index *LAI* simulated by *SWAP-WOFOST* model without or with reduced daily gross CO_2 assimilation rate A_{pgross} ($\text{kg ha}^{-1} \text{d}^{-1}$) by a factor of 0.80. This figure is based on the simulation for wheat at a farmer field (S4F16) in Sirsa district during the *rabi* (winter) season of the agricultural year 2001-02.

Fig. 7.3 suggests that the reduction in total dry matter *TDM* production is more or less linearly related to the reduction in other simulated plant organs such as total storage organs *TSO* and leaf area index *LAI*. Therefore, we can update the simulated plant organs i.e. leaf, stem, storage organ and root biomass with the calculated C_F (Eq. 7.4), whenever a TDM_{obs} is available.

7.3 Application to study sites in Sirsa district

We present the assimilation of TDM_{obs} for wheat in Sirsa district during the agricultural year 2001-02. First, ‘forcing’ and ‘updating’ methods were evaluated using the synthetic TDM_{obs} data, and second ‘calibration’ and ‘updating’ methods were evaluated using the observed TDM_{obs} data.

In this application, the meteorological data were used from the ICAR-CS, Sirsa (Chapter 3). The crop parameters of *SWAP-WOFOST* were the same as summarized by Bessembinder et al. (2003). The soil parameters were based on the calibration and validation at field S5F20 in Sirsa (Chapter 4). The groundwater level is deeper than 3.0 m, and therefore a free drainage (Eq. 3.14) condition was applied as lower boundary.

For synthetic TDM_{obs} data, a numerical ‘reference’ experiment for wheat was performed through a forward run of *SWAP-WOFOST* during the *rabi* (winter) season from Nov. 1, 2001 to April 30, 2002. The average crop and irrigation calendar were used to specify the crop emergence and irrigation dates for a wheat crop (Chapter 5). A total of 38.0 cm irrigation was applied through 6 irrigations with an irrigation depth of 8.0 cm for pre-sowing irrigation and 6.0 cm for the following irrigations. The simulated *TDM* after emergence of the crop during the ‘reference’ experiment was sampled at an interval of 16 days. This sampling frequency represents the revisit frequency of the Landsat TM7 image (*Landsat Enhanced Thematic*

Mapper, spatial resolution 30×30 m), which offers the remotely sensed TDM at regional scale. The accuracy of the observed LAI , TDM and ET through satellite remote sensing varies from 80 to 90% (Bastiaanssen and Bos, 1999). The error in TDM_{obs} data used for data assimilation is expected to affect the simulation of crop production, and hence was evaluated. Two different levels of random error (10% and 20%) were added in the synthetic TDM_{obs} data. For each error level, 40 series consisting of 10 TDM_{obs} data points were generated. A random number e.g. for 10% error level was drawn from a normally distributed population with a mean equal to TDM_{obs} and a standard deviation equal to 10% of TDM_{obs} .

For the observed TDM_{obs} data, a farmer field S5F20 was selected with a wheat-cotton combination in Sirsa district. This field was monitored during the *rabi* (winter) season (Nov. 1, 2001 to April 30, 2002) of the agricultural year 2001-02 (Chapter 3). The measured crop and irrigation calendars were used to specify the crop emergence and irrigation dates for the wheat crop. A total of 56.8 cm irrigation was applied through 8 irrigations with a depth ranging from 5.0 to 12.0 cm. The TDM_{obs} was observed four times during the crop growth period, and finally at harvest time of the crop. The four TDM_{obs} values, observed during the growth period, were used in the sequential ‘*updating*’ and ‘*calibration*’ process.

In the ‘*calibration*’ process, the sensitive and uncertain input parameters were calibrated to obtain an optimal agreement between TDM_{obs} and TDM_{sim} values. In *SWAP-WOFOST*, the simulation of TDM_{sim} is sensitive to crop parameters such as maximum CO_2 assimilation rate A ($kg\ ha^{-1}\ hr^{-1}$) and light use efficiency ϵ ($kg\ ha^{-1}\ hr^{-1}/J\ m^2\ s^{-1}$) (Fig 6.1). These crop parameters were calibrated within a realistic range through the optimisation algorithm PEST, which was linked to *SWAP-WOFOST* (Chapter 4). The calibration range for the parameter A was specified from 35.0 to 45.0 $kg\ ha^{-1}\ hr^{-1}$, and for parameter ϵ from 0.35 to 0.55 $kg\ ha^{-1}\ hr^{-1}/J\ m^2\ s^{-1}$. The ‘*calibration*’ process was started with an initial value of parameter A equal to 45.0 $kg\ ha^{-1}\ hr^{-1}$, and of parameter ϵ equal to 0.50 $kg\ ha^{-1}\ hr^{-1}/J\ m^2\ s^{-1}$. The weight factor W_{obs} (Eq. 7.1) for a particular TDM_{obs} value was assigned inversely proportional to the magnitude of the observation i.e. $1/TDM_{obs}$, which implies that every TDM_{obs} has equal importance during the ‘*calibration*’ process.

7.4 Results and discussion

7.4.1 The ‘*forcing*’ vs. ‘*updating*’ method

To assimilate the synthetic TDM_{obs} data into *SWAP-WOFOST*, the above described ‘*forcing*’ and ‘*updating*’ methods were implemented repetitively, each time with a different realization of the random observation error incorporated into the synthetic TDM_{obs} data. In this study, we did not calculate the optimal gain factor ‘ K_g ’ (Eq. 7.3) during the sequential ‘*updating*’ process, and used different values of K_g to investigate its effect on the assimilation results. Four different values of K_g were used: 0.00, 0.50, 0.75 and 1.00.

Table 7.1 presents the statistical properties for simulated crop production i.e. total dry matter TDM and total storage organs TSO , and water balance components i.e. transpiration T , evapotranspiration ET and percolation Q_{bot} at harvest time of the wheat crop. The statistical properties are mean, bias and standard deviation. The bias is equal to the absolute difference between the mean expected and the true value i.e. ‘*reference*’. The bias was small in all cases,

indicating that the number of 40 replications was large enough to derive the standard deviation. Note the negligible influence on the water balance components T , ET and Q_{bot} during the assimilation of synthetic TDM_{obs} data. It shows the possibilities of assimilating the remotely sensed or field observed TDM_{obs} with involved 10 and 20% random error into *SWAP-WOFOST* without affecting the simulation of water balance for the average wheat conditions in Sirsa district.

Table 7.1 Statistical properties (mean, bias and standard deviation) of total dry matter TDM , total storage organs TSO , transpiration T , evapotranspiration ET and percolation Q_{bot} as simulated by *SWAP-WOFOST* model without i.e. ‘reference’ and with synthetic TDM_{obs} data assimilation through ‘forcing’ and ‘updating’ methods. K_g is the optimal gain factor (Eq. 7.2) during the sequential ‘updating’ process. The numerical experiment was conducted for a wheat crop in Sirsa district during the *rabi* (winter) season of the agricultural year 2001-02. The results are based on the 40 generated synthetic TDM_{obs} data sets each having 10 data points, and two (a) 10% and (b) 20% random error level.

(a) 10% Random error level

Parameter / Method	TDM (ton ha ⁻¹)			TSO (ton ha ⁻¹)			T (mm)			ET (mm)			Q_{bot} (mm)		
	Mean	Bias	Std	Mean	Bias	Std	Mean	Bias	Std	Mean	Bias	Std	Mean	Bias	Std
<i>Reference</i>	14.0	--	--	7.5	--	--	243	--	--	340	--	--	-29	--	--
<i>Forcing</i>	13.8	0.2	0.9	7.4	0.1	0.5	243	0	2	340	0	1	-28	1	0
<i>Updating</i>															
$K_g = 0.00$	14.0	0.0	0.0	7.5	0.0	0.0	243	0	0	340	0	0	-29	0	0
$K_g = 0.50$	13.9	0.1	0.5	7.5	0.0	0.3	242	1	1	340	0	1	-29	0	0
$K_g = 0.75$	13.8	0.1	0.7	7.4	0.1	0.4	242	1	2	340	0	1	-29	0	0
$K_g = 1.00$	13.8	0.2	0.9	7.4	0.1	0.5	242	1	2	340	0	1	-29	0	0

(b) 20% Random error level

Parameter / Method	TDM (ton ha ⁻¹)			TSO (ton ha ⁻¹)			T (mm)			ET (mm)			Q_{bot} (mm)		
	Mean	Bias	Std	Mean	Bias	Std	Mean	Bias	Std	Mean	Bias	Std	Mean	Bias	Std
<i>Reference</i>	14.0	--	--	7.5	--	--	243	--	--	340	--	--	-29	--	--
<i>Forcing</i>	13.5	0.5	1.9	7.3	0.2	1.0	243	0	3	340	0	2	-28	1	0
<i>Updating</i>															
$K_g = 0.00$	14.0	0.0	0.0	7.5	0.0	0.0	243	0	0	340	0	0	-29	0	0
$K_g = 0.50$	13.8	0.2	1.1	7.4	0.1	0.6	242	1	3	339	1	2	-29	0	0
$K_g = 0.75$	13.6	0.4	1.4	7.3	0.2	0.8	242	1	3	339	1	2	-29	0	0
$K_g = 1.00$	13.5	0.5	1.9	7.3	0.2	1.1	242	1	4	339	1	2	-29	0	0

In case of the ‘forcing’ method, the standard deviations of TDM and TSO were the highest, and became double with the increased level of random error from 10% to 20% (Table 7.1a and 7.1b). It clearly shows that in case of data assimilation through the ‘forcing’ method, errors in the remotely sensed or observed biophysical variables e.g. TDM_{obs} will be propagated into the model.

In case of the ‘updating’ method, the standard deviation of TDM and TSO is approximately linearly related to the used value of the optimal gain factor ‘ K_g ’. With the used value of K_g equal to 1.00, the ‘updating’ method became equal to the ‘forcing’ method. This is obvious as

the K_g equal to 1.00 implies full weight to the erroneous synthetic TDM_{obs} data during the ‘*updating*’ process. As the value of K_g was decreased to 0.75 and 0.50, the standard deviations of TDM and TSO decreased. With the used value of K_g equal to 0.00, there was no deviation between TDM and TSO simulated during the ‘*updating*’ and the ‘*reference*’ situation, which implies no assimilation of the erroneous synthetic TDM_{obs} data.

In representing the natural conditions, the physical based *SWAP-WOFOST* conceptualises and aggregates the relatively complex processes and their heterogeneity through relatively simple mathematical equations, and therefore contains to a certain extent a modelling error. The modelling error might become large with over- or underparameterisation and with uncertainty involved, especially when applied in a distributed mode at regional scale. The assimilation of remotely sensed or field observed model state variables is expected to improve the model predictions. However, the remotely sensed or observed model variables also contain observation errors e.g. TDM_{obs} values with 10 and 20% random error level in this study. *In case of the ‘forcing’ method, the model forgets its own information, and follows the TDM_{obs} data as a driving state variable, including the observation errors.* The ‘*updating*’ method has more flexibility in assimilating TDM_{obs} data and its associated errors into the model. In case of the simple sequential ‘*updating*’ algorithm, the magnitude of the correction of TDM_{sim} depends on the used value of optimal gain factor ‘ K_g ’ (Eq. 7.2). If the errors in the model structure are very small i.e. $\sigma_{sim}^2 = 0$, the K_g value becomes equal to 0.00, and no weight will be given to the TDM_{obs} during the ‘*updating*’ process. Similarly, if errors in the observations are very small i.e. $\sigma_{obs}^2 = 0$, the K_g value becomes equal to 1.00, and full weight will be given to the TDM_{obs} .

Therefore, *an accurate calculation of the optimal gain factor K_g , associated with the errors into both modelling and observations, is essential during the sequential ‘updating’ process.* The Kalman filter, a statistical method, can be used to calculate the accurate values of K_g , which represents the Kalman gain in the adopted simple sequential ‘*updating*’ algorithm. The standard Kalman filter (Kalman, 1960) has limitations in its application to non-linear models such as *SWAP-WOFOST*. Instead, the developed Extended or Ensemble Kalman filter can be applied (Aubert et al., 2003; Walker et al., 2003; Makowski et al., 2003). Further research is recommended to investigate the implementation of these statistical models to assimilate TDM_{obs} into *SWAP-WOFOST*.

7.4.2 The ‘*calibration*’ vs. ‘*updating*’ method

In this section, the observations at a farmer field S5F20 were used for the implementation of ‘*calibration*’ and ‘*updating*’ methods to assimilate TDM_{obs} into *SWAP-WOFOST*.

Firstly, field S5F20 was simulated with *SWAP-WOFOST* without assimilation of TDM_{obs} , which is referred to as ‘*reference*’ model. The results are presented in Table 7.2. Note that the TDM and TSO values simulated with the ‘*reference*’ model were about 50% higher than the actual (observed) TDM and TSO values at the harvest time of the wheat crop. *SWAP-WOFOST* simulates the water and salt limited TDM and TSO accounting for the water and salt stress only. In addition to water and salt stress, management factors such as nutrient, pest and disease control affect the crop growth under actual field conditions. The low observed (actual)

wheat grain yield of 4.3 ton ha⁻¹ at field S5F20 despite the high irrigation of 568 mm shows the presence of nutritional, pest or disease stresses (Chapter 4).

Secondly, the ‘*calibration*’ process was performed to assimilate the four TDM_{obs} values observed during the *rabi* (wheat) growing season. In the ‘*calibration*’ process, the effect of so-called management factors on TDM and TSO is partially propagated into the model input variables. The sensitive crop parameter i.e. light use efficiency ε (kg ha⁻¹ hr⁻¹/ J m² s⁻¹) was optimised at 0.43 with a coefficient of variation equal to 4.42, and maximum CO₂ assimilation rate A (kg ha⁻¹ hr⁻¹) at 45.0 with a coefficient of variation equal to 3.75. In the ‘*updating*’ process, the same four observed TDM_{obs} values were used to update the simulated plant organs i.e. leaf, stem, storage organ and root biomass through the adopted simple sequential ‘*updating*’ algorithm. Instead of calculating the optimal gain factor ‘ K_g ’, we again used three optimal values of K_g : 0.50, 0.75 and 1.00.

Table 7.2 Total dry matter TDM , total storage organs TSO , transpiration T , evapotranspiration ET and percolation Q_{bot} as simulated by SWAP-WOFOST model without i.e. ‘*reference*’ and with observed TDM_{obs} data assimilation through ‘*calibration*’ and ‘*updating*’ methods. K_g is the optimal gain factor (Eq. 7.2) during the sequential ‘*updating*’ process. The field experiment was conducted for a wheat crop monitored at a farmer field (S5F20) in Sirsa district during the *rabi* (winter) season of the agricultural year 2001-02.

Parameter / Method	TDM (ton ha ⁻¹)	TSO (ton ha ⁻¹)	T (mm)	ET (mm)	Q_{bot} (mm)
Observation	9.22	5.43			
Reference	14.23	8.46	249	370	-164
Calibration	11.31	6.82	229	354	-173
Updating					
$K_g = 0.50$	11.00	6.64	248	369	-162
$K_g = 0.75$	9.92	6.05	247	368	-162
$K_g = 1.00$	9.24	5.68	245	367	-161

Fig. 7.4 presents the simulation of TDM without i.e. ‘*reference*’ and with the TDM_{obs} assimilation through ‘*calibration*’ and ‘*updating*’ methods. The ‘*calibration*’ process adjusted the sensitive crop parameters, mainly light use efficiency ε (kg ha⁻¹ hr⁻¹/ J m² s⁻¹), and provided an internal modelling consistency for the simulation of TDM during crop growth (Fig. 7.4a). As the physical description of underlying process is an acceptable representation of the natural system, the ‘*calibration*’ method is expected to give more representative input parameters and simulated crop production i.e. TDM and TSO and water balance components i.e. T , ET and Q_{bot} . This only applies if there are sufficient observations, and the observation error is small. Note that the TDM and TSO simulated during the ‘*calibration*’ process were not strictly equal to the observed TDM and TSO at the harvest time of the wheat crop (Table 7.2). This is attributed to the errors associated with the observations or suddenly reduction in TDM during crop growth due to pest or diseases in actual field conditions. If we assume that there is a sudden reduction in TDM due to pest or diseases attack, it is hard to assimilate such

effects through the ‘*calibration*’ process. Moreover, because of the optimisation procedure, PEST algorithm had to recall *SWAP-WOFOST* model 57 times during the ‘*calibration*’ process. Therefore, this approach requires a large amount of computation time to assimilate the remotely sensed TDM_{obs} data, especially in case of distributed modelling at regional scale.

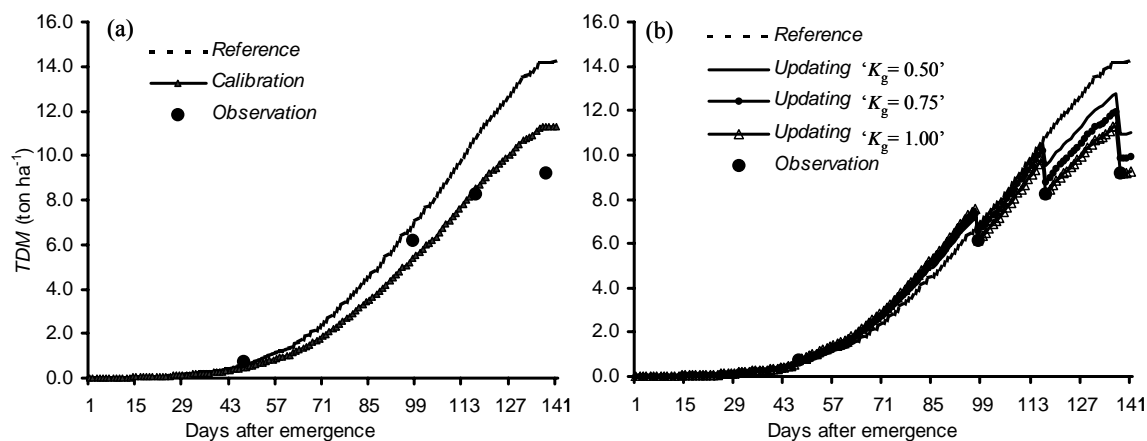


Figure 7.4 Total dry matter TDM (ton ha^{-1}) as simulated by *SWAP-WOFOST* model without i.e. ‘*reference*’ and with the observed TDM_{obs} data assimilation through (a) the ‘*calibration*’ and (b) the ‘*updating*’ method. K_g is the optimal gain factor (Eq. 7.2) during the sequential ‘*updating*’ process. The field experiment was conducted for a wheat crop monitored at a farmer field (S5F20) in Sirsa district during the *rabi* (winter) season of the agricultural year 2001-02.

In case of the ‘*updating*’ process, the simulation of TDM and TSO was improved with the use of increased K_g values. With the used value of K_g equal to 1.00, the simulated TDM and TSO were almost equal to the observed TDM and TSO at the harvest time of the wheat crop (Table 7.2). The value of K_g equal to 1.00 implies full weight to the TDM_{obs} data during the ‘*updating*’ process. Even with a value of K_g equal to 0.50, the ‘*updating*’ process performed almost equal to the ‘*calibration*’ process. Although relatively simple, the simple sequential ‘*updating*’ algorithm introduced some modelling inconsistency into the simulation of TDM during crop growth (Fig 7.4b). If there are sufficient observations and the observation error is small, the introduced inconsistency is expected to be small. Also, this inconsistency has minor influence on the simulated water balance components T , ET and Q_{bot} at field S5F20 (Table 7.2). In case of a sudden reduction in TDM due to pest or diseases attack, it might be incorporated through the ‘*updating*’ process. Further, adopting this sequential ‘*updating*’ algorithm, which requires only one run of the model, will significantly reduce the computation time as compared to the ‘*calibration*’ method. This feature is important for distributed modelling at regional scale.

7.5 Conclusions

The main conclusions, which could be drawn from this study, are as follows.

- The remotely sensed or field observed TDM_{obs} data with 10 to 20% random error can be assimilated into *SWAP* model without affecting the simulation of water balance for the average wheat growing conditions in Sirsa district.

- Errors in the remotely sensed or observed biophysical variables e.g. TDM_{obs} will be propagated into the model if the TDM_{obs} data with involved observation errors are assimilated through the ‘*forcing*’ method. In terms of error propagation, the ‘*updating*’ method is superior to the ‘*forcing*’ method.
- In order to improve predictions, the ‘*calibration*’ method provides the internal modelling consistency, and is expected to give more representative input parameters and simulated crop production i.e. TDM and TSO and water balance components i.e. T , ET and Q_{bot} . This only applies if there are sufficient observations, and the observation error is small. The potential drawback of this method is the use of an optimisation procedure, and therefore requires a large amount of computation time.
- Besides its scientific relevance, adopting the simple sequential ‘*updating*’ algorithm will significantly reduce the computation time as compared to the ‘*calibration*’ method, especially in case of distributed modelling at regional scale. The success of the simple sequential ‘*updating*’ algorithm relies on the accurate calculation of the optimal gain factor ‘ K_g ’, which is associated with the errors into both modelling and observations. The Extended or Ensemble Kalman filter methods should be investigated to calculate this factor K_g , and to update SWAP model’s state variables such as total dry matter, leaf area index and ET fluxes, whenever an observation is available.

Summary and conclusions

Problem Statement

In India, like in most of the Asian countries, the growing human population forces to *'produce more and more food from the limited land and water resources'*. At the same time, the irrigated agriculture, which contributes to nearly 60% of the total agricultural output, is faced with typical problems of water scarcity, poor groundwater quality, rising or declining groundwater levels, waterlogging and secondary salinization, and less than optimal production. These prevailing water management issues are very complex, and must be addressed by better planning and management.

In order to improve water management and its productivity, we need to reveal the cause-effect relationships between hydrological and biophysical variables under different ecohydrological conditions. The recently introduced concept of water productivity describes various aspects of water management such as production, utilization and economy. Keeping in mind the increasing demands of water for food and the increasing water scarcity, the concept of water productivity in agricultural production systems is focused on *'more crop per drop'* or *'producing more food with the same water resources'* or *'producing the same amount of food with less water resources'*. A profound water productivity *WP* analysis requires quantification of different hydrological variables such as transpiration T , evapotranspiration ET and percolation Q_{bot} , and biophysical variables such as grain (or seed) yields Y_g in relation to different irrigation and agricultural management practices. The problems, often encountered are:

- i) limited availability of ecohydrological information,
- ii) field experiments are expensive, laborious and time consuming,
- iii) measurements of ET and its partitioning into E and T under partial soil cover, and of Q_{bot} are rather difficult, and
- iv) tools are absent to make a detailed analysis of irrigation systems.

In recent decades, researchers have devoted much effort to quantify these required hydrological and biophysical variables by means of different approaches i.e. simulation modelling and satellite remote sensing. Estimation of water balance components such as Q_{bot} , and E and T separately is also not possible with the current remote sensing algorithms such as the Surface Energy balance Algorithm for Land (SEBAL), and therefore provides limited information on water productivity: crop yield per unit amount of evapotranspiration. The evaluation of alternative water management scenarios is also not possible with satellite remote sensing. However, satellite remote sensing provides spatial variables such as land use, which can be of great help in water productivity analysis at regional scale. The simulation modelling approach is able to estimate water balance components such as Q_{bot} , and E and T separately, and to evaluate alternative water management scenarios. Therefore, *the main research objective of this study was to integrate the operational knowledge of crop growth, soil water flow and salt transport modelling with field experiments, remote sensing and geographical information system (GIS) for water productivity analysis from field to regional scale.*

Study area

Sirsa district (Haryana), located in the northwest Indian irrigated plains, has been selected for a case study. It covers about 4270 km², of which 90% is under cultivation with a high cropping intensity of 157%. Wheat and mustard (oilseed) are the main crops during the *rabi* (winter) season, which are followed by cotton and rice during the *kharif* (summer) season. The climate is characterized by its dryness, extremes of temperature and scanty rainfall. Crop production without irrigation is very limited, even in the monsoon (rainy) season. To summarize, the major water management problems in Sirsa district are canal water scarcity, poor groundwater quality, rising and declining groundwater levels, waterlogging and secondary salinization, and low crop production. Current increase in crop yields is either marginal or reversed, especially in case of rice.

Framework for regional water productivity analysis

As presented in Chapter 3, a framework integrating crop growth, soil water flow and salt transport modelling with remote sensing and GIS is developed to describe the hydrological and biophysical processes at regional scale. *The main hypothesis postulated in this framework is that an ensemble of individually homogeneous regions can equivalently represent a spatially heterogeneous region.* It is further postulated that the effects of spatial heterogeneity on the regional water and salt balances, and on the water productivity can be analyzed by running a field scale model for all combinations of *weather-crop-soil-water* in the study area. This hypothesis is valid for only unsaturated zone conditions over the plain irrigated areas without significant runoff and with deep groundwater levels as is the case in Sirsa district.

In this study, a field scale ecohydrological model, Soil Water Atmosphere Plant (SWAP), was extended in a distributed mode to simulate the spatial water and salt balances and crop yields, and subsequently the water productivity from field to regional scale. SWAP simulates the vertical soil water flow and salt transport in close interaction with crop growth in the soil-water-atmosphere-plant continuum. Richards' equation is applied to compute transient soil water flow, and the convection-dispersion equation to compute salt transport.

SWAP includes both simple and detailed crop growth modules. In the simple crop module, crop growth is forced by the measured leaf area index, crop height and rooting depth as a function of crop development stage. The simple crop module does not simulate any interaction between the crop growth and the water and salt stress conditions. *However, the detailed crop module has the advantage of giving a feedback between crop growth and water and salt stress conditions.* The detailed crop growth module is based on the World Food Studies (WOFOST) model, which simulates the crop growth and its production based on the incoming photosynthetically active radiation (*PAR*) absorbed by the crop canopy, its photosynthetic leaf characteristics, and accounting for water and salt stress on the crop. The effects of nutrient supply, pests, weeds, and diseases on the crop growth and its production are not implemented in the present version of WOFOST. The above described both simple and detailed crop growth simulation approaches are included in the present version SWAP 3.03 model (Kroes and Van Dam, 2003). To distinguish the simulations in this study, SWAP 3.03 when used with the simple crop growth module is called *SWAP* hereafter, and when used with the detailed crop growth module is called *SWAP-WOFOST*.

The developed framework when applied for regional water productivity analysis requires a significant amount of information at different spatial and temporal scales. The information used in this study was collected in the framework of the WATPRO project in Sirsa district, and was derived from two different sources: specific field experiments and existing secondary information sources. Field experiments for two main crops (wheat and cotton) were conducted to obtain the detailed crop growth measurements, which were used to calibrate and validate the *SWAP-WOFOST*. To obtain existing ecohydrological conditions and its variation under actual field conditions, 24 farmer fields with main crop combinations (wheat-cotton and wheat-rice) were monitored in Sirsa district during the agricultural year 2001-2002. The spatial information on weather, soil, irrigation and groundwater was collected from existing Government agencies. Satellite remote sensing techniques provided the spatial land use and *ET* fluxes at regional scale. This substantial amount of data available in Sirsa district made it possible to perform such a detailed ecohydrological study at regional scale.

Calibration and validation of SWAP model

Successful application of models like SWAP depends on the accuracy and reliability of the input parameters for crop growth, soil water flow and salt transport. In Chapter 4, a profound analysis of input parameters and predicted results of SWAP was conducted at farmer fields in Sirsa district during the agricultural year 2001-02. The simple crop growth model, denoted as *SWAP*, was calibrated and validated using measurements at five fields representing various combinations of soil, crop, and irrigation amount and quality. Two fields represented the wheat-rice cultivation at heavy soil texture (i.e. clay loam to silt clay loam), and other three fields represented the wheat-cotton cultivation at light soils (i.e. sandy loam to loamy sand). Most of the input parameters were measured directly during the field experiments, and the remaining uncertain soil hydraulic parameters were estimated through the model calibration. The non-linear parameter estimation program PEST was linked with SWAP to perform automatic calibration, called inverse modelling, of soil hydraulic parameters using the observed soil moisture θ and salinity *EC* profiles at different fields. A good agreement between the observed and simulated θ and *EC* was achieved. Inverse modelling was found efficient in the calibration of soil hydraulic parameters using the observed θ and *EC* as system response. Further, the applicability of the detailed crop growth model, denoted as *SWAP-WOFOST*, for regional crop growth simulations was tested by its comparison with the calibrated and validated *SWAP* at different fields. The water and salt balances simulated by *SWAP-WOFOST* were comparable with those obtained from *SWAP*. The crop yields simulated by *SWAP-WOFOST* were also found to be properly corresponding to the water and salt stress at different fields.

The results of Chapter 4 provided confidence to apply *SWAP-WOFOST* for water productivity analysis at regional scale as described in Chapter 5. The calibrated and validated *SWAP-WOFOST* was applied in a distributed mode: independent runs for all combinations of *weather-crop-soil-water* in the study area. The process of aggregation of these combinations, denoted as ‘*simulation*’ units, was performed in a GIS environment by overlaying the thematic maps of weather, land use, soil, water supply, groundwater level and quality in Sirsa district. Field experiments, satellite images and existing geographical data were used to derive and aggregate the input parameters attached to all simulation units and boundary

conditions at the appropriate scales. Canal water and groundwater irrigations were aggregated for different crop combinations at village level. Pedotransfer functions, which relate the soil hydraulic functions $\theta(h)$ and $K(\theta)$ (Eq. 3.3 and 3.4) to easily measured soil information, were applied to estimate soil hydraulic parameters for different simulation units.

To evaluate the accuracy and reliability of spatial aggregation of input parameters, the actual evapotranspiration simulated by distributed *SWAP-WOFOST* modelling, denoted as ET_{SW} , was compared with independent satellite remote sensing based evapotranspiration data, denoted as ET_{RS} , at different spatial and temporal scales. There was a close agreement between ET_{RS} and ET_{SW} over the wheat, mustard and rice areas, with a slightly lower simulation of ET_{SW} over the cotton area. A high discrepancy between ET_{RS} and ET_{SW} over the bare soil/settlements area showed the importance of proper land use classification in distributed modelling approach. The low accuracy of land use classification can mislead the parameterization of *SWAP-WOFOST*, which subsequently can result in unrealistic water and salt balances. Despite the simplifications involved, the proposed aggregation methods for spatial input parameters (such as average crop and irrigation calendar, irrigation water distribution, and the use of pedotransfer functions) resulted into the simulated water and salt balances and crop yields, which compared well with other independent data based on satellite remote sensing and field measurements.

Current water management and its productivity in Sirsa district

The current water productivity of the main crops wheat, mustard, rice and cotton in Sirsa district was analysed at both field (Chapter 4) and regional scale (Chapter 5). Experimental year, the agricultural year 2001-02, might be characterised as ‘dry’ year with a low rainfall of 99 mm only. Water productivity was computed for different scales and in different forms viz., $kg Y_g$ (grain or seed yield) / m^3 water used in T (transpiration), ET (evapotranspiration), or ETQ (evapotranspiration ET plus percolation Q_{bot} from irrigations and seepage losses Q_{SL} from the conveyance system) (Table 3.1). This flexibility in defining water productivity provides useful indicators to evaluate irrigation water utilization, and to identify where and when water can be saved.

Firstly, we analysed water productivity WP values (Table 3.1) using the water balance components T , ET and Q_{bot} simulated by *SWAP*, and the grain (or seed) yields Y_g measured at the selected farmer fields (Table 4.7). WP_T refers to Y_g/T , and sets the lower limit of water used by crop: the crop transpiration only. The average WP_T ($kg m^{-3}$) was 1.88 for wheat, 1.73 for rice and 0.29 for cotton. *This presents wheat as highest efficient crop in terms of physical crop production in Sirsa district.*

The average WP_{ET} , expressed as Y_g/ET ($kg m^{-3}$), was 1.39 for wheat, 0.94 for rice and 0.23 for cotton. This corresponds to kind of average values of WP_{ET} for the climatic and growing conditions in Northwest India. The ET is mostly considered as the total amount of water used in crop production. The average WP_{ET} was significantly lower than the average WP_T : about 46% for rice, 26% for wheat and 22% for cotton. *Improving agronomic practices such as soil mulching and especially dry rice cultivation could reduce the non-beneficial loss of water through soil evaporation E , and subsequently will improve WP_{ET} at field scale.*

The percolation from field irrigations further reduces the WP_{ET} to WP_{ETQ} at field scale. The average WP_{ETQ} , expressed as Y_g/ETQ (kg m^{-3}), was 1.04 for wheat, 0.84 for rice and 0.21 for cotton.

Secondly, we analysed water productivity WP values (Table 3.1) using the water balance components T , ET and Q_{bot} , and the grain (or seed) yields Y_g simulated by *SWAP-WOFOST* at the same farmer fields (Table 4.7). Note that *SWAP-WOFOST* simulates the crop growth and its production accounting for water and salt stress only. In addition to water and salt stress, management factors such as nutrient, pest and disease control affect the crop growth under actual field conditions. For wheat, the simulated water and salt limited Y_g were 20 to 60% higher than the actual (measured) Y_g . This is attributed to almost negligible water and salt stress at the selected wheat fields: relative transpiration (T/T_p) ranged from 0.85 to 1.00. In this field scale analysis, we concluded that improved crop management in terms of timely sowing, optimum nutrient supply and better pest and disease control for wheat will multiply its WP_{ET} by a factor of 1.5 in Sirsa district.

In the following *kharif* (summer) season, severe water stress was observed at the selected cotton fields: $T/T_p < 0.65$. For cotton, the simulated water and salt limited Y_g were 1.5 to 3.5 times lower than the simulated potential Y_g . Therefore, benefits in terms of increased crop yields and improved water productivity will be gained by ensuring irrigation supply at cotton fields, especially during 'dry' years such as the year 2001-02.

In Chapter 5, *SWAP-WOFOST* was applied in a distributed mode to simulate the water and salt limited WP_T , WP_{ET} and WP_{ETQ} values for the entire Sirsa district during the agricultural year 2001-02 (Table 5.7). These values are based on the simulation results, and might deviate to a certain extent from the real values. However, they represent the current utilization of water resources and their effect on existing physical environment. The mean WP_{ET} , expressed as Y_g/ET (kg m^{-3}), was 1.37 for wheat, 0.36 for cotton and 0.47 for mustard and rice. Considerable variation was observed in WP_{ET} with a coefficient of variation of 15% for wheat and cotton, 19% for mustard and 64% for rice. *This presents a large potential of the improvement of water productivity in Sirsa district.*

The soil evaporation E accounted for 20 to 47% of the evapotranspiration ET , especially for rice, and is identified as a major non-beneficial loss of water. Further, the high seepage losses Q_{SL} (34 to 43% of total canal water inflow) from the conveyance system along with percolation Q_{bot} from the field irrigations are responsible for a reduction of 25 to 30% from WP_{ET} to WP_{ETQ} .

The simulated water and salt limited WP_T , WP_{ET} and WP_{ETQ} values for wheat, cotton and especially rice were higher in the southern (FB) and central (GHG and SUK) commands than in the northern (BMB) command (Fig. 5.14). The low water productivity in BMB is related to the poor quality groundwater in the northern parts of Sirsa district. In BMB, the mean WP_{ET} for rice was 47% lower than its mean value of 0.47 kg m^{-3} for the entire district. Also, the high percolation from rice fields is contributing to the rising groundwater levels in this command. Therefore, *efforts to improve the water productivity must focus on the northern parts, and replacing rice cultivation by cotton should be promoted in BMB command.*

The current cultivation and irrigation practices in Sirsa district are leading to unfavorable ecohydrological conditions. For instance, the high intensity of more water consuming wheat and rice crops and relatively low canal inflow in GHG and SUK commands, inducing high groundwater use, are resulting in the declining groundwater levels in the central parts. On the other side, relatively high canal water inflow and low groundwater pumping in BMB, restricted due to relatively poor groundwater quality, are contributing to the rising groundwater levels in the northern parts. *This presents a threat to the sustainability of irrigated agriculture in Sirsa district (Fig. 5.13).*

Alternative water management scenarios in Sirsa district

Productive and sustainable water management can be achieved through the identification and implementation of efficient water management options. Problems and prospects associated with a particular water management option are often not recognised until they are well advanced. Although the developed distributed modelling is based on certain assumptions and simplifications of real situations, it provides the opportunity to compare and understand the cause-effect relationships. The simulated water and salt balances and crop production can help to evaluate alternative water management scenarios at the desired scale.

In Chapter 6, feasible water management options in Sirsa district are proposed and elaborated. The proposed 5 alternative water management scenarios include:

- Scenario 1: *'Business as usual'* or *'reference'* situation,
- Scenario 2: Increased (10 to 15%) crop yields,
- Scenario 3: Reduced seepage losses at 25 to 30%,
- Scenario 4: Canal water reallocation (15%) from the BMB to the GHG and SUK, and
- Scenario 5: Combination of Scenario 2, 3 and 4.

These scenarios intend to improve the water productivity, and to halt the rising and declining groundwater levels in Sirsa district. They were evaluated through the distributed *SWAP-WOFOST* modelling over a period of 10 years (1991-2001).

Sirsa district as a whole has nearly a closed water balance as the total annual surface inflow, accounting for both rainfall and canal water inflow, was almost equal to the simulated annual evapotranspiration. This is also confirmed by the measured groundwater levels, which show a marginal average annual net groundwater recharge R of 11 mm y^{-1} during the period from 1990 to 2000. At the same time, Scenario 1 i.e. *'Business as usual'* shows a large spatial variation of the estimated R and salt build-up ΔC over the main commands BMB, SUK, GHG and FB (Table 6.2). *This suggests that interventions are required for a productive and sustainable water management in Sirsa district.*

The average actual grain (or seed) yields Y_g (ton ha^{-1}) in Sirsa district over the last 10 years (1991-2001) are recorded at 4.1 for wheat, 1.2 for mustard (oilseed), 3.2 for rice and 1.2 for cotton (Fig. 2.10). In case of *'Business as usual'* (Scenario 1), the simulated water and salt limited Y_g during the same period were 1.2 to 2.0 times higher than the recorded Y_g , especially for rice and cotton (Table 6.3). *This indicates that there exists substantial nutritional, pest or disease stresses on crop production in Sirsa district.*

Efforts to increase the crop yields will certainly improve WP_{ET} , which represents the actual amount of water used i.e. ET . In this study, the simulated 12 to 17% increased water and salt limited Y_g (Scenario 2) increased the water and salt limited WP_{ET} by 12% for wheat and cotton, 14% for mustard and 18% for rice.

Reduction in seepage losses from the conveyance system is strongly recommended, especially in the northern BMB command with relatively poor quality groundwater. In this study, the simulated reduction in seepage losses from 39-41% (Scenario 1) to 25-27% (Scenario 3) improved the water and salt limited WP_T , WP_{ET} and especially WP_{ETQ} by 6 to 12% for all crops. Moreover, Scenario 3 contributed to the decrease of net groundwater recharge R in BMB and salt build-up ΔC over the entire Sirsa district.

Canal water reallocation (15%) from BMB to SUK and GHG (Scenario 4) will have a slightly adverse impact in BMB in terms of simulated water and salt limited WP_T , WP_{ET} and WP_{ETQ} values for all crops, and salt build-up ΔC . This reduction of 15% canal water inflow in BMB might be made up again by the reduction of seepage losses from the conveyance system (Scenario 3). However, Scenario 4 has a tremendous favorable impact by decreasing R in BMB faced with a rise in groundwater levels. Further, Scenario 4 increased R in GHG and SUK, and will have a favorable impact in checking the declining groundwater levels in central parts of Sirsa district.

In Scenario 5, ‘Combining scenarios 2, 3 and 4’, the water and salt limited WP_T , WP_{ET} and WP_{ETQ} values, and the large fluctuations of the estimated R and high ΔC have been significantly improved as compared to Scenario 1 ‘business as usual’ (Table 8.1).

Table 8.1 Relative impact (%) of the combined alternative water management scenarios (Scenario 2, 3 and 4) (Table 6.1) on the regional water productivity WP_T , WP_{ET} and WP_{ETQ} , and on the net groundwater recharge R and salt build-up ΔC in Sirsa district and its four main commands (Fig. 5.3). Positive values represent an increase and negative represent a decrease. These values are based on the distributed *SWAP-WOFOST* simulations for the unsaturated zone (0-300 cm) over the period of 10 years (1991-2001), and apply to the entire area (cropped as well as bare soil).

Performance indicators	Wheat	Mustard	Cotton	Rice	
WP_T	9	17	8	8	
WP_{ET}	13	16	12	21	
WP_{ETQ}	23	29	23	26	
	Sirsa	BMB	GHG	SUK	FB
R	-85	-99	47	45	-81
ΔC	-20	4	-163	-24	-50

Table 8.1 suggests that the combined impact of increased crop yields (Scenario 2), reduction in seepage losses (Scenario 3) and canal water reallocation (15%) from the northern BMB to the central SUK and GHG commands (Scenario 4) will significantly improve the regional water productivity, and contribute to halt the rising and declining groundwater levels in Sirsa district.

Data assimilation

Although ecohydrological models offer the possibilities for future predictions, they may become inaccurate due to over- or underparameterisation, especially in distributed modelling at regional scale. In principle, the simulated state variables contain a modelling error due to the simplified mathematical representation of the complex processes in natural situations. The uncertainty in input parameters increases this modelling error. This could be accommodated by data assimilation, which uses field observations characterizing the system behaviour such as soil moisture, leaf area index, dry matter production and evapotranspiration fluxes. However, these state observations also involve a certain extent of random observation errors.

In Chapter 7, different data assimilation methods such as ‘*calibration*’, ‘*forcing*’ and ‘*updating*’ were explored to assimilate the observed total dry matter production in the detailed crop module of SWAP, denoted as *SWAP-WOFOST*. In the most common ‘*calibration*’ method, sensitive and uncertain crop input parameters, e.g. light use efficiency and maximum CO₂ assimilation rate, were optimized to minimize the deviation between observed total dry matter TDM_{obs} and simulated total dry matter TDM_{sim} . The ‘*forcing*’ method directly replaced the TDM_{sim} with TDM_{obs} as state variable into the model. A simple sequential ‘*updating*’ algorithm was developed to update the TDM_{sim} , whenever a TDM_{obs} was available. First, ‘*forcing*’ and ‘*updating*’ methods were evaluated using the synthetic (numerical) TDM_{obs} data, and second ‘*calibration*’ and ‘*updating*’ methods were evaluated using the observed TDM_{obs} data.

The results with synthetic TDM_{obs} data (Table 7.1) showed that the remotely sensed or field observed TDM_{obs} with 10 to 20% random error can be assimilated into *SWAP-WOFOST* without affecting the simulation of water balance components for the average wheat growing conditions in Sirsa district. In case of the ‘*forcing*’ method, the model loses its own information, and the observation error of TDM_{obs} data is propagated into the simulated crop production. The ‘*updating*’ method is superior to the ‘*forcing*’ method in terms of error propagation.

The success of the sequential ‘*updating*’ algorithm relies on the accurate calculation of the optimal gain factor ‘ K_g ’, which is associated with errors in the modelling as well as in the observations. Extended or Ensemble Kalman filter methods might be used to calculate K_g accurately, and to update SWAP model state variables e.g. TDM , whenever an observation is available. A major drawback of the sequential ‘*updating*’ might be the introduced internal modelling inconsistency for simulated crop production (Fig. 7.4b). The results of field scale application with the observed TDM_{obs} data showed that this introduced inconsistency during the ‘*updating*’ process had a minor influence on the simulated water balance components T , ET and Q_{bot} (Table 7.2).

The ‘*calibration*’ method assures the internal modelling consistency (Fig. 7.4a), and is expected to give more representative input parameters, and simulated crop production and water balance components. This applies only if there are sufficient observations, and the observation error is small. The potential drawback of the ‘*calibration*’ method is the large amount of computation time due to the use of an optimisation procedure.

Besides its scientific relevance, adopting the simple sequential ‘*updating*’ algorithm will significantly reduce the computation time as compared to the ‘*calibration*’ method, especially in distributed modelling at regional scale. Moreover, the ‘*updating*’ algorithm is able to incorporate suddenly reduced crop production due to pest or diseases, which might not be possible with the ‘*calibration*’ method.

Key conclusions and recommendations

The following key conclusions and recommendations are made *to improve water management and its productivity in Sirsa district*:

- Sirsa district as a whole has nearly a closed water balance as the total annual surface inflow, accounting for both rainfall and canal water inflow, is almost equal to the simulated annual evapotranspiration. At the same time, there exists a large spatial variation of the estimated net groundwater recharge and salt build-up over the main commands (BMB, SUK, GHG and FB). *This presents a threat to the sustainability of irrigated agriculture in Sirsa district.*
- Considerable spatial variation in water productivity WP_{ET} was observed not only for different crops but also for the same crop. Efforts to increase crop yields will certainly improve the WP_{ET} , which represents the actual amount of water used i.e. evapotranspiration. *Soil evaporation, which contributes 20 to 47% of evapotranspiration, especially for rice, is identified as a major non-beneficial loss of water.* Improving rice cultivation, e.g. dry rice cultivation, may help to reduce this non-beneficial loss of water, and to improve the water productivity.
- The simulated water and salt limited crop yields were 1.2 to 2.0 times higher than the actual (recorded) crop yields over the period from 1991-2001. *This indicates substantial nutritional, pest or disease stresses on crop production in Sirsa district.* Therefore, an agronomic management program focusing on improved crop management in terms of timely sowing, optimum nutrient supply, and better pest or disease control should be launched to achieve this higher simulated water and salt limited crop production.
- Reduction in seepage losses from the conveyance system is strongly recommended, especially in the northern BMB command with relatively poor quality groundwater. The conveyance efficiency must be improved from the current level of 60% to 75% through proper lining and adequate maintenance of the irrigation system. *Most of the canals and watercourses in Sirsa district are lined, while the field channels that distribute canal water among fields are still unlined.*
- Canal water reallocation (15%) from BMB to GHG and SUK in combination with the reduction in seepage losses at 25 to 30% is suggested to halt the rising groundwater levels in the northern parts, and the declining groundwater levels in the central parts of Sirsa district.

The following key conclusions and recommendations are made with respect to *distributed modelling for water management and its productivity analysis at regional scale*:

- *Effects of spatial heterogeneity on the regional water and salt balances, and on the water productivity can be analyzed by distributed modelling: running a field scale model for all combinations of weather-crop-soil-water in the study area.*
- The physical based field scale ecohydrological SWAP model, when coupled with field experiments, remote sensing and GIS demonstrated the potential of producing information required to evaluate water management and its productivity at different spatial and temporal scales.
- Integration of distributed SWAP modelling with satellite remote sensing observations such as leaf area index, dry matter production and evapotranspiration fluxes through data assimilation techniques should be investigated to improve its predictive performance at regional scale.
- The developed distributed SWAP modelling can quantify the net groundwater recharge, which is a necessary component for groundwater management. Spatially-temporally quantification of net groundwater recharge from the unsaturated zone can serve as input to regional saturated groundwater flow models. *Combination of both distributed SWAP modelling and regional groundwater flow models should be investigated for regional surface and sub-surface water management.*
- A comprehensive water productivity analysis of an irrigation system requires a substantial amount of ecohydrological information at different spatial and temporal scales. In order to obtain this information, a measurement program through field experiments, satellite remote sensing and existing Government Agencies should be launched in different irrigation systems, and *an accessible digital database must be maintained.*

Samenvatting en conclusies

Probleembeschrijving

Net als in de meeste Aziatische landen, dwingt in India de groeiende bevolking tot het ‘*produceren van steeds meer voedsel op beperkte hoeveelheden land en water*’. Gelijktijdig wordt de geïrrigeerde landbouw, die bijna 60% van de totale landbouwopbrengst levert, geconfronteerd met problemen van waterschaarste, slechte grondwaterkwaliteit, stijgende en dalende grondwaterstanden, verzouting, en verminderde productie. Deze urgente waterbeheersproblemen zijn zeer complex, en dienen benaderd te worden met betere planning en beheer.

Teneinde waterbeheer en –productiviteit te verbeteren, dienen we de causale relaties bloot te leggen tussen hydrologische grootheden en biofysische grootheden onder verschillende ecohydrologische omstandigheden. Het recent geïntroduceerde concept van waterproductiviteit beschrijft diverse aspecten van waterbeheer, zoals productie, gebruik en financiële opbrengst. Rekening houdend met de toenemende vraag naar water voor voedselproductie en de toenemende waterschaarste, richt het concept van waterproductiviteit in landbouwkundige productiesystemen zich op ‘*more crop per drop*’ of ‘*meer gewasproductie met dezelfde hoeveelheid water*’ of ‘*dezelfde gewasproductie met minder water*’. Een degelijke analyse van waterproductiviteit vereist kwantificering van hydrologische grootheden als plantverdamping, bodemverdamping en percolatie, en biofysische grootheden als drogestof- en graanopbrengsten in relatie tot verschillende irrigatie- en landbouwkundige beheersmaatregelen. De problemen bij zo’n analyse zijn vaak:

- i) beperkte beschikbaarheid van ecohydrologische informatie,
- ii) dure, arbeidsintensieve en tijdrovende veldexperimenten,
- iii) moeizame metingen van evapotranspiratie ET en, bij gedeeltelijke gewasbedekking, haar verdeling over evaporatie E en transpiratie T , en van percolatie Q_{bot} ,
- iv) hulpmiddelen ontbreken voor een gedetailleerde analyse van irrigatiesystemen.

De afgelopen decaden hebben onderzoekers veel moeite gedaan om de benodigde hydrologische en biofysische grootheden vast te stellen. Hiervoor gebruikten zij onder andere modelmatige simulatie en remote sensing met satellieten. Meting van waterbalanscomponenten zoals Q_{bot} , en onderscheiding van E en T is echter niet mogelijk met de huidige remote sensing algoritmes zoals de Surface Energy Balance Algorithm for Land (SEBAL). Daardoor verschaft remote sensing beperkte informatie voor een analyse van waterproductiviteit. Ook de evaluatie van alternatieve scenario's voor waterbeheer is niet mogelijk met satellietbeelden. Satellietbeelden verschaffen echter ruimtelijke informatie over grootheden als landgebruik en evapotranspiratie, hetgeen zeer nuttig kan zijn voor een regionale analyse van waterproductiviteit. Simulatiemodellen zijn in staat waterbalanscomponenten als Q_{bot} , E en T apart te berekenen, en kunnen tevens gebruikt worden om alternatieve scenario's voor waterbeheer te evalueren. Daarom is het belangrijkste onderzoeksdoel van dit proefschrift *het integreren van operationele kennis van gewasgroei, bodemvochtstroming en verzouting met veldexperimenten, remote sensing en geografische informatiesystemen (GIS) voor analyse van waterproductiviteit van veld tot regionale schaal.*

Studiegebied

Sirsa district (Haryana), gelegen in de geïrrigeerde vlaktes in het noordwesten van India, is gekozen als studiegebied. Het gebied beslaat 4270 km², waarvan 90% gecultiveerd wordt met een gemiddelde gewasintensiteit van 157%. Tarwe en mosterd zijn de belangrijkste gewassen tijdens het *rabi* (winter) seizoen, en katoen en rijst tijdens het *kharif* (zomer) seizoen. Het klimaat wordt gekarakteriseerd door haar droogte, extremen in temperatuur en onregelmatige neerslag. Gewasproductie zonder irrigatie is zeer beperkt, zelfs in het moesson seizoen. Samenvattend zijn de belangrijkste problemen met betrekking tot waterbeheer in Sirsa district de schaarste van kanaalwater, slechte grondwaterkwaliteit, stijgende en dalende grondwaterstanden, verzouting en lage gewasproductie. Op dit moment is de toename in gewasproductie marginaal of, zoals in het geval van rijst, neemt de gewasproductie af.

Raamwerk voor regionale analyse van waterproductiviteit

In Hoofdstuk 3 wordt een raamwerk gepresenteerd voor integratie van gewasgroei, bodemvochtstroming, en bodemzouttransport met remote sensing en GIS voor de beschrijving van hydrologische en biofysische processen op regionale schaal. *De belangrijkste hypothese achter dit raamwerk is dat een verzameling van individueel homogene subgebieden representatief kan zijn voor een ruimtelijke heterogeen gebied.* Verder wordt aangenomen dat de effecten van ruimtelijke heterogeniteit op de regionale water- en zoutbalans en op de waterproductiviteit kunnen worden geanalyseerd door toepassing van een veldschaalmodel op alle combinaties van *weer-gewas-bodem-water* in het studiegebied. Deze hypothese geldt alleen voor de onverzadigde zone van geïrrigeerde gebieden met diepe grondwaterstanden en zonder noemenswaardige afstroming, hetgeen het geval is in Sirsa district.

In deze studie is het veldschaal, ecohydrologische, Soil-Water-Atmosphere-Plant model (SWAP) gedistribueerd toegepast om de water- en zoutbalansen en gewasproductie te simuleren van veld tot regionale schaal. SWAP simuleert verticale bodemvochtstroming en zouttransport in nauwe interactie met gewasgroei. Voor bodemvochtstroming wordt de Richards' vergelijking toegepast, en voor zouttransport de convectie-dispersie vergelijking.

SWAP heeft zowel een simpele als gedetailleerde gewasgroeimodule. In de simpele gewasmodule, wordt gewasgroei voorgeschreven aan de hand van gemeten bladoppervlakte-index, gewashoogte en worteldiepte als functie van gewasontwikkelingsstadium. De simpele gewasmodule simuleert geen interacties tussen gewasgroei en condities van bodemvocht en –zout. *Echter, de gedetailleerde gewasgroeimodule heeft het voordeel dat gewasgroei afhankelijk is van bodemvocht en bodemzout en omgekeerd.* De gedetailleerde gewasgroeimodule is gebaseerd op de World Food Studies (WOFOST). De module simuleert gewasgroei aan de hand van inkomende fotosynthetisch-actieve straling (*PAR*) die wordt geabsorbeerd door de bladeren, de fotosynthetische karakteristieken van de bladeren en condities met betrekking tot bodemvocht en –zout. Effecten van nutriëntentekort, plagen, onkruiden en ziekten zijn niet opgenomen in de huidige versie van WOFOST. De hiervoor beschreven simpele en gedetailleerde gewasgroeimodule zijn opgenomen in SWAP versie 3.03 (Kroes and Van Dam, 2003). Om onderscheid te maken in de simulaties in deze studie, noemen we SWAP 3.03 simulaties met het simpele gewasgroeimodel *SWAP*, en SWAP 3.03 simulaties met het gedetailleerde gewasgroeimodel *SWAP-WOFOST*.

Toepassing van het ontwikkelde raamwerk voor regionale analyse van waterproductiviteit vereist een grote hoeveelheid gegevens op verschillende ruimte- en tijdschalen. De informatie in deze studie is verzameld in het kader van het project WATPRO in Sirsa district. Twee gegevensbronnen zijn gebruikt: veldexperimenten en bestaande documentatie. Voor de twee belangrijkste gewassen (tarwe en katoen) zijn veldexperimenten uitgevoerd om gedetailleerde gewasgroeigegevens te verkrijgen voor de calibratie en validatie van *SWAP-WOFOST*. Voor de bestaande ecohydrologische condities, inclusief de lokale variatie, zijn in het landbouwjaar 2001-02 gegevens verzameld op 24 landbouwvelden met de belangrijkste gewasrotaties (tarwe – katoen en tarwe – rijst). Ruimtelijke informatie van weer, bodem, irrigatie en grondwater is verzameld bij overheidsdiensten. Remote sensing metingen met satellieten verschaften het landgebruik en de verdampingsfluxen op regionale schaal. De grote hoeveelheid gegevens die beschikbaar is in Sirsa district maakte het mogelijk deze gedetailleerde ecohydrologische studie op regionale schaal uit te voeren.

Calibratie en validatie van het SWAP model

Succesvolle toepassing van modellen als SWAP hangt af van de nauwkeurigheid en betrouwbaarheid van de invoergegevens voor gewasgroei, bodemvochtstroming en zouttransport. In hoofdstuk 4 is een grondige analyse uitgevoerd van de invoergegevens en SWAP berekeningsresultaten voor de landbouwvelden in Sirsa district tijdens het landbouwjaar 2001-02. Het simpele gewasgroeimodel, aangeduid als *SWAP*, werd gecalibreerd en gevalideerd met gegevens van 5 landbouwvelden met verschillende combinaties van bodem, gewas, irrigatiehoeveelheid en waterkwaliteit. Twee velden vertegenwoordigden verbouw van tarwe en rijst op gronden met zware textuur (clay loam tot silt clay loam) en drie andere velden vertegenwoordigden verbouw van tarwe en katoen op gronden met lichte textuur (sandy loam tot loamy sand). De meeste invoergegevens werden direct gemeten tijdens de veldexperimenten. De overblijvende onbekende bodemfysische parameters werden geschat door kalibratie van het model. Het niet-lineaire programma voor parameterschattingen PEST werd gebruikt om met SWAP automatisch parameters te kalibreren. Met name de bodemfysische parameters van de verschillende velden werden geschat met behulp van de profielen van bodemvocht θ and bodemzout *EC*. Er werd een goede overeenstemming bereikt tussen gemeten en gesimuleerde θ en *EC*. Tevens is de toepasbaarheid getest van het gedetailleerde gewasgroeimodel voor regionale gewasproductie door *SWAP-WOFOST* te vergelijken met de gekalibreerde en gevalideerde *SWAP* voor verschillende velden. De water- en zoutbalansen zoals gesimuleerd door *SWAP-WOFOST* zijn vrijwel gelijk aan die gesimuleerd door *SWAP*. Ook reageerde de gesimuleerde gewasgroei door *SWAP-WOFOST* naar verwachting op de aanwezige water- en zoutstress in de velden.

De resultaten van Hoofdstuk 4 gaven vertrouwen om *SWAP-WOFOST* toe te passen voor regionale analyse van waterproductiviteit, zoals beschreven in Hoofdstuk 5. De gekalibreerde en gevalideerde *SWAP-WOFOST* werd gedistribueerd toegepast: er werden onafhankelijke runs gedaan voor alle combinaties van *weer-gewas-bodem-water* in het studiegebied. Het proces van aggregatie van deze combinaties, aangeduid als ‘*simulatie-eenheden*’, werd uitgevoerd in een GIS omgeving door combinatie van thematische kaarten van Sirsa district over weer, landgebruik, bodemtype, waterbeschikbaarheid, grondwaterstand en grondwaterkwaliteit. Veldexperimenten, satellietbeelden, en bestaande geografische gegevens werden

gebruikt om invoergegevens af te leiden voor de simulatie-eenheden op de geschikte schaal. Irrigaties van kanaalwater en grondwater werden geaggregeerd voor verschillende gewasrotaties per dorp. Bodemvertaalfuncties, welke de bodemfysische relaties $\theta(h)$ en $K(\theta)$ relateren aan eenvoudig meetbare bodeminformatie, werden gebruikt om bodemfysische parameters te schatten voor de simulatie-eenheden.

Om de nauwkeurigheid en betrouwbaarheid van het ruimtelijk aggregeren van de invoerparameters te evalueren, werd op verschillende ruimte- en tijdschalen de actuele evapotranspiratie zoals gesimuleerd door *SWAP-WOFOST* (ET_{SW}) vergeleken met de onafhankelijk gemeten actuele evapotranspiratie door de satellieten (ET_{RS}). Er bestond nauwe overeenstemming tussen ET_{SW} en ET_{RS} voor de gebieden met tarwe, mosterd en rijst, terwijl voor gebieden met katoen ET_{SW} iets lager werd gesimuleerd. De grote afwijking tussen ET_{SW} en ET_{RS} voor kale gronden en stedelijk gebied liet het belang zien van nauwkeurige classificatie van landgebruik. Een geringe nauwkeurigheid van landgebruik classificatie kan de parameterisatie van *SWAP-WOFOST* verstoren, wat vervolgens kan leiden tot onnauwkeurige water- en zoutbalansen. Ondanks de gemaakte vereenvoudigingen, resulteerde de voorgestelde aggregatie-methoden voor ruimtelijk variabele invoergegevens (zoals een gemiddelde gewas- en irrigatiekalender, de verdeling van irrigatiewater en het gebruik van bodemvertaalfuncties) in gesimuleerde water- en zoutbalansen en gewasopbrengsten die goed overeenkwamen met onafhankelijke gegevens van satellietbeelden en veldmetingen.

Huidige waterbeheer en –productiviteit in Sirsa district

De huidige waterproductiviteit van de hoofdgewassen tarwe, rijst en katoen in Sirsa district is geanalyseerd op zowel veld (Hoofdstuk 4) als regionale schaal (Hoofdstuk 5). Het landbouwkundige jaar 2001-02 kan met een neerslag van slechts 99 mm worden gekarakteriseerd als een ‘droog’ jaar. De waterproductiviteit is berekend voor verschillende schalen en voor verschillende eenheden, namelijk $kg Y_g$ (graan- of zaadopbrengst) / m^3 gebruikt water in T (transpiratie), ET (evapotranspiratie), of ETQ (evapotranspiratie ET plus percolatie Q_{bot} van irrigaties en plus wegzijgingsverliezen Q_{SL} van het kanalsysteem) (zie Tabel 3.1). Deze verschillende definities van waterproductiviteit verschaffen nuttige indicatoren voor het evalueren van het gebruik van irrigatiewater en om aan te geven waar en wanneer water bespaard kan worden.

Eerst analyseerden we op geselecteerde landbouwvelden de waterproductiviteitswaarden WP met door *SWAP* gesimuleerde waterbalanscomponenten T , ET en Q_{bot} , en de gemeten graanopbrengsten Y_g (Tabel 4.7). WT_T staat voor Y_g/T en geeft de minimale hoeveelheid aan van waterverbruik door het gewas: uitsluitend de gewastranspiratie. De gemiddelde WT_T ($kg m^{-3}$) was 1.88 voor tarwe, 1.73 voor rijst en 0.29 voor katoen. *Dit geeft aan dat in Sirsa tarwe het meest efficiënte gewas is in termen van waterverbruik voor fysische gewasproductie.*

De gemiddelde WT_T , uitgedrukt in Y_g/ET ($kg m^{-3}$), was 1.39 voor tarwe, 0.94 voor rijst en 0.23 voor katoen. Dit komt overeen met gemiddelde waarden voor de klimaat- en groeiomstandigheden in het noordwesten van India. In het algemeen wordt ET beschouwd als de hoeveelheid verbruikt water in gewasproductie. De gemiddelde WP_{ET} was significant lager dan de gemiddelde WP_T : circa 46% voor rijst, 26% voor tarwe en 22% voor katoen.

Verbetering van cultuurmaatregelen zoals ‘mulching’ en vooral verbouw van droge rijst, kan het verlies van water door bodemverdamping E aanzienlijk reduceren en daarmee WP_{ET} op veldschaal verhogen.

Op veldschaal reduceert percolatie WP_{ET} tot WP_{ETQ} . De gemiddelde WP_{ETQ} (kg m^{-3}) bedroeg 1.04 voor tarwe, 0.84 voor rijst en 0.21 voor katoen.

Vervolgens analyseerden we op dezelfde landbouwvelden WP waarden met resultaten van *SWAP-WOFOST* voor de waterbalanscomponenten T , ET en Q_{bot} , en de graan- of zaadopbrengsten Y_g (Tabel 4.7). De combinatie *SWAP-WOFOST* simuleert gewasgroei en – productie waarbij het alleen rekening houdt met water- en zoutstress. Behalve water- en zoutstress, wordt de gewasgroei onder werkelijke veldcondities ook gereduceerd door factoren als nutriëntentekort, plagen en ziekten. Voor tarwe waren de water- en zoutgelimiteerde waarden voor Y_g 20 tot 60% hoger dan de gemeten Y_g in het veld. Op de geselecteerde tarwevelden was de water- en zoutstress gering: de relatieve verdamping (T/T_p) varieerde tussen 0.85 en 1.00. Uit de veldanalyse concluderen we dat verbeterd beheer van het gewas, zoals tijdig zaaien, optimale hoeveelheid nutriënten en effectieve bestrijding van plagen en ziekten, de WP_{ET} voor tarwe in Sirsa met 50% kan laten toenemen.

In het daaropvolgende *kharif* seizoen werd ernstige waterstress gemeten op de geselecteerde katoenvelden: $T/T_p < 0.65$. De gesimuleerde water- en zoutgelimiteerde Y_g voor katoen was 1.5 tot 3.5 keer lager dan de gesimuleerde potentiële Y_g . Daarom zullen de gewasproductie en waterproductiviteit van katoen toenemen als de irrigatiehoeveelheid voor katoen gegarandeerd is, vooral in droge seizoenen zoals 2001-02.

In Hoofdstuk 5 werd *SWAP-WOFOST* toegepast op een gedistribueerde wijze om water- en zoutgelimiteerde WP_T , WP_{ET} en WP_{ETQ} waarden te simuleren voor het gehele Sirsa district in het landbouwjaar 2001-02 (Tabel 5.7). De waarden in Tabel 5.7 zijn gebaseerd op simulatieresultaten en kunnen in zekere mate afwijken van de werkelijke waarden. Echter, de waarden vertegenwoordigen het huidige gebruik van water en het effect op de bestaande natuurlijke omgeving. De gemiddelde WP_{ET} , uitgedrukt in Y_g/ET (kg m^{-3}) bedroeg 1.37 voor tarwe, 0.36 voor katoen en 0.47 voor mosterd en rijst. De variatie in WP_{ET} was aanzienlijk, met een variatiecoëfficiënt van 15% voor tarwe en katoen, 19% voor mosterd en 64% voor rijst. Dit geeft aan dat er een groot potentiële bestaat voor verbetering van de waterproductiviteit in Sirsa district.

De bodemverdamping E bedroeg 20 tot 47% van de evapotranspiratie ET , en was vooral hoog voor rijst. De bodemverdamping is een van de belangrijkste verliesposten. Verder zijn de hoge wegzijgingsverliezen, Q_{SL} (34-43%), van het kanalsysteem en de percolatie tijdens en na irrigaties, Q_{bot} , verantwoordelijk voor een reductie van WP_{ET} tot WP_{ETQ} met 25-30%.

De water- en zoutgelimiteerde WP_T , WP_{ET} en WP_{ETQ} waarden voor tarwe, katoen en vooral rijst waren hoger in de zuidelijke (FB) en centrale (GHG en SUK) gebieden dan in de noordelijke (BMB) gebieden (Fig. 5.14). De lage waterproductiviteit in BMB hangt samen met de slechte grondwaterkwaliteit in de noordelijke delen van Sirsa district. In BMB was de gemiddelde WP_{ET} voor rijst 47% lager dan de gemiddelde waarde van 0.47 kg m^{-3} voor het

gehele district. Bovendien draagt de hoge percolatie van de rijstvelden in dit gebied bij aan stijgende grondwaterstanden. *Daarom dienen maatregelen om de waterproductiviteit te verhogen zich te concentreren op de noordelijke delen, en vervanging van rijst door katoen dient gestimuleerd te worden in het BMB gebied.*

De huidige landbouw- en irrigatiemethoden in Sirsa district leiden tot ongunstige ecohydrologische condities. Bijvoorbeeld, de hoge intensiteit van veel water gebruikende gewassen als tarwe en rijst en de relatief lage instroming via kanalen in de GHG en SUK gebieden, veroorzaken veel grondwateronttrekking en daling van grondwaterstanden in de centrale delen. Aan de andere kant dragen de hoge instroming via kanalen en geringe grondwateronttrekking door slechte waterkwaliteit in het BMB gebied bij aan stijgende grondwaterstanden in de noordelijke delen. Dit betekent een bedreiging voor de duurzaamheid van de geïrrigeerde landbouw in Sirsa district (Fig. 5.13).

Alternatieve scenario's voor waterbeheer in Sirsa district

Productieve en duurzaam waterbeheer kan bereikt worden door het identificeren en uitvoeren van de juiste opties voor waterbeheer. Problemen en gevolgen van specifieke waterbeheersmaatregelen worden vaak niet herkend voor zij vergevorderd zijn. Hoewel het ontwikkelde raamwerk voor gedistribueerd modelleren gebaseerd is op zekere aannamen en vereenvoudigingen van de werkelijke situatie, verschaft het de mogelijkheid oorzaak-gevolg relaties op te sporen en te analyseren. De gesimuleerde water- en zoutbalansen en gewasproductie kunnen een hulp zijn om alternatieve scenario's voor waterbeheer op de gewenste schaal te evalueren.

In Hoofdstuk 6 worden mogelijke alternatieven voor waterbeheer in Sirsa district voorgesteld en uitgewerkt. De voorgestelde 5 alternatieven zijn:

- Scenario 1: *'Business as usual'* of referentie-situatie,
- Scenario 2: Toegenomen (10 tot 15%) gewasopbrengsten,
- Scenario 3: Gereduceerde wegzijgingsverliezen met 25-30%,
- Scenario 4: Herverdeling van kanaalwater (15%) van BMB naar GHG en SUK, en
- Scenario 5: Combinatie van scenario's 2, 3 en 4.

Deze scenario's hebben tot doel de waterproductiviteit te verhogen en de daling, respectievelijk stijging, van grondwaterstanden een halt toe te roepen. De scenario's zijn geëvalueerd met het gedistribueerde *SWAP-WOFOST* model voor een periode van 10 jaar (1991-2001).

Sirsa district in het geheel heeft een nagenoeg gesloten waterbalans, aangezien de som van instroming via kanalen en neerslag vrijwel gelijk was aan de gesimuleerde evapotranspiratie. Dit wordt bevestigd door de gemeten grondwaterstanden, welke in de periode 1990-2000 een geringe netto grondwateraanvulling van 11 mm/j laten zien. Tegelijkertijd laat Scenario 1 (*'Business as usual'*) een grote ruimtelijke variatie zien van gesimuleerde grondwateraanvulling R and zoutophoping ΔC in de gebieden BMB, SUK, GHG en FB (Tabel 6.2). *Dit geeft aan dat er interventies nodig zijn voor een productief en duurzaam waterbeheer in Sirsa district.*

De gemiddelde gemeten graanopbrengsten Y_g (ton ha⁻¹) in Sirsa district over de periode 1991-2001 bedroegen 4.1 voor tarwe, 1.2 voor mosterd, 3.2 voor rijst en 1.2 voor katoen (Fig. 2.10). In case of 'Business as usual' was de gesimuleerde water- en zoutgelimiteerde Y_g in deze periode 1.2 tot 2.0 keer hoger dan de genoemde gemeten Y_g , vooral in het geval van rijst en katoen (Tabel 6.3). Dit geeft aan dat in Sirsa district de gewasproductie een aanzienlijke stress ondervindt door nutriëntentekort, plagen en/of ziekten.

Pogingen om de gewasproductie te verhogen zullen zeker ook de WP_{ET} verhogen. In Scenario 2 werd de water- en zoutgelimiteerde Y_g verhoogd met 12 tot 17%. Dit verhoogde WP_{ET} voor tarwe en katoen met 12 %, voor mosterd met 14% en voor rijst met 18%.

Reductie van de wegzijgingsverliezen in het kanalsysteem wordt sterk aanbevolen, vooral in het noordelijke gebied (BMB) met een slechte waterkwaliteit. In Scenario 3 werden de oorspronkelijke wegzijgingsverliezen van 39-41% verminderd tot 25-27%. Dit verhoogde de water- en zoutgelimiteerde WP_T , WP_{ET} en vooral WP_{ETQ} met 6 tot 12% voor alle gewassen. Bovendien verminderde in Scenario 3 de netto grondwateraanvulling R in BMB en de zoutophoping ΔC over het gehele Sirsa district.

Herverdeling van 15% van het kanaalwater van BMB naar SUK en GHG (Scenario 4) heeft enigszins negatieve gevolgen in BMB in termen van water- en zoutgelimiteerde WP_T , WP_{ET} en WP_{ETQ} waarden voor alle gewassen en in termen van zoutophoping ΔC . Deze reductie van 15% kanaalwater in BMB kan teniet worden gedaan door vermindering van de wegzijgingsverliezen van het kanalsysteem (Scenario 3). Scenario 4 heeft het grote voordeel dat in BMB, waar de grondwaterstanden stijgen, de grondwateraanvulling R verminderd wordt. Bovendien neemt in Scenario 4 in GHG en SUK R toe, wat daling van de grondwaterstanden in de centrale delen van Sirsa district tegengaat.

In Scenario 5 (combinatie van Scenario's 2, 3 en 4) wordt, vergeleken met 'business as usual', een significante verbetering bereikt van water- en zoutgelimiteerde WP_T , WP_{ET} en WP_{ETQ} waarden, en een vermindering van de grote ruimtelijke verschillen van R en de zoutophoping ΔC (Tabel 8.1).

Tabel 8.1 Relatieve effect (%) van de gecombineerde Scenario's 2, 3, en 4 voor waterbeheer (Tabel 6.1) op de regionale waterproductiviteit WP_T , WP_{ET} en WP_{ETQ} , en op de netto grondwateraanvulling R en zoutophoping ΔC in Sirsa district en haar vier deelgebieden (Fig. 5.3). Positieve waarden geven een toename aan, negatieve waarden een afname. De waarden zijn gebaseerd op gedistribueerde SWAP-WOFOST simulaties voor de onverzadigde zone (0-300 cm) over een periode van 10 jaar (1991-2001), en gelden voor de gehele landoppervlakte (zowel gecultiveerd als braak).

Indicator	Tarwe	Mosterd	Katoen	Rijst	
WP_T	9	17	8	8	
WP_{ET}	13	16	12	21	
WP_{ETQ}	23	29	23	26	
	Sirsa	BMB	GHG	SUK	FB
R	-85	-99	47	45	-81
ΔC	-20	4	-163	-24	-50

Tabel 8.1 geeft aan dat een combinatie van toename van gewasopbrengsten (Scenario 2), reductie van wegzijgingsverliezen (Scenario 3) en herverdeling van kanaalwater (15%) van het noordelijke BMB naar de centrale SUK en GHG gebieden, zullen leiden tot een significante verbetering van de regionale waterproductiviteit, en tot een vermindering van stijgingen, respectievelijk dalingen, van de grondwaterstanden in Sirsa district.

Data-assimilatie

Hoewel ecohydrologische modellen mogelijkheden bieden voor kwantitatieve voorspellingen, kunnen zij onnauwkeurig worden door teveel of te weinig systeemparameters, vooral in het geval van gedistribueerd simuleren op regionale schaal. De gesimuleerde toestandsvariabelen bevatten altijd een modelfout door vereenvoudigde analytische uitdrukkingen van de complexe processen in onze natuurlijke omgeving. Onnauwkeurigheden van invoerparameters vergroten de modelfout. De fout kan worden verminderd door data-assimilatie, waarbij gebruik wordt gemaakt van veldmetingen die het systeem karakteriseren, zoals bodemvocht, bladoppervlakte-index, drogestof-productie of verdampingsfluxen. Echter, ook deze veldmetingen bevatten in zekere mate willekeurige meetfouten.

In Hoofdstuk 7 worden verschillende data-assimilatie methoden verkend, zoals ‘*calibration*’, ‘*forcing*’ en ‘*updating*’, om gemeten drogestof-productie op te nemen in de combinatie *SWAP-WOFOST*. In de meest algemene ‘*calibration*’ methode, worden gevoelige en onzekere gewasinvoerparameters, zoals light use efficiency en maximale CO₂ assimilatie flux, geoptimaliseerd om de verschillen te minimaliseren tussen gesimuleerde totale drogestof TDM_{sim} en gemeten totale drogestof TDM_{obs} . In de ‘*forcing*’ methode wordt de toestandsvariabele TDM_{sim} in het model eenvoudig vervangen door TDM_{obs} . Een eenvoudig ‘*updating*’ algoritme is ontwikkeld om TDM_{sim} aan te passen op het moment dat een TDM_{obs} beschikbaar is. Eerst zijn de ‘*forcing*’ en ‘*updating*’ methoden geanalyseerd met synthetische TDM_{obs} gegevens. Vervolgens zijn de ‘*calibration*’ en ‘*updating*’ methoden geanalyseerd met gemeten TDM_{obs} gegevens.

De analyse met de synthetische TDM_{obs} gegevens (Tabel 7.1) laat zien dat metingen van TDM door remote sensing of direct in het veld met 10 tot 20% willekeurige fout, geassimileerd kunnen worden in *SWAP-WOFOST* zonder de simulatie van de waterbalans-componenten voor gemiddelde groeiomstandigheden in Sirsa district te beïnvloeden. In geval van de ‘*forcing*’ methode, verliest het model zijn eigen informatie en worden de meetfouten van TDM_{obs} opgenomen in de gesimuleerde gewasproductie. De ‘*updating*’ methode is beter dan de ‘*forcing*’ methode in termen van fouten voortplanting.

Het succes van het ‘*updating*’ algoritme schuilt in de optimale ‘gain factor K_g ’, welke afhangt van zowel de modelfouten als de meetfouten. Extended of Ensemble Kalman filtermethoden kunnen worden gebruikt om K_g nauwkeurig te berekenen. De SWAP toestandsvariabelen, zoals TDM , worden met K_g aangepast op het moment dat een meting beschikbaar is. Een belangrijk nadeel van een ‘*updating*’ algoritme voor TDM kan zijn dat de simulatie van de gewasproductie door het model intern inconsistent wordt. Resultaten van de toepassing op veldschaal met gemeten TDM_{obs} waarden laten zien dat de geïntroduceerde inconsistentie

tijdens het ‘*updating*’ proces slechts een geringe invloed had op de gesimuleerde waterbalanscomponenten T , ET en Q_{bot} (Tabel 7.2).

Bij de ‘*calibration*’ methode is men verzekerd van interne consistentie van het model (Fig. 7.4a). Deze methode geeft naar verwachting meer representatieve invoerparameters, gesimuleerde gewasproductie en waterbalanscomponenten. Dit geldt bij voldoende metingen en een geringe meetfout. Een groot nadeel van de ‘*calibration*’ methode, vooral op regionale schaal, is de grote hoeveelheid rekentijd in verband met het gebruik van een optimalisatieprocedure.

Naast haar wetenschappelijke relevantie, zal het gebruik van een ‘*updating*’ algoritme de rekentijd in vergelijking met de ‘*calibration*’ methode aanzienlijk reduceren, vooral in geval van gedistribueerd rekenen voor regionale studies. Bovendien kan het ‘*updating*’ algoritme goed omgaan met plotselinge afnamen in de gewasproductie door bijvoorbeeld plagen of ziekten, hetgeen niet mogelijk is met de ‘*calibration*’ methode.

Conclusies en aanbevelingen

De belangrijkste conclusies en aanbevelingen voor verbetering van het waterbeheer en haar productiviteit in Sirsa district, zijn:

- Sirsa district in haar geheel heeft een nagenoeg gesloten waterbalans aangezien de totale jaarlijkse instroming via neerslag en kanaalwater vrijwel gelijk is aan de gesimuleerde jaarlijkse verdamping. Er bestaat echter een grote ruimtelijke variatie in de berekende netto grondwateraanvulling en zoutophoping in de hoofdgebieden (BMB, SUK, GHG, en FB). *Dit bedreigt de duurzaamheid van geïrrigeerde landbouw in Sirsa district.*
- Voor de waterproductiviteit WP_{ET} werd een grote variatie gemeten, zowel voor verschillende gewassen als voor hetzelfde gewas. Pogingen om de gewasopbrengsten te verhogen zullen ook de WP_{ET} verhogen, welke de werkelijke hoeveelheid gebruikt water (evapotranspiratie) vertegenwoordigt. *Bodemverdamping is verantwoordelijk voor 20 tot 47% (hoogste bij rijst) van de evapotranspiratie, en wordt gezien als de grootste nutteloze verliespost van water.* Verbetering van methoden voor de verbouw van rijst, zoals verbouw van droge rijst, dragen bij aan vermindering van de bodemverdamping en daarmee aan verhoging van de waterproductiviteit.
- De gesimuleerde water- en zoutgelimiteerde gewasopbrengsten waren 1.2 tot 2.0 keer groter dan de werkelijk gemeten gewasopbrengsten over de periode 1991-2000. *Dit geeft aan dat er een aanzienlijke stress door nutriëntentekort, plagen en/of ziekten bestaat in Sirsa district.* Daarom dient er een landbouwkundig programma opgezet te worden dat zich richt op verbeterd gewasbeheer zoals tijdig zaaien, optimale nutriëntenvoorziening, en verbeterde bestrijding van plagen en ziekten.
- Reductie van wegzijgingsverliezen in het kanalsysteem wordt sterk aanbevolen, vooral in het noordelijke BMB gebied met een slechte grondwaterkwaliteit. De

‘conveyance efficiency’ dient verhoogd te worden van het huidige niveau van 60% naar 75% door geschikte kanaalbekleding en voldoende onderhoud. De meeste van de hoofdkanalen en tertiaire kanalen in Sirsa zijn bekleed, echter de veldkanalen die het water verdelen over de landbouwvelden zijn niet bekleed.

- Herverdeling van 15% van het kanaalwater van BMB naar GHG en SUK in combinatie met reductie van wegzijgingsverliezen tot 25-30% wordt aanbevolen om de stijging van grondwaterstanden in de noordelijke delen, en de daling van de grondwaterstanden in de centrale delen van Sirsa district tegen te gaan.

De volgende hoofdconclusies en –aanbevelingen zijn getrokken met betrekking tot *gedistribueerd modelleren van waterbeheer en haar productiviteit op regionale schaal*:

- *Effecten van ruimtelijke heterogeniteit op de regionale water- en zoutbalansen en op de waterproductiviteit kunnen worden geanalyseerd met gedistribueerd modelleren: pas het veldschaalmodel toe op alle combinaties van weer-gewas-bodem-water in het studiegebied.*
- Het deterministische, veldschaal, ecohydrologische model SWAP blijkt in staat, in combinatie met veldexperimenten, remote sensing en GIS, waardevolle informatie te leveren voor evaluatie van waterbeheer en haar productiviteit op verschillende ruimte- en tijdschalen.
- Integratie van gedistribueerd modelleren met SWAP met satellietwaarnemingen, zoals bladoppervlakte-index, productie van drogestof en verdampingsfluxen, via moderne data-assimilatietechnieken dient onderzocht te worden om de voorspellingskracht te verhogen, vooral op regionale schaal.
- Het ontwikkelde raamwerk voor gedistribueerd modelleren met SWAP kan de netto grondwateraanvulling berekenen, welke een belangrijke component is voor grondwaterbeheer. De grondwateraanvulling op verschillende ruimte- en tijdschalen kan dienen als invoer voor modellen van regionale grondwaterstroming. *De combinatie van gedistribueerd modelleren met SWAP en een regionaal grondwatermodel dient onderzocht te worden voor regionaal beheer van oppervlakte- en grondwater.*
- Een degelijke waterproductiviteitsanalyse van een irrigatiesysteem vereist een grote hoeveelheid ecohydrologische informatie op verschillende ruimte- en tijdschalen. Om deze informatie te verkrijgen, dient via veldexperimenten, remote sensing met satellieten en bestaande overheidsorganen een meetprogramma opgezet te worden in verschillende irrigatiesystemen, en *een toegankelijke, digitale database dient onderhouden te worden.*

References

- Aggarwal, M.C. and C.W.J. Roest, 1996. Towards improved water management in Haryana state. *Final report of the Indo-Dutch operational research project on hydrological studies*. Chaudhary Charan Singh Haryana Agricultural University, Hisar, International Institute for Land Reclamation and Improvement, Wageningen and DLO Winand Staring Centre for Integrated Land, Soil and Water Research, now Alterra, Wageningen, The Netherlands, 80 p.
- Aggarwal, P.K., K.K. Talukdar and R.K. Mall, 2000. Potential yields of rice-wheat system in the Indo-Gangetic plains of India. *Rice-Wheat Consortium Paper Series 10*, Rice-Wheat Consortium for Indo-Gangetic plains, New Delhi, India, 16 p.
- Aggarwal, P. K., R.P. Roeter, N. Kalra, H. Van Keulen, C.T. Hoanh and H.H. Van Laar (Eds.), 2001. Land use analysis and planning for sustainable food security: with an illustration for the state of Haryana, India. Indian Research Institute, New Delhi, International Rice Research Institute, Los Banos and Wageningen University and Research Centre, Wageningen, The Netherlands, 167 p.
- Ahuja, R.L., D. Ram, B.S. Panwar, M.S. Khud and Jagan Nath, 2001. Soils of Sirsa district (Haryana) and their management. *Research Report*. Department of Soil Sciences, CCS Haryana Agricultural University, Hisar, India, 81 p.
- Allen, R.G., L.S. Pereira, D. Raes, and M. Smith, 1998. Crop evapotranspiration, Guidelines for computing crop water requirements. *Irrigation and Drainage Paper 56*, FAO, Rome, Italy, 300 p.
- Angstrom, A., 1924. Solar and atmospheric radiation. *Q. J. R. Meteorol. Soc.* 50: 122-125.
- Arora, V.K., P.R. Gajri and M.R. Chaudhary, 1993. Effects of conventional and deep tillage on mustard for efficient water and nitrogen use in coarse textured soils. *Soil & tillage Research*, 26: 327-340.
- Aubert D., C. Loumagne and L. Oudin, 2003. Sequential assimilation of soil moisture and streamflow data in a conceptual rainfall-runoff model. *J. Hydrol.*, 280: 145-161.
- Aulakh, M. S. and N. S. Pasricha, 1999. Effect of rate and frequency of applied P on crop yields, P uptake, and fertilizer P use-efficiency and its recovery in a groundnut-mustard rotation. *Journal of agricultural science*, 132: 181-188.
- Bastiaanssen, W.G.M., R. Singh, and S. Kumar, 1996. Analysis and recommendations for integrated on-farm water management in Haryana, India: a model approach. *Report 118*, Alterra Green World Research, Wageningen, The Netherlands, 152 p.
- Bastiaanssen W.G.M., R.A. Feddes, A.A.M. Holtslag, M. Menenti, 1998. A remote sensing surface energy balance algorithm for land (SEBAL) 1. Formulation. *J. Hydrol.*, 212-213: 198-212.
- Bastiaanssen, W.G.M and M.G. Bos, 1999. Irrigation performance indicators based on remotely sensed data: a review of literature. *Irrigation and Drainage Systems*, 13: 291-311.

- Bastiaanssen, W.G.M., D.J. Molden, S. Thiruvengadachari, A.A.M.F.R. Smit, L. Mutuwatte and G. Jayasinghe, 1999. Remote sensing and hydrologic models for performance assessment in Sirsa Circle, India, *Research Report 27*, International Water Management Institute, Colombo, Sri Lanka, 29 p.
- Bastiaanssen, W.G.M., J.C. van Dam and P. Droogers, 2003a. Introduction. In Dam, J.C. van, and R.S. Malik (Eds.), 2003. *Water productivity of irrigated crops in Sirsa district, India. Integration of remote sensing, crop and soil models and geographical information systems*. WATPRO final report, including CD-ROM. ISBN 90-6464-864-6: 11-19.
- Bastiaanssen, W.G.M., S.J. Zwart and H. Pelgrum, 2003b. Remote sensing analysis. In Dam, J.C. van, and R.S. Malik (Eds.), 2003. *Water productivity of irrigated crops in Sirsa district, India. Integration of remote sensing, crop and soil models and geographical information systems*. WATPRO final report, including CD-ROM. ISBN 90-6464-864-6: 85-100.
- Bear, J., 1972. Dynamics of fluids in porous media. *Elsevier*, Amsterdam, The Netherlands.
- Belmans, C., J.G. Wesseling and R.A. Feddes, 1983. Simulation of the water balance of a cropped soil: SWATRE. *J. Hydrol.*, 63: 271-286.
- Berkoff, J. 1990. Irrigation management on the Indo-Gangetic Plain. *Technical Paper 129*. Washington D.C., World bank.
- Bessembinder, J.J.E., A.S. Dhindwal, P.A. Leffelaar, T. Ponsioen and S. Singh, 2003. Analysis of crop growth. In Dam, J.C. van, and R.S. Malik (Eds.), 2003. *Water productivity of irrigated crops in Sirsa district, India. Integration of remote sensing, crop and soil models and geographical information systems*. WATPRO final report, including CD-ROM. ISBN 90-6464-864-6: 59-82.
- Black, T.A., W.R. Gardner and G.W. Thurtell, 1969. The prediction of evaporation, drainage, and soil water storage for a bare soil. *Soil Sci. Soc. Am. J.*, 33: 655-660.
- Boegh E., M. Thorsen, M.B. Butts, S. Hansen, J.S. Christiansen, P. Abrahamsen, C.B. Hasager, N.O. Jensen, P. van der Keur, J.C. Refsgaard, K. Schelde, H. Soegarrd and A. Thomsen, 2004. Incorporating remote sensing data in physical based distributed agro-hydrological modelling. *J. Hydrol.*, 287: 279-299.
- Boels, D., M. Abdel Khalek, C.W.J. Roest and M.F.R. Smit, 1989. Simulation of water management in Arab Republic of Egypt: Reuse of drainage water model. *Reuse report 25*. Drainage Research Institute, Cairo, Egypt and DLO Winand Staring Centre, now Alterra, Wageningen, The Netherlands, 52 p.
- Boels, D., A.A.M.F.R. Smit, R.K. Jhorar, R. Kumar and J. Singh. 1996. Analysis of water management in Sirsa District in Haryana: model testing and application. *Report 115*. DLO Winand Staring Centre, now Alterra, Wageningen, The Netherlands, 50 p.
- Boesten, J.J.T.I. and A.M.A. van der Linden, 1991. Modelling the influence of sorption and transformation on pesticide leaching and persistence. *J. Environ. Qual.*, 20: 425-435.

- Boons-Prins, E.R., G.H.J. De Koning, C.A. Van Diepen and F.W.T. Penning de Vries, 1993. Crop specific simulation parameters for yield forecasting across the European Community. *Simulation Reports CABO-TT no. 32*. CABO-DLO, Wageningen, The Netherlands, 43 p.
- Boonstra, J. and N.A. de Ridder, 1990. Numerical Modelling of Groundwater Basins (2nd Ed.). International Institute for Land Reclamation and Improvement (ILRI), The Netherlands, 226 p.
- Boonstra, J., J. Singh and R. Kumar, 1996. Groundwater model study, Sirsa District, Haryana. Indo-Dutch Operational Research Project on Hydrological Studies. *Technical Report*. International Institute for Land Reclamation and Improvement. Wageningen, The Netherlands, 87 p.
- Brown, L.R. and R. Kane, 1994. Full house. The World Watch Environmental Alert Series. Norton, New York, USA.
- Cardon G.E. and J. Letey, 1992. Plant water uptake terms evaluated for soil water and solute movement models. *Soil Sci. Soc. Am. J.*, 32: 1876-1880.
- Chaudhary, T.N., 1997. Vision-2020. DWMR Perspective Plan. Directorate of Water Research, Patna, India, 73 p.
- District Statistical Abstract, Sirsa, 2001. Issued by Economic and Statistical Organization, Planning Department, Government of Haryana, 2002.
- De Wit, C.T., 1958. Transpiration and crop yields. Verslaa, van Landbouw, *Onderzoek No. 64.6*: 88 p.
- Doherty, J., L. Brebber and P. Whyte, 1995. PEST: Model independent parameter estimation. Australian Centre for Tropical Freshwater Research, James Cooke University, Townsville, Australia, 140 p.
- Doorenbos, J., and A.H. Kassam, 1979. Yield response to water. *FAO Irrigation and Drainage Paper 33*, FAO, Rome, Italy.
- Droogers, P., W.G.M. Bastiaanssen, M. Beyazgül, Y. Kayam, G.W. Kite, and H. Murray-Rust, 2000. Distributed agro-hydrological modelling of an irrigation system in western Turkey. *Agric. Water Manage.*, 43: 183-202.
- Droogers, P. and G. Kite, 2001. Estimating productivity of water at different spatial scales using simulation modelling. *Research Report 53*, International Water Management Institute, Colombo, Sri Lanka, 16 p.
- Droogers, P. and W.G.M. Bastiaanssen, 2002. Irrigation performance using hydrological and remote sensing modelling. *J. of Irrigation and Drainage Engineering*, 128: 11-18.
- Droogers, P. and G.W. Kite, 2002. Remotely sensed data used for modelling at different hydrological scales. *Hydrol. Process.*, 16: 1543-1556.
- D'Usro, G., M. Menenti, and A. Santini, 1999. Regional application of one-dimensional water flow models for irrigation management. *Agric. Water Manage.*, 40: 291-302.
- Feddes, R.A., P.J. Kowalik and H. Zaradny, 1978. Simulation of field water use and crop yield. *Simulation Monographs*, Pudoc, Wageningen, The Netherlands, 189 p.

- Feddes, R.A., 1985. Crop water use and dry matter production: state of the art. *Technical bulletin no. 63*. Institute for Land and Water Management Research (ICW), Wageningen, The Netherlands, 221-234.
- Goudriaan, J., 1977. Crop meteorology: a simulation study. *Simulation monographs*, Pudoc, Wageningen, The Netherlands.
- Gribb, M.M., 1996. Parameter estimation for determining hydraulic properties of fine sand from transient flow measurements. *Water Resour. Res.*, 32: 1965-1974.
- Groundwater Atlas of Sirsa District, 2002. Assistant Geologist (Groundwater Cell), Department of Agriculture, Sirsa (Haryana), India.
- Hanks, R.J. 1974. Model for predicting plant yield as influenced by water use. *Agron. J.*, 66: 660-665.
- Hanks, R.J., 1983. Yield and water use relationships: an overview. In Taylor, H.M., W.R. Jordan and T.R. Sinclair (Eds.), (1983). *Limitations to efficient water use in crop production*. Amer. Soc. Agron.: 393-411.
- Hellegers, P. and C. J. Perry, 2003. Water as an economic good in irrigated agriculture-Theory and practice. *Research Report 3.04.12*. Agricultural Economics Research Institute, The Hague, The Netherlands, 152 p.
- Houser P.R., W.J. Shuttleworth, J.S. Famiglietti, H. V. Gupta, Kamran H. Syed and D. Goodrich, 1998. Integration of soil moisture remote sensing and hydrologic modelling using data assimilation. *Water Resour. Res.*, 34(12): 3405-3420.
- Hussain, I., R. Sakthivadivel, U. Amarasinghe, M. Mudassar and D. Molden, 2003. Land and water productivity of wheat in the western Indo-Gangatic plains of India and Pakistan: a comparative analysis. *Research Report 65*, International Water Management Institute, Colombo, Sri Lanka, 50 p.
- IWRS, 1999. Water Vision 2050. Indian Water Resources Society (IWRS).
- Ines, A.V.M., A. Das Gupta and R. Loof, 2002. Application of GIS and crop growth models in estimating water productivity. *Agric. Water Manage.*, 54: 205-225.
- IWMI, 2000. Water issues for 2025. A research perspective. Research contribution to the World Water Vision. International Water Management Institute, Colombo, Sri Lanka, 50 p.
- Jacobs, C. and J.de Jong. 1997. Constraints and opportunities for implementation of improved irrigation management in a waterlogged area-the case of Hisar District. *MSc Thesis*, Wageningen University and Research Centre and University of Twente. The Netherlands, 88 p.
- Jhorar, R.K., 2002. Estimation of effective soil hydraulic parameters for water management studies in semi-arid zones. *PhD Thesis*, ISBN 90-5808-644-5, Wageningen University and Research Centre, Wageningen, The Netherlands, 157 p.
- Kalman, R.E., 1960. A new approach to linear filtering and prediction problems. *J. Basic Engi.* 82 D: 35-45.

- Kijne, J., R. Barker and D. Molden (Eds.), 2003. Water productivity in agriculture: limits and opportunities for improvement. *Comprehensive assessment of Water Management in Agriculture, Series No. 1*, CABI press, Wallingford, UK, 352 p.
- Kool, J.B., and J.C. Parker, 1988. Analysis of the inverse problem for transient unsaturated flow. *Water Resour. Res.*, 24: 817-830.
- Kroes, J.G. and J.C. van Dam (eds), 2003. Reference Manual SWAP version 3.03. Alterra Green World Research, *Alterra report 773*, ISSN 1566-7197. Wageningen University and Research Centre, Wageningen, The Netherlands, 211 p.
- Kroes, J.G., P. Droogers, R. Kumar, W. Immerzeel, R. Singh, A. Roelevink, H.W. ter Maat and D. S. Dabas, 2003. A regional approach to model water productivity. In Dam, J.C. van, and R.S. Malik (Eds.), 2003. *Water productivity of irrigated crops in Sirsa district, India. Integration of remote sensing, crop and soil models and geographical information systems*. WATPRO final report, including CD-ROM. ISBN 90-6464-864-6: 101-119.
- Kumar, S., R.K. Jhorar and M.C. Aggarwal, 1996. (Re)use of saline irrigation waters for cereal crops. CCS Haryana Agricultural University, Hisar, India, 96 p.
- Kumar, P., 2001. Future demands for food in India and Haryana State. In Aggarwal, P. K., R.P. Roeter, N. Kalra, H. Van Keulen, C.T. Hoanh and H.H. Van Laar (Eds.), 2001. *Land use analysis and planning for sustainable food security: with an illustration for the state of Haryana, India*. Indian Research Institute, New Delhi, International Rice Research Institute, Los Banos and Wageningen University and Research Centre, Wageningen, The Netherlands: 27-32.
- Leffelaar, P.A., J.C. van Dam, J.J.E. Bessembinder and T. Ponsioen, 2003. Integration of remote sensing and simulation of crop growth, soil water and solute transport at regional scale. In Dam, J.C. van, and R.S. Malik (Eds.), 2003. *Water productivity of irrigated crops in Sirsa district, India. Integration of remote sensing, crop and soil models and geographical information systems*. WATPRO final report, including CD-ROM. ISBN 90-6464-864-6: 121-134.
- Lövenstein H.M., R. Rabbinge and H. Van Keulen, 1992. World Food Production. *Textbook 2: Biophysical factors in agricultural production*. Open university, Heerlen. ISBN 90-358-1111-1: 247 p.
- Lövenstein H.M., E. A. Lantinga, R. Rabbinge and H. Van Keulen, 1995. Principles of production ecology: text for course F 300-001, p.8, Figure 8. Department of Theoretical production ecology, Wageningen University and Research Centre, Wageningen, The Netherlands, 121 p.
- Maas, E.V., and G.J. Hoffman, 1977. Crop salt tolerance-current assessment. *J. Irrig. and Drainage Div.*, 103: 115-134.
- Makowski D., M.H. Jeuffroy and M. Guerif, 2003. Bayesian methods for updating crop-model predications, applications for predicting biomass and grain protein content. *Proceedings of the Frontis workshop on Bayesian Statistics and Quality Modelling in the agro-food production chain*. Wageningen, The Netherlands: 57-68. <http://www.wageningen-ur.nl/frontis>

- Malik, R.S., R. Kumar, D.S. Dabas, A.S. Dhindwal, S. Singh, U. Singh, D. Singh, J. Mal, R. Singh and J.J.E. Bessembinder, 2003. Measurement program and description database. In Dam, J.C. van, and R.S. Malik (Eds.), 2003. *Water productivity of irrigated crops in Sirsa district, India. Integration of remote sensing, crop and soil models and geographical information systems*. WATPRO final report, including CD-ROM. ISBN 90-6464-864-6: 29-39.
- Mandal, S., 2003. Evaluation of the current warabandi system for equitable water distribution. *M. Tech. Thesis*, CCS Haryana Agricultural University, Hisar (Haryana), India, 63 p.
- Ministry of Water Resources, 2003. 4th Editor's Conference on Social Sector issues – 28th August, 2003, Ministry of Water Resources, India, 36 p. <http://wrmin.nic.in>
- Molden, D., 1997. Accounting for water use and productivity. *SWIM Paper 1*. International Irrigation Management Institute, Colombo, Sri Lanka.
- Molden D, and R. Sakthivadivel, 1999. Water accounting to assesses and productivity of water. *J. Water Resources Development*, 15 (1/2): 55-72.
- Molden, D., H. Murray-Rust, R. Sakthivadivel and I. Makin, 2001. A water productivity framework for understanding and action. *Workshop on Water productivity*. Wadduwa, Sri Lanka, November 12 and 13, 2001.
- Monteith, J.L., 1965. Evaporation and the Environment. In G.E. Fogg (Eds.), 1965. *The state and movement of water in living organisms*, Cambridge University Press: 205-234.
- Moulin S., A. Bondeau and R. Delecolle, 1998. Combining agricultural crop models and satellite observations: from field to regional scales. *Int. J. Remote Sensing*, 19(6): 1021-1036.
- Monteith, J.L., 1981. Evaporation and surface temperature. *Quarterly J. Royal Soc.*, 107: 1-27.
- Mualem, Y., 1976. A new model for predicting the hydraulic conductivity of unsaturated porous media. *Water Resour. Res.*, 12: 513-522.
- Navalawala, B.N. 1999a. Improving management of irrigation resources. *Yojana*, January: 81-87.
- Navalawala, B.N. 1999b. Water resources development and management. *Yojana*, July: 4-9.
- Nielsen, D.R., M.Th. van Genuchten and J.W. Biggar, 1986. Water flow and solute transport in the unsaturated zone. *Water Resour. Res.*, 22, supplement: 89S-108S.
- Paniconi C., M. Marrocu, M. Putti and M. Verbunt, 2003. Newtonian nudging for a Richards equation-based distributed hydrological model. *Advances in Water Resources*, 26: 161-178.
- PARC, 1982. Consumptive use of water for crops in Pakistan, Pakistan Agricultural Research Council, *Final Technical report: PK-ARS-69/FG Pa 251*, Islamabad, Pakistan, 193 p.
- Penning de Vries, F.W.T., D.M. Jansen, H.F.M. Ten Berge and A. Bakema, 1989. Simulation of ecofysiological processes of growth in several annual crops. *Simulation monographs no. 29*. IIRI Los Banos/Pudoc, Wageningen, The Netherlands.

- Perreira, A.R., N.A. Villa Nova, A.S. Pereira and V. Barbieri, 1995. A model for the Class A pan coefficient. *Agr. and Forest Met.*, 76: 75-82.
- Reidinger, R.B., 1971. Water Management by Administrative Procedures in an Indian Irrigation System, In E.W. Coward Jr. (Eds.), 1971. *Irrigation and agricultural development in Asia - Perspectives from the Social Sciences*, Cornell University Press, Ithaca/London, 1980: 263-288.
- Ritter, A., F. Hupet, R. Munoz-Carpena, S. Lambot and M. Vancloster, 2003. Using inverse methods for estimating soil hydraulic properties from field data as an alternative to direct methods. *Agric. Water Manage.*, 59: 77-96.
- Roelevink, A., 2003. Stratification and parameterization for regional water productivity analysis of Sirsa District, Haryana (India). *MSc Thesis*, Wageningen University and Research Centre, Wageningen, The Netherlands, 42 p.
- Russo, D., 1988. Determining soil hydraulic properties by parameter estimation: on the selection of a model for the hydraulic properties. *Water Resour. Res.*, 24: 453-459.
- Schuermans, J.M., P.A. Troch, A.A. Veldhuizen, W.G.M. Bastiaanssen and M.F.P. Bierkens, 2003. Assimilation of remotely sensed latent heat flux in a distributed hydrological model. *Advances in Water Resources*, 26: 151-159.
- Sharma, H.C., 1995. Proposed cropping pattern and irrigation needs for sustainable agriculture in Haryana. In Oswal and Dhindwal (Eds.), 1995. *Proc. of Agricultural Water Management*, October 1995, CCS Haryana Agricultural University, Hisar (Haryana), India.
- Sijtsma, B.R., D. Boels, T.N.M. Visser, C.W.J. Roest and M.F.R. Smit, 1995. SIWARE Users' Manual. *Reuse Report 27*, DLO Winand Staring Centre, now Alterra, Wageningen, The Netherlands, 158 p.
- Singh, D. P. and H. C. Sharma, 1993. Irrigation management in field crops. In Singh, D. P. and H. C. Sharma (Eds.), 1993. *Important aspects of on-farm water management*. CCS Haryana Agricultural University, Hisar (Haryana), India: 132-146.
- Singh, B.P., 1996. Response of mustard and chickpea to moisture in soil profile and plant population on aridisols. *Indian J. Agric. Sci.*, 53(7): 543-549.
- Singh, S., R. K. Pannu and Tejinder Singh, 1996. Effect of sowing time on growth and yield of Brassica genotypes. *Annals of biology*, 12(2): 287-293.
- Singh, P., 2000. Methods of irrigation in different crops. In Kumar, V., A.S. Dhindwal, M.S. Kuhad and B.C. Sethi (Eds.), 2000. *Efficient management of irrigation water in Haryana*. CCS Haryana Agricultural University, Hisar, India: 41-54.
- Singh, K.B., P.R. Gajri, and V.K. Arora, 2001. Modelling the effect of soil and water management practices on the water balance and performance of rice. *Agric. Water Manage.*, 49: 77-95.
- Smith, M., 1992. CROPWAT, a computer program for irrigation planning and management. *Irrigation and Drainage Paper 46*, FAO, Rome, Italy.

- Spitters, C.J.T., H. van Keulen and D.W.G. van Kraalingen, 1989. A simple and universal crop growth simulator: SUCROS87. In Rabbinge, R., S.A. Ward and H.H. van Laar (Eds.), 1989. *Simulation and systems management in crop protection*, Simulation Monographs, Pudoc, Wageningen, The Netherlands: 147-181.
- Statistical Abstract of Haryana, 2001. Issued by Economic and Statistical Organization, Planning Department, Government of Haryana. *Publication No. 693*, 2002.
- Stewart, J.I., R.H. Cuenca, W.O. Pruitt, R. Hagana and J. Tosso, 1977. Determination and utilization of water production functions for principal California crops. *W-67 Calf. Contrib. Proj. Rep.* University of California, Davis, USA.
- Supit, I., A.A. Hooyer and C.A. van Diepen (Eds.), 1994. System description of the WOFOST 6.0 crop simulation model implemented in CGMS. Vol. 1: Theory and algorithms. *EUR publication 15956, Agricultural series*, Luxembourg, 146 p.
- Tanji, K.K. (Ed.), 1990. Agricultural salinity assessment and management. *ASCE Manuals and reports on engineering practice no. 71*. American Society of Civil Engineers, USA, 619 p.
- Taylor, S.A., and G.M. Ashcroft, 1972. Physical Edaphology. *W.H. Freeman and Co.*, San Francisco: 434-435.
- Tuong, T.P. and B.A.M. Bouman, 2003. Rice production in water-scarce environments. In Kijne, J., R. Barker and D. Molden (Eds.), 2003. *Water productivity in agriculture: limits and opportunities for improvement*. Comprehensive assessment of Water Management in Agriculture, Series No. 1, CABI press, Wallingford, UK, 352 p.
- Tyagi, N.K., 1996. Irrigation management in unit command areas: concepts, indicators and evaluation. *J. of Water Management*, 4 (1&2): 52-57.
- Van Dam, J.C., J. Huygen, J.G. Wesseling, R.A. Feddes, P. Kabat, P.E.V. van Walsum, P. Groenendijk and C.A. van Diepen, 1997. Theory of SWAP version 2.0. Simulation of water flow, solute transport and plant growth in the Soil-Water-Atmosphere-Plant environment. Report 71, Sub department of Water Resources, Wageningen University, *Technical document 45*, Alterra Green World Research, Wageningen, The Netherlands, 167 p.
- Van Dam, J.C., 2000. Simulation of field-scale water flow and bromide transport in a cracked clay soil. *Hydrol. Proces.*, 14: 1101-1117.
- Van Dam, J.C. and R.A. Feddes, 2000. Numerical simulation of infiltration, evaporation and shallow groundwater levels with Richards's equation. Simulation of field-scale water flow and bromide transport in a cracked clay soil. *J. Hydrol.* 233: 72-85.
- Van Dam, J.C., and R.S. Malik (Eds.), 2003. Water productivity of irrigated crops in Sirsa district, India. Integration of remote sensing, crop and soil models and geographical information systems. *WATPRO final report, including CD-ROM*. ISBN 90-6464-864-6: 173 p.
http://library.wur.nl/way/catalogue/documents/WATPRO_final_report.pdf

- Van Genuchten, M.Th., and R.W. Cleary, 1979. Movement of solutes in soil: computer simulated and laboratory results. In Bolt, G.H. (Eds.), 1979. *Soil Chemistry B, Physico-Chemical Models*, Elsevier, Amsterdam, The Netherlands: 349-386.
- Van Genuchten, M.Th., 1980. A closed form equation for predicting the hydraulic conductivity of unsaturated soils. *Soil Sci. Soc. Am. J.*, 44: 892-898.
- Van Heemst, H.D.J., 1988. Plant data values required for simple crop growth simulation models: review and bibliography. *Simulation report CABO-TT nr. 17*. CABO/Theoretical production ecology, Wageningen, The Netherlands, 100 p.
- Walker, J.P., G. R. Willgoose and J. D. Kalma, 2001. One-dimensional soil moisture profile retrieval by assimilation of near-surface observations: a comparison of retrieval algorithms. *Advances in Water Resources*, 24: 631-650.
- Wesseling, J.G., J.A. Elbers, P. Kabat and B.J. van den Broek, 1991. SWATRE: instructions for input. *Internal note*, Winand Staring Centre, Wageningen, The Netherlands. International Waterlogging and Salinity Research Institute, Lahore, Pakistan, 29 p.
- Wösten, J.H.M., A. Lilly, A. Nemes and C. Le Bas, 1998. Using existing soil data to derive hydraulic parameters for simulation models in environmental studies and in land use planning. *Report 156*, Alterra Green World Research, Wageningen, The Netherlands, 106 p.
- Zwart, S.J. and W.G.M. Bastiaanssen, 2003. Review of measured crop water productivity values for irrigated wheat, rice, cotton and maize. *Agric. Water Manage.*, 69(2): 115-133.

Appendix A: Determination of solar net radiation (R_n)

$$R_n = R_{s\downarrow} - R_{L\uparrow} \quad (\text{A.1})$$

where $R_{s\downarrow}$ is the incoming net short wave radiation [$\text{MJ m}^{-2} \text{ day}^{-1}$], and $R_{L\uparrow}$ is the outgoing net long wave radiation [$\text{MJ m}^{-2} \text{ day}^{-1}$].

$$R_{L\uparrow} = \sigma \left[\frac{T_{\max, K} + T_{\min, K}}{2} \right] \left(0.34 - 0.14 \sqrt{e_a} \right) \left(1.35 \frac{R_s}{R_{s0}} - 0.35 \right) \quad (\text{A.2})$$

where σ is the Stefan-Boltzmann constant [$4.903 \cdot 10^{-9} \text{ MJ K}^{-4} \text{ m}^{-2} \text{ day}^{-1}$], $T_{\max, K}$ is the maximum absolute temperature during the 24-hour period [$K = ^\circ\text{C} + 273.16$], $T_{\min, K}$ is the minimum absolute temperature during the 24-hour period [$K = ^\circ\text{C} + 273.16$], e_a is the actual vapour pressure [kPa], R_s / R_{s0} is the relative short wave radiation (limited to ≤ 1.0), R_s is the measured or calculated solar radiation [$\text{MJ m}^{-2} \text{ day}^{-1}$], and R_{s0} is the calculated clear-sky radiation [$\text{MJ m}^{-2} \text{ day}^{-1}$].

$$R_{s\downarrow} = (1 - \alpha) R_s \quad (\text{A.3})$$

where α is the albedo or canopy reflection coefficient, which is 0.23 for the hypothetical grass reference crop [-], R_s is the incoming solar or short wave radiation [$\text{MJ m}^{-2} \text{ day}^{-1}$].

$$R_s = \left[a_s + b_s \frac{n}{N} \right] R_a \quad (\text{A.4})$$

where R_a is the extraterrestrial radiation [$\text{MJ m}^{-2} \text{ day}^{-1}$], n is the actual duration of sunshine [hour], N is the maximum possible duration of sunshine or daylight hours [hour], n/N = relative sunshine duration [-], a_s is the regression constant, expressing the fraction of extraterrestrial radiation reaching the earth on overcast days ($n = 0$), $a_s + b_s$ is the fraction of extraterrestrial radiation reaching the earth on clear days ($n = N$).

$$N = \frac{24}{\pi} \omega_s \quad (\text{A.5})$$

where ω_s = sunset hour angle.

$$\omega_s = \text{arc cos} \left[-\tan(\varphi) \tan(\delta) \right] \quad (\text{A.6})$$

where φ = latitude [rad.], and δ = solar declination [rad.].

$$\delta = 0.409 \sin \left[\frac{2\pi}{365} J - 1.39 \right] \quad (\text{A.7})$$

$$R_a = \frac{24(60)}{\pi} G_{sc} d_r \left[\omega_s \sin(\varphi) \sin(\delta) + \cos(\varphi) \cos(\delta) \sin(\omega_s) \right] \quad (\text{A.8})$$

where G_{sc} is the solar constant ($= 0.0820 \text{ MJ m}^{-2} \text{ min}^{-1}$) and d_r is the inverse relative distance Earth-Sun.

$$d_r = 1 + 0.033 \cos \left(\frac{2\pi}{365} J \right) \quad (\text{A.9})$$

Appendix B: Soil profiles in Sirsa district (Haryana), India

(According to 'Soils of Sirsa district (Haryana) and their Management', Ahuja et al., 2001)

Series	Horizon	Depth (cm)	Size class in % and particle size diameter in mm			Organic carbon	EC _{1:2} (dS m ⁻¹)	pH
			Sand (2-0.05)	Silt (0.05-0.002)	Clay (< 0.002)			
Series name	Nimla							
Series number	1							
Classification	Typic Torripsamment							
	Ap	18	92.0	4.0	4.0	0.03	0.09	7.9
	C1	32	92.0	4.0	4.0	0.03	0.09	8.1
	C2	30	86.0	6.0	8.0	0.02	0.11	8.2
	C3	20	84.0	6.0	10.0	0.02	0.11	8.2
	C4	60	82.0	8.0	10.0	0.02	0.14	8.2
Series name	Saimpal							
Series number	2							
Classification	Typic Torripsamment							
	Ap	24	92.0	4.0	4.0	0.11	0.09	8.2
	C1	41	92.0	4.0	4.0	0.08	0.06	8.3
	C2	30	92.0	4.0	4.0	0.07	0.06	8.2
	C3	80	90.0	4.0	6.0	0.07	0.06	8.2
	C4	60	86.0	8.0	6.0	0.03	0.16	8.2
Series name	Ganga							
Series number	3							
Classification	Typic Torripsamment							
	Ap	15	90.0	4.0	6.0	0.11	0.22	8.3
	C1	25	86.0	8.0	6.0	0.07	0.10	8.2
	C2	37	88.0	6.0	6.0	0.07	0.10	8.1
	C3	103	84.0	10.0	6.0	0.06	0.10	8.2
Series name	Lambi							
Series number	4							
Classification	Coarsy Fine Loamy, Aridic Haplusepts							
	Ap	20	80.6	10.4	9.0	0.24	0.50	8.1
	B1	26	73.2	14.0	12.8	0.24	0.20	8.3
	B2	31	76.0	12.3	11.7	0.19	0.60	8.1
	B3	43	75.6	12.4	12.0	0.16	1.10	8.1
	C1	35	82.7	8.5	8.8	0.14	1.20	8.2
	C2	45	84.6	8.0	7.4	0.14	2.50	8.2
Series name	Darbi							
Series number	5							
Classification	Fine Loamy, Aridic Haplusepts							
	Ap	14	36.0	50.0	14.0	0.37	0.14	7.9
	AB	8	42.0	42.0	16.0	0.37	0.20	8.4
	B1	28	24.0	54.0	22.0	0.07	0.23	8.7
	B2	40	12.0	66.0	22.0	0.07	0.33	8.6
	B3	85	10.0	68.0	22.0	0.05	0.41	8.5

Continued...

Series	Horizon	Depth (cm)	Size class in % and particle size diameter in mm				Organic carbon	EC _{1:2} (dS m ⁻¹)	pH
			Sand (2-0.05)	Silt (0.05-0.002)	Clay (< 0.002)				
Series name	F. Baidwala								
Series number	6								
Classification	Fine Loamy, Aridic Haplusepts								
	Ap	10	16.0	64.0	20.0	0.52	0.24	8.4	
	AB	30	12.0	68.0	20.0	0.18	0.45	8.4	
	B1	30	14.0	62.0	24.0	0.12	0.32	8.9	
	B2	30	18.0	68.0	14.0	0.07	0.27	8.7	
	B3	50	18.0	60.0	22.0	0.05	0.27	8.8	
Series name	H. Khurd								
Series number	7								
Classification	Fine Silty, Typic Haplusepts								
	Ap	15	30.0	48.0	22.0	0.32	0.40	8.0	
	B1	20	16.0	60.0	24.0	0.21	0.40	8.5	
	B21	35	4.0	64.0	32.0	0.14	0.38	8.8	
	B22	25	18.0	50.0	32.0	0.07	0.34	8.6	
	B23	25	10.0	60.0	30.0	0.07	0.30	8.6	
	C	75	8.0	66.0	26.0	0.07	0.23	8.5	
Series name	Phaggu								
Series number	8								
Classification	Coarse Loamy, Typic Fluvaquents								
	Ap	5	80.0	14.0	6.0	0.31	13.50	9.0	
	C1	10	80.0	12.0	8.0	0.17	3.24	8.9	
	C2	25	60.0	28.0	12.0	0.12	1.80	8.8	
	C3	20	60.0	28.0	12.0	0.09	1.98	8.8	
Series name	Khaireka								
Series number	9								
Classification	Fine Loamy, Typic Ustifluvents								
	Ap	5	29.0	52.5	18.5	0.28	0.24	8.3	
	C1	25	82.5	9.5	8.0	0.38	0.12	8.5	
	C2	8	30.1	51.4	18.5	0.28	0.21	8.5	
	C3	34	92.6	3.4	4.0	0.28	0.14	8.6	
	C4	8	30.5	52.0	17.5	0.25	0.18	8.3	
	C5	23	16.1	53.5	30.4	0.20	0.08	8.7	
	C6	37	67.7	15.6	18.7	0.25	0.12	8.5	
	C7	10	87.0	6.0	7.0	0.26	0.16	8.6	
Series name	Jhunpra								
Series number	10								
Classification	Coarse Loamy, Typic Ustifluvents								
	Ap	10	86.0	4.0	10.0	0.33	0.69	7.8	
	C1	45	78.0	11.0	15.9	0.33	0.39	7.7	
	C2	23	86.6	4.3	9.1	0.32	0.26	7.7	
	C3	49	87.3	4.2	8.5	0.18	0.27	7.8	
	C4	47	18.1	46.1	35.8	0.29	0.35	7.7	

List of frequently used symbols

<i>Symbol</i>	<i>Description</i>	<i>Dimension</i>	<i>SI Unit</i>
A	Rate of photosynthetic assimilation of CO ₂	$M L^{-2} T^{-1}$	$kg m^{-2} s^{-1}$
b	Vector containing parameters to be optimised	variable	variable
C	Solute concentration of soil water	$M L^{-3}$	$kg m^{-3}$
C	Differential water capacity ($d\theta/dh$)	L^{-1}	m^{-1}
ΔC	Change in salt storage	$M L^{-2}$	$kg m^{-2}$
C_{air}	Specific heat capacity of moist air per unit mass	$L^{-2} T^{-2} \Theta^{-1}$	$J kg^{-1} K^{-1}$
c_{conf}	Vertical resistance of semi-confined layer	T	d
C_{FC}	Soil salinity concentration at field capacity	$M L^{-3}$	$kg m^{-3}$
e_a	Actual vapour pressure	$M L^{-1} T^{-2}$	Pa
e_{sat}	Saturation vapour pressure	$M L^{-1} T^{-2}$	Pa
E	Actual soil evaporation rate	$L T^{-1}$	$m s^{-1}$
E	Actual soil evaporation integrated over time	L	m
E_{emp}	Soil evaporation rate according to an empirical function	$L T^{-1}$	$m s^{-1}$
E_{max}	Maximum soil evaporation rate according to Darcy's law	$L T^{-1}$	$m s^{-1}$
E_p	Potential soil evaporation rate	$L T^{-1}$	$m s^{-1}$
E_p	Potential soil evaporation integrated over time	L	m
E_{pan}	Pan evaporation	L	m
E_w	Evaporation of ponding water integrated over time	L	m
$EC_{1:2}$	Electrical conductivity of one part soil mixed with two parts distilled water	-	$dS m^{-1}$
EC_{FC}	Soil electrical conductivity at field capacity	-	$dS m^{-1}$
EC_e	Electrical conductivity of the saturated soil paste	-	$dS m^{-1}$
EC_{gw}	Electrical conductivity of groundwater	-	$dS m^{-1}$
EC_{obs}	Observed soil salinity in field condition	-	$dS m^{-1}$
EC_{max}	Critical level of salinity tolerance for a crop	-	$dS m^{-1}$
EC_{slope}	Decline per unit increase in electrical conductivity beyond EC_{max}	-	$\% dS m^{-1}$
ET	Actual evapotranspiration rate	$L T^{-1}$	$m s^{-1}$
ET	Actual evapotranspiration integrated over time	L	m
ET_p	Potential evapotranspiration rate	$L T^{-1}$	$m s^{-1}$
ET_p	Potential evapotranspiration integrated over time	L	m
ET_{p0}	Potential evapotranspiration rate of a wet crop	$L T^{-1}$	$m s^{-1}$
ET_{ref}	Reference evapotranspiration integrated over time	L	m
ETQ	Actual evapotranspiration ET plus percolation Q_{bot} and seepage losses Q_{SL} integrated over time	L	m

<i>Symbol</i>	<i>Description</i>	<i>Dimension</i>	<i>SI Unit</i>
G	Soil heat flux density	$M T^{-3}$	$W m^{-2}$
h	Soil water pressure head	L	m
h_1	Pressure head below which roots start to extract water from the soil	L	m
h_2	Pressure head below which roots start to extract water optimally from the soil	L	m
h_{3h}	Pressure head below which roots cannot extract optimally any more, at a high potential transpiration rate	L	m
h_{3l}	Pressure head below which roots cannot extract water optimally any more, at a low potential transpiration rate	L	m
h_4	Pressure head below which no water uptake by roots is possible ('wilting point')	L	m
I	Irrigation integrated over time	L	m
I_{cw}	Canal water irrigation integrated over time	L	m
I_{gw}	Groundwater irrigation integrated over time	L	m
J	Solute flux density	$M L^{-2} T^{-1}$	$kg m^{-2} s^{-1}$
K	Hydraulic conductivity	$L T^{-1}$	$m s^{-1}$
k	Crop growing stage	-	-
K_{gr}	Extinction coefficient for global solar radiation	-	-
K_{sat}	Saturated hydraulic conductivity	$L T^{-1}$	$m s^{-1}$
K_y	Yield response factor	-	-
L_{dis}	Dispersion length	L	m
LAI	Leaf area index	-	-
n	Empirical shape factors in the Van-Genuchten model	-	-
P	Rainfall integrated over time	L	m
P_i	Rainfall interception rate	$L T^{-1}$	$m s^{-1}$
q	Water flux density	$L T^{-1}$	$m s^{-1}$
q_{bot}	Bottom flux density (positive upward)	$L T^{-1}$	$m s^{-1}$
Q_{bot}	Bottom flux from soil column integrated over time (positive upward)	L	m
Q_{cw}	Canal water inflow integrated over time	L	m
Q_{SL}	Seepage losses from the conveyance system (% of the canal water inflow Q_{cw})	-	%
r_{air}	Aerodynamic resistance	$L^{-1} T$	$s m^{-1}$
r_{crop}	Crop resistance	$L^{-1} T$	$s m^{-1}$
R	Net groundwater recharge integrated over time	L	m
R_n	Net radiation flux density	$M T^{-3}$	$W m^{-2}$

<i>Symbol</i>	<i>Description</i>	<i>Dimension</i>	<i>SI Unit</i>
S_a	Actual root water extraction rate	T^{-1}	s^{-1}
S_e	Relative saturation	-	-
S_{max}	Maximum root water extraction rate	T^{-1}	s^{-1}
SR	Surface runoff integrated over time	L	m
T	Actual transpiration rate	$L T^{-1}$	$m s^{-1}$
T	Actual transpiration integrated over time	L	m
T_p	Potential transpiration rate	$L T^{-1}$	$m s^{-1}$
T_p	Potential transpiration integrated over time	L	$m s^{-1}$
W	Weighting function to account for the relative influence of each data point in objective function, Φ	-	-
ΔW	Change in soil water storage integrated over time	L	m
Y	Actual crop yield	$M L^{-2}$	$kg m^{-2}$
Y_g	Actual grain (or seed) yield	$M L^{-2}$	$kg m^{-2}$
Y_{FM}	Actual fresh matter yield	$M L^{-2}$	$kg m^{-2}$
Y_p	Potential crop yield	$M L^{-2}$	$kg m^{-2}$
z	Vertical coordinate (positive upward)	L	m
z_{root}	Rooting depth	L	m
t	time	T	s
ρ_{air}	Air density	$M L^{-3}$	$kg m^{-3}$
Δ_v	Slope of the vapour pressure curve	-	$Pa K^{-1}$
Φ	Objective function	-	-
ϕ_{aquif}	Hydraulic head in a semi-confined layer	L	m
ϕ_{gw1}	Groundwater level in aquifer	L	m
γ_{air}	Psychrometric constant	$L^{-1} M T^{-2} \Theta^{-1}$	$Pa K^{-1}$
α	Empirical parameter in the Van-Genuchten model	L^{-1}	m^{-1}
α_{rs}	Reduction coefficient for salinity stress as used in SWAP	-	-
α_{rw}	Reduction coefficient for water stress as used in SWAP	-	-
α_s	Surface albedo	-	-
ε	Actual light use efficiency of crop	$L^{-2} T^2$	$kg J^{-1}$
λ	Empirical parameter in the Van-Genuchten model	-	-
ρ_w	Density of water	$M L^{-3}$	$kg m^{-3}$
λ_w	Latent heat of vaporization	$L^2 T^{-2}$	$J kg^{-1}$
θ	Volumetric soil water content	-	$m^3 m^{-3}$
θ_{res}	Residual volumetric water content	-	$m^3 m^{-3}$
θ_{sat}	Saturated volumetric water content	-	$m^3 m^{-3}$

List of abbreviations

<i>Abbreviation</i>	<i>Description</i>
<i>APAR</i>	Actual Photo synthetically Active Radiation absorbed by a plant
BMB	Bhakra Main Branch
BRU	Baruwali distributary
CCA	Culturable Command Area: area suitable for agriculture with attached water rights
CRS	Cotton Research Station
CCS HAU	CCS Haryana Agricultural University
<i>CV</i>	Coefficient of Variation
DM	Dry Matter
F	denotes the Farmer field
FB	Fathebad Branch
GIS	Geographical Information System
<i>HSMITC</i>	Haryana State Minor Irrigation and Tubewell Corporation
ICAR-CRS	Indian Council of Agricultural Research – Cotton Research Institute
IWMI	International Water Management Institute
IWRS	Indian Water Resources Society
JDW	Jandwala distributary
<i>kharif</i>	Summer crop season (April – October)
<i>PAR</i>	Photo synthetically Active Radiation
PEST	Parameter ESTimation
<i>rabi</i>	Winter crop season (October – April)
<i>RMSE</i>	Root Mean Square Error
<i>rostering</i>	Rotation of water supply among distributary canals
RS	Remote Sensing
SEBAL	Surface Energy Balance Algorithm for Land
S	denotes the field Site (four farmer fields at one site)
SGC	Southern Ghagger Canal
SGMP	Standard Groundwater Model Package
SIC	Sirsa Irrigation Circle
SU	Simulation Unit
SUK	Sukchain distributary
SWAP	Soil-Water-Atmosphere-Plant
SIWARE	SImulation of Water management in Arid REgions
<i>warabandi</i>	Available canal water is spread to all farmers in proportion to their land holding
WOFOST	WOrld FOod STudies
<i>WP</i>	Water Productivity

Curriculum vitae

Ranvir Singh was born on August 12, 1974, in the village Nahri in Haryana, India. After finishing his secondary school in 1992, he studied the Bachelor of Engineering (Agricultural Engineering) at CCS Haryana Agricultural University (CCS HAU), Hisar, Haryana. Following studies in agriculture, he joined the Master of Technology (Soil and Water Engineering) at the same university. He passed his post-graduation in 1999. Thereafter, he worked as Research Associate at the Department of Soil and Water Engineering at CCS HAU. In April 2003, he started with his Doctoral thesis at Wageningen University and Research Centre, Wageningen, The Netherlands. His research interest is focused on the mutual benefit between the detailed crop and soil models, remote sensing and GIS, with the aim to develop a decision support system for improved regional irrigation water management and its productivity.

Wageningen University and Research Centre (WUR) supported the research reported in this thesis through a 'Sandwich fellowship'. The extended period of the fellowship was financed from the WATER PROductivity (WATPRO) project of the Sub-department of Water Resources, WUR. Their financial support is gratefully acknowledged.